

Reliability Based Seismic Design of Open Ground Storey Framed Buildings

Haran Pragalath D.C.



**Department of Civil Engineering
National Institute of Technology Rourkela
Rourkela -769008, India**

Reliability Based Seismic Design of Open Ground Storey Framed Buildings

*Thesis submitted in partial fulfillment
of the requirements for the degree of*

Doctor of Philosophy

in

Civil Engineering

by

**Haran Pragalath D.C.
(511CE105)**

under the guidance of

**Dr. Pradip Sarkar
&
Dr. P. Robin Davis**



Department of Civil Engineering
National Institute of Technology Rourkela
Odisha-769008, India.

2015



Department of Civil Engineering
National Institute of Technology Rourkela
Rourkela-769 008, Odisha, India.

CERTIFICATE

This is to certify that the thesis entitled titled “**Reliability Based Seismic Design of Open Ground Storey Framed Buildings**” by **Haran Pragalath D.C.** to the National Institute of Technology Rourkela for the award of the degree of Doctor of Philosophy is a bonafide record of research work carried out by him under our supervision. The contents of this thesis, in full or in parts, have not been submitted to any other Institute or University for the award of any degree or diploma.

Research Guides

Rourkela-769008
Date:

Prof. Pradip Sarkar Prof. P.Robin Davis
Department of Civil Engineering

DECLARATION

I hereby declare that, I am the sole author of this thesis. This thesis contains no material that has been submitted previously, in whole or in part, for the award of any other academic degree or diploma. Except where otherwise indicated, this thesis is my own work.

Haran Pragalath D.C.
Department of Civil Engineering
NIT Rourkela

ACKNOWLEDGEMENTS

This thesis is the result of my twenty three years of education, in which five years of stay at NIT Rourkela, during the stay I have been supported by many people. Now, I have the opportunity to express my gratitude to all of them.

First and foremost, I would like to thank Prof. S. K. Sarangi, Director, NIT Rourkela for making the college environment more active by conducting a series of programmes throughout the year, which makes research scholars to loosen up and work effectively.

From the bottom of my heart, I would like to thank my research guide Prof. Pradip Sarkar, who supported me during critical times. His advice at the right time makes me to concentrate on research works. I would like to thank for the freedom you have given to me and the faith on me, which makes me to feel more comfortable during the stay. I remember the funs and chats we had together in picnics and dinner parties. I enjoyed driving your car during the stay at Rourkela, mostly during the ICSEM-13 conference. I really enjoyed working with you throughout the stay. Many thanks for the efforts taken on correcting and updating the thesis and bringing it into readable form. I also thank Mrs. Sutanuka Sarkar for her affection and support during the stay at Rourkela.

I would like to thank Prof. Robin Davis, who shaped my research work throughout. I enjoyed reading the papers and understanding the concepts along with you. I remember the fun we had while discussing the research findings. I am happy to discuss the small findings in research work with you to see the smile on your face. I have seen the meaning of hard work from your day-to-day life process. You are the coolest Professor I ever had. I am most lucky to have you as my co-guide during my research work. Special thanks for providing your Scooty, whenever I required.

I would like to thank Prof. M. Panda, Prof. S.K. Sahu, Prof. A.V. Asha, Prof. M.R. Barik, Prof. N. Roy, Prof. S.P. Singh, Prof. S.K. Das and Prof. Ujjal Chattaraj for their encouragement, guidance and support during my stay at rourkela. I also thank Mrs. Sudeshna Chattaraj for her efforts on correcting my thesis. I thank, my hostel (V.S.Hall) warden Prof. Sumit Kumar Pal for allowing my E-cycle to use inside the hostel for charging, which really makes my mode of transportation easier.

I remember the early stage of my research period was more challenging as most of the time I was alone. I want to thank my immediate juniors Mr. Hemanth Kumar Godke, Miss. Soumya Subhashree and Mr. Paramananda Kundu who supported me during this period and made my stay more colourful. I remember the fun, chit-chats and project discussions we had in structural engineering lab and PG lab. I cherish the moments we had together in never ending parties, fests and cultural.

I would like to thank Padmakar Maddala, sports secretary at NIT Rourkela, who arranged countless cricket matches with friends and professors and the fun we all had together in playing cricket in flood lights. I would like to thank Alagappan Kuppumanikandan and S. Krishna Kumar for organising several parties and for making whole classmates together. I remember the birthday celebration fun, picnics and parties had with Naveen Sandesh, Rahul Venugopal Nair, Arshaghosh Ajayan, Vikas Kachhap, Adyasha Priyadarshini, Ashish Singh, Ranjith Kumar Chokkarapu, Sreelatha Vuggumudi, Satish Kumar and Miss Meera. I thank for their strong affection towards me.

I also like to thank my juniors Subhash Karthik, Subhashree Samantasinghar, Ganesh Ravi, Sanju J. Thachampuram, Minnu Mathew, Pavani Murakonda, Chethan Jaya Naik and Nagendra kola for their endless love. I remember the fun we had in Diwali, Holi celebrations and the parties. The last week rush-up project works done after the seminar dates are announced that was really a funny moments, I am thankful to all for being a part of it.

Special thanks to my research colleagues Monalisa Priyadharshini, Rima Sahini, Avadhoot Bhosale, Ramkumar Chandran, Shubhashree Behera, Biraja Prasad Mishra, Saleema Panda, and Prateek Dhir. Heartly thanks to Madhusmita Biswal for providing her Scooty!

I would like to thank my childhood friend Steffi Lawrence, who is there for me always to share my feelings. It's been a great pleasure to have you as my friend, who always encourages me.

My time at NIT Rourkela was made colourful due to all my friends. I deeply thank you all and cherish these memories with all my friends.

Lastly I am holding for the best, my father and mother they know me well. They travelled with me by correcting my mistakes, adjusting themselves with my wishes and gave me a peaceful happy life. I thank for their encouragements, support, advice and the endless love towards me. I would also like to thank my brother for his care and affection towards me.

HARAN PRAGALATH D.C.

I would like to dedicate this work to my father **G.Devadhas**,
mother **K.Chellam** and my brother **D.C.Haran Pramoth**

ABSTRACT

Open Ground Storey (OGS) framed buildings in which the ground storey is kept open without providing any infill walls and mainly used for parking, are increasingly common in urban areas. Vulnerability of this type of buildings has been exposed in the past earthquakes. OGS buildings are conventionally designed considering a bare frame analysis, ignoring the stiffness of the infill walls present in the upper storeys, which under-estimates the inter-storey drift and the force demand in the ground storey columns. To compensate this, a multiplication factor (MF) is introduced by various international codes while calculating the design forces (bending moments and shear forces) in the ground storey columns.

Present study focuses on the evaluation of seismic performances of OGS buildings designed with alternative MFs through performance-based design approach using a probabilistic framework. The probabilistic seismic demand models and corresponding fragility curves for all the selected OGS buildings are developed for different performance levels. Reliability curves are developed for the OGS building frames against the seismic hazard associated with maximum seismic zone of India (Zone-V of IS 1893, 2002). Similar analyses are also carried out on bare frames and fully infilled frames for reference.

It is found from the present study that the application of MF only in ground storey, as suggested by many literatures and design codes (including Indian standards), is not an appropriate solution for design of OGS buildings as it leads to vulnerable adjacent storey. This study proposes an effective scheme of MF for design of OGS buildings that yields acceptable levels of reliability index.

Keywords: *open ground storey building, multiplication factor, probabilistic seismic demand model, fragility curves, reliability index`*

TABLE OF CONTENTS

Title.....	Page No.
ACKNOWLEDGEMENTS	i
ABSTRACT	v
TABLE OF CONTENTS	vii
LIST OF TABLES	xi
LIST OF FIGURES	xiii
ABBREVIATIONS	xvii
NOTATIONS	xix

CHAPTER 1 INTRODUCTION

1.1 Background and Motivation.....	1
1.2 Objectives	3
1.3 Scope of the study	4
1.4 Methodology	5
1.5 Organization of thesis	6

CHAPTER 2 LITERATURE REVIEW

2.1 Introduction	9
2.2 International codes of practice on OGS building	9
2.3 Previous research on OGS building	14
2.4 Modes of failure of masonry infill	20
2.5 Previous research on modelling of infilled masonry	22
2.5.1 Studies on micro models	22
2.5.2 Studies of macro models	23
2.6 Previous research on seismic risk assessment.....	30
2.7 Review on reliability based structural design	39
2.7.1 Reliability Analysis Methodologies.....	40
2.7.2 A Review on Reliability in Conventional Design	43

2.7.3	Previous Researches on Reliability based Seismic Design.....	44
2.9	Summary.....	46

CHAPTER 3 METHODOLOGY

3.1	Introduction.....	49
3.2	Earthquake risk assessment.....	49
3.2.1	Seismic hazard analysis	53
3.2.2	Development of fragility curves.....	58
3.3	Building performance levels	61
3.3.1	Damage limitation (<i>DL</i>).....	62
3.3.2	Significant damage (<i>SD</i>).....	62
3.3.3	Collapse prevention level or Near Collapse level (<i>CP</i>).....	62
3.4	Sampling of variables	63
3.5.	Summary.....	66

CHAPTER 4 MODELLING AND ANALYSIS

4.1	Introduction.....	67
4.2	Material models.....	67
4.2.1	Concrete modelling.....	68
4.2.2	Reinforcement modelling.....	70
4.2.3	Infill wall modelling	72
4.3	Element model.....	74
4.4.	Nonlinear dynamic analysis.....	75
4.4.1	Mass matrix.....	76
4.4.2	Damping matrix.....	76
4.4.3	Stiffness matrix - fibre based Element.....	77
4.4.4	Analysis.....	81
4.5	Validation study	83
4.5.1	Validation I: One storey one bay RC infilled frame.....	84
4.5.2	Validation II: Four storey three bay ICONS frame-bare and infilled frame.....	85
4.6.	Indian seismic code design	87
4.6.1	Seismic weight.....	88
4.6.2	Lumped mass.....	88

4.6.3	Calculation of lateral forces	88
4.6.4	Load combinations.....	90
4.7	Frames considered	91
4.8	Latin Hypercube sampling	98
4.9	Limit state capacities (S_C)	100
4.10	Selection of appropriate intensity measure	108
4.11	Selection of ground motions	111
4.11.1	Natural ground motions from Indian region	111
4.11.2	Synthetic ground motion records.....	113
4.11.3	Effect of earthquake records on fragility curves	116
4.12	Summary	119

CHAPTER 5 FRAGILITY BASED ASSESSMENT OF OGS BUILDINGS

5.1	Introduction.....	121
5.2	Response of OGS frames – A deterministic study.....	121
5.3	Probabilistic Seismic Demand Models.....	125
5.4	Validation of the SAC-FEMA method.....	126
5.5	Probabilistic Seismic Demand Models for OGS buildings	128
5.6	Fragility curves.....	139
5.6.1	Two storey buildings.....	139
5.6.2	Four storey buildings	141
5.6.3	Six storey buildings	143
5.6.4	Eight storey buildings	146
5.7	Summary and Conclusions	148

CHAPTER 6 RELIABILITY BASED ASSESSMENT OF OGS BUILDINGS

6.1	Introduction.....	151
6.2	Selection of seismic hazard curve	152
6.3	Performance objectives.....	153
6.4	Reliability curves.....	154
6.4.1	Two storey frames	156
6.4.2	Four storey frames	156
6.4.3	Six storey frames	156

6.4.4	Eight storey frames	157
6.5	Reliability index for different performance objectives.....	160
6.5.1	Two storey frames	160
6.5.2	Four storey frames	161
6.5.3	Six storey frames	161
6.5.4	Eight storey frames	162
6.6	Effect of MF schemes on the behaviour of OGS frame	165
6.7	Target reliability	168
6.7.1	Evaluation based on target reliabilities of Aoki <i>et al.</i> (2000).....	169
6.7.2	Evaluation based on achieved reliability of fully infilled frame	170
6.8	Suitable MF schemes for the design of OGS Buildings	173
6.9	Summary	175

CHAPTER 7 CONCLUSIONS

7.1	Summary	177
7.2	Conclusions	179
7.3	Contribution of the research.....	180
7.4	Scope of future work	181

APPENDIX A	183
-------------------------	-----

APPENDIX B	189
-------------------------	-----

APPENDIX C	197
-------------------------	-----

REFERENCES	209
-------------------------	-----

LIST OF PUBLICATIONS	225
-----------------------------------	-----

LIST OF TABLES

Table No.	Title	Page No.
2.1	Characterization of soft-storey building as per international design codes.....	10
2.2	Characterization of weak-storey building as per international design codes	11
2.3	MFs recommended by international codes/literatures	19
4.1	Details of computer processor available in NEEShub.....	83
4.2	Design base shear details of selected frames	93
4.3	Details of random variables used in LHS scheme.....	98
4.4	Limit state capacities for 2-storey frames.....	104
4.5	Limit state capacities for 4-storey frames.....	105
4.6	Limit state capacities for 6-storey frames.....	106
4.7	Limit state capacities for 8-storey frames.....	107
4.8	Selected Indian ground motions events	112
4.9	Far-field ground motions events suggested by FEMA P695 (2012).....	115
4.10	Comparison of PSDM models developed from two suites of ground motions	117
5.1	PSDMs for two storeyed frames	130
5.2	PSDMs for four storeyed frames.....	131
5.3	PSDMs for six storeyed frames.....	133
5.4	PSDMs for eight storeyed frames	135
6.1	Different earthquake levels at selected regions.....	152
6.2	Target reliability index used by Aoki <i>et al.</i> (2000)	169
6.3	Target reliability index based on achieved reliability index of fully infilled frame .	169
6.4	Comparison of proposed schemes with the schemes available in literature.....	174
6.5	Expected probability of failure (at Guwahati) for proposed schemes.....	175

LIST OF FIGURES

Figure No.	Title	Page No.
1.1	A typical OGS building located at Rourkela, India.....	1
1.2	Failures of OGS building during 2001 Bhuj Earthquake	2
1.3	Flowchart showing the methodology	5
2.1	Corner crushing and shear cracking modes of infill wall failure	20
2.2	Diagonal cracking mode of infill wall failure.....	21
2.3	Parameters relevant for equivalent strut modelling.....	25
2.4	Schematic force-displacement response of the infill strut model	27
2.5	Force-displacement relationship of the diagonal struts used by Celarec <i>et al.</i> (2012)....	30
2.6	Probability Density for Limit-state $g(.)$	41
3.1	Reliability curve generation using non-linear time history analyses	51
3.2	Fragility-hazard interface, identifying dominant contribution to the risk (Elingwood, 2001)	52
3.3	Typical seismic hazard curve -possibility of intense ground shaking at a site	55
3.4	Steps for performing a PSHA (Baker, 2008)	56
3.5	Typical performance levels for bare frame.....	61
3.6	Typical performance levels for fully infilled frame	62
3.7	Typical Latin Hypercube sampling method.....	66
4.1	Parameters of monotonic envelopes of Concrete02 model (OpenSees,2013).....	69
4.2	Stress-strain relationships of steel reinforcement (Menegotto- Pinto model)	70
4.3	Force-displacement relationship of the diagonal struts used by Celarec <i>et al.</i> (2012)....	72
4.4	Pinching hysteresis model.....	74
4.5	Typical building model and corresponding computational model.....	75
4.6	Computational model- fiber-based element and section discretization.....	78
4.7	Force and deformation variables at element and section levels.....	79
4.8	Infilled frame tested by Colangelo (1999)	84

4.9	Displacement history E-W component of Friulli earthquake (1976)	85
4.10	Comparison of base shear histories obtained from experimental and computational study.....	85
4.11	Time history analysis of the record, Acc-475	86
4.12	Comparison of roof displacement time histories for ICON frame - Bare	87
4.13	Comparison of roof displacement history for ICON infilled frame	87
4.14	Response spectra for 5 percent damping (IS 1893, 2002)	89
4.15	Building model under seismic load	90
4.16	Configurations of selected frames: Two-storeyed.....	94
4.17	Configurations of selected frames: Four-storeyed	95
4.18	Configurations of selected frames: Six-storeyed	96
4.19	Configurations of selected frames: Eight-storeyed	97
4.20	PDF Distribution for random variables and selected points based on LHS scheme... 99	
4.21	Envelope Stress vs. Strain Curve for 44 models developed according LHS Scheme	100
4.22	Typical performance levels for bare frame	102
4.23	Typical performance levels for fully infilled frame	102
4.24	Evaluation of storey limit state capacity for typical frame (4O ₁)	103
4.25	PSDMs of selected bare frame (4B)	109
4.26	Fragility Curves of selected bare frame (4B)	109
4.27	Relation between Sa[T1] and PGA	110
4.28	Fragility curves of frame for different performance levels in terms of PGA and Sa[T1]	110
4.29	Response Spectra for natural ground motions	113
4.30	Response Spectra for 22 pairs of synthetic ground motion records.....	116
4.31	Cloud analysis results and corresponding PSDM	117
4.32	Fragility curves for SD performance levels	118
4.33	Fragility curves for CP performance levels	118
5.1	Maximum displacement profile for four storeyed frames subjected to particular ground motion	122
5.2	Inter-storey-drift for four storeyed frames.....	123
5.3	ISD versus MF for 4O _x frames.....	124
5.4	Comparison between LHS-Monte Carlo and 2000 SAC-FEMA method	127
5.5	PSDMs and fragility curves for each storey of four storey fully infilled frame (4F)	129

5.6	PSDMs model for two storeyed frame	130
5.7	PSDMs model for four storeyed frame.....	132
5.8	PSDMs model for six storeyed frame.....	135
5.9	PSDMs model for eight storeyed frame	138
5.10	Fragility curves for two storey frames.....	140
5.11	Comparison of different schemes of MF at CP for 2-storey frames	141
5.12	Fragility curves for four storey frames	142
5.13	Comparison of different schemes of MF at CP for 4-storey frames	143
5.14	Typical displacement profile for four storied OGS frame	143
5.15	Fragility curves for six storey frames.....	144
5.16	Comparison of different schemes of MF at CP for 6-storey frames	145
5.17	Typical displacement profile for six-storeyed OGS frame	145
5.18	Fragility curves for eight-storey frames	147
5.19	Comparison of different schemes of MF at CP for 8-storey frames	148
5.20	Typical displacement profile for eight storied OGS frame.....	148
6.1	Seismic hazard curves of selected regions.....	153
6.2	Seismic performance and design objective matrix as per SEAOC (1995).....	154
6.3	Schematic representation for development of reliability index (β_{pf})	155
6.4	Reliability curves for 2 storey frame	158
6.5	Reliability curves for 4 storey frame	158
6.6	Reliability curves for 6 storey frame	159
6.7	Reliability curves for 8 storey frame	159
6.8	Reliability index for different performance objectives for 2- storey frames	163
6.9	Reliability index for different performance objectives for 4- storey frames	163
6.10	Reliability index for different performance objectives for 6- storey frames	164
6.11	Reliability index for different performance objectives for 8- storey frames	164
6.12	Variation of Reliability index with various scheme of MF (Guwahati region).....	166
6.13	Variation of Reliability index with various scheme of MF (Bhuj region).....	167
6.14	κ_{ak} values for all the benchmark frames.....	171
6.15	κ_{ff} values for all the benchmark frames	172

ABBREVIATIONS

3-D	-	Three Dimensional
2-D	-	Two Dimensional
BF	-	bare frame
C	-	Capacity
CPU	-	Central Processing Unit
CESMD	-	Center for Engineering Strong Motion Data
CP	-	Collapse Prevention
CCDF	-	Complementary Cumulative Distribution Function
D	-	Demand
DL	-	Damage Limitation
DOF	-	Degrees of Freedom
DSHA	-	Deterministic Seismic Hazard Analysis
EQ	-	Earthquake
EDP	-	Engineering Damage Parameter
E-W	-	East-West
G	-	Ground
GLD	-	Gravity Load Design
IO	-	Immediate Occupancy
IM	-	Intensity Measure
ISD	-	Inter-Storey Drift
FEM	-	Finite Element Model
FF	-	Fully infilled frame

LHS	-	Latin Hyper-cube Sampling
LHS-MC	-	Latin Hyper-cube Sampling Monte Carlo
LS	-	Limit State
MF	-	Multiplication Factor
NEEShub	-	Network for Earthquake Engineering Simulation hub
NTHA	-	Non-linear Time History Analysis
OGS	-	Open Ground Storey
OpenSees	-	Open System for Earthquake Engineering Simulation
PGA	-	Peak Ground Acceleration
PGV	-	Peak Ground Velocity
PGD	-	Permanent Ground Deformation
PSDM	-	Probabilistic Seismic Demand Model
PSHA	-	Probabilistic Seismic Hazard Analysis
POA	-	Pushover Analysis
R	-	Response Reduction factor
RC	-	Reinforced Concrete
SD	-	Significant Damage
SHA	-	Seismic Hazard Analysis
TCL	-	Tool Command Language

NOTATIONS

English Symbols

a	strain hardening ratio
a_i	area of i^{th} fiber
A_w	cross-sectional area of the infill panel
b_w	equivalent strut width
$B(x)$	first order strain-deformation transformation matrix
$[C]$	damping matrix
$C(x)$	strain-deformation transformation matrix which consists of the first derivatives of displacement interpolation matrix
d	diagonal length of infill wall
d_i	inter-storey drifts
E_c	elastic modulus of the column in the bounding frame
E_s	modulus of elasticity of steel, and the hardening ratio
E_{ti}	tangent modulus at i^{th} fiber
E_w	elastic modulus of the infill wall
f_{cc}	compressive strength of confined concrete
f_c	compressive strength
f_{ck}	characteristic strength of concrete
f_{cc}^{resid}	residual strength of confined concrete
f_{co}	compressive strength of unconfined concrete
f_m	shear strength of masonry
f_o	compressive strength of concrete
f_y	yield strength of steel
F_{cr}	cracking load
F_i	lateral strength of i^{th} storey of the building
F_{max}	crushing load or maximum load
F_{res}	residual strength
$F_R(x)$	seismic fragility
$f_M(m)$	probability density functions for magnitude.

$f_R(r)$	probability density functions for distance
g	acceleration due to gravity
$G(x)$	strain-deformation transformation matrix
$G_A(x)$	seismic hazard function
G_w	elastic shear modulus of the infill material
h	height of column between centrelines of beams
h_w	clear height of infill wall
H	height of the infill panel
I_c	moment of inertia of the column
k	confinement factor
$k_s(x)$	section stiffness
K_{deg}	degrading stiffness
K_e	initial stiffness
K_{el}	stiffness of infill material up to first cracking
K_i	lateral stiffness of i^{th} storey of the building
K_{sec}	secant stiffness
$[K]$	stiffness matrix
$[K_c]$	last committed stiffness
$[K_i]$	tangent stiffness
$[K_l]$	current tangent stiffness
L	element length
L_w	clear length of Infill wall
m	magnitude
m^{\min}	minimum magnitude
m^{\max}	maximum magnitude
M	bending moment
$[M]$	mass matrix
MDOF	multi-degrees-of-freedom
M_i	range of magnitude
ncpus	number of effective CPU
n_M	discretized intervals for magnitude
n_R	discretized intervals for distance
nn	number of nodes
N -value	standard penetration resistance

N	normal force
N_t	number of intervals
N_s	number of storeys
N_p	number of PSDM
$O_{x,y}$	Open Ground Storey frame designed with MF of 'x' in the ground storey and 'y' in the first storey
p	element level force
ppn	number of tasks per node
$P[LS_i]$	limit state probability
$q(x)$	section level of force
q	behaviour factor
r	distance
$r_s(x)$	resisting force
R	residual stress ratio
R_i	range of distance
R_0, cR_1, cR_2	parameter that controls the transition from elastic to plastic branches
R square	coefficient of determination
S_a	spectral acceleration
S_d	spectral displacement
$S_a[T_1]$	spectral acceleration at a fundamental period
S_a/g	spectral acceleration per unit g
S_C	chosen limit state capacity
S_D	chosen demand
SDOF	single-degree-of-freedom
t_w	thickness of infill wall
u	element level deformation
$v_s(x)$	section level deformations
V_B	design base shear
V_{RW}	lateral resistance of masonry infill in that storey
V_{ED}	shear forces acting on structural vertical elements
w	width of the equivalent strut
x	relative displacement
\dot{x}	relative velocity

\ddot{x} relative acceleration

Greek Symbols

α_{cap}	slope of the post capping branch as a fraction of initial stiffness
α_{pinch}	cut-off limit for the force once the cap is reached
β	pinching ratio
β_c	dispersions in capacities
β_{AIM}	dispersions in the intensity measure
β_M	dispersions in modelling
β_{Pf}	reliability index
β_q	quality and completeness of the nonlinear analysis model
δ_{cap}	displacement at the peak load
δ	stiffness-proportional damping coefficient
δ_{cap}	cap displacement
δ_c	displacement at residual stress/load
ε	axial strain
ε_i	strain at i^{th} fiber
ε_o	strain corresponding to compressive strength of concrete
ε_{cc}	strain corresponding to compressive strength of confined concrete
ε_{co}	strain corresponding to compressive strength of unconfined concrete
ε_{cu}	ultimate strain of confined concrete
η	mass-proportional damping coefficient
κ_{ak}	parameter defines the performance of buildings with respect to Target reliability of Akoi <i>et al.</i> (2000)
κ_{ff}	parameter defines the performance of buildings with respect to achieved reliability of fully infilled frame
λh	relative stiffness
ω_n	natural frequency for n^{th} mode
ϕ	diameter of rebars
ϕ_o	curvature
$\phi ()$	standard normal distribution
σ_i	stress at i^{th} fiber
τ_{cr}	shear stress at cracking stage

θ	slope of the infill wall diagonal to the horizontal line
θ_{max}	maximum inter storey drift
ξ	global damping
ξ_n	critical-damping ratio

CHAPTER 1

INTRODUCTION

1.1 BACKGROUND AND MOTIVATION

Proper utilisation of space has become a major concern in developing countries like India due to rapid urbanisation and population growth. As a result, multi-storey residential buildings in urban areas are forced to have parking in the ground floor. In such framed buildings, the ground storey is generally built without any infill walls to allow easy movement of vehicles but the upper storeys are covered with infill walls. This type of framed building is referred as ‘open ground storey (OGS) building’ in this study. Fig. 1.1 presents a typical OGS building located in Rourkela, India.



Fig.1.1: A typical OGS building located at Rourkela, India.

Although this type of OGS buildings has many functional advantages, they possess a potentially dangerous type of vertical irregularity. The sudden reduction in lateral stiffness and strength of the ground storey in OGS building results in large lateral displacements in ground storey level, which increases the curvature and force in the ground storey columns. The collapse of this type of buildings is predominantly due to the formation of soft-storey mechanism in the ground storey columns. Past earthquakes have demonstrated the vulnerability of OGS buildings. A number of OGS framed buildings have experienced severe damage during the 2001 Bhuj earthquake (Fig. 1.2).



Fig.1.2: Failures of OGS building during 2001 Bhuj Earthquake (www.nicee.org)

In conventional design practice, the stiffness contribution of infill walls present in upper storeys of OGS framed buildings is ignored in the structural analysis ('bare frame' analysis). Design based on such analysis results in underestimation of the bending moments and shear forces in the ground storey columns and this is perhaps responsible for the failures of such buildings. To address this problem, Indian Standard IS 1893 (2002) recommends a factor to magnify the forces in ground storey columns. This factor is referred as 'multiplication factor (MF)' in this study. IS 1893 (2002) states: "The columns of the OGS (soft-storey) are to be designed for 2.5 times the storey shears and moments calculated under seismic loads of bare frame".

ASCE/SEI 7 (2010) and NZS1170.5 (2004) do not recommend OGS buildings as they fall in the extreme soft/weak storey irregularity category. ICC IBC (2012) relies on ASCE/SEI 7 for its provisions related to structural design and earthquake loads. Different other international codes and published literature addressed this problem through MF in line with Indian code. A review of the MFs suggested by various international design codes is reported by Kaushik *et al.* (2006) and the corresponding expression/values of MF are shown in Table 2.3 (Chapter 2). This table shows that there is a wide disparity in the MF values suggested by international codes.

Many previous literatures (Fardis and Panagiotakos, 1997, Fardis *et al.*, 1999) reported that the MF proposed by the Eurocode 8 (2003) lacks a rational basis. This may also be true for other international design codes. The MFs recommended by existing literatures do not consider the uncertainties associated with earthquake loading and structural properties. However, the current trend of seismic design is moving towards the probabilistic approach considering possible uncertainties (Ghobarah, 2000). Also, there is no literature found on performance-based design approach for OGS buildings. In this circumstance it is very important to undertake a thorough study on the behaviour of OGS buildings considering uncertainties involved using a performance-based design approach and arrive at a MF on the basis of more rational methods such as reliability-based design. This is the underlying motivation of the present study.

1.2 OBJECTIVES

Based on the literature review presented in Chapter 2, the main objective of the present study has been identified as to propose suitable schemes of MF for seismic design of OGS buildings considering a desired degree of reliability. To achieve this objective the problem is being divided into different parts with following sub-objectives:

- i) To establish limit state capacities of each storey of framed building for various performance levels.
- ii) To develop probabilistic seismic demand model (PSDM) and fragility curves for benchmark OGS framed buildings designed with various schemes of MF.
- iii) To develop reliability index for OGS framed buildings designed with various schemes of MF.
- iv) To propose appropriate schemes of MF for the design of OGS buildings based on the reliability indices achieved by the benchmark frames.

1.3 SCOPE OF THE STUDY

- i) The present study is limited to framed buildings up to eight-storey designed as per prevailing Indian Standards.
- ii) The present study is limited to OGS reinforced concrete multi-storey frames that are regular in plan. Hence, representative plane frames are used in the present study. The plan asymmetry arising from possible irregular distribution of infill walls are not considered in the analysis.
- iii) The infill walls are assumed to be non-integral with the surrounding frames.
- iv) Out-of-plane action of masonry walls is not considered in the study.
- v) Uncertainties in structural properties and loading are considered as applicable to Indian context.
- vi) The present study uses an equivalent single strut approach based on recent studies (Celarec *et al.*, 2012) for modelling infill walls.
- vii) Random variables considered in the present study (concrete strength, steel strength, infill strength and damping ratio) are assumed to be uncorrelated.

1.4 METHODOLOGY

The methodology worked out to achieve the above-mentioned objectives is shown in Fig.1.3 through a flowchart. Step by step methodology is presented as follows:

- i) To review the existing literature and different international design code provision on the design of OGS buildings.
- ii) To select benchmark building frames ranging from 2-8 storey and design them considering different schemes of MFs.

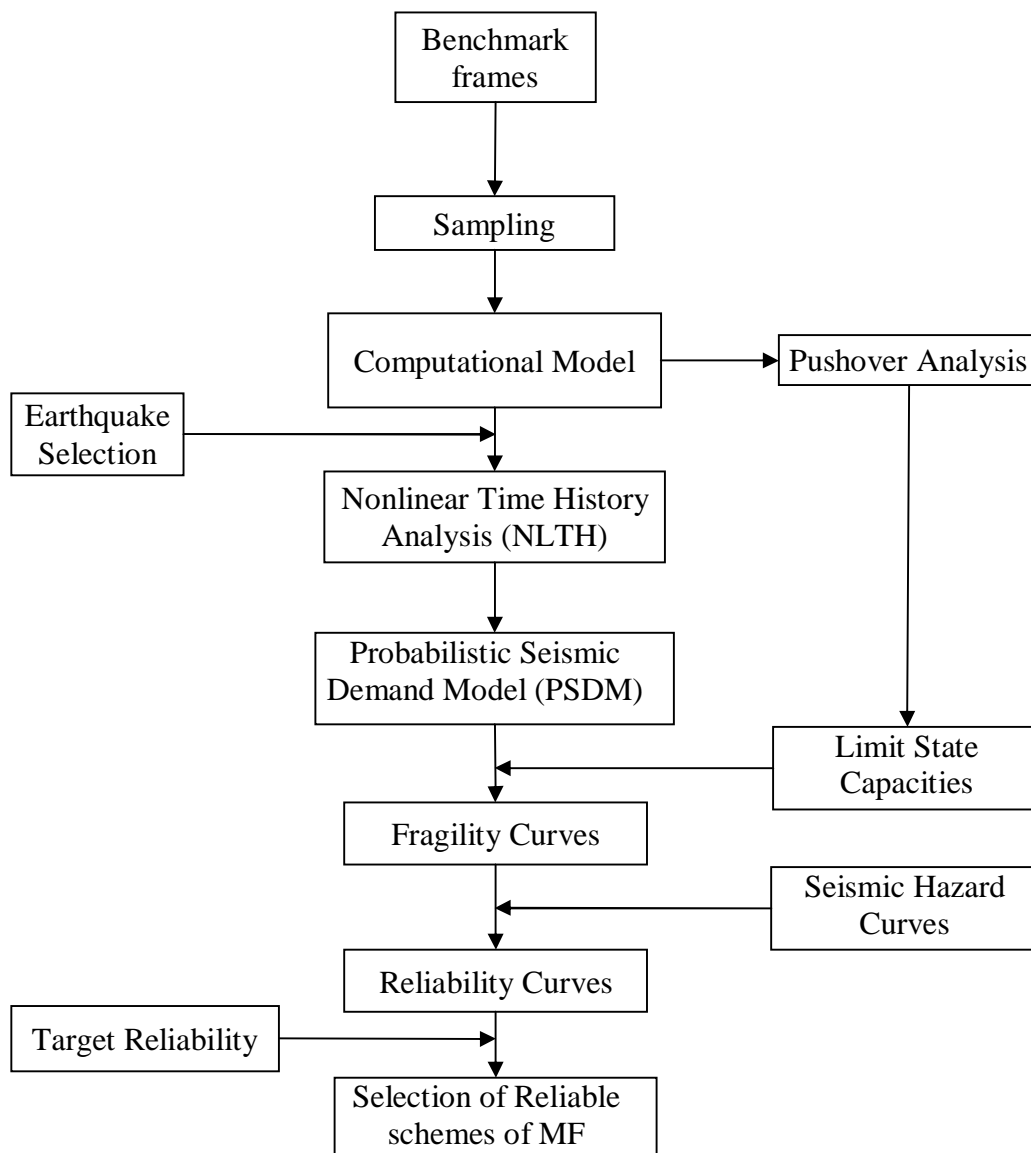


Fig.1.3: Flowchart showing the methodology

- iii) To develop computational model of selected frames to perform Pushover analysis (POA) and Nonlinear time history analysis (NTHA).
- iv) Estimate the limit state capacities of different storeys of selected frames at each performance levels
- v) Develop Probabilistic Seismic Demand Models (PSDMs), fragility curves and reliability indices for the selected frames
- vi) Select the appropriate scheme of MF for design of OGS buildings that yields acceptable levels of reliability index.

1.5 ORGANIZATION OF THESIS

A brief introduction of OGS buildings, MF values, disparity of MF values in design codes are discussed in this introductory chapter (Chapter 1). The objectives and scope of the proposed research work along with the methodology are discussed here.

Chapter 2 is devoted to the state of the art literature review on different topics related to OGS buildings. An overview of existing design guidelines for OGS buildings by various international codes and literatures is presented here. Further, a review on fragility and reliability analysis conducted on RC framed buildings are summarised and various macro-models available in literature for modelling infill walls are also discussed in this chapter.

A detailed methodology adapted for seismic risk assessment in the present study is discussed in Chapter 3. Seismic risk assessment involves the development of probabilistic seismic demand models (PSDMs), fragility curves and probabilistic seismic hazard analysis (PSHAs). The sampling scheme used to consider the uncertainties are discussed in this chapter.

Chapter 4 discusses the non-linear modelling procedure used in the present study. A number of studies are presented to validate the modelling procedure adopted in the present study. This chapter also describes the selected frame configurations designed with different schemes of MF. The material and structural properties developed through sampling to consider the uncertainties are discussed in this chapter. This chapter presents the pushover analyses of the designed frames carried out to obtain the structural capacities at different limit states. This chapter also discusses the selection of earthquake for time history analyses.

PSDM and corresponding fragility curves are developed for all the selected frames at each limit state and their comparisons are discussed in Chapter 5.

Chapter 6 discusses seismic hazard curves from selected regions required for the estimation of reliability index. The procedure for the computation of reliability index involving numerical integration of fragility curve and seismic hazard curve is explained in Chapter 6. This chapter also discusses the performance objectives required for calculation of reliability indices. A review on the target reliability index is discussed and compared with the achieved reliability indices for selected frames. This chapter finally presents the proposed schemes of MF for the design of OGS buildings.

Chapter 7 presents the summary, significant conclusions and the contributions drawn from the present study. This chapter also discusses the scope for future work in the area of OGS framed building.

CHAPTER 2

LITERATURE REVIEW

2.1 INTRODUCTION

In the first chapter, the problem of designing OGS buildings and the need for a systematic assessment of seismic risk and reliability in current design practice is outlined. This chapter deals with the current state of the art in the design of OGS buildings. It starts with a review of relevant international codes of practice followed by a review of published literature on OGS buildings. Computational modelling of masonry infill is an integral part of this research. The later part of this chapter presents a detailed review on nonlinear structural models of masonry infill available in literature. A review on probability-based assessment of building response and reliability based seismic design is presented at the end of this chapter.

2.2 INTERNATIONAL CODES OF PRACTICE ON OGS BUILDING

International design codes recognise OGS buildings as soft or weak storey buildings that require special attention. The design codes reviewed here are almost identical to define the soft storey and weak storey buildings. Tables 2.1 and 2.2 summarise the characterization of soft storey and weak storey buildings, respectively, as per the design codes. It is to be noted that OGS buildings, in most of the cases, fall either in the extreme soft storey or extreme weak storey category or both. Majority of the design codes do not recommend the construction of such extreme soft/weak storey buildings.

Table 2.1: Characterization of soft-storey building as per International design codes

Design Codes	Soft Storey Building	Extreme Soft Storey Building
IS 1893:2002	$K_i < 0.7K_{i+1}$ or $K_i < 0.8\left(\frac{K_{i+1} + K_{i+2} + K_{i+3}}{3}\right)$	$K_i < 0.6K_{i+1}$ or $K_i < 0.7\left(\frac{K_{i+1} + K_{i+2} + K_{i+3}}{3}\right)$
ASCE/SEI 7 (2010)	Same as IS 1893:2002	Same as IS 1893:2002
ICC IBC (2012)	Same as IS 1893:2002	Same as IS 1893:2002
Eurocode 8 (2003)	×	×
NZS 1170.5:2004	Same as IS 1893:2002	×
SI 413:1995	Same as IS 1893:2002	×
NBC 201:1995	Qualitative	×
FCEACR 1986	×	$K_i < 0.5K_{i+1}$
K_i = The lateral stiffness of i^{th} storey of the building '×' represents that the code does not explicitly define		

International Building Code (ICC IBC, 2012), American Standard ASCE/SEI 7 (2010) and New Zealand Code NZS 1170.5 (2004) require dynamic analysis (and do not allow equivalent static analysis) procedure for the design of buildings with soft/weak storey irregularity as this type of irregularity induce lateral loads that are significantly different from the predominantly first mode distribution assumed in the equivalent static analysis method. However, Indian Standard IS 1893 (2002), Eurocode 8 (2003), Israel Standard SI 413 (1995), Nepal National Building Code NBC 201 (1994) and Costa Rica Code FCEACR (1986) among others permit the use of equivalent static analysis procedure with suitable modifications for the design of OGS buildings. ICC IBC (2012) and ASCE/SEI 7 (2010) do not allow construction of '*extreme soft or weak storey building*' in seismic areas. The various code provisions with regard to the design of OGS building using equivalent static approach are described and compared in this section.

Table 2.2: Characterization of weak-storey building as per International design codes

Design Codes	Weak Storey Building	Extreme Weak Storey Building
IS 1893 (2002)	$F_i < 0.8F_{i+1}$	×
ASCE/SEI 7-(2010)	Same as IS 1893:2002	$F_i < 0.65F_{i+1}$
ICC IBC (2012)	Same as IS 1893:2002	Same as ASCE/SEI 7 (2010)
Eurocode 8 (2003)	×	×
NZS 1170.5 (2004)	$F_i < 0.9F_{i+1}$	×
SI 413 (1995)	Same as IS 1893:2002	×
NBC 201 (1994)	Qualitative	×
FCEACR (1986)	×	$K_i < 0.5K_{i+1}$
F_i = The lateral strength of i 'th storey of the building '×' represents that the code does not explicitly define		

Indian Standard IS 1893 has been revised in 2002 to include new recommendations for the design of OGS buildings. Although IS 1893 (2002) defines extreme soft storey category of building irregularity it is silent about any design guideline for this building type. However, in the Clause 7.10.3(a), the code recommends the use of equivalent static method for analysis and design of soft storey type buildings with certain modifications as follows: “*The columns and beams of the soft storey are to be designed for 2.5 times the storey shears and moments calculated under seismic loads of bare frame*”. This is to be noted that the code recommends the MF of 2.5 even for the beams whereas the research (Fardis and Panagiotakos, 1997) has shown that the increase in the beam strength will further increase the seismic demands on the columns. Indian Standard IS 1893:2002 does not explicitly recommend any guideline for the analysis and design of weak-storey buildings.

Eurocode 8 (2003) does not categorise the irregular buildings as soft-storey or weak storey buildings. But if there are considerable irregularities in building elevation (due to drastic

reduction of infills in one or more storeys compared to the others), Eurocode 8 (2003) imposes a local increase of the seismic action effects in vertical elements of the respective storeys. The MF to increase the seismic action effects is defined as follows:

$$\eta = 1 + \frac{\Delta V_{RW}}{\sum V_{ED}} \leq q \quad (2.1)$$

where, ΔV_{RW} is the total reduction of the lateral resistance of masonry infill in the ground storey compared to that in the upper storey. As there is no infill wall in the ground storey of an OGS building, ΔV_{RW} is equal to the resistance of masonry in the first storey itself and $\sum V_{ED}$ is the sum of seismic shear forces acting on all structural vertical elements of the storey concerned. The term ‘ q ’ is called behaviour factor, which accounts for energy dissipation capacity of the structure and the value varies from 1.50 to 4.68 depending upon the type of building systems, ductility classes, and plan regularity in the building (*Kaushik et al.*, 2006).

Israel Standard SI 413 (1995) allows a flexible (soft) or a weak storey, including open ground storey, in buildings with low or medium ductility levels only, which correspond to the buildings of little or moderate importance only. While other international codes recommend to increase the design force only in the ground storey columns, SI 413:1995 requires to increase the design force of the columns of the adjacent storeys also in addition to the columns of the ground storey. As per this standard the design forces for the flexible or weak storey members, and for the members in the storey above and below, are required to be increased by a factor $0.6R$ (where ‘ R ’ is the response reduction factor). For masonry infill RC frame buildings, R is 3.5 for low ductility level, and 5.0 for medium ductility level. Therefore, beams and columns of the flexible or weak storey and also of the two adjacent

storeys are required to be designed for at least 2.1-3.0 times the actual design forces for the irregular storey, depending upon the ductility level of the building. SI 413 (1995) also imposes some special requirements with regard to the reinforcement detailing. Confinement in columns in the flexible or weak storey, and in the storey above and below, is required to be increased in such a way that the maximum spacing of shear reinforcement (min. 8mm diameter) shall not exceed 100 mm throughout the height of columns. In addition, the overlapping length of column longitudinal bars in the flexible or weak storey, and in the two adjacent stories is required to be 30% more than that for the corresponding regular columns.

Nepal code (NBC-201, 1995) restricts the vertical irregularity using some thumb rules. There should be at least two lateral load resisting walls along the two principal directions at any level of the building.

Costa Rica Code FCEACR (1986) requires that all structural-resisting systems must be continuous from the foundation to the top of buildings, and stiffness of a storey must not be less than 50% of that of the storey below. Also, the weight of two adjacent stories must not differ by more than 15%, except at the roof level and at those stories located in the first 20% of the height of tall buildings. These clauses are intended to help reduce the adverse effects of the vertical irregularities in buildings.

To summarise, the vertical irregularity associated with strength and stiffness of multi-storey frames buildings are classified into the following two categories by the international codes: (a) soft/weak storey and (b) extreme soft and weak storey buildings. Majority of these codes prohibits the construction of extreme soft and weak storey buildings in seismic areas. However all the international codes reviewed here permit the other category of buildings

(soft or weak storey) with some restriction in analysis and design methods. Some of the international codes allow only dynamic analysis for design of such soft and weak storey buildings with appropriate model including masonry infill whereas others permit equivalent static analysis of a bare frame model with some MF to improve the design forces of the members of soft stores. Israel Standard SI 413 (1995) required to improve the design forces of members in not only the soft storey alone but also the adjacent storeys. The design codes published in the recent years recommended to increase the design forces of only the vertical members of the soft storey and not the horizontal members. The magnitude of the MF varies from code to code. Also, none of these international codes justify the magnitude of MF recommended in it.

2.3 PREVIOUS RESEARCH ON OGS BUILDING

Esteva (1992) conducted a parametric study to show the influence of OGS on the nonlinear dynamic response of shear-beam systems representative of buildings characterised by different number of stories and time periods. The stiffness of each storey is represented by an elastoplastic shear element whereas all the masses are assumed to be concentrated at the floor level. P- Δ effects are also considered in the analysis. This paper concludes that the response of soft ground storey buildings is very sensitive to the ratio of the mean over-strength factors at the upper storeys to that of the ground storey.

The behaviour of RC framed buildings with OGS subjected to seismic loads was reported by Arlekar *et al.* (1997). A case study of four storeyed OGS building is presented using equivalent static and response spectrum analysis method to show the differences between the response of OGS frame, bare frame and fully infilled frame. This infill walls are modelled as

panel elements for the linear elastic analyses carried out in this study. This paper shows that the stiffness of OGS can be less than 10% of the stiffness of the storey above (infilled) for both 220mm and 110mm thick brick wall. The drift and the strength demands in the first storey columns are reported to be very large for buildings with soft ground storeys. This paper concludes stating that it is difficult to provide such capacities in the columns of the first storey.

Scarlet (1997) evaluated equivalent static forces to be taken into account in the design of lateral load resisting elements of soft stories in a soft storey building based on energy approach. It was based on interpolation between two extreme situations: uniform structures and rigid structures supported by a soft storey. This paper calculated the value of MFs for buildings up to 20 storeys subjected to two types of loading patterns: (a) inverted triangular load and (b) concentrated load at the top. It also showed the variation of MFs for varying support conditions (fixed and elastic support). This study also recommended the use of MF's in the columns of soft storey and adjacent storey.

A newly constructed RC building with soft first storey collapsed during the 1995 Hyogoken-Nanbu earthquake. Nonlinear dynamic analysis of this building considering strength deterioration was conducted by Yoshimura (1997) to simulate how the building behaved and eventually collapsed during the earthquake. It was reported that the collapse of this building was unavoidable even for base shear strength of as much as 60% of the total weight.

Studies conducted by Fardis and Panagiotakos (1997) show that soft-storey effect is considerable only for higher percentage of infill weight compared to building weight and the

provisions of the Eurocode 8 (2003) for designing the weak storey elements against the effects of infill irregularities are found to be quite effective.

Fardis *et al.*(1999) observed that the bending of the columns in the more infilled storey (first storey of OGS building) under the lateral load is in a direction that is opposed to that of the less infilled storey (ground storey). Based on this observation, an alternate capacity design rule was proposed and validated through experimental testing. According to this rule, the demand on the beams in the first floor was also to be increased, depending on the capacity of the columns in the first storey.

Monotonic tests, on fully infilled and OGS frames having two bays and five storeys, were conducted by Selvakoodalingam *et al.* (1999). It was reported that the ultimate strength of OGS building is around 65% of that of fully infilled building.

The vulnerability and seismic reliability of two 10-storey, three-bay in-filled frames (a fully in-filled one and one with a soft ground storey) were derived by Dymiotis *et al.* (2001) and subsequently compared with values corresponding to the bare frame counterpart. This paper demonstrated a methodology for the probabilistic assessment of RC frames infilled with clay brick walls and subjected to earthquake loading.

Dolsek and Fajfar (2001) conducted nonlinear dynamic analysis of four storeyed uniformly infilled frame building. The study demonstrated that soft-storey mechanism can be formed even in uniformly infilled frame if the intensity of ground motion is above a certain limit.

Das and Nau (2003) have studied the response of RC buildings with different types of vertical irregularities including OGS. The result of this study showed that the formation of storey mechanism in OGS caused high ductility demands at ground-storey columns.

However, it was found that shear force is not a governing factor for initiating the collapse mechanism. The 'damage indices' calculated for OGS buildings were shown to have very high value that indicated severe damage beyond the threshold of repair. It was claimed that the stiffness and strength of masonry infill did not affect the value of damage indices of OGS buildings.

Kanitkar and Kanitkar (2004) investigated the seismic performance of OGS through linear static and nonlinear static analyses. Case studies of some of the buildings that failed in the 2001 Bhuj earthquake were considered for pushover analysis by Murty (2002). The mode of failure of such buildings is verified in this study.

Davis *et al.* (2004) concluded that the presence of masonry infill panels modifies the structural force distribution significantly in an OGS building. The total storey shear force increases as the stiffness of the building increases in the presence of masonry infill at the upper floor of the building. Also, the bending moments in the ground floor columns increase (more than two fold), and the mode of failure is soft storey mechanism (formation of hinges in ground floor columns).

Hashmi and Madan (2008) conducted performance-based seismic analyses of Indian code designed RC OGS framed buildings considering the effect of infill walls using NTHA and pushover analysis. The study concludes that the MF prescribed by IS 1893 (2002) for OGS building is adequate for preventing collapse and limiting the seismic damage.

Patel (2012) conducted both linear and nonlinear analyses for low-rise OGS framed building with infill wall stiffness as an equivalent diagonal strut model. The analysis results shows that a factor of 2.5 is too high to be multiplied to the beam and column forces of the ground

storey of low-rise OGS buildings. This study concluded that the problem of OGS buildings cannot be identified properly through elastic analysis as the stiffness of OGS building and a similar bare-frame building are almost same.

Fragility based seismic vulnerability of buildings with consideration of soft storey and quality of construction was demonstrated by Rajeev and Tesfamariam (2012) on three-, five-, and nine-storey RC frames designed prior to 1970s. A soft ground storey was modelled analytically by increasing the height of the columns of ground storey and not by introducing masonry infill. Probabilistic seismic demand model for those gravity load designed structures was developed, using the nonlinear finite element analysis, considering the interactions between soft storey and quality of construction. This paper concluded that the structural irregularities have significant influence on the PSDM parameters.

Favvata *et al.* (2013) studied the seismic performance of reinforced concrete (RC) frame structures with soft first floor (OGS) using Capacity Spectrum Method (ATC-40) and on the Coefficient Method (FEMA 356) procedures. The effects of the first floor irregularity on the RC frame structure performance stages at global and local level (limit states) are investigated. Results in terms of failure modes, capacity curves, inter storey drifts, ductility requirements and infill behaviour are presented. This study concludes that the global capacity of the structures is decreased due to the considered first floor morphology irregularities in comparison to the capacities of the regular structure. An increase of the demands for inter storey drift is observed at the first floor level due to the considered irregularities while the open ground building (pilotis type) led to even higher values of inter storey drift demands at the first storey.

Kumar (2013) studied on the behaviour of OGS buildings with different MFs proposed by different International codes in a probabilistic frame work using fragility curves (2000 SAC-FEMA method) and reported that application of MF only in the ground storey may not provide the required performance, rather it leads to more damage to the adjacent storeys.

There are many literatures available (Kaushik *et al.*, 2009; Tian and Symans, 2012; Sahoo and Rai, 2013 and many others) on the various techniques of retrofitting OGS buildings.

Review of the literatures on RC multi-storeyed framed buildings with OGS (soft and weak storey) are presented in this section. There are some studies on the wood-frame buildings with soft ground storey; OGS precast buildings where the stiffness and strength irregularity may arise from weak connections, etc., available in published literature, are kept outside the scope of the review presented here. Tables 2.3 summarise the MF recommended by various international codes and past literatures for OGS buildings

Table 2.3: MFs recommended by international codes/literatures

Code	Expression/Value for MF
IS 1893 (2002)	2.5
SI 413 (1995)	0.6R R=3.5 for low ductility R=5 for medium ductility
Bulgarian Seismic Code (1987)	3.0
Eurocode 8 (2003)	$\left[1 + \frac{\Delta V_{RW}}{\sum V_{ED}} \right]$
Scarlet (1997)	1.86 to 3.28 (for 6 storey to 20 storey)
Davis <i>et al.</i> (2004)	$(0.656 + 0.044N^{0.979} \beta^{-0.279}) \geq 1.0$
K_i - Lateral stiffness of i^{th} storey considered, R - Response reduction factor ΔV_{RW} – strength of infill in the storey above, $\sum V_{ED}$ – sum of design lateral force in the storey	

2.4 MODES OF FAILURE OF MASONRY INFILL

Different failure modes of masonry infilled frames have been proposed in literature (Thomas, 1953; Wood, 1958; Mainstone, 1962; Liauw and Kwan, 1983; Mehrabi and Shing, 1997; Al-Chaar, 2002) based on both experimental and analytical results. Some of these failure modes are associated with the failure of surrounding frame members and others are the failure of the masonry infill. In general, there are three basic failure modes for masonry infill found in literature: (a) corner crushing failure at the compressive corners of the infill, (b) shear cracking failure along the bedding joints of the brick work and (c) diagonal cracking of the slender infill wall. Apart from this failure may also occur due to out of plane effects where the damage takes place in the central region as a result of arching action of the infill wall.

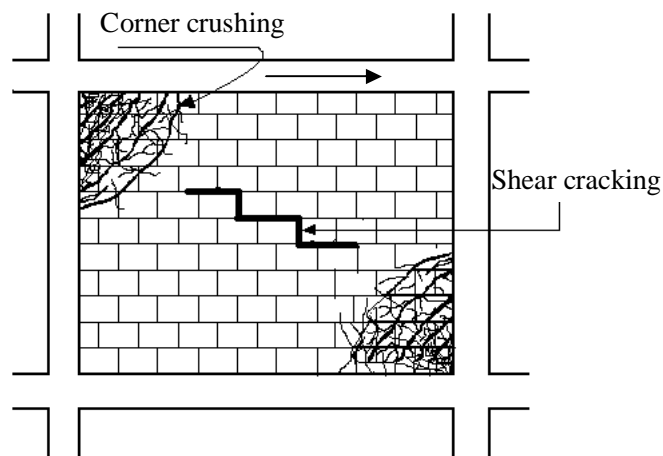


Fig. 2.1: Corner crushing and shear cracking modes of infill wall failure

The corner crushing mode of failure usually occurs through crushing of the infill in at least one of its corners, as shown in the Fig. 2.1. This mode of failure is most common and it takes place when the infill material has a low compressive strength.

Shear failure through the bed joints of a masonry infill wall may occur due to weak mortar joints as shown in Fig. 2.2. When mortar joints are weak in comparison to the masonry units, or when shear stress predominates over normal stress (low to medium aspect ratio), cracking usually occurs via de-bonding along the mortar joints (<http://framedinfill.org/resources/>). The cracking may be horizontal or along the diagonal, with a stepped pattern.

When the infill wall material has a high compressive strength, diagonal cracking may be observed connecting the two corners where contact between the infill and the frame takes place, as shown in Fig. 2.2. This is due to the tensile stress developed in perpendicular direction.

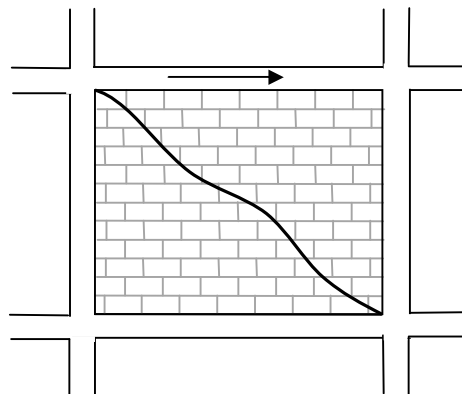


Fig. 2.2: Diagonal cracking mode of infill wall failure

The failure modes discussed above are for solid infill wall without any openings. The modes of failure of infill frames with openings are far more complex than those of solid infill panels. Experimental studies (Al-Chaar, 2002; Asteris *et al.*, 2011 and others) indicate that the behaviour of infilled frames with openings differs considerably from that of solid infill frames. The size and the location of the opening in infill wall have a significant effect on the overall behaviour of the global system of infilled frame.

2.5 PREVIOUS RESEARCH ON MODELLING OF INFILLED MASONRY

Several attempts have been made during last few decades to define the seismic behaviour of masonry infilled reinforced concrete frames and to develop methods for simulating the behaviour of infilled frame structure. Nonlinear modelling of structural elements is essential for this purpose. A lot of research efforts are found in literature to establish the nonlinear models of RC elements and there are many well known approaches to model RC beams and columns. However, the same is not true for the case of masonry infill. There are only few experimental and theoretical studies on masonry infill frames available in order to develop appropriate simulation models. This section, is therefore, devoted to report the review of published literature on the different models of masonry infill.

Different techniques proposed in the literature for modelling infill masonry can be categorized in to following two groups (a) micro-models and (b) macro-models. Micro-models are more detailed finite element models (FEMs) that consider the local effects of the wall. Macro-models includes simplified models (generally equivalent diagonal struts) based on physical understanding of the behaviour of infill masonry.

2.5.1 Studies on Micro Models

Micro-modelling is a modelling technique which considers the effect of mortar joints as a discrete element in the model. Micro-modelling is the most accurate analytical approach because it can take into consideration the masonry unit – mortar joint interface conditions, frame – infill wall interface conditions, constitutive relationships for the frame, brick, mortar and the interfaces, and several other modelling parameters. Dhanasekar and Page (1986), Mehrabi and Shing (1997), Stavridis and Shing (2010) and Koutromanos *et al.*

(2011) conducted works in this field. A detailed review of the literatures on micro models can be available in Sattar (2013) and in the web link <http://framedinfill.org/resources>.

2.5.2 Studies of Macro Models

Macro-models are based on a physical understanding of the behaviour of each infill panel as a whole. The infill panel is typically represented by a single global structural member, most often by equivalent diagonal struts. It is always convenient to use the macro models for infill wall when behaviour of multi-storeyed infilled framed building is primary focus of the analysis. An extensive literature review was carried out on the '*macro models*' for modelling infill wall, as the present study deals with the effect of OGS on the seismic response of multi-storeyed building. This section presents a brief report on the previous works in this area.

At the macro level, it has been found that the infill panel separates from the surrounding frame at relatively low lateral load levels, after which contact between the frame and infill was limited to the two opposite compression corners (Mehrabi and Shing, 2002). Experimental and conceptual studies have suggested that a diagonal strut with the appropriate geometrical and material characteristics can be used to model the response of composite infilled frame structures. This approach is known as the equivalent diagonal strut approach.

Holmes (1961) modelled the infill wall as an equivalent pin-jointed diagonal strut with the same elastic material properties as masonry, the same thickness as the infill panel, and a width equal to one third of the length of the strut. Failure strength of the strut was predicted

from an assumed ultimate strain. This model was based on results of the monotonic tests on masonry infilled steel frames conducted by Polyakov (1960).

Researchers have refined this model for computing the characteristics of the struts intended to represent the masonry infill. Smith (1962), Mainstone and Weeks (1970), and Mainstone (1971), among others, proposed methods for calculating the effective width of the diagonal strut considering various parameters such as the frame/infill wall relative stiffness, dimensions of the infill wall and the columns of the surrounding frame. Smith (1962) developed a chart which relates the effective width of the strut to the aspect ratio (L_w/h_w) of the infill panel.

Smith and Carter (1969) developed analytical techniques to calculate the effective width and the ultimate failure load of the equivalent strut. This approach considered a variable width for the equivalent strut that decreases as length of contact decreases. Length of contact decreases if the stiffness of the frame relative to the masonry wall decreases or if the load in the equivalent strut increases. The relative stiffness of the infill wall is expressed as a non-dimensional variable λh as follows:

$$\lambda h = h \times \sqrt[4]{\frac{E_w t_w \sin 2\theta}{4E_c I_c h_w}} \quad (2.2)$$

Here, E_w = elastic modulus of the infill wall, E_c = elastic modulus of the column in the bounding frame, I_c = moment of inertia of the column, h_w = clear height of infill wall, h = height of column between centrelines of beams, t_w = thickness of infill wall, d = diagonal length of infill wall, θ = slope of the infill wall diagonal to the horizontal. Refer Fig. 2.3 for the detailed dimensions.

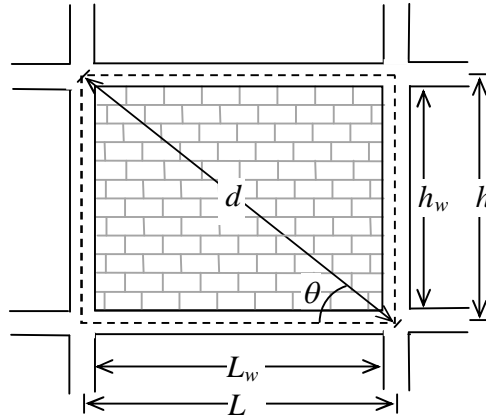


Fig. 2.3: Parameters relevant for equivalent strut modelling

The width of the equivalent strut is expressed as the length of contact (αh) which is inversely proportional to the relative stiffness of the infill wall (λh) as follows

$$\frac{\alpha}{h} = \frac{\pi}{2\lambda h} \quad (2.3)$$

Mainstone (1971) proposed following two equations (Eqs. 2.4-2.5) defining the width of the equivalent strut (w) as a function of relative stiffness of the infill wall (λh), based on the experiments conducted on masonry infilled frames.

$$\frac{w}{d} = 0.16 \lambda h^{-0.3} \quad (2.4)$$

$$\frac{w}{d} = 0.175 \lambda h^{-0.4} \quad (2.5)$$

Liauw and Kwan (1984) developed a semi-empirical equation, as shown in Eq. 2.6, to compute the width of the strut as the function of λh . This equation predicts a bigger equivalent width compared to Eq. 2.5.

$$\frac{w}{h \cdot \cos \theta} = \frac{0.95}{\sqrt{\lambda h}} \quad (2.6)$$

All of these models define the effective width of the strut, which in turn is used to compute the stiffness and ultimate strength of the infill panel. However, they do not specifically define the force-displacement behaviour of the strut. One of the early attempts to define the complete force-displacement behaviour of the infill panel was conducted by Klingner and Bertero (1976). This study proposed a nonlinear hysteretic response for the equivalent diagonal strut model based on the findings of the experiments conducted on masonry infilled RC frames. This model considers the strength degradation and reloading stiffness deterioration.

Saneinejad and Hobbs (1995) also tried to predict the nonlinear behaviour of the infill panel and proposed a force-deformation model for equivalent diagonal strut that considers low ductility, cracking and crushing load, aspect ratio of the infill wall and beam to column strength/stiffness ratio. The area of the equivalent strut is calculated from the diagonal load at failure. This approach is based on ultimate strength of the equivalent strut. This bilinear model predicts the initial stiffness (K_e), cracking load (F_{cr}), crushing load (F_{max}), stiffness and displacement (cap) at the peak load, as shown in Fig. 2.4a. However, this model does not define the post-peak response of the infill. This bilinear model was developed based on the experimental and finite element analysis results on steel frames with masonry infill.

Continuing to improve understanding of strength and nonlinear behaviour of the infilled systems, Zarnic and Gostic (1997) proposed an empirical equation, which was later modified by Dolsek and Fajfar (2008), to compute the shear ultimate strength of the masonry infill panel.

Specifically, Dolsek and Fajfar (2008) defined a tri-linear response of the single strut model including elastic, hardening, and post-capping branch, as shown in Fig. 2.4b. They arbitrarily assumed 1:5 ratios for post-capping slope of the infill response to the infill initial stiffness and assumed the cracking load as 60% of the ultimate strength from the Zarnic and Gostic (1997) predictions. They also assumed that the capping displacement occurs at 0.2% drift ratio. For the initial stiffness, they used an equation proposed in Pinto A. V (1996) - ECOEST-PREC 8 Report. This equation predicts the stiffness of the infill as the function of shear modulus and configuration of the infill panel. Flanagan and Bennett (1999) used a piecewise-linear equivalent strut to model infill and proposed an analytical procedure to calculate the strength of the infill, based on experimental results on steel frames with clay tile infill walls.

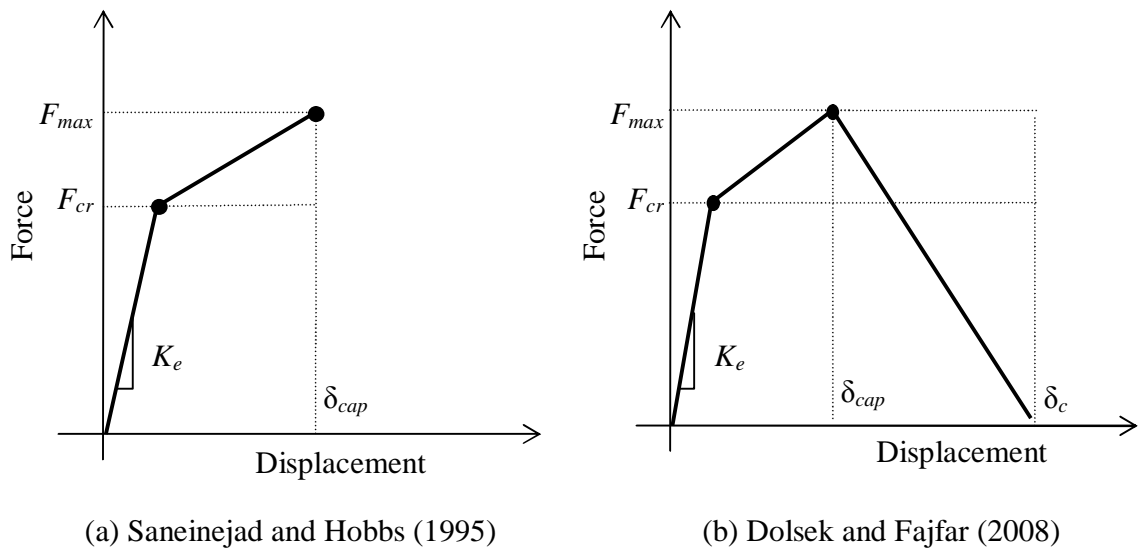


Fig. 2.4: Schematic force-displacement response of the infill strut model

Celarec *et al.* (2012) used infill wall model based on the approach developed by Panagiotakos and Fardis (1996). The first branch of the quadrilinear force-displacement

envelope curve corresponds to the linear elastic behaviour up to the first cracking of the infill with a stiffness of

$$K_{el} = \frac{G_w A_w}{h_w} \quad (2.7)$$

where, A_w is the cross-sectional area of the infill panel, G_w is the elastic shear modulus of the infill material, and h_w is the clear height of the infill panel. The shear cracking strength is given by

$$F_{cr} = \tau_{cr} A_w \quad (2.8)$$

where, τ_{cr} is the shear stress at cracking stage. The second branch of the envelope runs from the first cracking point up to the point of maximum strength, which is estimated as

$$F_{max} = 1.30 \cdot F_{cr} \quad (2.9)$$

The corresponding displacement is evaluated assuming secant stiffness up to the maximum strength, by Mainstone's formula (1971), i.e. assuming an equivalent strut width equal to

$$b_w = 0.175(\lambda_h h_w)^{-0.4} d_w \quad (2.10)$$

where, d_w is the clear diagonal length of the infill panel, and the coefficient λ_h is defined by the expression

$$\lambda_h = \sqrt{\frac{E_w t_w \sin(2\theta)}{4E_c I_c h_w}} \quad (2.11)$$

where E_w and E_c are the Young's modulus of the infill walls and of the RC frame, respectively, $\theta = \tan^{-1}(h_w/l_w)$ is the inclination of the diagonal with respect to horizontal plane, H and L are, respectively, the height and the length of the infill panel, t_w is the thickness of the masonry infill and I_c is the moment of inertia of the RC column.

Considering, Eqs. (2.10) & (2.11), the secant stiffness which targets the maximum strength of the infill can be calculated from the expression:

$$K_{\text{sec}} = \frac{E_w b_w t_w}{\sqrt{L^2 + H^2}} \cos^2 \theta \quad (2.12)$$

The third branch of the envelope is the post-capping degrading branch, which runs from the maximum strength to the residual strength. Its stiffness depends on the elastic stiffness, and is defined by means of the parameter α as:

$$K_{\text{deg}} = -\alpha_{\text{cap}} \cdot K_{\text{el}} \quad (2.13)$$

where, α_{cap} is the ratio between post-capping stiffness to the elastic stiffness.

There is a lack of data regarding the estimation of the parameter α_{cap} . However, in the literature (e.g. Panagiotakos and Fardis, 1996) it has been suggested that α_{cap} should be within the range of values between 0.005 (less brittle) and 0.1 (more brittle). In the case of the presented study, α_{cap} was assumed to have a value of 0.05 for all the masonry infills (as used by Celarec *et al.*, 2012). The fourth branch of the envelope is the horizontal branch corresponding to the residual strength, which was conservatively assumed to be equal to 2% of the maximum strength.

Panagiotakos and Fardis (1996) have suggested that ' α_{cap} ' should be within the range of values between 0.005 and 0.1, although the upper value corresponds to a brittle failure. In the present study, α_{cap} is assumed to have a value of 0.05 for all the masonry infill. The fourth branch of the envelope is the horizontal branch corresponding to the residual strength, which is conservatively assumed to be equal to 2% of the maximum strength. The typical quadrilinear force-displacement relationship of the diagonal struts (in compression), measured in the axial direction is shown in Fig.2.5. This equivalent diagonal strut approach can model the global force-displacement behaviour of the infilled frame

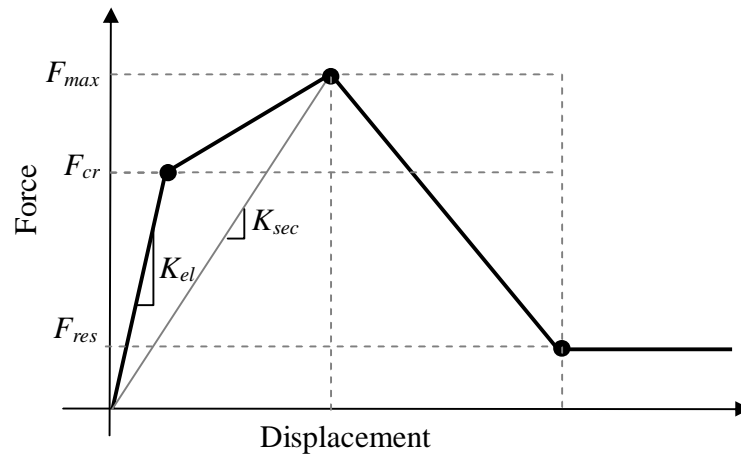


Fig. 2.5: Force-displacement relationship of the diagonal struts used by Celarec *et al.* (2012)

2.6 PREVIOUS RESEARCH ON SEISMIC RISK ASSESSMENT

In the past few decades, failure of structures has exposed the weakness in current design procedures of building structures and has shown the importance to improve the current design practice. Seismic risk analysis has become more popular due to recent developments in earthquake engineering to ensure risk management in accordance with building codes and to provide an insight into the performances of building structures under seismic excitations. Development of seismic risk assessment for structures is undergoing drastic changes triggered by a variety of reasons. However, the current trend of procedure for seismic risk assessment of buildings structures requires identification of the seismic hazard, analysis of structural fragilities, and calculation of limit state probabilities. The structural fragility curves are said to be the key component while quantifying the seismic risk assessment. Fragility curves are usually defined as the probability of exceeding a specific limit state of building for a given level of ground motion intensity.

Broadly, generation of fragility curves can be divided into three approaches namely (i) professional judgment, (ii) Empirical based (iii) Analytical based (Lupoi, 2005).

Professional judgement is based on the experience; ATC-13 (1985) presents expert-opinion on earthquake damage and loss estimates for industrial, commercial, residential, utility and transportation facilities in California. It is one of the first applications of fragility modelling to civil infrastructure subjected to earthquake load. Empirical based fragility curves are based on damage data associated with experimental tests or past earthquakes. Singhal and Kiremidjian (1998), Basoz and Kiremidjian (1999) and Shinozuka *et al.* (2000) have developed empirical fragility curves based on damage state of structure from past earthquakes/experimental tests. Lupoi (2005) has developed empirical fragility curves for free standing equipment based on experimental test and regression analysis. Analytical based fragility curves are based on numerical analysis for particular system with well-defined limit states. Several authors in the past used analytical fragility curves to assess the performance of buildings for various limit states. Following section summarizes the work done on seismic risk assessment using fragility curves.

Hwang and Jaw (1990) proposed a procedure to calculate fragility curves taking into account uncertainties in ground-motion and structure. Latin hypercube sampling technique was used considering these uncertainties to construct the samples of structural systems. NTHA were performed for each sample and response from each analysis was recorded and used to draw fragility curves. Five limit states representing various degrees of structural damages were defined to draw fragility curves as a function of peak ground acceleration.

Singhal and Kiremidjian (1996) developed fragility curves for low, mid, and high rise RC frames that were designed using seismic provisions. Monte Carlo simulations were considered to quantify the uncertainties in structural capacity and demand. NTHA were performed for stochastically generated frame models, with randomly paired simulated ground

motion records. Structural demand versus seismic intensity relationships were determined from so-called stripe analyses. The structural demand at each seismic intensity level was assessed using ground motions scaled to that particular intensity level and was represented by a lognormal probability density function. The lognormal model of demand was then utilized to compute fragility estimates (for the performance limits considered) at that particular level. Finally, fragility curves were represented by lognormal cumulative distribution functions that were fit to individual fragility estimates, computed at several seismic intensity levels. Singhal and Kiremidjian (1998) later presented a Bayesian method for updating the fragility curves which they had developed earlier for low-rise RC frames and estimating confidence bounds on those fragility curves, by using the observed building damage data from the 1994 Northridge earthquake.

Mosalam *et al.* (1997) studied on behaviour of low-rise Lightly Reinforced Concrete (LRC) frames with and without masonry infill walls using fragility curves. Adaptive nonlinear static pushover analyses were performed for the frame models. Monte Carlo simulation was used to generate the frame models considering uncertainties in material properties. Idealised single-degree-of-freedom (SDOF) systems developed from the pushover analysis results were employed in further analyses. Each model was paired with each ground motion and structural responses of these SDOF models were used to determine the fragility curves for different performance limits. Based on the obtained fragility curves, it was concluded that adding masonry infill walls to low-rise LRC frame buildings significantly reduces the likelihood of seismic damage.

Shinozuka *et al.* (2000) developed empirical and analytical fragility curves for bridges. The observed bridge damage data from the 1998 Kobe earthquake was used for developing

empirical fragility curves. Analytical fragility curves were developed from NTHA of stochastically generated models of two bridges, taking into account the uncertainty in material properties. Both fragility curves were represented by lognormal distribution functions with the distribution parameters estimated using the maximum likelihood method. Confidence intervals for the distribution parameters were also provided.

Porter *et al.* (2001) proposed an assembly-based vulnerability framework for assessing the seismic vulnerability of buildings. The proposed approach differs from usual fragility analysis discussed in literature. This approach accounts for the detailed structural and non-structural design of buildings. This is probabilistic analysis that considers the uncertainty associated with ground motion, structural response, assembly fragility, repair cost, repair duration and loss due to downtime. It is reported that the effectiveness of alternative retrofit scheme can be examined using this approach.

Cornell *et al.* (2002) developed a probabilistic framework for seismic design and assessment of structures in a demand and capacity format addressing the uncertainties in hazard, structural, damage, and loss analyses. Structural-demand versus seismic-intensity relationships were determined from a so-called cloud analysis (i.e. NTHA using accelerograms not scaled to the same intensity levels). The structural demand was assessed using a suite of ground motions and the median structural demand was represented by a log-linear function of seismic intensity. The structural demand was assumed to be distributed lognormally about the median with constant logarithmic standard deviation. This framework provided the probabilistic basis for the design recommendations that resulted from the SAC project.

Erberik and Elnashai (2004) studied the performance of mid-rise-flat-slab RC building with masonry infill walls using fragility curves as per the same methodology adopted by Singhal and Kiremidjian (1996). Uncertainties are considered by stochastically generated building models paired with each ground motion records rather than random sampling. Nonlinear static pushover analyses were carried out to identify performance limits for developing fragility curves.

Kim and Shinozuka (2004) developed fragility curves of two sample bridges before and after column retrofit for southern California region. Monte Carlo simulation was performed to study nonlinear dynamic responses of the bridges. Peak ground acceleration (PGA) was considered as intensity measure for developing fragility curves which is represented by lognormal distribution function with two parameters. It was found that the fragility curves after column retrofit with steel jacketing shows excellent improvement (less fragile) compared to those before retrofit.

Rossetto and Elnashai (2005) developed fragility curves for low-rise code designed RC frames with masonry infill walls for Italy region. Structural demand versus seismic intensity relationships was determined using the methodology given by Erberik and Elnashai (2004). Capacity spectrum method with adaptive pushover analysis was employed for estimating drift demand. A response surface equation was fit to the demand versus intensity data. Fragility curves were then developed using a larger data set at refined seismic intensity levels generated through a re-sampling process from the response surface equation. Confidence bounds were also identified on the fragility curves.

Kwon and Elnashai (2006) developed fragility curves for low-rise gravity load designed (GLD) RC frames. However, the problematic reinforcement details, such as the inadequate joint shear capacity and the insufficient positive beam bar anchorage, were not considered. The finite element model of the three-storey frame was validated using experimental data from the shake table tests (Bracci *et al.*, 1995). The methodology given in Erberik and Elnashai (2004) was followed to derive the fragility curves. The frames were modelled with randomly generated material strength parameters. The statistical analysis of structural demand indicated that the effect of material uncertainty is negligible with respect to that of ground motion uncertainty. The comparison of fragility curves developed using different sets of ground motions revealed that the fragility curves depend considerably on the choice of the ground motions.

Ramamoorthy *et al.* (2006) developed fragility curves for low-rise RC frames. Cloud analysis was carried out based on NTHA to develop the structural demand. A bilinear function was used here to represent the median demand instead of a linear function given in Cornell *et al.* (2002).

Kircil and Polat (2006) developed fragility curves for mid-rise RC buildings in Istanbul region designed according to the Turkish seismic design code. Typical buildings with different storeys were considered ranging from 3 to 7 storeys. Twelve artificial ground motions were used to perform incremental dynamic analyses to determine the yielding and collapse capacity of each sample building. This study proposes an equation for immediate occupancy (*IO*) and collapse prevention (*CP*) performance levels as a function of number of storeys and concluded that these equations may be used for the preliminary evaluation of

mid-rise RC framed structures designed with 1975 version of the Turkish seismic design code.

Nielson and Desroches (2007) developed fragility curves analytically for nine classes of bridges common to the central and south-eastern United States. 3-D analytical models of bridges including the contribution of multiple bridge components were considered for NTHA. Bridge components were columns, fixed bearings, expansion bearings, and abutments in both the longitudinal and transverse directions. A suite of 96 synthetic ground motions were used for NTHA. Probabilistic seismic demand model was estimated using Cornell *et al.* (2002), where the median of the seismic demand is assumed to be a power function of the selected intensity measure (*IM*). Dispersion in intensity measure and capacity were considered. Fragility curves were developed for each component separately (columns, fixed bearings, expansion bearings, and abutments) and the results concluded that multi span steel girder bridges are the more vulnerable than single-span bridges.

Lagaros (2008) conducted fragility analyses for two groups of reinforced concrete buildings. The first group of structures was composed of fully infilled, weak ground storey and short columns frames and the second group consists of building frames designed with different values of behavioural factors. Four limit state fragility curves were developed on the basis of nonlinear static analysis and 95% confidence intervals of the fragility curves were calculated. This study concludes that the probability of exceedance of the slight damage state for the design earthquake (0.30g) is of the same order for first group of building frames. On the other hand, it was found that the probability of exceedance for the fully infilled frame is one and three orders of magnitude less than that of the weak ground storey and short column

frames for the moderate and complete damage states, respectively. This study shows that the behaviour factor significantly affect the fragility curves of the buildings.

Guneyisi and Altay (2008) developed fragility curves for high-rise RC office building retrofitted with fluid viscous dampers for Istanbul region. Three different scheme of viscous dampers (effective damping ratios as 10%, 15% and 20%.) were used. For fragility analysis, a suit of 240 artificially generated ground motions compatible with the design spectrum was used to represent the variability in ground motions. Nonlinear dynamic responses of the structures before and after retrofit were studied. Slight, moderate, major, and collapse damage states were considered to express the condition of damage. The fragility curves, represented by lognormal distribution functions with two parameters, developed in terms of peak ground acceleration (*PGA*), spectral acceleration (S_a) and spectral displacement (S_d). Comparing the fragility curves this study concludes that viscous damper is an excellent retrofit scheme that improves the performance of buildings considerably.

Celik and Ellingwood (2010) studied the effects of uncertainties in material, structural properties and modelling parameters for gravity load designed RC frames. It was found that damping, concrete strength, and joint cracking have the greatest impact on the response statistics. However, the uncertainty in ground motion dominated the overall uncertainty in structural response. The study concluded that fragility curves developed using median (or mean) values of structural parameters may be sufficient for earthquake damage and loss estimation in moderate seismic regions.

Ozel and Guneyisi (2011) developed fragility curves for mid-rise RC building retrofitted using eccentric steel braces. Six storey mid-rise RC building designed with 1975 version of

the Turkish Seismic Code was chosen for the study. Four limit states (namely slight, moderate, major and collapse) were considered and pushover analyses were performed to identify performance limits for these limit states. Probabilistic seismic demand model (PSDM) was considered as power law as per Cornell *et al.* (2002) and developed from the regression analysis. A two-parameter lognormal distribution function was used to represent the fragility curves. This study concluded that fragility curves after retrofitting with steel braces show good performance (less fragile) compared to those before retrofit.

Tavares *et al.* (2012) developed the fragility curves analytically for five bridge classes commonly found in Quebec, Canada. Each bridge class was represented by 3-D nonlinear analytical models subjected to a suite of bidirectional ground motions for eastern Canada region. Slight, moderate, extensive, and complete limit states for bridge systems were considered for the development of fragility curves. To consider uncertainties, Latin Hypercube Sampling (LHS) was used to derive statistically significant bridge samples from the random variables. Probabilistic seismic demand model (PSDM) was considered as power law model of Cornell *et al.* (2002) which was developed from the regression analysis on the computed responses. Dispersions in intensity measures and the quality in construction were considered in this study. It was concluded that concrete-girder bridges are found to be more vulnerable than steel-girder bridges and continuous-span bridges are more vulnerable than the simply supported span bridges.

Haldar *et al.* (2012) studied the seismic performance of Indian code designed RC framed buildings with and without masonry infill walls using fragility curves. HAZUS methodology along with nonlinear static analysis was used to identify performance limits. This study

concludes that infill walls result in a significant increase in the seismic vulnerability of RC frames and their effects needs to be properly incorporated in design codes.

Fragility based seismic vulnerability of buildings with consideration of soft storey and quality of construction was demonstrated by Rajeev and Tesfamariam (2012) on three-, five-, and nine-storey RC frames designed prior to 1970s. A soft ground storey was modelled analytically by increasing the height of the columns of ground storey and not by introducing masonry infill. Probabilistic seismic demand model for those gravity load designed structures was developed, using the nonlinear finite element analysis, considering the interactions between soft storey and quality of construction. This paper concludes that the structural irregularities have significant influence on the Probabilistic Seismic Demand Models (PSDM).

An extensive literature review in this area found that majority of the literature presented work related to fragility assessment of buildings. There are only few literatures found on seismic risk assessment based on fragility and seismic hazard analyses.

2.7 REVIEW ON RELIABILITY BASED STRUCTURAL DESIGN

Most of the current codes and standards for seismic design are developed using reliability based methodology. The first part of this section describes the reliability analysis methodologies used in different codes. It also discusses the reliability criteria recommended in different international codes. Finally this section presents, a review on previous studies on the reliability based seismic design.

2.7.1 Reliability Analysis Methodologies

The reliability of a system is the probability that it will perform its intended function, under the operating conditions considered, in the considered time period (Krishnan, 2006):

$$\text{Reliability} = 1 - \text{Probability of failure} (P_f) \quad (2.14)$$

The building frames may be considered to be the ‘system’ whereas ‘Failure’ could refer to the frames reaching a defined level of non-performance (such as yielding). This non-performance is defined by a ‘limit state function’ (LSF) or ‘performance function’.

Generally, the limit-state indicates the margin of safety between the resistance and the load of structures. The limit-state function, $g(\cdot)$, and probability of failure, P_f , can be defined as:

$$g(X) = R(X) - S(X) \quad (2.15)$$

$$P_f = P[g(\cdot) < 0] \quad (2.16)$$

Where, R is the resistance and S is the loading of the system. Both $R(\cdot)$ and $S(\cdot)$ are functions of random variables X . The notation $g(\cdot) < 0$ denotes the failure region. Likewise, $g(\cdot) = 0$ and $g(\cdot) > 0$ indicate the failure surface and safe region, respectively.

The reliability index indicates the distance of the mean margin of safety from $g(\cdot) = 0$. Fig. 2.1 shows a geometrical illustration of the reliability index in a one-dimensional case. The idea behind the reliability index is that the distance from location measure μ_g to the limit-state surface provides a good measure of reliability. The distance is measured in units of the uncertainty scale parameter σ_g . The shaded area of Fig. 2.6 identifies the probability of failure. The probability of failure is

$$P_f = \int_{-\infty}^0 f_g(g) dg \quad (2.17)$$

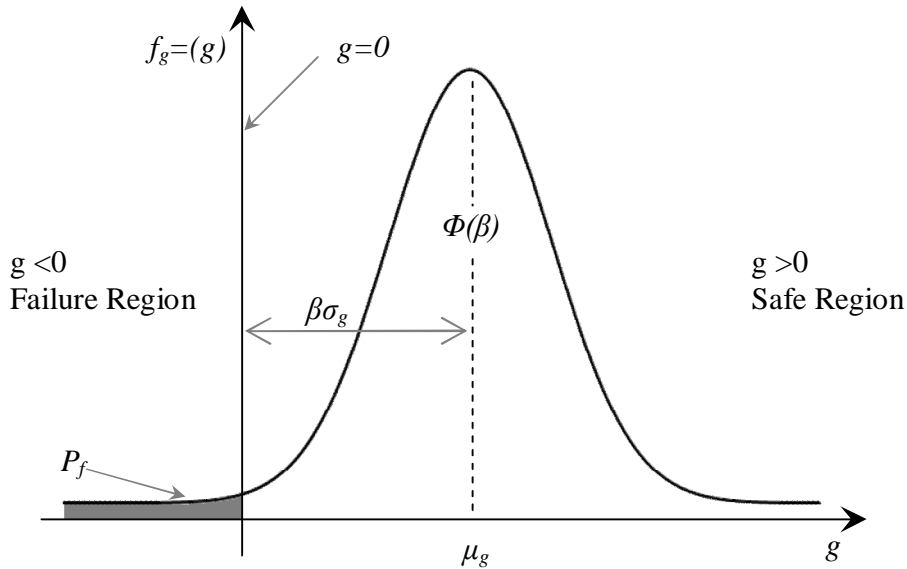


Fig. 2.6: Probability Density for Limit-state $g(\cdot)$

The reliability index, β , was defined by Hassofer and Lind (1974) as the shortest distance from the origin to the LSF, in a standard normal variable space. This form of defining β makes it independent of the form of the limit state function. β is commonly used in code calibration work (Cornell, 1969). This measure of reliability can be related to a nominal probability of failure, P_f :

$$\beta = -\phi^{-1}(P_f) \quad (2.18)$$

A number of methods exist to estimate probability of failure. These include simulation, first and second order reliability methods and the response surface method. In the first order reliability method (FORM) the failure surface is linearised (taking only the first term of a Taylor's series expansion) at the design point. The design point is identified by optimisation

– through the HLRF (Hassofer Lind Rackwitz Fiessler) algorithm (Liu and Der Kiureghian, 1991) – to find the minimum distance to the failure surface. This method requires details of the distributions, the performance function and its rate of change with respect to each random variable (often computed numerically, for example, by the central difference method). The second order reliability method (SORM) is used when the performance function is more non-linear. Here a second order Taylor’s series expansion is used at the design point – *i.e.*, a quadratic surface. In response surface method, the performance function is first fitted using deterministic analysis by varying each random variable. All these reliability methodologies approximate the failure function.

In the simulation method the integral is solved using, for example, Monte Carlo methods – by generating instances of the random variables probabilistically and performing deterministic checks for failure. Monte Carlo simulation is an iterative procedure, the probability of failure, P_f , being estimated as

$$P_f = \frac{N_f}{N} \quad (2.19)$$

where N_f is the number of failures in N iterations. As the number of iterations increases, the estimated probability of failure converges. The convergence of P_f is observed from the reduction of the coefficient of variation of this estimated P_f , $CoV(P_f)$. This is defined in terms of the estimated probability of failure, P_f and the number of iterations, N (Melchers, 1999) as:

$$CoV(P_f) = \sqrt{\frac{(1 - P_f)}{N P_f}} \quad (2.20)$$

Although it is computationally intensive, simulation can overcome many of the shortcomings of the analytical methods. The variance of the estimated probability of failure can be reduced by a number of methods. Importance sampling is a method of variance reduction that involves sampling points only in the region of failure – thus reducing the computational intensity. However, this requires some prior knowledge of the probability of failure. Also, erroneous selection of the sampling function can result in serious errors in the estimated probability of failure.

2.7.2 A Review on Reliability in Conventional Design

Probability based limit states design is the basis of most new structural design standards and specifications worldwide. Structural reliability methods provide tools for quantifying the safety levels implied by codes and have been utilised in setting the nominal (or characteristic) loads), load factors and load combinations, and resistance or material factors found in specifications for building designs.

Traditional earthquake design practice has been to include the earthquake effects in load combinations, as with other loads. In the first set of general probability based load combinations for buildings and other structures the following load combinations for earthquake design were developed using first order reliability methods:

$$\phi R_n = k_1(D) + k_2(EQ) + k_3(L) \quad (2.21)$$

$$\phi R_n = k_4(D) + k_5(EQ) \quad (2.22)$$

Where, ϕ is the resistance factor, R_n is the nominal strength, D is the dead load, EQ is the earthquake load, L is the live load and k_i are the load factors. The load factors are different for different codes.

The first generation of probability based limit state design codes are based on a code calibration process in which (i) the reliabilities of member designed by existing conventional earthquake-resistant design practise were determined and (ii) these reliabilities set the benchmarks for new criteria. The basic assumption in this process is that traditional design procedures have provided acceptable structures (in terms of reliability) for different combinations of loads. For load combinations involving earthquake forces, these assumptions are arguable.

Using advanced first order reliability analysis (Melchers, 1987), it was found that the reliability index, β (50 year basis), fell within the range of 1.75-2.25 for structures with periods between 0.5s and 1.0s. For a building designed with only gravity load combinations the reliability index, β fell in the range of 2.50-4.00.

These studies without exceptions lead to a conclusion that the apparent limit state probability when the design is governed by the seismic load provisions is less than when the design is governed by one of the gravity load combinations.

2.7.3 Previous Researches on Reliability based Seismic Design

An extensive literature review did not reveal any published work on the reliability based design of OGS buildings. However, there are many previous works on reliability based seismic design of RC framed building reported in literature. These literatures have been reviewed to gain insight of this subject. This section summarizes the previous research works on reliability based seismic design.

Ellingwood (1994) evaluated the role of structural reliability methods in providing an improved basis for code design provisions. It also describes the treatment of uncertainty in code safety checking. Prospects for improving current earthquake-resistant design procedures based on a more rational probability-based treatment of uncertainty are assessed.

Wen (1995) presented the reliability evaluation and comparison of buildings designed in accordance with different international codes. It also discussed the development of design procedures in international codes based on multi-level, probabilistic structural performance criteria.

Collins *et al.* (1996) proposed a reliability-based seismic design procedure for building structures. An equivalent system methodology and uniform hazard spectra are used to evaluate structural performance. The performance criteria are expressed in probabilistic terms, and deterministic design-checking equations are derived from these criteria. The design-checking equations incorporate design factors (analogous to load and resistance factors) which account for the uncertainties in different relevant parameters. Chen and Collins (2001) extended the procedure developed by Collins *et al.* (1996) for asymmetric building structures that accounts for the torsional effects. The only required change here is to use three-dimensional static pushover analyses to calibrate the parameters of the equivalent SDOF model.

A probabilistic method for reliability evaluation of plane frame structures with respect to ultimate limit state is proposed by Val *et al.* (1997). This method is based on finite element structural model and FORM. Implementation of the FORM for nonlinear analysis of RC

structures is considered. A sensitivity analysis is performed to evaluate the influence of uncertainties associated with structural model on structural reliability.

Wen (2001) proposed a reliability-based framework for structural design considering large uncertainty in loading and complex building behaviour in the nonlinear range. Minimum lifecycle cost criteria were proposed to arrive at optimal target reliability for performance based design under multiple natural hazards. The effects of structural configurations and ductility capacity amongst others are investigated. A uniform-risk redundancy factor is proposed to ensure uniform reliability for structural systems of different degree of redundancy.

Ellingwood (2001) highlighted the importance of the probabilistic analysis of building response in understanding the perspective of building behaviour. This paper outlined a relatively simple procedure for evaluating earthquake risk based on seismic fragility curve and seismic hazard curve. This study shows the importance of inherent randomness and modelling uncertainty in forecasting building performance through a building fragility assessment of a steel frame.

There are many past literatures (Nie and Ellingwood, 2005; Khatibinia *et al.*, 2013; Kermani and Fadaee, 2013; etc.) available on reliability based seismic analysis using different alternative methods.

2.8 SUMMARY

This chapter presents the international design code perspective on the OGS buildings. All the international codes recognise OGS building as a potentially vulnerable vertically irregular

building that requires special attention for designing. Some of the codes do not even permit the construction of such buildings in seismic areas. Other codes recommend different MF for designing the columns of OGS buildings. There is large disparity in the MF values suggested by international design codes.

Past earthquakes demonstrated the vulnerability of OGS frames. There is no literature found on the quantification of seismic forces in the ground storey column of OGS frames. Many previous literature (Fardis and Panagiotakos, 1997, Fardis *et al.* 1999) concluded that the MFs proposed by the international codes lack theoretical background. Some of the literatures reported research effort to improve the MFs given in the international codes. However, MFs recommended through deterministic approach by most of the literatures are empirical in nature and do not have rational basis. Uncertainties associated with earthquake loading and structural properties are not considered in these studies.

A number of studies are available on the probabilistic fragility analysis of OGS buildings that establishes the poor performance of OGS buildings. However, these research efforts are not extended to the formulation of MFs required for performance-based seismic design of OGS buildings.

CHAPTER 3

METHODOLOGY

3.1 INTRODUCTION

The study in this thesis is based on risk assessment of OGS buildings considering uncertainties in load and resistance. This chapter explains the detailed procedure of seismic risk assessment in a probabilistic framework using fragility and seismic hazard analysis. Defining limit state performance levels are necessary for fragility analysis of buildings. The second part of the chapter defines the selected building performance levels. Finally, this chapter briefly explains the Latin Hypercube Sampling techniques used in the present study for modelling uncertainties.

3.2 EARTHQUAKE RISK ASSESSMENT

The methodology reported by Ellingwood (2001) for estimation of seismic risk involves three parts. First part is the identification of the seismic hazard, $P [A = a]$, described by the annual probability of occurrence of specific levels of earthquake motion. The seismic hazard at a site is usually represented through a seismic hazard curve, $G_A(x)$ which is a plot of $P [A = a]$ versus the level peak earthquake acceleration (a) expressed in terms of gravitational acceleration (g). Second part is the analysis of global response of the structural system subjected to different levels of earthquake motions. The response analyses of the structure are carried out by conducting NTHA for different earthquakes, and the response is expressed in terms of maximum inter- storey drift at any storey. Third part is the calculation of limit state probabilities of attaining a series of (increasingly severe) limit states, LS_i , through the Eq. (3.1).

$$P[LS_i] = \sum_a P[LS_i | A = a]P[A = a] \quad (3.1)$$

The step by step procedure for estimation of seismic risk in a framed building is explained as follows (also shown schematically in Fig. 3.1):

- i) Assemble a suite of 'N' number of ground motions relevant to the area of interest. This suite should represent a broad range of values for the chosen intensity measure.
- ii) Generate 'N' number of statistical samples of the subject structure. These samples should be generated by sampling on various modeling parameters which may be deemed significant (e.g. damping ratio, material strength). This can be done using different sampling techniques. Thus, N statistically significant yet nominally identical building samples are made.
- iii) Perform a full NTHA for each ground motion for the subject structure. Key responses should be monitored throughout the analysis.
- iv) For each analysis, peak responses are recorded and plotted versus the value of the intensity measure. A regression of this data is then used to estimate the constants of PSDMs and fragility curves are developed as explained later in Section 3.2.2.
- v) Probabilistic seismic hazard curves for specific site is developed as explained in Section 3.2.1
- vi) Then reliability index is calculated by combining the fragility curve and hazard curve using the Eq. 3.2.

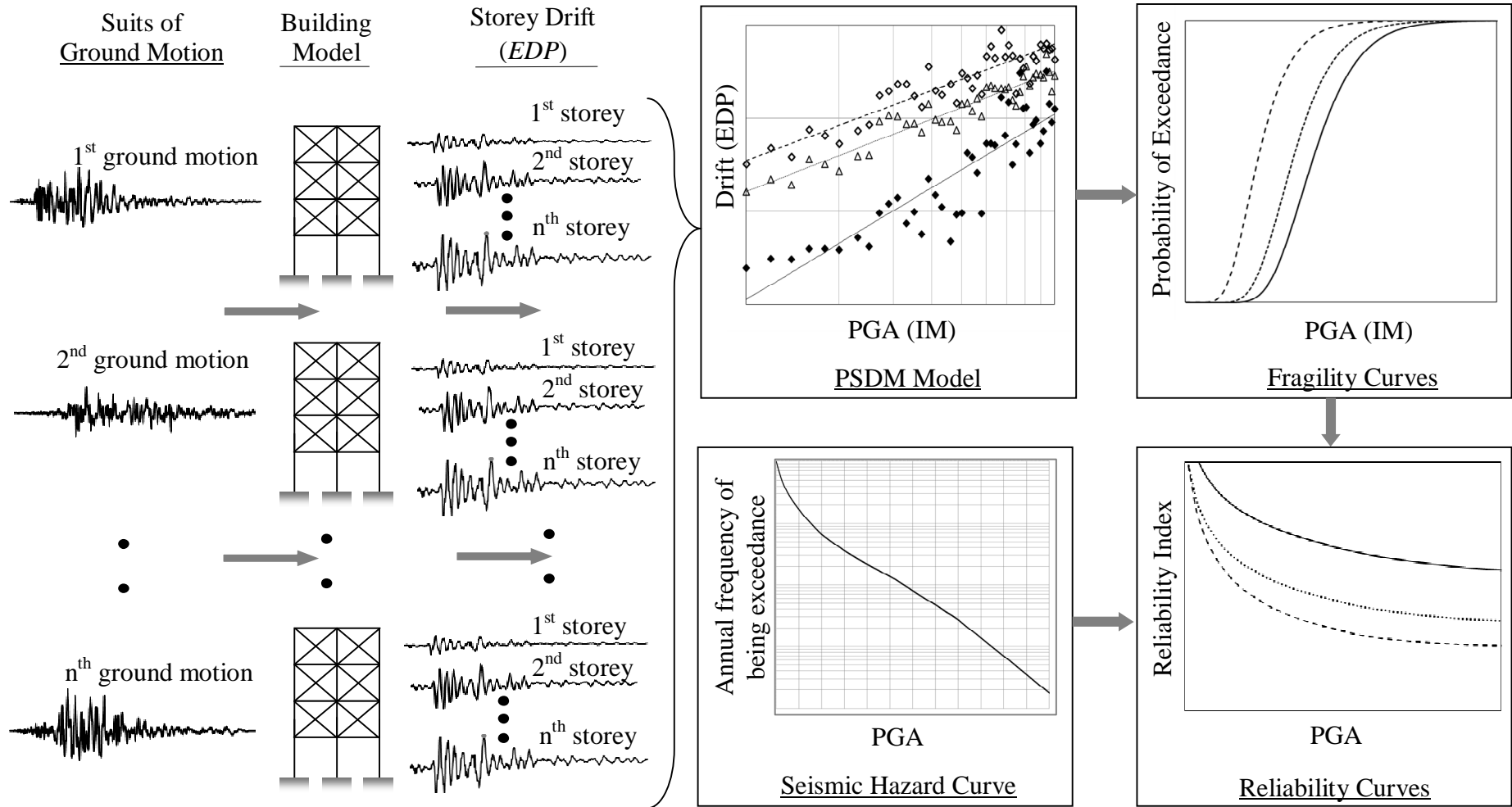


Fig. 3.1: Reliability curve generation using NTHA

The conditional probability, $P[LS_i/A=a]$ in Eq. 3.1 is denoted as the seismic fragility, $F_R(x)$. This is the probability of meeting or exceeding a specified level of damage, LS , given a ground motion which has a certain level of intensity, a . This conditional probability is often assumed to follow a two parameter lognormal probability distribution (Cornell *et. al*, 2002; Song and Ellingwood, 1999).

A point estimate of the limit state probability of state ‘ i ’ can be obtained by convolving the fragility $F_R(x)$ with the derivative of the seismic hazard curve, $G_A(x)$, thus removing the conditioning on acceleration as per Eq. (3.1).

$$P[LS_i] = \int F_R(x) \frac{dG_A}{dx} dx \quad (3.2)$$

Fig. 3.2 shows fragility-hazard interface, identifying dominant contribution to the risk. The parameters of the fragility-hazard interface must be dimensionally consistent for the probability estimate to be meaningful.

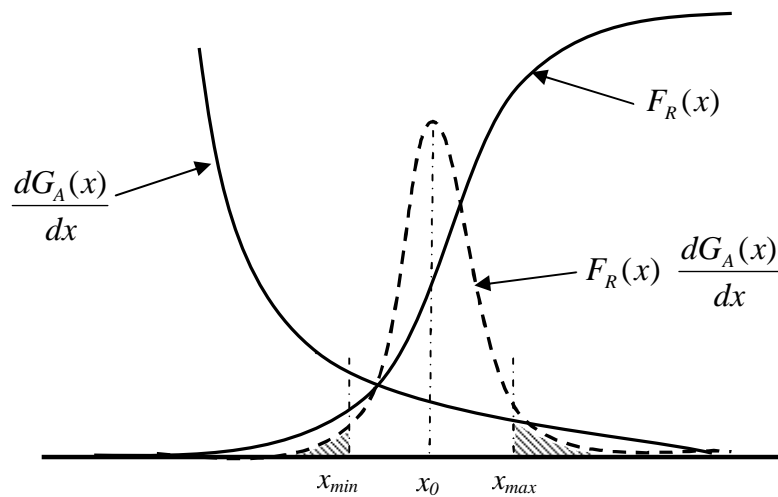


Fig.3.2: Fragility-hazard interface, identifying dominant contribution to the risk (Elingwood, 2001)

Reliability Index, that gives a direct measure of the safety margin, is used in the present study to assess the performance of OGS buildings. Reliability Index corresponding to the probability of failure can be found by the following standard equation as shown below:

$$\beta_{pf} = -\phi^{-1}(P[LS_i]) \quad (3.3)$$

where $\phi ()$ represents the standard normal distribution.

Therefore the methodology of the present study can be summarized as to develop a seismic hazard curve for the area of interest using probabilistic seismic hazard analysis and fragility curves for the selected buildings and to arrive at the probability of failure (Eq. 3.2) and associated reliability index (Eq. 3.3) for different limit states. Following two sections reports the methods of developing seismic hazard curve and fragility curve.

3.2.1 Seismic Hazard Analysis

Seismic Hazard Analysis (SHA) is to quantify the probabilities of occurrence of future earthquake. Two basic approaches have been reported in literature to be used for finding out the probabilities of occurrence of future earthquake: deterministic and probabilistic seismic hazard analyses. Following paragraphs briefly describes these two approaches:

Deterministic Seismic Hazard Analysis (DSHA)

A basic DSHA is a simple process that is useful especially where tectonic features are reasonably active and well-defined. The focus is generally on determining the maximum credible earthquake (MCE) motion at the site. The steps in the process are as follows (Reiter, 1990):

- i) Identify nearby seismic source zones - these can be specific faults or distributed sources
- ii) Identify distance to site for each source (nearby distributed sources are a problem)

- iii) Determine magnitude and other characteristics (i.e. fault length, recurrence interval) for each source
- iv) Establish response parameter of interest for each source, as a function of magnitude, distance, soil conditions, etc., using either the envelope or the average of several ground motion attenuation relationships
- v) Tabulate the values from each source and use the largest value of response parameter.

The DSHA method is simple and has been used by many researchers (Anderson, 1997; Krinitzsky, 2002) in the past to identify the response parameter of interest. However, this method is not considered in the present study as it does not treat uncertainties well. Rudimentary statistics can be incorporated into the procedure by taking one standard deviation above median at each step (magnitude, PGA, etc.), which gives a very big, very conservative estimate. However, the DSHA does not account for the probability of an earthquake occurring on a fault.

Probabilistic Seismic Hazard Analysis (PSHA)

PSHA aims to quantify the uncertainties such as location, size, and resulting shaking intensity of future earthquake and combine them to produce an explicit description of the distribution of future shaking that may occur at a site. In order to assess risk to a structure from earthquake shaking, we must determine the annual probability of exceeding some level of earthquake ground shaking at a site, for a range of intensity levels. Typical seismic hazard curve is as shown in Fig. 3.3, which shows that low levels of intensity are exceeded relatively often while high intensities are rare.

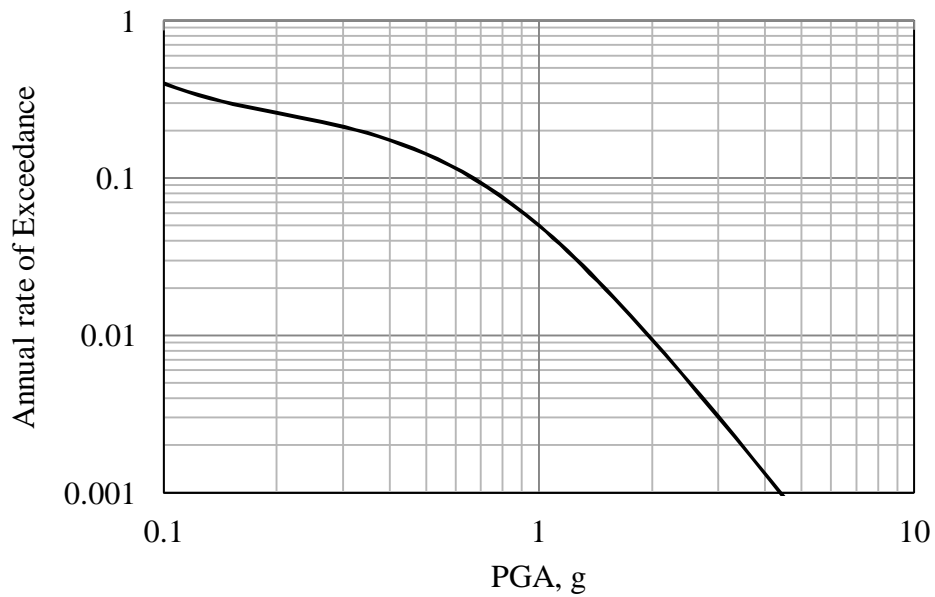
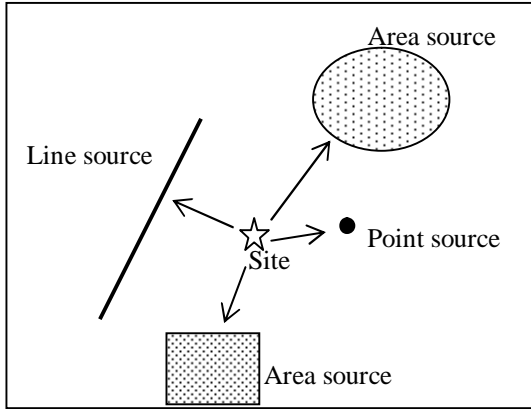


Fig.3.3: Typical Seismic Hazard curve -possibility of intense ground shaking at a site

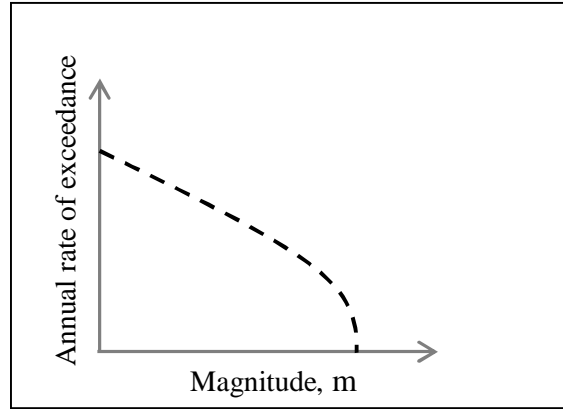
If one was willing to observe earthquake shaking at a site for thousands of years, it would be possible to obtain this entire curve experimentally. But for seismic risk it is not possible experimentally due to various uncertainties in the size, location and resulting shaking intensity caused by an earthquake and we do not have enough observations to extrapolate to the low rates of interest. Due to these challenging tasks, seismic hazard data for a particular site can be obtained by mathematically combining models for the location and size of potential future earthquakes with predictions of potential shaking intensity caused by these future earthquakes. Thus the mathematical approaches used for performing these calculations are termed as Probabilistic Seismic Hazard Analysis, or PSHA.

Procedure for Developing the Seismic Hazard Curve using PSHA

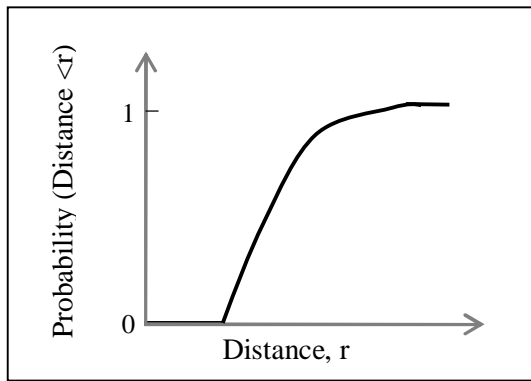
This section presents the step-by-step procedure for developing the seismic hazard curve using PSHA as per Baker (2008). The steps in performing a PSHA are also shown in Fig. 3.4 schematically. Uncertainties are incorporated in each step of the PSHA process. The steps consist of:



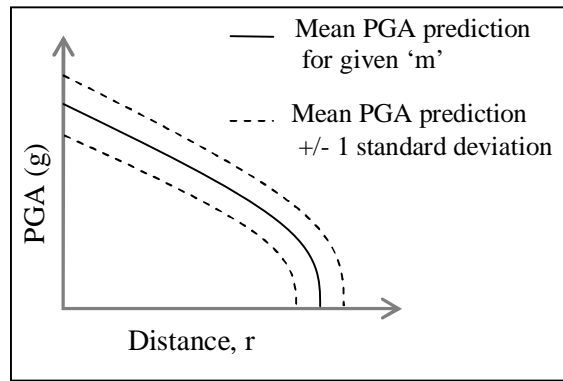
i) Identify earthquake sources



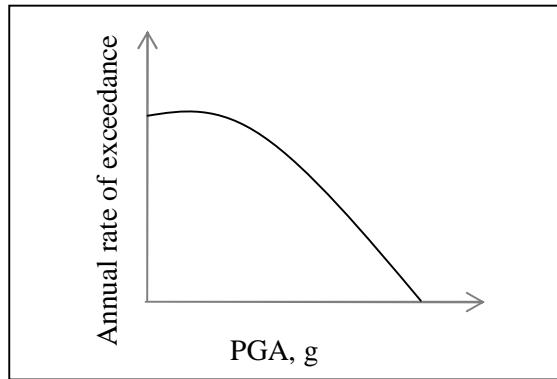
ii) Characterize the distribution of earthquake magnitudes from each source



iii) Characterize the distribution of source-to-site distances from each source.



iv) Predict the resulting distribution of ground motion intensity.



v) Combine information from parts i-iv to compute the annual rate of exceeding a given ground motion intensity

Fig. 3.4: Steps for performing a PSHA (Baker, 2008)

- i) Identify all earthquake sources capable of producing damaging ground motions.
- ii) Characterize the distribution of earthquake magnitudes (the rates at which earthquakes

of various magnitudes are expected to occur).

- iii) Characterize the distribution of source-to-site distances associated with potential earthquakes.
- iv) Predict the resulting distribution of ground motion intensity as a function of earthquake, magnitude, distance, etc.
- v) Combine uncertainties in earthquake size, location and ground motion intensity, using a calculation known as the total probability theorem.

At first, compute the probability of exceeding an IM intensity level x , given occurrence of a future earthquake from a single source using the total probability theorem representing the following equation:

$$P(IM > x) = \int_{m_{\min}}^{m_{\max}} \int_0^{r_{\max}} P(IM > x | m, r) f_M(m) f_R(r) \cdot dr \cdot dm \quad (3.4)$$

where $P(IM > x | m, r)$ is the ground motion model, $f_M(m)$ and $f_R(r)$ are Probability Density Functions (PDFs) for magnitude (m) and distance (r), respectively.

Eq. 3.4 is a probability of exceedance given an earthquake and does not include any information about how often earthquakes occur on the source of interest. Small modification to that equation, to compute the rate of $IM > x$, rather than the probability of $IM > x$ given occurrence of an earthquake can be written as:

$$\lambda(IM > x) = \lambda(M > m_{\min}) \int_{m_{\min}}^{m_{\max}} \int_0^{r_{\max}} P(IM > x | m, r) f_M(m) f_R(r) \cdot dr \cdot dm \quad (3.5)$$

where $\lambda(M > m_{\min})$ is the rate of occurrence of earthquakes greater than a minimum magnitude (m_{\min}) from the source, and $\lambda(IM > x)$ is the rate of $IM > x$

To generalize the analysis further, for the cases with more than one source, Eq. 3.5 can be modified to the sum of the rates of $IM > x$ from each individual source as follows:

$$\lambda(IM > x) = \sum_{i=1}^{n_{sources}} \lambda(M_i > m_{\min}) \int_{m_{\min}}^{m_{\max}} \int_0^{r_{\max}} P(IM > x | m, r) f_{M_i}(m) f_{R_i}(r) \cdot dr \cdot dm \quad (3.6)$$

where $n_{sources}$ is the number of sources considered, and M_i/R_i denote the magnitude/distance distributions for source i . Further it is to discretize to continuous distributions for M and R , and convert the integrals into discrete summations, as follows:

$$\lambda(IM > x) = \sum_{i=1}^{n_{sources}} \lambda(M_i > m_{\min}) \sum_{j=1}^{n_M} \sum_{k=1}^{n_R} P(IM > x | m_j, r_k) \cdot P(M_i = m_j) \cdot P(R_i = r_k) \quad (3.7)$$

where the range of possible M_i and R_i have been discretized into n_M and n_R intervals, respectively using the discretization technique.

Eq. 3.6 (or Eq. 3.7) is the equation most commonly associated with PSHA for development of seismic hazard curve. Typical seismic hazard curve developed based on the PSHA is shown in Fig 3.3.

3.2.2 Development of Fragility Curves

The fragility function represents the probability of exceedance of a selected Engineering Demand Parameter (EDP) for a selected structural limit state (LS) for a specific ground motion intensity measure (IM). Fragility curves are cumulative probability distributions that indicate the probability that a component/system will be damaged to a given damage state or a more severe one, as a function of a particular demand. The seismic fragility, $F_R(x)$ can be expressed in closed form using the following equation (Celik and Ellingwood, 2010),

$$P(D \geq C | IM) = 1 - \phi \left(\frac{\ln \frac{S_C}{S_D}}{\sqrt{\beta_{D|IM}^2 + \beta_c^2 + \beta_M^2}} \right) \quad (3.8)$$

where, D is the drift demand, C is the drift capacity at chosen limit state, S_C and S_D are the chosen limit state and the median of the demand (LS) respectively. $\beta_{D|IM}$, β_c and β_M are

dispersions in the intensity measure, capacities and modelling respectively. A fragility curve can be obtained for different limit states using Eq. 3.8.

Probabilistic Seismic Demand Model (PSDM)

The seismic demand (S_D) is usually described through probabilistic seismic demand models (PSDMs) particularly for NTHA which are given in terms of an appropriate intensity measure (IM). It has been suggested by Cornell *et. al.* (2002) (also known as 2000 SAC FEMA method) that the estimate of the median demand, $EDP(S_D)$ can be represented in a generalized form by a power model as given in Eq. 3.9.

$$EDP = a(IM)^b \quad (3.9)$$

where, a and b are the regression coefficients of the PSDM. Eq. 3.8 can be rewritten for system fragilities as follows:

$$P(D \geq C | IM) = 1 - \phi \left(\frac{\ln(S_C) - \ln(a \cdot IM^b)}{\sqrt{\beta_{D|IM} + \beta_c + \beta_M}} \right) \quad (3.10)$$

The dispersion, $\beta_{D|IM}$, of inter-storey drifts (d_i) from the time history analysis can be calculated using Eq. 3.11 where $a(IM)^b$ represents the mean inter-storey drift.

$$\beta_{D|IM} \cong \sqrt{\frac{\sum [\ln(d_i) - \ln(aIM^b)]^2}{N - 2}} \quad (3.11)$$

Uncertainty associated with building definition and construction quality (β_c) accounts for the possibility that the actual properties of structural elements (e.g., material strength, section properties, and details such as rebar location) might be different than those otherwise believed to exist. Values of β_c are assigned based on the quality and confidence associated with building definition. For existing buildings, this will depend on the quality of the available drawings documenting the as-built construction, and the level of field investigation performed to verify their accuracy. For new buildings, this will be determined based on

assumptions regarding how well the actual construction will match the design. ATC 58 (2012) recommends values for β_c under representative conditions. In the present study, β_c is considered as 0.25 which represents the building design is completed to a level typical of design development, construction quality assurance and inspection are anticipated to be of limited quality.

According to ATC 58 (2012), modelling uncertainty (β_m) is the result from inaccuracies in component modelling, damping and mass assumptions. For the purpose of estimating β_m , this uncertainty has been associated with the dispersion of building definition and construction quality assurance (β_c) and the quality and completeness of the nonlinear analysis model (β_q).

The total modelling dispersion can be estimated as follows:

$$\beta_m = \sqrt{\beta_c^2 + \beta_q^2} \quad (3.12)$$

β_q recognizes that hysteretic models may not accurately capture the behaviour of structural components, even if the details of construction are precisely known. Values of β_q are assigned based on the completeness of the mathematical model and how well the components deterioration and failure mechanisms are understood and implemented. Dispersion should be selected based on an understanding of how sensitive response predictions are to key structural parameters (*e.g.*, strength, stiffness, deformation capacity, in-cycle versus cyclic degradation) and the likely degree of inelastic response.

In this study, β_q is assumed to be 0.25 representing that numerical model for each component is robust over the anticipated range of displacement or deformation response. Strength and stiffness deterioration is fairly well represented though some failure modes are simulated indirectly. The mathematical model includes most structural components and non-structural components in the building that contribute significant strength or stiffness.

3.3 BUILDING PERFORMANCE LEVELS

To define the fragility function demand, parameters are compared with the selected structural limit states or building performance levels. Building performance levels are defined as approximate limiting levels of structural and non-structural damage that may be expected during an earthquake. It can be described qualitatively in terms of the following parameters:

- i) safety afforded to building occupants, during and after an earthquake.
- ii) cost and feasibility of restoring the building to pre-earthquake conditions.
- iii) length of time, the building is removed from service to conduct repairs.
- iv) economic, architectural, or historic impacts on the community at large.

These performance characteristics will be directly related to the extent of damage sustained by the building during a damaging earthquake. Three important performance levels (Damage Limitation, Significant Damage and Collapse Prevention) are being considered in the present study as discussed in the following sections and illustrated graphically in Figs. 3.5-3.6 for bare and infilled frame (Dolsek and Fajfar, 2008).

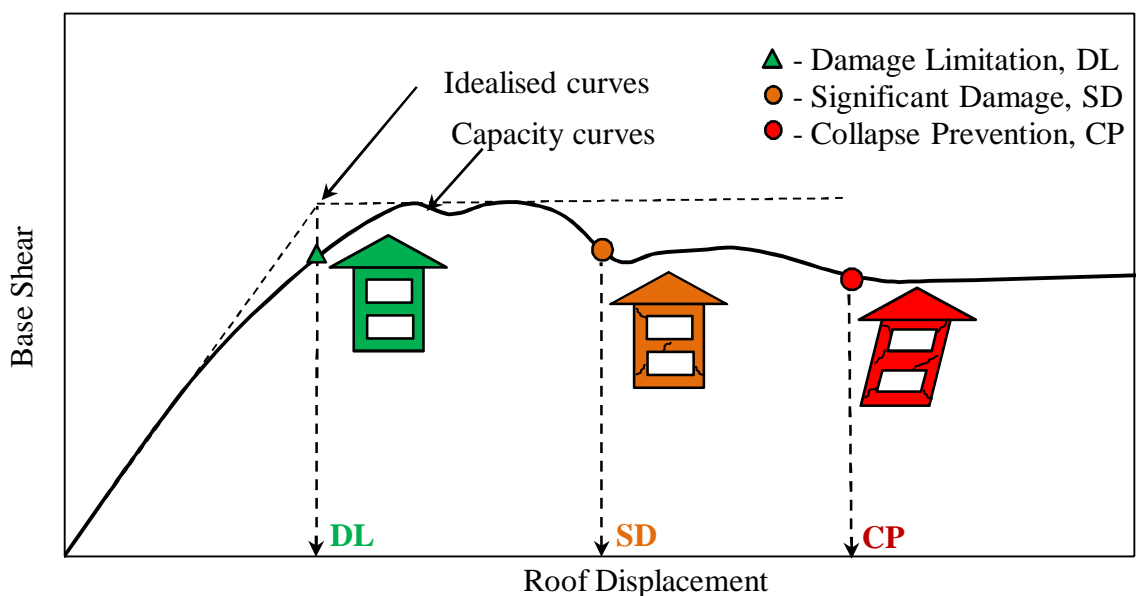


Fig. 3.5: Typical performance levels for bare frame

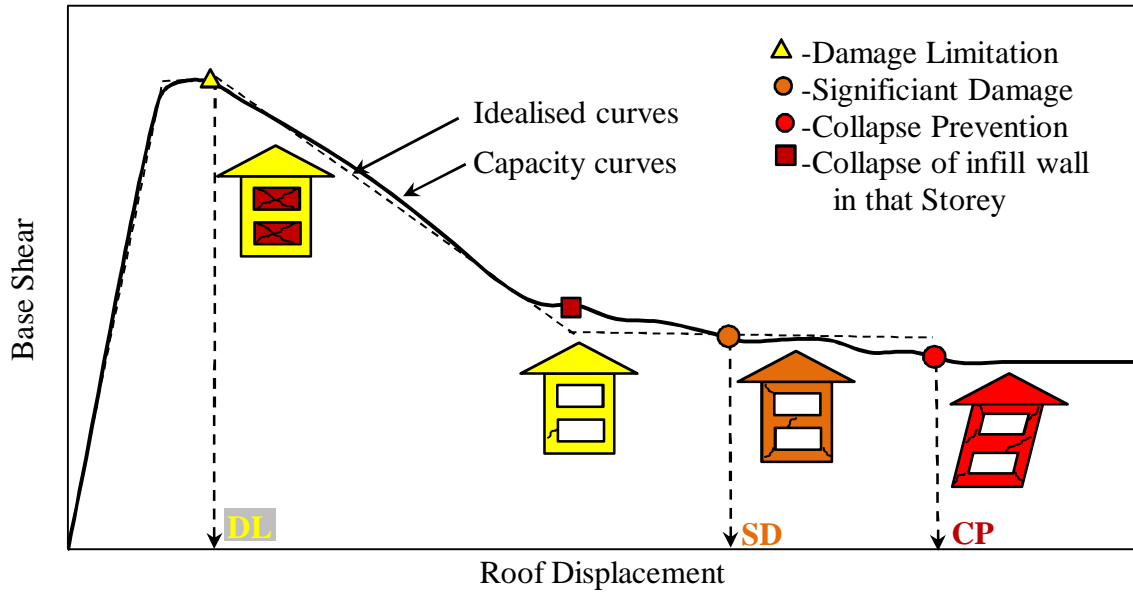


Fig. 3.6: Typical performance levels for fully infilled frame

3.3.1 Damage Limitation (DL)

In this performance level, overall damage to the building is light. Damage to the structural systems is very less, however, somewhat more damage to non-structural systems is expected. Non-structural components such as cladding and ceilings and mechanical and electrical components remain secured; however, repair and cleanup may be needed. It is expected that utilities necessary for normal function of all systems will not be available, although those necessary for life safety systems will be available. Many building owners may wish to achieve this level of performance when the building is subjected to moderate levels of earthquake ground motion. In addition, some owners may desire such performance for very important buildings, under severe levels of earthquake ground shaking. At this limit state, masonry infill walls attain its maximum strength.

3.3.2 Significant Damage (SD)

Structural and non-structural damage in this performance level is significant. The building may lose a substantial amount of its pre-earthquake lateral strength and stiffness, but the

gravity-load bearing elements function. Out-of-plane wall failures and tipping of parapets are not expected, but there will be some permanent drift and select elements of the lateral-force resisting system may have substantial cracking, spalling, yielding, and buckling. Non-structural components are secured and do not present any a falling hazard, but many architectural, mechanical, and electrical systems are damaged. The building may not be safe for continued occupancy until repairs are done. Repair of the structure is feasible, but it may not be economically attractive to do so. Masonry infill walls lose its complete strength at this level.

3.3.3 Collapse Prevention Level or Near Collapse Level (CP)

The structure sustains severe damage. The lateral-force resisting system loses most of its pre-earthquake strength and stiffness. Load-bearing columns and walls function, but the building is near collapse. Substantial degradation of structural elements occurs, including extensive cracking and spalling of masonry and concrete elements, and buckling and fracture of steel elements. Infills are completely failed. The building has large permanent drifts. Non-structural components experience substantial damage and may be falling hazards. The building is unsafe for occupancy. Repair and restoration is probably not practically achievable. This building performance level results in mitigation of the most severe life-safety hazards at relatively low cost.

3.4 SAMPLING OF VARIABLES

During development of fragility curves, it is very important to consider possible uncertainties associated with them. In structural engineering, material properties like strength and stiffness, structural properties like damping ratio are random in nature. These properties depend on many parameters like type of construction, quality of construction, etc. It is not a proper way

to represent these parameters by considering mean value; hence sampling is required to estimate the most accurate results. To estimate the characteristics of the whole population, a subset of individuals within the population are selected which is normally known as sampling. Broadly sampling is divided in to two parts: (i) Probability Sampling Method and (ii) Non-Probability Sampling Method.

The techniques of random sampling are more powerful and useful for performing probabilistic analyses. However, in most cases, the problems being analyzed are extremely complex and the time needed to evaluate the solution may be very long. As a result, the time needed to perform hundred or thousand of simulation may be unfeasible. To overcome this problem, McKay *et al.* (1979) proposed an attractive alternative method in computer experiments called as Latin Hypercube Sampling (LHS). This method is a technique for reducing the number of simulations needed to obtain reasonable results. Several authors (Ayyub and Lai, 1989; Iman and Conover, 1980; Tavares *et al.*, 2012) have used LHS method successfully to consider uncertainties in materials for developing fragility curves. This sampling scheme is used in the present study for considering the uncertainties.

In LHS sampling scheme, the range of possible data of each random input variable is partitioned into subset and a value from each subset is randomly selected as a representative value. The representative values for each subset are then combined so that each representative value is considered only once in the simulation process. In this way, all possible values of the random variables are represented in the simulation. The maximum number of combinations for an LHS of N_t divisions and M_t variables can be computed (McKay et al., 1979) with the following formula:

$$\left(\prod_{n=0}^{N_t-1} (N_t - M_t) \right)^{M_t-1} = (N_t!)^{M_t-1} \quad (3.13)$$

For example, a LHS of $N_t = 4$ divisions with $M_t = 2$ variables (i.e., a square) will have 24 possible combinations. A Latin hypercube of $N_t = 4$ divisions with $M_t = 3$ variables (i.e., a cube) will have 576 possible combinations. Fig. 3.7 shows the graphical representation of typical LHS scheme when number of intervals (N_t) is five.

LHS Scheme of Sampling Procedure

This section discusses the step-by-step procedure of LHS scheme for sampling the random variables as given in Ranganathan, (1999). Let's consider that we need to simulate values of some function Z described by

$$Z = f(A_1, A_2, \dots, A_k) \quad (3.14)$$

where $f(\)$ is deterministic function (but possibly not known in closed form) and the A_i ($i = 1, 2, 3, \dots, K$) are the random input variables. Partition the range of each A_i into N_t intervals. The partitioning should be done so that the probability of a value of A_i occurring in each interval is $1/N_t$.

- i) For each A_i variable and each of its N_t intervals, randomly select a representative value for the interval. In practical applications, if the number of intervals is large, the centre point (i.e., the middle value) of each interval can be used instead of doing random sampling.
- ii) After steps 1, there will be N_t representative values for each of the K random variables. There are $N_t K$ possible combinations of these representative values. The objective of Latin hypercube sampling is to select N_t combinations such that each representative value appears once and only once in the N_t combinations.
- iii) To obtain the first combination, randomly select one of the representative values for each of the K input random variables. To obtain the second combination, randomly select one of the $N_t - 1$ remaining representative values of each random variable. To obtain the third combination, randomly select one of the $N_t - 2$ remaining

representative values of each random variable. Continue this selection process until you have N_t combinations of values of the input random variables.

- iv) Evaluate Eq. 3.14 for each of the N combinations of input variables generated above. This will lead to N_t values of the function. These values will be referred to as $Z_i (i = 1, 2, \dots, N_t)$.

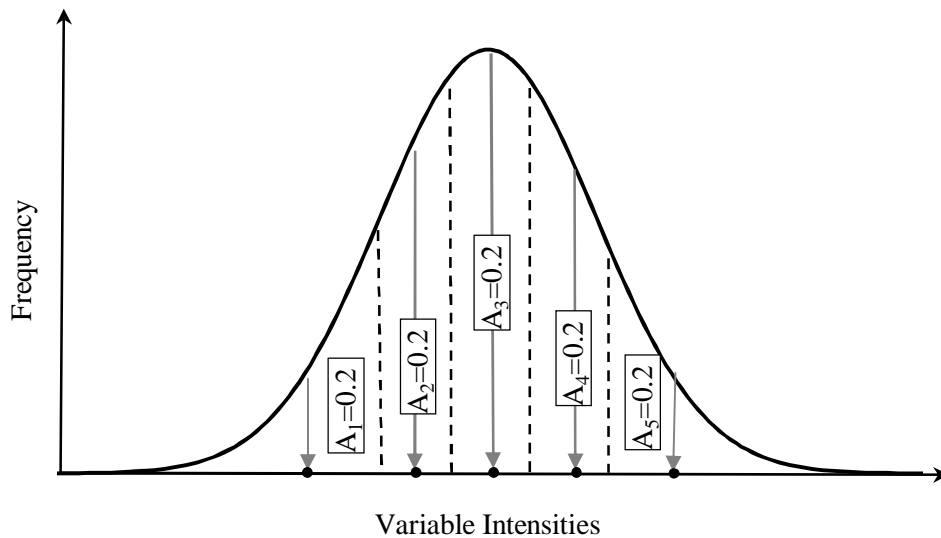


Fig. 3.7: Typical Latin Hypercube Sampling method

3.5. SUMMARY

This chapter presents detailed methodology of seismic risk assessments of OGS building (Ellingwood, 2001) followed in the present study. This involves the development of probabilistic seismic hazard curves for specific site and development of fragility curves based on power law PSDMs (Cornell *et al.*, 2002) and selected building performance levels. Selected building performance levels are discussed in detail. Procedure for sampling random variables using LHS scheme to incorporate uncertainties are also explained.

CHAPTER 4

MODELLING AND ANALYSIS

4.1 INTRODUCTION

The study in this thesis is based on NTHA of a family of structural models representing OGS framed buildings designed with different scheme of MFs. Accurate modelling of the nonlinear properties of various structural elements is very important for nonlinear analysis. In the present study, frame elements were modelled using fibre elements with spread plasticity. The first part of this chapter presents a summary of various parameters defining the constitutive relations used for modelling reinforced concrete and infill wall elements. Validation studies are performed and reported in the next part of this chapter to demonstrate the efficacy of modelling approach considered in the present study. The details of selected building frame configurations are also discussed in this chapter. Latin Hypercube Sampling (LHS) has been used for estimating the random variables considered in the present study and accordingly the structural models are developed. This chapter presents a brief discussion on the random variables and sampling. The estimation of structural limit state capacities to be used for developing fragility curves is also discussed. Last part of this chapter explains the selection of earthquake ground motion records required for the evaluation of building performances.

4.2 MATERIAL MODELS

An elemental cross-section in an RC member is composed of three types of materials: unconfined concrete, confined concrete and reinforcing steel. All reinforced concrete components are detailed with transverse steel which provide both shear resistance and

confining action. The confining effects of transverse steel are considered implicitly by modifying the stress-strain response of the core concrete. Numerous researchers have developed stress-strain models of confined concrete based on observed experimental behaviour. The concrete cover will typically spall at relatively small strain levels; therefore, the modelling of unconfined concrete is generally not critical for damage limit states in the inelastic range. The response of RC components and consequently the system is a function of the behaviour of the confined core concrete and the longitudinal steel.

4.2.1 Concrete Modelling

Concrete outside the transverse reinforcements in the RC section has no confinement, whereas concrete inside the transverse reinforcements is confined. In order to consider the effect of confinement, cover concrete (outside the transverse reinforcement) and core concrete (inside the transverse reinforcement) materials are considered separately and the corresponding parameters are calculated based on the Mander *et al.* (1988). Concrete02, material is used to model concrete in Open System for Earthquake Engineering Simulation (OpenSees, 2013). The Concrete02 model is an uniaxial material model that includes tensile strength and linear tension softening. The idealized model is shown in Fig. 4.1, where the basic inputs for the model are:

f_{co} :	Compressive strength of concrete
ε_o :	Concrete strain at maximum strength
f_u :	Concrete crushing strength
ε_u :	Concrete strain at crushing strength
$\lambda = E_u / E_c$:	Ratio of unloading slope at ε_u to initial slope
f_t :	Concrete tensile strength
E_{ts} :	Concrete tension softening stiffness

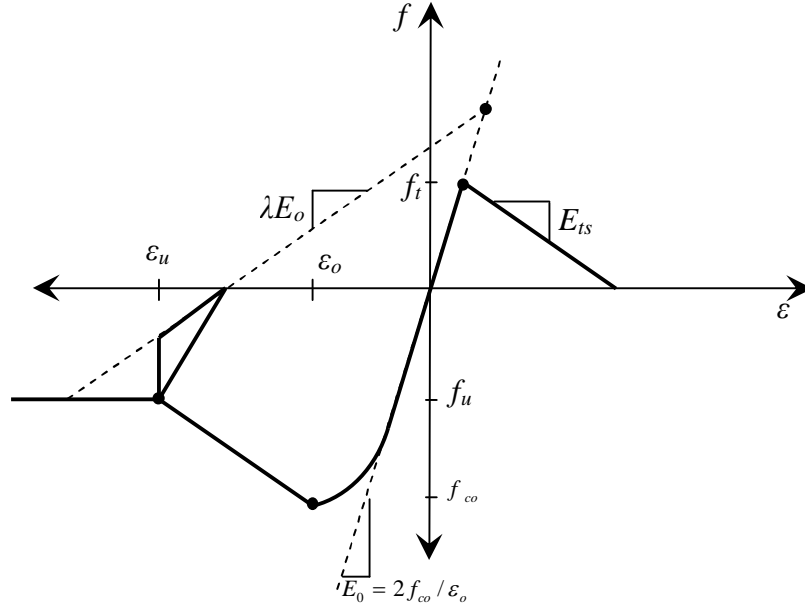


Fig.4.1: Parameters of monotonic envelopes of Concrete02 model (OpenSees, 2013)

The concrete compressive strength at 28 days is specified as the peak compression strength of unconfined concrete. Confinement factor (k) is calculated according to the stirrups/lateral ties proposed by Mander *et al.* (1988) as shown in Eq. (4.1):

$$\frac{f_{cc}}{f_{co}} = 2.254 \sqrt{1 + 7.94 \frac{f_L}{f_{co}}} - 2 \frac{f_L}{f_{co}} - 1.254 \quad (4.1)$$

where, f_{cc} and f_{co} are confined and unconfined concrete strength respectively, f_L is the effective lateral confining pressure. The constants that appear in the Eqn. (4.1) were obtained from empirical calibration of experimental data. The ratio between unloading slope at second step and initial slope (λ) is considered as 0.1 as per Attarchian *et al.* (2013). The initial slope is given by 2 times of f_c/ϵ_o , as it is correlated well with the experimentally determined elastic modulus of concrete (Heo and Kunnath, 2008). A residual stress of the confined concrete, f_{cc}^{resid} , is assumed as $0.2f_{cc}$, while it is assumed zero for the unconfined concrete.

4.2.2 Reinforcement Modelling

Steel reinforcing bars are modelled using Menegotto and Pinto, (1973) model with Isotropic Strain Hardening (referred to as Steel02 in the OpenSees material library) as shown in Fig. 4.2 with a schematic cyclic behaviour. This model consists of explicit algebraic stress-strain relationship, in finite terms, for branches between two subsequent reversal points (loading branches). The parameters involved are updated after each strain reversal. The Menegotto-Pinto $\sigma = f(\varepsilon)$ expression is:

$$\sigma^* = b\varepsilon^* + \frac{(1-b)\varepsilon^*}{(1 + \varepsilon^{*R})^{1/R}} \quad (4.2)$$

$$\varepsilon^* = \frac{\varepsilon - \varepsilon_r^n}{\varepsilon_y^{n+1} - \varepsilon_r^n}, \quad \sigma^* = \frac{\sigma - \sigma_r^n}{\sigma_y^{n+1} - \sigma_r^n} \quad (4.3)$$

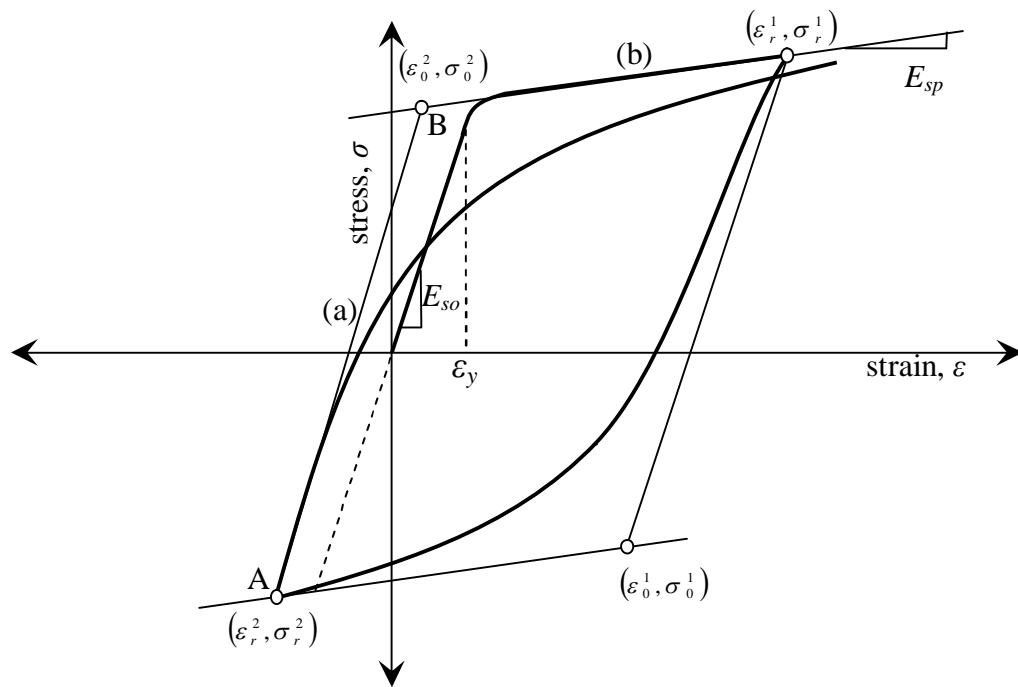


Fig.4.2: Stress-strain relationships of steel reinforcement (Menegotto- Pinto model)

The above relation represents a curved transition from a straight-line asymptote with slope E_{so} to another asymptote with slope $E_{sp} = bE_{so}$. The strain ε_y^{n+1} and stress σ_y^{n+1} denote the point where the two asymptotes of the branch under consideration meet. The

strain ε_r^n and stress σ_r^n denote the last reversal point. The plastic excursion at the current semi cycle is defined as:

$$\xi_p^n = \xi_r^n - \varepsilon_y^n \quad (4.4)$$

$$\varepsilon_y^n = \varepsilon_r^{n-1} + \frac{\sigma_y^n - \sigma_r^{n-1}}{E} \quad (4.5)$$

where, ε_r^n is the strain of the last reversal point and ε_y^n is the strain corresponding to the yield stress σ_y^n at the n^{th} semi cycle, the curvature of the branch is then defined as:

$$R = R_0 - \frac{cR_1 \cdot \xi_p^{\max}}{cR_2 + \xi_p^{\max}} \quad (4.6)$$

where the coefficients R_0 , cR_1 and cR_2 depend on the mechanical properties of steel. R is a parameter which influences the shape of the transition curve and allows a good representation of the Bauschinger effect. The stress-strain relationship of Menegotto-Pinto model is shown in Fig. 4.2. Isotropic strain hardening is taken into account according to Filippou *et al.* (1983) that considers a shifting of the asymptote of the hardening branch by a quantity given by:

$$\sigma_{shift} = \sigma_y a_1 \left(\frac{\varepsilon_{\max}}{\varepsilon_y} - a_2 \right) > 0 \quad (4.7)$$

where ε_{\max} is the maximum strain reached in the opposite direction with respect to that of current loading; ε_y and σ_y are, respectively the yield strain and stress; a_1 defines the amount of isotropic hardening and a_2 defines the value beyond which the phenomenon occurs. These factors can be experimentally evaluated. The shift of asymptote is considered to be same for both tension and compression. This material model is employed in OpenSees as steel02 (Mazzoni *et al.*, 2009) to simulate the behaviour steel bars. Parameters required to define the relationship are the yield strength f_y , the modulus of

elasticity E_s , the hardening ratio (a) and the parameters controlling the transition from elastic to plastic branches (R_0 , cR_1 and cR_2).

4.2.3 Infill Wall Modelling

Infill walls are modelled as equivalent diagonal single strut in both diagonals of each bay as used by several authors (Klingner and Bertero, 1978; Madan *et al.*, 1997; Negro and Colombo, 1997; Combescure and Pegon, 2000; Crisafulli *et al.*, 2000; Dolsek and Fajfar, 2001; Dolsek and Fajfar 2002; Dolsek and Fajfar, 2008; Ravichandran and Klinger, 2012). This approach allows easy analytical representation of multi-storey, multi-bay frames as it requires less computational effort than micro-modelling approaches (such as the finite element method) yet still provides reasonable accuracy. In the equivalent-strut approach, the infill is represented as a combination of two compression-only truss elements, each acting independently. Each equivalent strut element is assigned with an appropriate hysteretic force- deformation relationship, generally including a descending post-peak strength, in-cycle degradation, and pinching. Fig. 4.3 shows the typical quadrilinear force-displacement relationship of the diagonal struts (in compression), used in the present study as per Celarec *et al.* (2012). This model is discussed in detail in section 2.5.2.

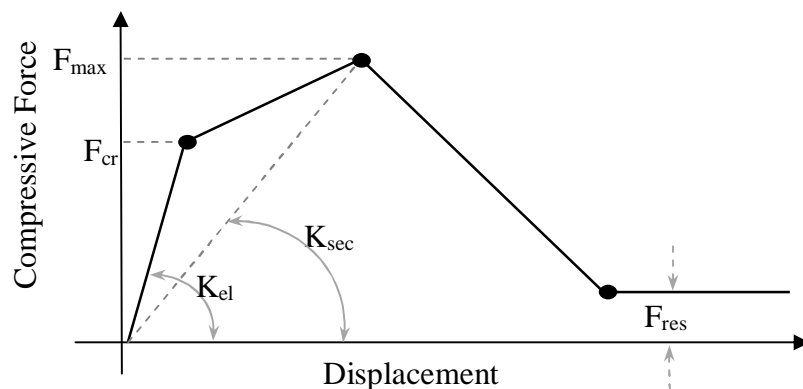


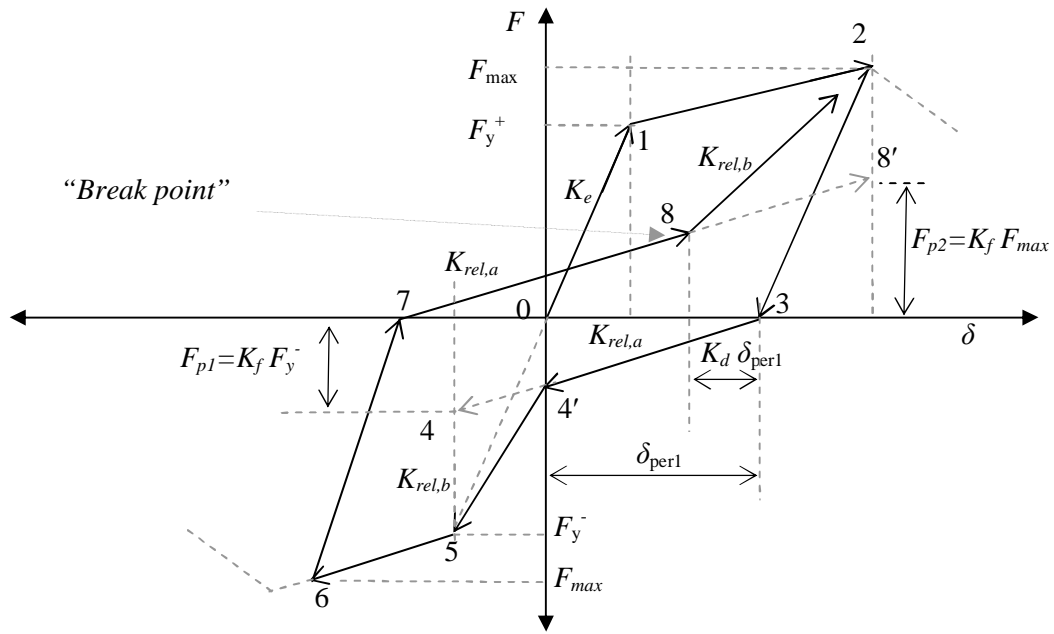
Fig.4.3: Force-displacement relationship of the diagonal struts used by Celarec *et al.* (2012)

The parameters involved to define the force-deformation relationship are maximum strength (F_{max}), Shear cracking strength (F_{cr}), Residual strength (F_{res}), Secant stiffness (K_{sec}) and Elastic stiffness (K_{el}). In order to consider the strength and stiffness degradation of the infill walls, in the time history analysis, pinching material model is used to model the equivalent strut. This is implemented in OpenSees by Ibarra *et al.* (2005). Details of this model are elaborated in Janardhana (2010). Pinching material model is used for hysteretic modelling of infill walls under cyclic loading by many studies (Landi *et al.*, 2012; Ravichandran and Klinger, 2012; etc).

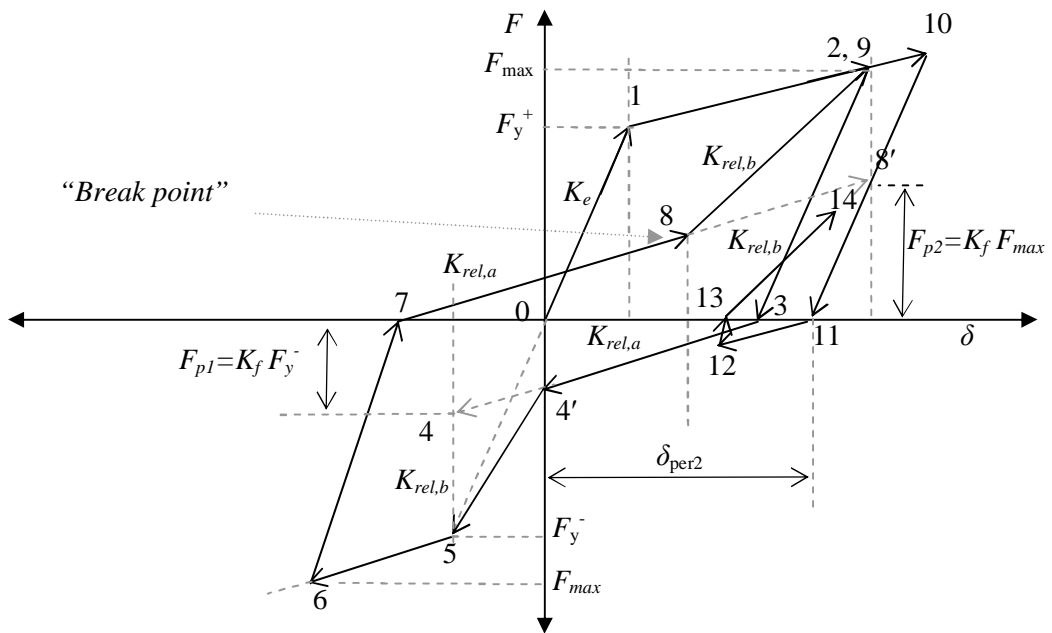
Pinching Model:

In the pinching model, the reloading path consists of two parts. In the first part, the reloading path is directed towards a point denoted as “breakpoint”, which is a function of the maximum permanent deformation and the maximum load experienced in the direction of loading. The break point is defined by the parameter K_f which modifies the maximum “pinched” strength (points ‘4’ and ‘8’ of Fig. 4.4a), and K_d defines the displacement of the break point (points ‘4’ and ‘8’). The first part of the reloading branch was defined by $K_{rel,a}$ and once the break point has reached (points 4 and 8), the reloading path was directed towards the maximum deformation of earlier cycles in the direction of loading ($K_{rel,b}$).

And second part, is reloading without $K_{rel,a}$, if the absolute deformation at reloading (point 13, Fig. 4.4b) is larger than absolute value of $(1-K_d) \delta_{per}$, where δ_{per} is the displacement at which the unloading curve touches the horizontal axis. The reloading path consists of a single branch that is directed towards the previous maximum deformation in the direction of loading.



a) Basic model rules



b) Reloading deformation at the right of break point

Fig 4.4: Pinching hysteresis model

4.3 ELEMENT MODEL

OpenSees (2013) a software framework for simulating the seismic response of structural systems, is used for non-linear static and time history analysis of selected buildings models. OpenSees is open source software written on C++ platform and can be edited

\ddot{x} is the acceleration vector relative to the ground, \dot{x} is the relative velocity vector, x is the relative displacement vector and the external load vector is $\{P(t)\} = -[M]\{1\}\ddot{a}_g$ in the case of earthquake loading, where \ddot{a}_g is the ground acceleration. $[M]$ $[C]$ and $[K]$ are the mass, damping, and stiffness matrix, respectively. These matrices are described in the following sections.

4.4.1 Mass Matrix

The mass of a structure can be modelled in an equivalent lumped or a consistently distributed matrix (Clough and Penzien, 1975). Past many studies used lumped mass system on dynamic analyses. In the present study, the lumped mass approach is considered. All permanent weight that moves with the structure is lumped at the appropriate nodes. This includes all the dead loads and part of the live loads which is expected to be present in the structure during the ground shaking. It is common practice (Indian code) to include 25% of the design live load in intermediate floors and no loads on terrace, while calculating the seismic mass of the structure.

4.4.2 Damping matrix

Damping is the dissipation of energy from a vibrating structure. In this context, the term ‘dissipate’ is used to mean the transformation of energy into the other form of energy and, therefore, a removal of energy from the vibrating system. In reality, damping forces may be proportional to the velocity or to some power of velocity.

In this study, a Rayleigh damping is used for dynamic analysis (Rayleigh, 1954). Rayleigh damping is assumed to be proportional to the mass and stiffness matrices as follows:

$$[C] = \eta[M] + \delta[K] \quad (4.9)$$

where, η is the mass-proportional damping coefficient and δ is the stiffness-proportional damping coefficient. These coefficients can be derived by assuming suitable damping ratios for any two modes of vibrations. Relationships between the modal equations and orthogonality conditions allow this equation to be rewritten as

$$\xi_n = \frac{\eta}{2\omega_n} + \delta \frac{\omega_n}{2} \quad (4.10)$$

where, ξ_n is the damping ratio and ω_n is the natural frequency for n^{th} mode. In linear dynamic analysis, damping matrix is constant as mass and stiffness matrices are constant. However, in nonlinear dynamic analysis, the stiffness matrix of the system changes with the nonlinear steps. In this context, the damping matrix can be expressed in proportion to either initial tangent stiffness $[K_i]$ or current tangent stiffness $[K_t]$ or last committed stiffness $[K_c]$. Although the first method (consideration of initial tangent stiffness) is the simplest, the next two methods would be the most appropriate. It is reported by Filippou *et al.* (1992) that the effect of viscous damping is very small compared to hysteretic damping in the nonlinear dynamic analysis of structures that are subjected to large post-yield deformations. In this study initial tangent stiffness $[K_i]$ is considered in order to avoid numerical problems. In this study, damping ratio (ξ_n) is considered as a random variable. First and second modes are considered to evaluate the required damping coefficients (η and δ).

4.4.3 Stiffness matrix - Fibre based Element

In fibre model the each element is divided into number of sections and sections are subdivided into a number of fibres. Fibres are rigidly bonded and do not have relative slip. The main advantage of fibre model is that it adopts uniaxial material constitutive relation to consider the coupling axial force and biaxial bending. The response of each

fibre can be integrated to get the force and deformation response of a section based on plane section assumption.

The integration scheme plays a significant role in the fibre based element. It determines the location of integration points where the fibre sections are placed. Fig.4.6 presents a schematic diagram of fibre-based element and section discretization. Accuracy of model can be obtained from sufficient cross-section subdivisions and appropriate constitutive model of materials. For different materials, different uni-axial constitutive models can be assigned to the corresponding fibres according to their location and area. For the same material, different uniaxial constitutive models can be assigned to the fibres which have different mechanical behaviour due to different lateral restraints, such as the restraints from stirrups, steel tube and carbon fibre sheet, etc. Fibre-based element model is effective for different cross-sectional shape and different composition of material properties.

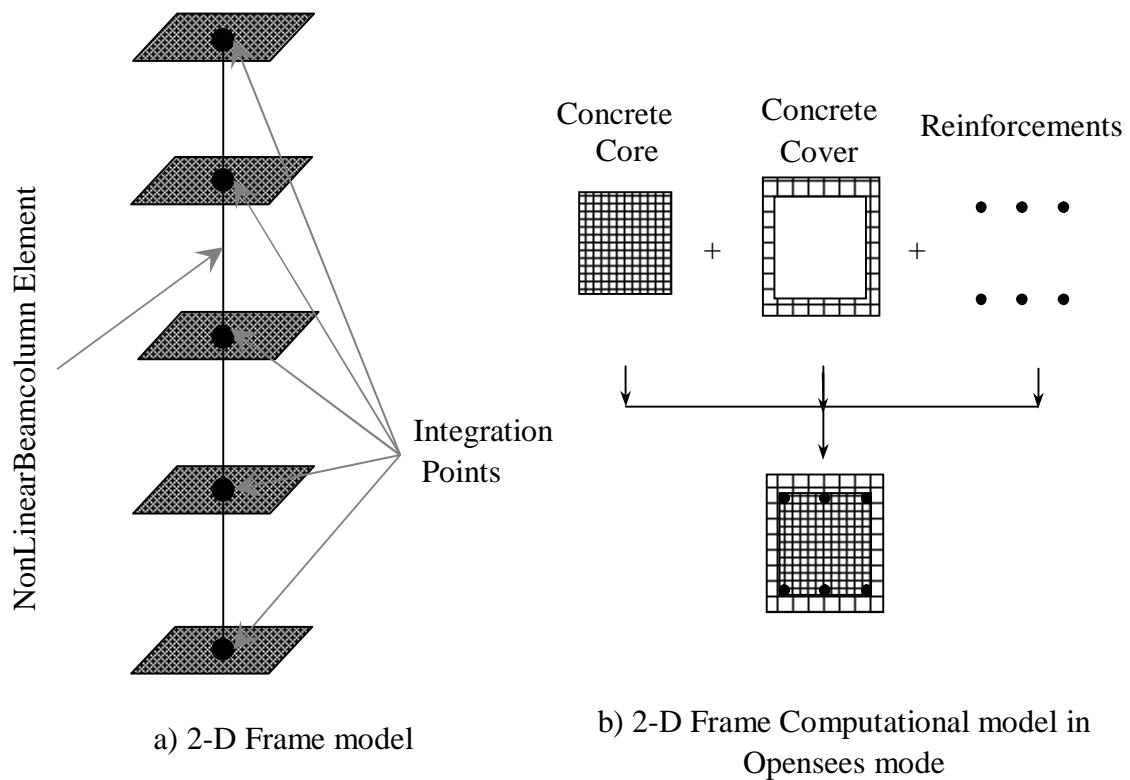


Fig. 4.6: Computational model- Fibre-based element and section discretization

Formulations of Stiffness matrix

Force and deformation variables at the element and section levels are shown in Fig 4.7.

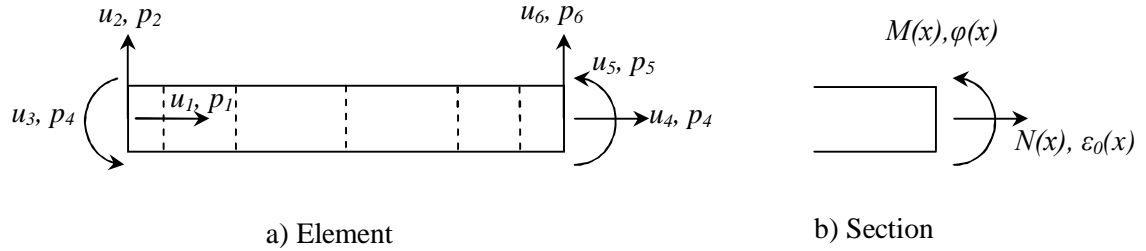


Fig 4.7: Force and deformation variables at element and section levels

From the Fig. 4.7, the element force and deformation vectors are given by

$$\text{Force, } \mathbf{p} = [p_1, p_2, \dots, p_6]^T \quad (4.11)$$

$$\text{Deformation, } \mathbf{u} = [u_1, u_2, \dots, u_6]^T \quad (4.12)$$

On the other hand, the section force and deformation vectors are given by

$$\text{Force, } \mathbf{q}(x) = [N(x), M(x)]^T \quad (4.13)$$

$$\text{Deformation, } \mathbf{v}_s(x) = [\varepsilon_0(x), \phi(x)]^T \quad (4.14)$$

The normal force N , bending moment M , axial strain at the reference axis ε_0 , and curvature ϕ , are functions of the section position x . The strain increment in the i^{th} fibre is defined by:

$$\begin{aligned} d\varepsilon_i &= d\varepsilon_0(x) - y_i d\phi(x) \\ &= a_s(y) dv_s(x) \end{aligned} \quad (4.15)$$

where $a_s(y) = [1, -y_i]$, $dv_s(x) = [d\varepsilon_0(x), d\phi(x)]^T$ and y_i is the distance between the i^{th} fibre and the reference axis. Section deformations $v_s(x)$ are determined from the strain-deformation relationship such that

$$\mathbf{v}_s(x) = \left[\mathbf{B}(x) + \frac{1}{2} \mathbf{G}(x) \right] \mathbf{u}_{n+1} \quad (4.16)$$

where $u_{n+1} = u_n + \Delta u$ is the element deformation vector at the load step $n+1$, $B(x)$ is the first order strain-deformation transformation matrix which consists of the well-known first and second derivatives of the displacement interpolation matrix assuming small deformations, and $G(x)$ is another strain-deformation transformation matrix such that $\frac{1}{2}G(x)$ represents the second-order term of the strain-deformation relationship. $G(x)$ can be expressed as

$$G(x) = \begin{bmatrix} 1 \\ 0 \end{bmatrix} \{C(x)u_{n+1}\}^T C(x) \quad (4.17)$$

where, $C(x)$ is a strain-deformation transformation matrix which consists of the first derivatives of displacement interpolation matrix.

Tangent modulus E_{ti} and stress σ_i are determined from the strain ε_i using a particular constitutive relationship for the material of the i^{th} fibre. In this way, the section stiffness $k_s(x)$ and resisting force $r_s(x)$ are determined using the principle of virtual work such that

$$k_s(x) = \int_{A(x)} a_s^T(y) E_t(x, y) a_s(y) dA \quad (4.18)$$

$$r_s(x) = \int_{A(x)} a_s^T(y) E_t(x, y) dA \quad (4.19)$$

These integrals can be evaluated by the midpoint rule with n fibres. Thus, $k_s(x)$ and $r_s(x)$ are numerically obtained as follows:

$$k_s(x) = \sum_{i=1}^n a_{si}^T E_{ti} a_{si} a_i \quad (4.20)$$

$$r_s(x) = \sum_{i=1}^n a_{si}^T E_{ti} a_i \quad (4.21)$$

where, the cross-sectional area $A(x) = \sum_{i=1}^n a_i$. For nonlinear analysis, the force-displacement relationship at the element level is commonly expressed in terms of an incremental form such that $\Delta p = k_e \Delta u$ where k_e is the element tangent stiffness matrix. Once $v_s(x)$, is determined, the section stiffness $k_s(x)$ and resisting forces $r_s(x)$ are

evaluated. Subsequently, the element stiffness (k_e) and resisting forces (r_e) are derived from the principle of virtual work and can be expressed as follows:

$$k_e = \int_L T^T(x) k_s(x) T(x) dx + \int_L C^T(x) C(x) N_s(x) dx \quad (4.22)$$

$$r_e = \int_L T^T(x) r_s(x) dx \quad (4.23)$$

where $T(x) = B(x) + G(x)$, $N_s(x)$ is a component of $r_s(x)$ representing the axial force resultant and L is the element length. Formulations for fibre based element are summarized in Lee and Mosalam (2004). Five integration points are used in the present study as suggested by Kunnath (2007).

4.4.4 Analysis

All the analyses (NTHA and POA) in the present study are carried out using OpenSees based on the algorithm developed by Mazzoni and McKenna (available from: <http://opensees.berkeley.edu/>), where the following objects have to be specified to perform analyses:

- i) CONSTRAINTS handler – This object deals with the boundary conditions and imposed displacements. The constraint handler object determines how the constraint equations are enforced in the analysis. Constraint equations enforce a specified value for degrees of freedom (DOF) or a relationship between DOFs. The DOF can be broken down into the retained DOF's and the condensed DOF's. In this study transformation constraints that transforms the stiffness matrix by condensation of constrained degrees of freedom is used for NTHA whereas plain constraints are used for pushover analysis.
- ii) DOF NUMBERER – It determines the mapping between equation numbers and DOF in the domain. *i.e.*, how the DOFs are numbered. In this study Reverse

Cuthill-McKee algorithm (RCM) is used, which renumbers the DOF to minimize the matrix band-width.

- iii) SYSTEM – It describes how to store and solve the system of equations in the analysis. There are different solvers available in OpenSees, each solver is tailored to a specific matrix topology. In this study, BandGeneral solver is used which represents direct solver for banded unsymmetric matrices.
- iv) ALGORITHM - It determines the sequence of steps taken to solve the non-linear equation. Newton algorithm uses the tangent at the current iteration to iterate to convergence and the tangent is updated at each iteration. This algorithm is used in the present study for POA. Modified-Newton algorithm is used for gravity load analysis that precedes the NTHA. Modified-Newton-Raphson method uses the tangent stiffness of the first iteration to iterate to convergence in all the iterations.
- v) INTEGRATOR- This object deals with the direct time integration method for NTHA. The Integrator object is used for the following: In this study Newmark Integrator is used that considers average acceleration in one time step of analysis as per Newmark's method. Newmark parameter γ and β are considered as 0.5 and 0.25, respectively (Chopra, 2012).
- vi) ANALYSIS- It defines the type of analysis to be performed. There the tree types of analysis possible in OpenSees: such as, static, transient and variable transient analysis. Transient analysis is considered for NTHA in this study that has constant time steps.
- vii) CONVERGENCE TEST – It deals with the convergence of iteration steps. This command requires a convergence tolerance (TolDynamic) and the maximum number of iterations (maxNumIterDynamic) to be performed before 'failure to convergence' is returned. Ten (10) iterations and a convergence tolerance of 10^{-8}

are used in the study. Dynamic test type is set to EnergyIncr, it specifies a tolerance on the inner product of the unbalanced load and displacement increments at the current iteration type and the flag used to print information on convergence is set to “0” to print the minimum output. Numeric representation for CONVERGENCE TEST in Opensees is available in Lee and Mosalam (2006).

In order to have statistically significant conclusions the number of analyses planned to be carried out in the present study was very high. Therefore, parallel computing is utilised for running NTHAs for various frames to reduce the analysis running time. OpenSees Laboratory tool developed by McKenna *et al.* (2014) that has the facility to use parallel computing is used in the present study. Depending upon the complexity of the job and the analysis running time, the required number of processors can be chosen. Table 4.1 shows the details of presently available venues, number of processors and wall time in NEEShub (<https://nees.org/>) for parallel computing. These venues were used in the present study according to the slot availability, size of the analyses and user feasibility.

Table 4.1: Details of computer processor available in NEEShub

Venue	Maximum number of effective CPUs (ncpus)	Maximum number of nodes (nn)	Maximum number of tasks per node (ppn)	Maximum wall time (hr:min:sec)
Stampede	4096	256	16	24:00:00
Kraken	512	42	12	24:00:00
Hansen	48	12	4	720:00:00
Carter	64	4	16	72:00:00
Local	16	1	16	24:00:00

4.5 VALIDATION STUDY

The modelling and analysis techniques used in the present study are discussed in the previous sections. A validation is undertaken to ensure the applicability of these

approaches. Three experiments (one seismic excitation test and two pseudo dynamic tests) on reinforced concrete structures available on literature are selected for the validation study. Following sections presents the results obtained from the numerical studies comparing the experimental responses.

4.5.1 Validation I: One storey one bay RC infilled frame

The pseudo-dynamic experimental test carried out by Colangelo (1999, 2004) on single storey infilled plane frame as shown in Fig. 4.8 is chosen for validating the computational model. The frame was tested with a pseudo-dynamic load using the E-W component of the 1976 Friulli earthquake as shown in Fig. 4.9.

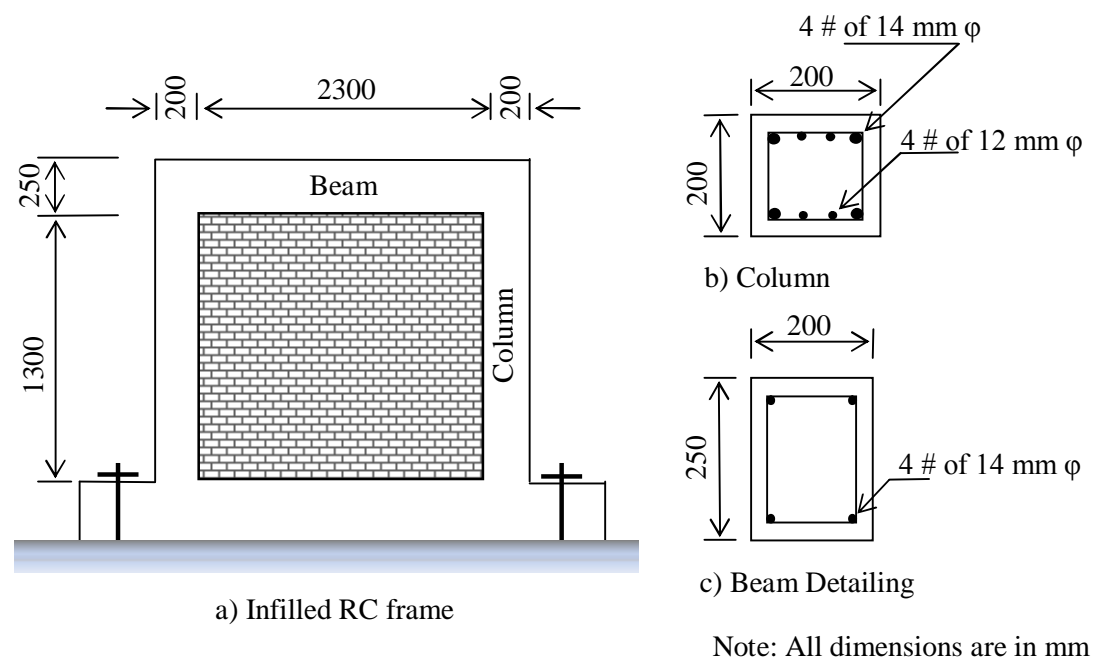


Fig. 4.8: Infilled frame tested by Colangelo (1999)

Detailed description of the test-rig, the material properties, as well as the loading regime, can be found in Biondi *et al.* (2000) and Seismosoft (2013). The nonlinear pseudo-dynamic time history analysis is conducted and the base shear time histories are recorded. Fig. 4.10 shows the comparison between the base shear time history obtained from the

experimental study and the present computational study. It can be seen that the two results match closely.

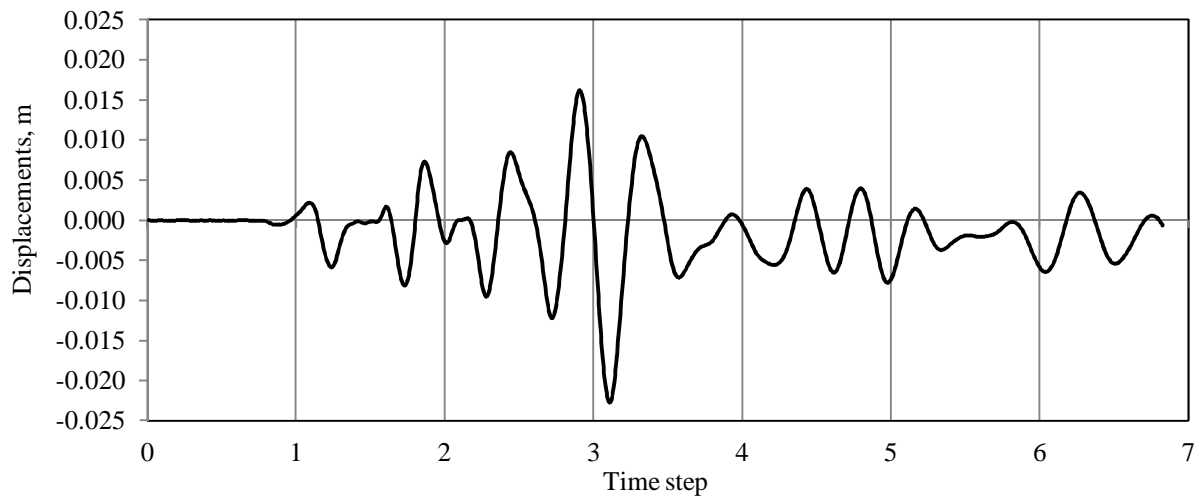


Fig. 4.9: Displacement history E-W component of Friulli earthquake (1976)

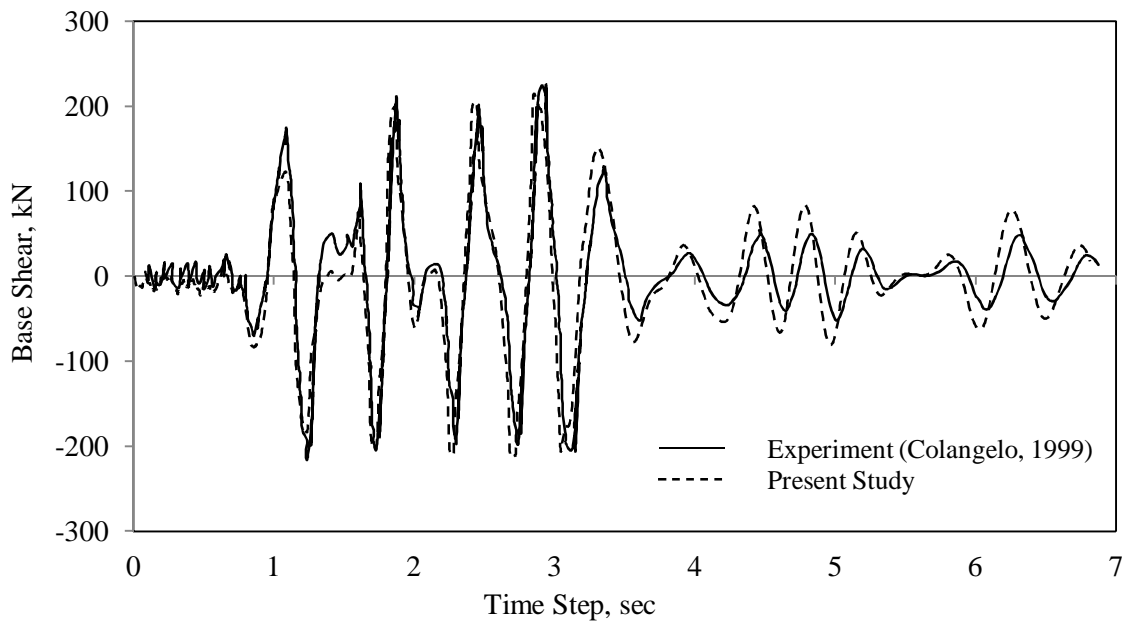


Fig. 4.10: Comparison of base shear histories obtained from experimental and computational study.

4.5.2 Validation II: Four storey three bay ICONS frame-bare and infilled frame

The pseudo-dynamic experimental test conducted at European Laboratory for Structural Assessment (ELSA test laboratory) on four storey three bay, RC full scale frames (ICON

frame – bare and infilled) are considered. The building frames are tested under two subsequent unidirectional pseudo-dynamics loading, first using Acc-475 input motion and then the Acc-975 input motion. Detailed description of the test specimens, material properties and the loading schemes are available in Pinho and Elnashai, 2000 and SeismoStruct verification report (2013). The test specimens are modeled in OpenSEES as per the approach explained in Section 4. The nonlinear pseudo-dynamic time history analysis for the record, Acc-475 is conducted. Acc-475 time history record is shown in Fig.4.11 and the top displacement time histories are recorded. Figs. 4.12 and 4.13 show the comparisons between the roof displacement histories obtained in present computational study and from the experimental study, for the bare and infilled frames respectively.

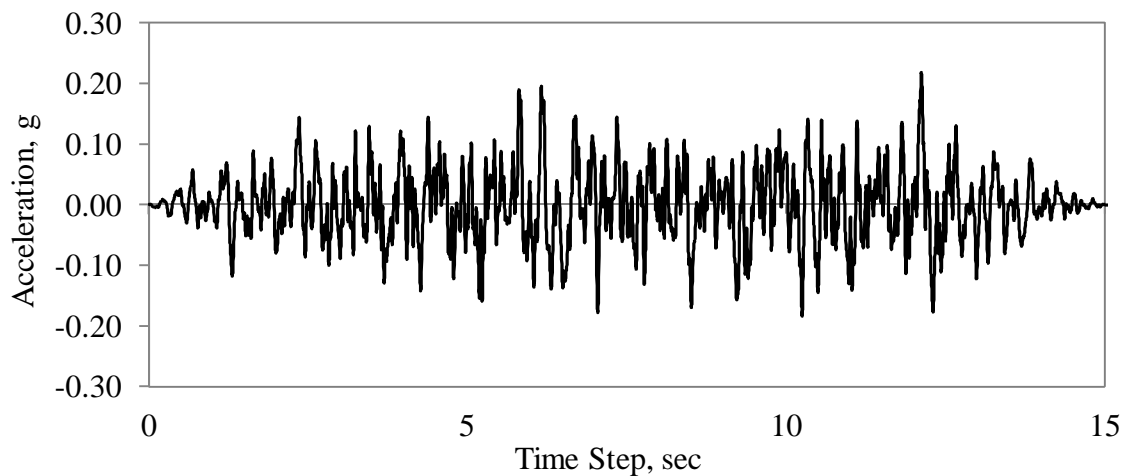


Fig. 4.11: Time history analysis of the record, Acc-475

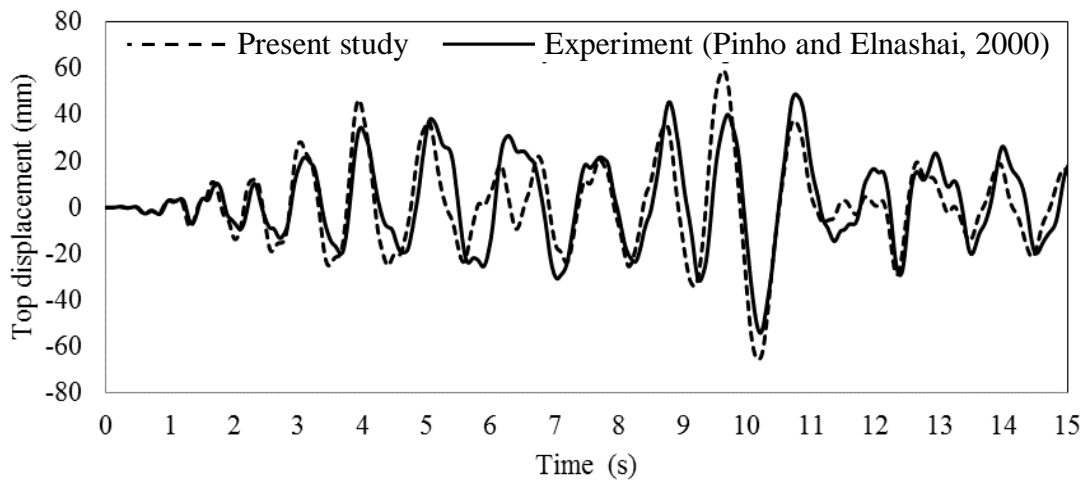


Fig. 4.12: Comparison of roof displacement time histories for ICON frame - Bare

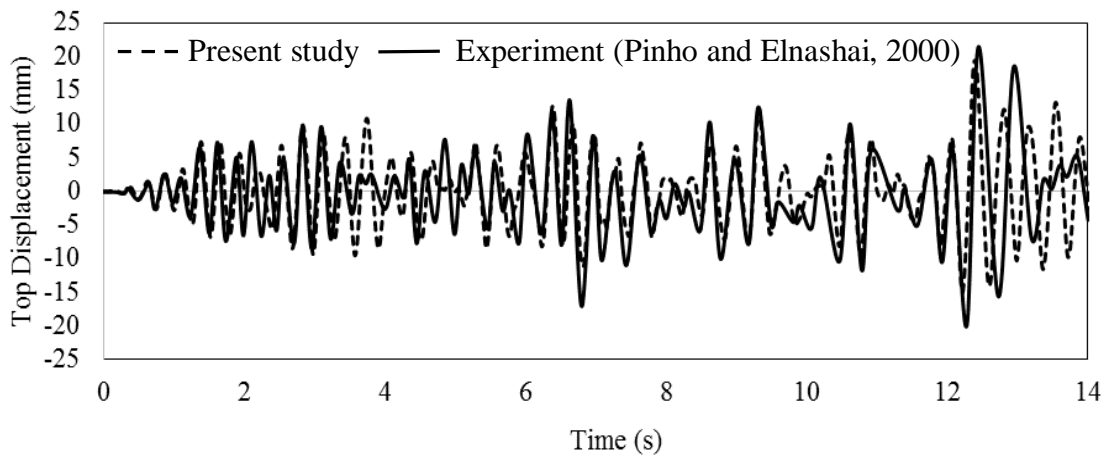


Fig. 4.13: Comparison of roof displacement history for ICON infilled frame

From these studies, it is clear that the computational model and the analysis procedure adopted in the present study yields the reasonably accurate behaviour of structures when subjected to dynamic and pseudo-dynamic loading.

4.6 INDIAN SEISMIC CODE DESIGN

The two different linear analysis methods recommended in IS 1893 (2002) are Equivalent Static Method (ESM) and Response spectrum method. Any one of these methods can be used to calculate the expected seismic demands on the lateral load resisting elements. Present work is based on ESM and it is explained in this section

In the ESM, the lateral force equivalent to the design basis earthquake is applied statically. The equivalent lateral forces at each storey level are applied at the design ‘centre of mass’ locations. It is located at the design eccentricity from the calculated ‘centre of rigidity (or stiffness)’.

4.6.1 Seismic weight

The seismic weight of each floor of the structure includes the dead load and fraction of the live load (as per Table 8 of IS 1893, 2002) acting on the floor. The weight of the columns and walls (up to the tributary height) are to be included. The tributary height is between the centreline of the storey above and centre line of the storey below.

4.6.2 Lumped mass

The lumped mass is the total mass of each floor that is lumped at the design centre of mass of the respective floor. The total mass of a floor is obtained from the seismic weight of that floor.

4.6.3 Calculation of lateral forces

The base shear ($V = V_B$) is calculated as per Clause 7.5.3 of IS 1893 (2002).

$$V_B = A_n W \quad (4.24)$$

$$A_n = \left(\frac{Z}{2} \right) \frac{I}{R} \frac{S_a}{g} \quad (4.25)$$

where, W = seismic weight of the building, Z = zone factor, I = importance factor, R = response reduction factor, S_a / g = spectral acceleration coefficient determined from Figure 4.14, corresponding to an approximate time period (T_a) which is given by

$$T_a = 0.075 h^{0.75} \text{ for RC moment resisting frame without masonry infill} \quad (4.26a)$$

$$T_a = \frac{0.09h}{\sqrt{d}} \text{ for RC moment resisting frame with masonry infill} \quad (4.26b)$$

The base dimension of the building at the plinth level along the direction of lateral forces is represented as d (in metres) and height of the building from the support is represented as h (in metres). The response spectra functions can be calculated as follows:

For Type I soil (rock or hard soil sites):

$$\frac{S_a}{g} = \begin{cases} 1+15T & 0.00 \leq T \leq 0.10 \\ 2.50 & 0.10 \leq T \leq 0.40 \\ \frac{1}{T} & 0.40 \leq T \leq 4.00 \end{cases}$$

For Type II soil (medium soil):

$$\frac{S_a}{g} = \begin{cases} 1+15T & 0.00 \leq T \leq 0.10 \\ 2.50 & 0.10 \leq T \leq 0.55 \\ \frac{1.36}{T} & 0.55 \leq T \leq 4.00 \end{cases}$$

For Type III soil (soft soil):

$$\frac{S_a}{g} = \begin{cases} 1+15T & 0.00 \leq T \leq 0.10 \\ 2.50 & 0.10 \leq T \leq 0.67 \\ \frac{1.67}{T} & 0.67 \leq T \leq 4.00 \end{cases}$$

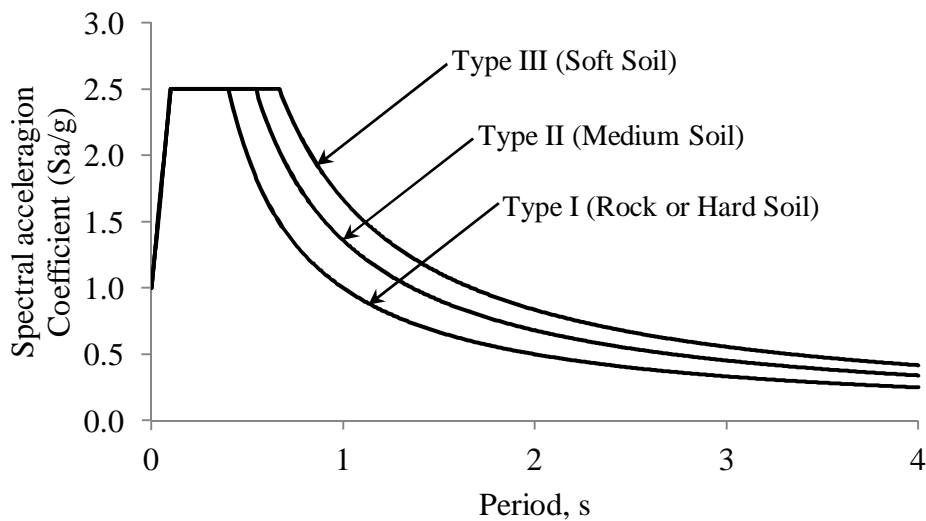


Fig. 4.14: Response spectra for 5 percent damping (IS 1893, 2002)

The design base shear is to be distributed along the height of building as per Clause 7.7.1 of IS 1893 (2002). The design lateral force at floor i is given as follows

$$Q_i = V_B \frac{W_i h_i^2}{\sum_{j=1}^n W_j h_j^2} \quad (4.27)$$

Here W_i = Seismic weight of floor i , h_i = Height of floor measured from base, n = Number of storeys in the building equal to the number of levels at which masses is located (Figure 4.15).

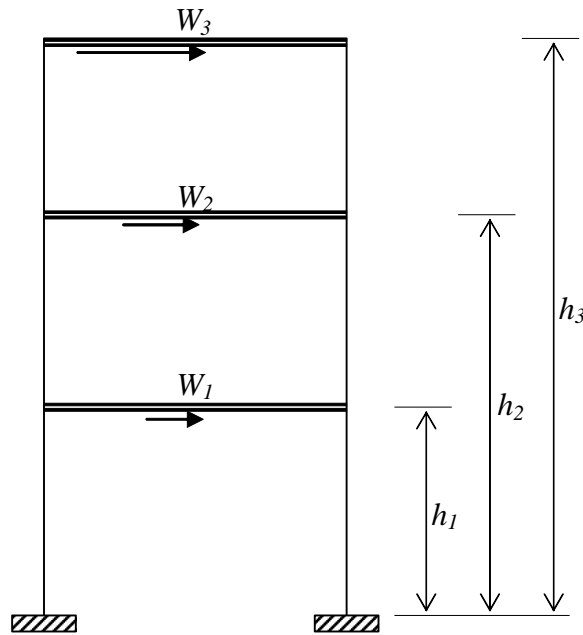


Fig. 4.15: Building model under seismic load

4.6.4 Load Combinations

The analysis results are to be for the following load combinations (IS 1893, 2002):

$$\text{COMB1} = 1.5(\text{DL} + \text{IL})$$

$$\text{COMB2} = 1.2(\text{DL} + \text{IL} + \text{EL})$$

$$\text{COMB3} = 1.2(\text{DL} + \text{IL} - \text{EL})$$

$$\text{COMB4} = 1.5(\text{DL} + \text{EL})$$

$$\text{COMB5} = 1.5(\text{DL} - \text{EL})$$

$$\text{COMB6} = 0.9\text{DL} + 1.5\text{EL}$$

$$\text{COMB7} = 0.9\text{DL} - 1.5\text{EL}$$

Here, DL = Dead load, IL = Live load, and EL = Earthquake Load. The dead load and the live load are taken as per IS 875, 1987. When the lateral load resisting elements are not orthogonally oriented, the design forces along two horizontal orthogonal directions (X- and Y-) should be considered. One method to consider this is the following.

- 100% of the design forces in X-direction and 30% of the design forces in Y-direction.
- 100% of the design forces in Y-direction and 30% of the design forces in X-direction.

An alternative method to consider the effect of the forces along X- and Y- directions is the square root of the sum of the squares (SRSS) basis.

$$EL = \sqrt{EL_x^2 + EL_y^2} \quad (4.28)$$

The vertical component is considered only for special elements like horizontal cantilevers in Zones IV and V. The maximum value of a response quantity from the above load combinations gives the demand.

4.7 FRAMES CONSIDERED

The building frame considered for numerical analysis in the present study is designed for the highest seismic zone (zone V with PGA of 0.36g) as per Indian standard IS 1893 (2002) considering medium soil conditions (N-value of 10 to 30). The characteristic strength of concrete and steel are taken as 25MPa and 415MPa respectively. The

buildings are assumed to be symmetric in plan, and hence a single plane frame is considered to be representative of the building along one direction. Typical bay width and column height in this study are selected as 5m and 3.2m respectively, as observed from the study of typical existing residential buildings. A configuration of building storey height ranging from 2 storeys to 8 storeys are considered in the present study with two bays for two, four and six storey frames and four bays for eight storey frame.

The dead load of the slab (5 m × 5 m panel) including floor finishes is taken as 3.75 kN/m² and live load as 3 kN/m². The design base shear (V_B) is calculated as per equivalent static method (IS 1893, 2002) as shown in Table 4.2. The structural analysis for all the vertical and lateral loads is carried out by ignoring the infill wall strength and stiffness (conventional). The design of the RC elements are carried out as per IS 456 (2000) and detailed as per IS 13920 (1993).

In order to study the effect of MF values on the probability of failure of OGS building, different MF values such as 1.5, 2.0, 2.5 and 3.0 are considered to design the columns of ground storey and/or storeys above.

Fully infilled (F) frame and bare frame (B) are also considered in the study for comparison which are designed without applying any MF (MF = 1.0). Depending on the number of storeys, value of MF at the design stage and the modelling of infill walls during nonlinear analysis, various naming schemes are introduced to represent all the frames considering in the present study. For the frames designated as ‘O’ (Open Ground Storey) and ‘F’ (Fully Infilled Frames), the stiffness and strength of the infill walls are modelled in the nonlinear analysis. As different MF values are used in the different stories, subscripts are used to represent the MF values in the corresponding stories differentiate between each OGS frame.

For example, NO_{x,y} indicates, a frame having ‘N’ number of storey with Open Ground Storey having MF in the ground storey as ‘x’ and that used in the first storey as ‘y’. Figs. 4.16- 4.19 show all frames with various MF values and infill wall configurations considered in the study along with their designations. Appendix B summarizes the details of columns and beam sections of each frame.

Table 4.2: Design base shear details of selected frames

Frame Identity	Height (m)	Base Dimension (m)	Fundamental Period as per IS 1893 (s)	Seismic Weight (kN)	Base Shear (kN)
2-storey	6.40	10	0.302	835	75
4-storey	12.8	10	0.508	1811	163
6-storey	19.2	10	0.688	2787	198
8-storey	25.6	20	0.854	7405	425

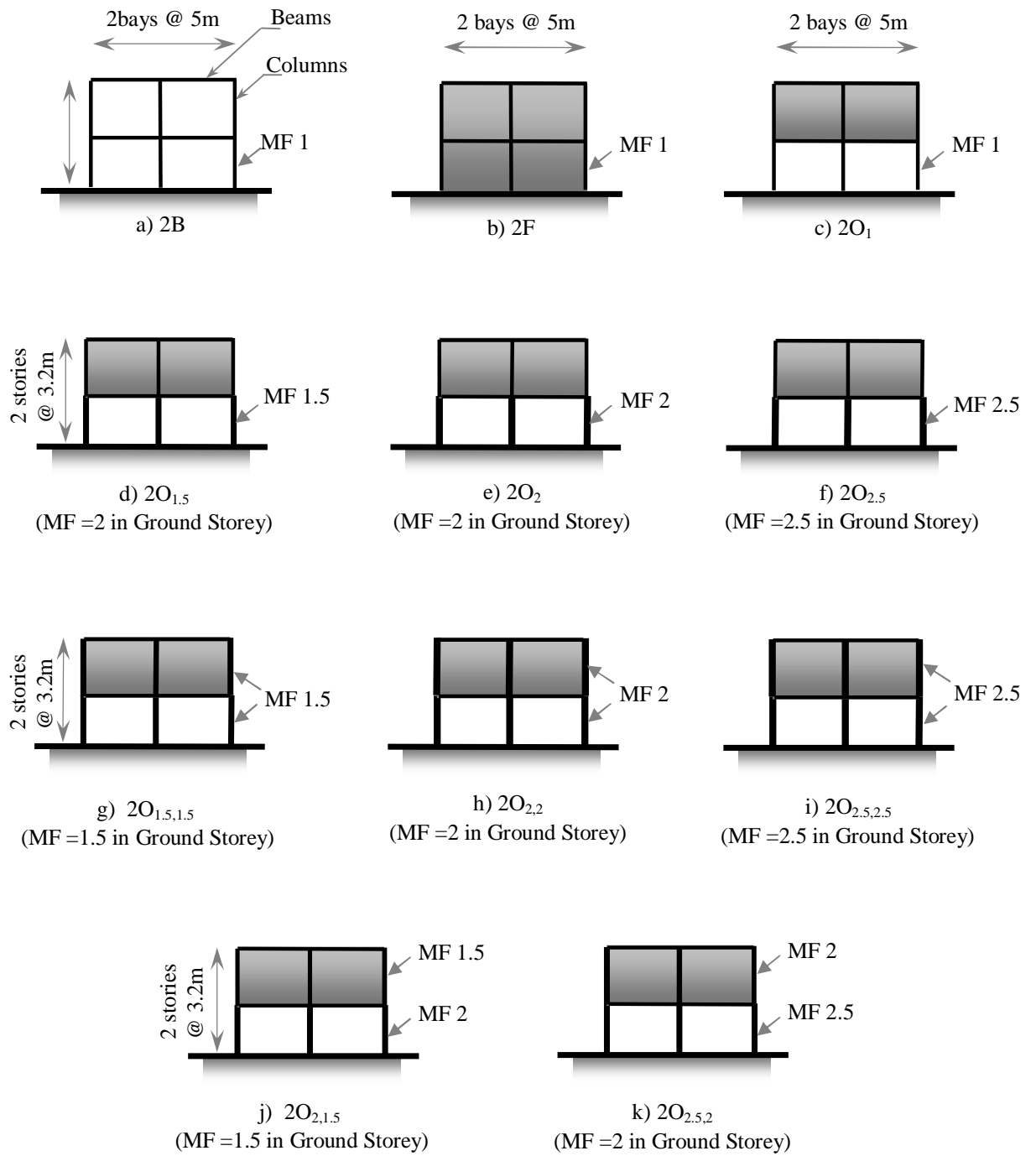


Fig. 4.16: Configurations of selected frames: Two-storeyed

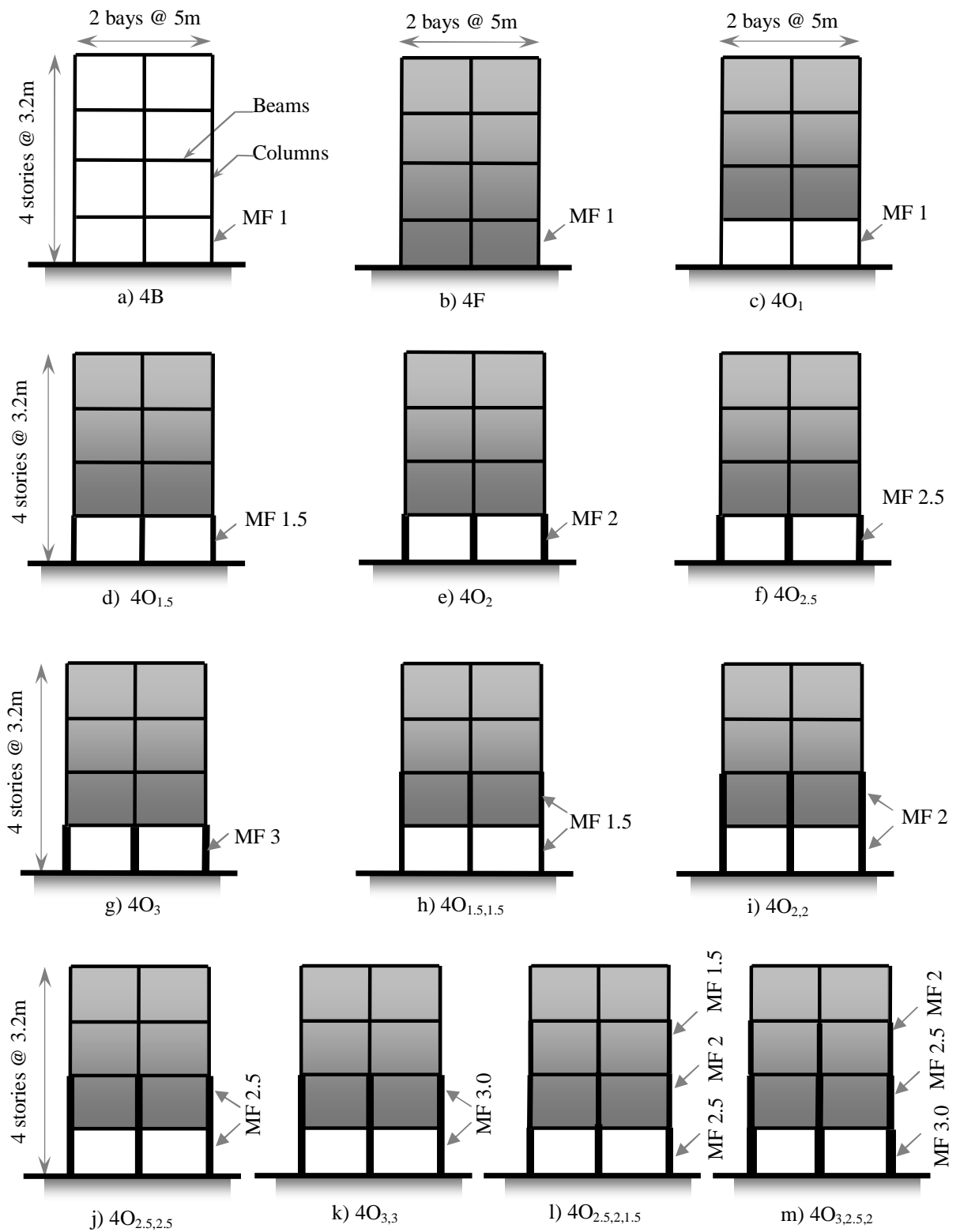


Fig. 4.17: Configurations of selected frames: Four-storeyed

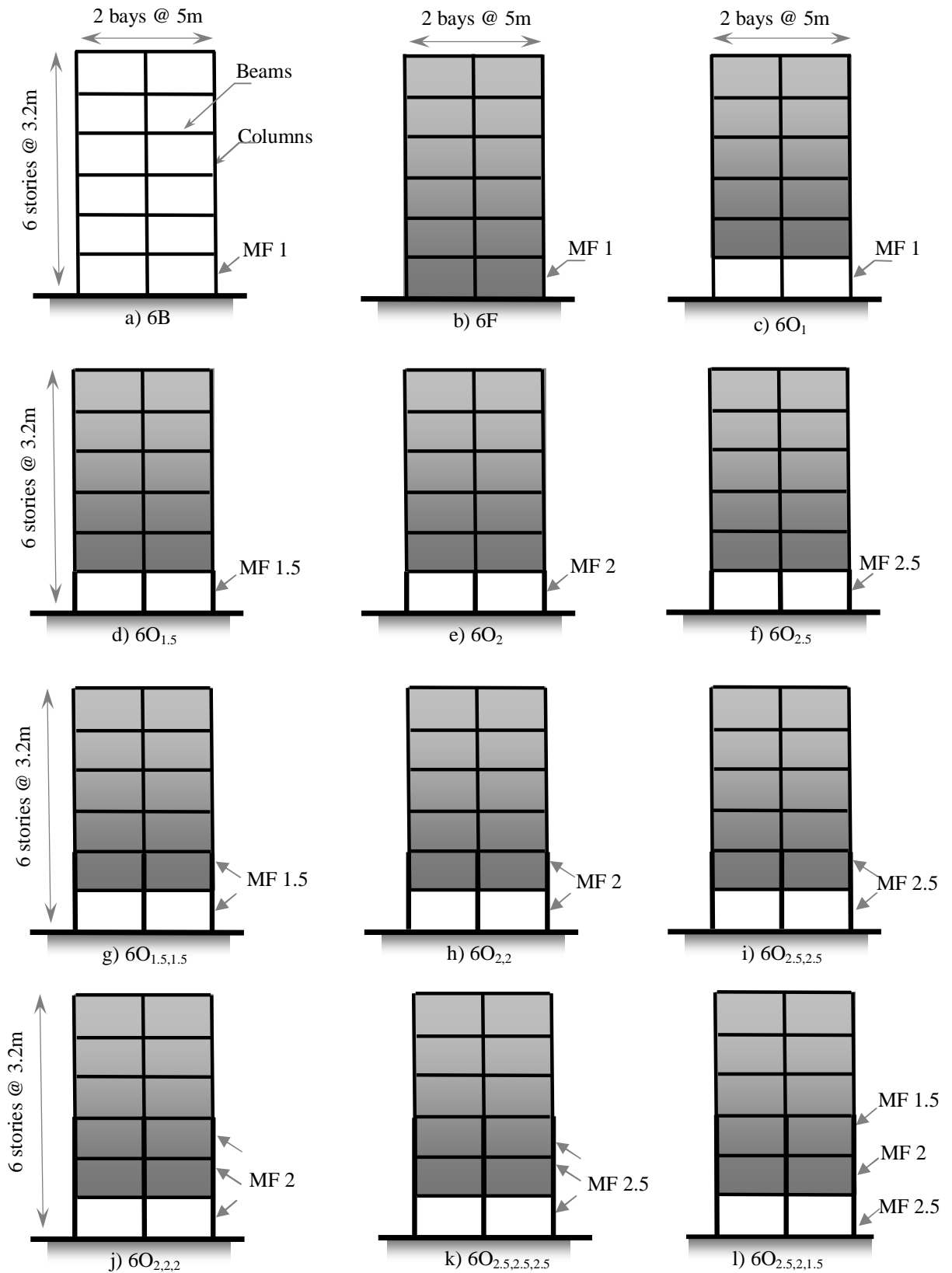


Fig. 4.18: Configurations of selected frames: Six-storied

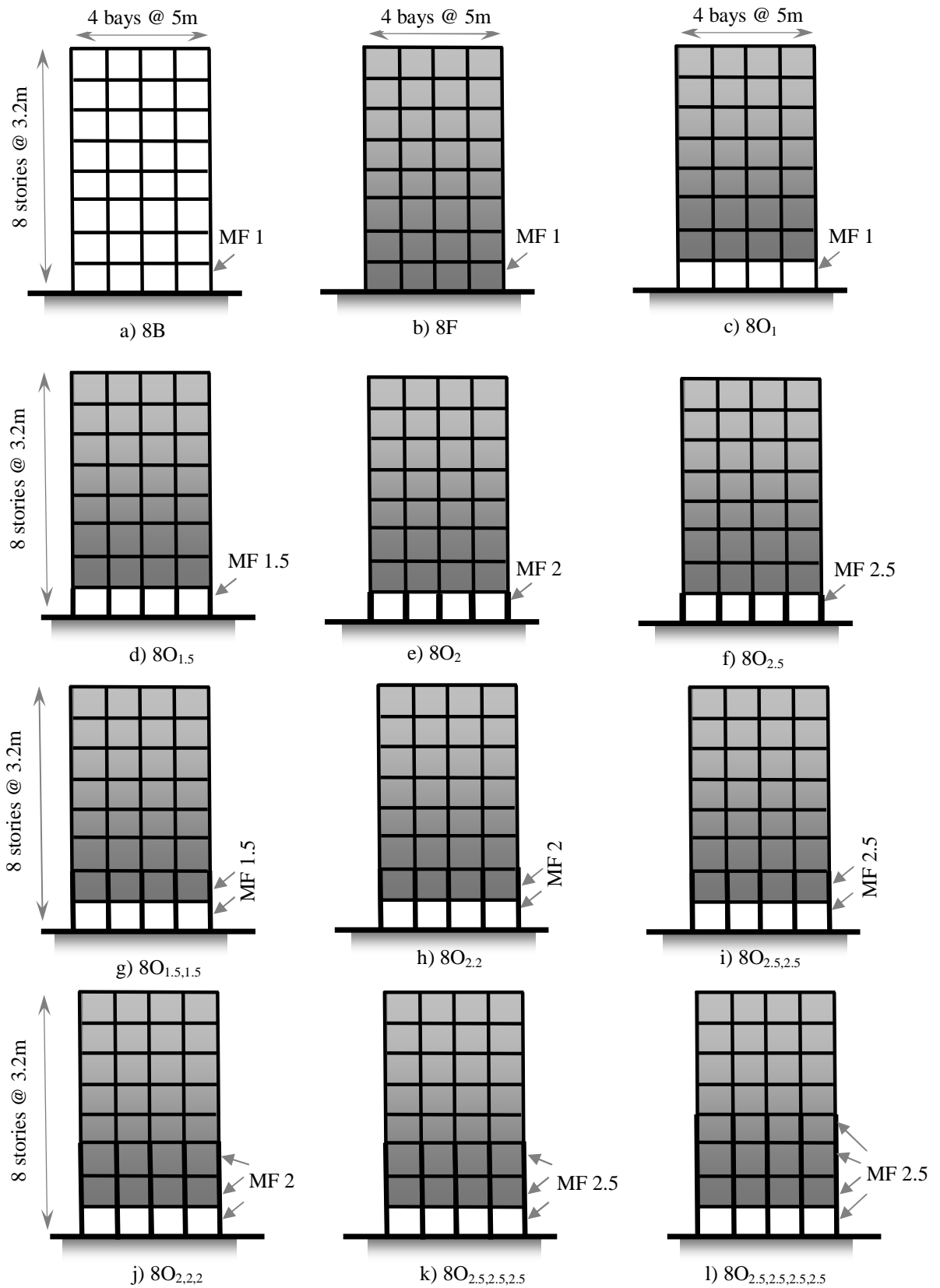


Fig. 4.19: Configurations of selected frames: Eight-storeyed

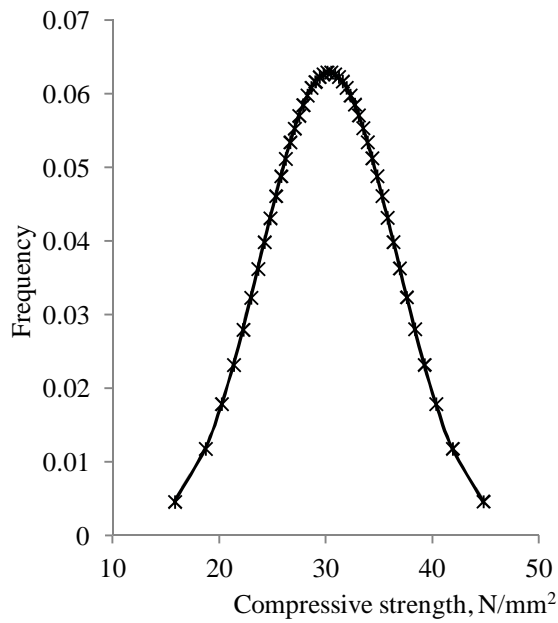
4.8 LATIN HYPERCUBE SAMPLING

In this study uncertainties are adopted based on LHS scheme as discussed in the Section 3.4. Several parameters are considered as random variables such as characteristic strength of concrete (f_{ck}), yield strength of the steel, (f_y), shear strength of masonry (f_m) and global damping ratio (ζ). Mean and co-efficient of variations of each property are shown in the Table 4.3. Statistical parameters for concrete and steel are adopted from Ranganathan (1999), for masonry taken from Agarwal and Thakkar (2001). Mean value for damping ratio for RC structures is assumed to be 5% as per IS-1893 (2002) and coefficient of variation is taken from Davenport and Carroll (1986).

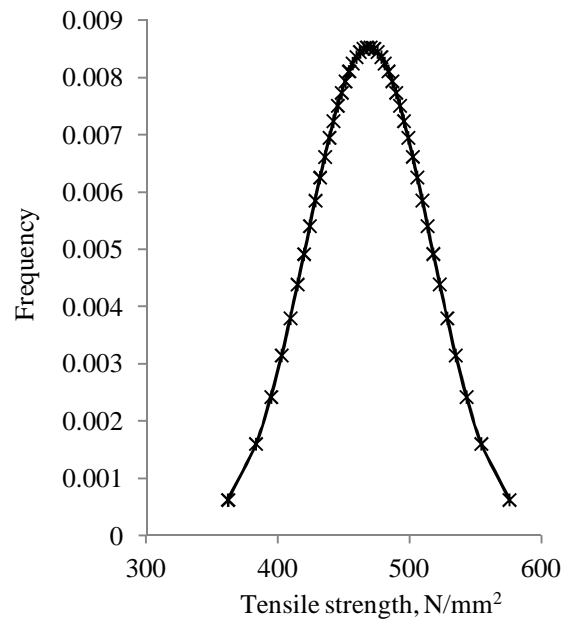
Table 4.3: Details of random variables used in LHS scheme

Material/Property	Variable	Mean	COV (%)	Distribution	Remarks
Concrete	f_{ck}	30.28 MPa	21	Normal	Uncorrelated
Steel	f_y	468.90 MPa	10	Normal	Uncorrelated
Global Damping ratio	ζ	5%	40	Normal	Uncorrelated
Masonry (Shear Strength)	τ_c	0.2041 MPa	12	Normal	Uncorrelated

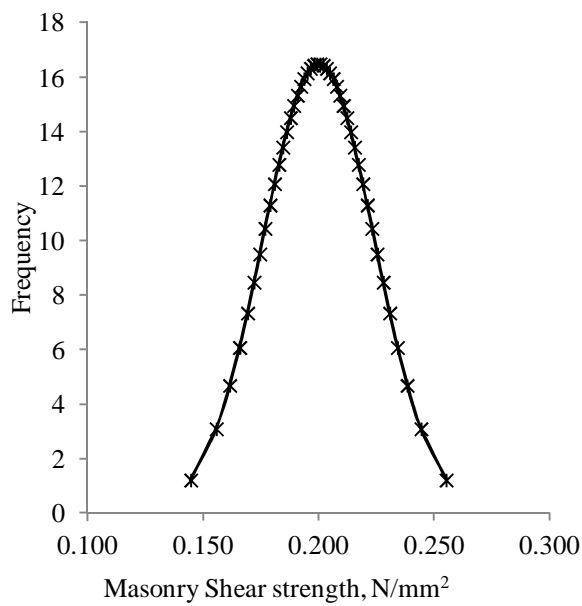
A set of models are generated based on LHS scheme and the stress-stain curves are developed for each samples. Fig. 4.20 shows the distribution of random variables generated based on LHS. Fig. 4.21 presents the stress-strain relation in compression for confined and unconfined concrete, steel reinforcement and masonry strut. Stress-strain curves for steel reinforcement in tension are identical to those shown in Fig. 4.20c. 44 numbers of models are generated to represent each of the selected building frames considering these parameters selected randomly.



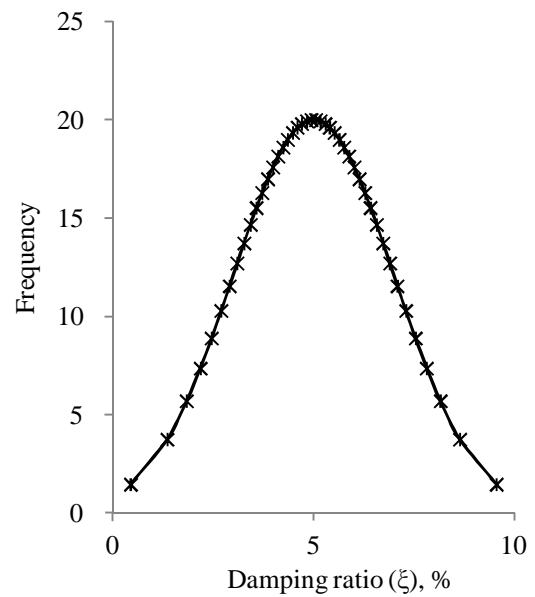
a) Concrete



b) Reinforcements



c) Masonry



d) Damping Ratio

Fig. 4.20: PDF Distribution for random variables and selected points based on LHS scheme

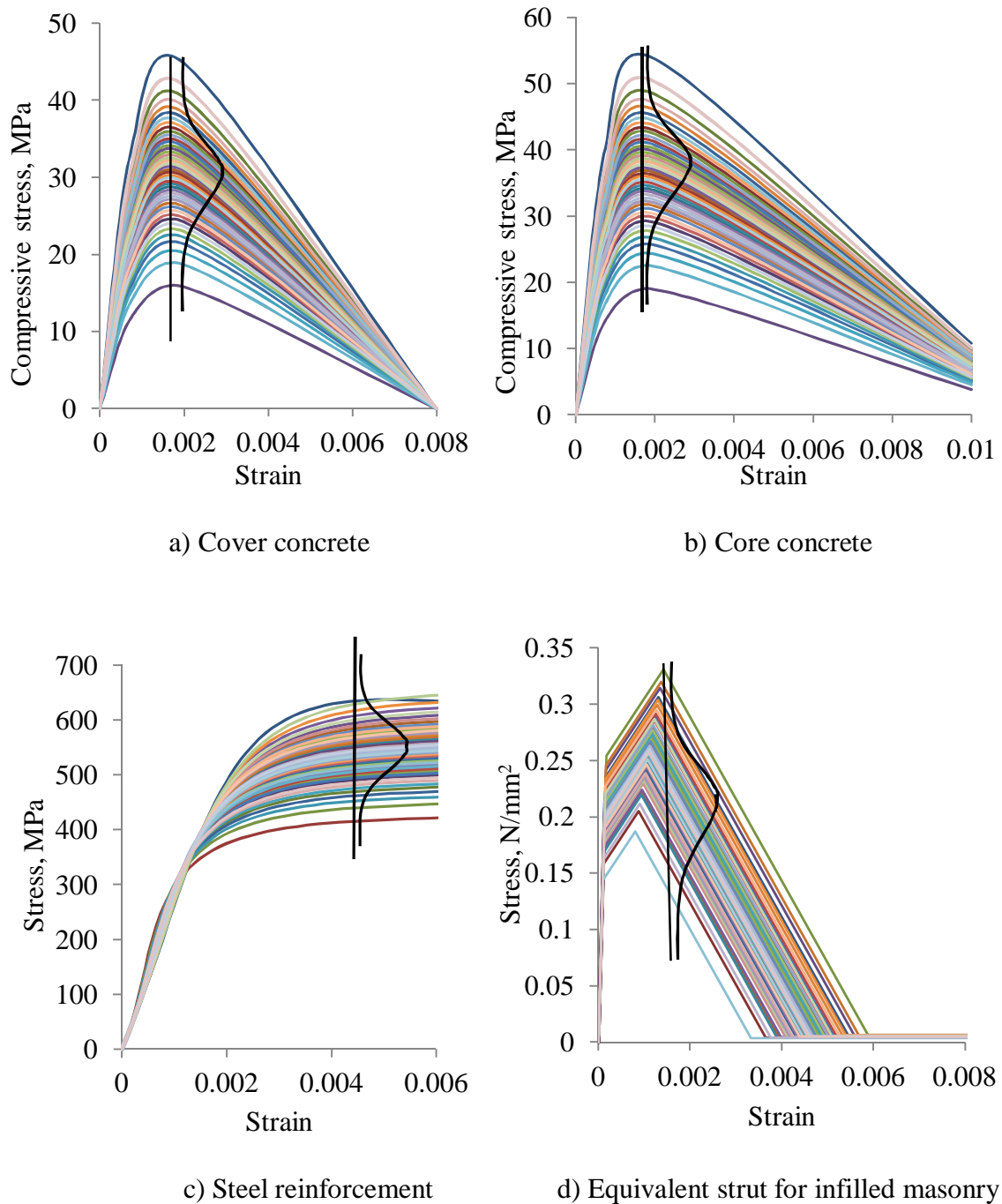


Fig. 4.21: Envelope Stress vs. Strain Curve for 44 models developed according LHS Scheme

4.9 LIMIT STATE CAPACITIES (S_c)

In seismic risk assessment, demand is compared with capacity for different limit states to develop fragility curves. Several literatures and codes (such as ASCE/SEI 41-06: 2007; Ghojarah, 2000; etc.) define capacities for RC moment resisting frames with and without

infill walls. However, these recommendations cannot be adopted for Indian code designed frames due to differences in material properties, construction qualities, loading conditions and other parameters. To define limit state capacity of building, FEMA HAZUS-MH (2003) suggests to perform a pushover analysis considering first mode shape as lateral load pattern and from resulting pushover curves limit states capacities can be identified. Similarly, N2 method (Fajfar, 2000) combines pushover analysis of a multi-degree-of-freedom (MDOF) model with the response spectrum analysis of an equivalent single-degree-of-freedom (SDOF) system and calculates the limit state capacities from resultant pushover curves. Rajeev and Tesfamariam (2012) reported that, HAZUS does not consider the presence of different irregularities (including soft storey) in the assessment; as a result, it can underestimate the level of expected losses. These methods define the limit state capacities globally and cannot consider the presence of irregularities in different storeys. To overcome this problem, pushover analyses are carried out in each storey level to define the capacities of each storey in terms of inter storey drifts. Then fragility curves are drawn separately for each storey levels from the results of NTHA. The three different limit states *DL*, *SD* and *CP* as discussed in Chapter 3 is used in the present study. Figs. 4.22-4.23 present the limit state capacities of individual storey for bare frame and fully infilled frame respectively. For the bare frame, the *DL* limit state is assumed to be attained at the yield displacement of the idealized pushover curve. In the case of infilled frames, the *DL* limit state is attained at the deformation when the last infill in a storey starts to degrade (Dolsek & Fajfar, 2008). Whereas for *SD* and *CP* level for bare and infilled frames are assumed to be same.

In this study different frames designed with various MF schemes are considered as explained in the Section 4.7. Pushover analyses are carried out for each storey to find out the storey capacities by modelling the mean values of material properties. The procedure

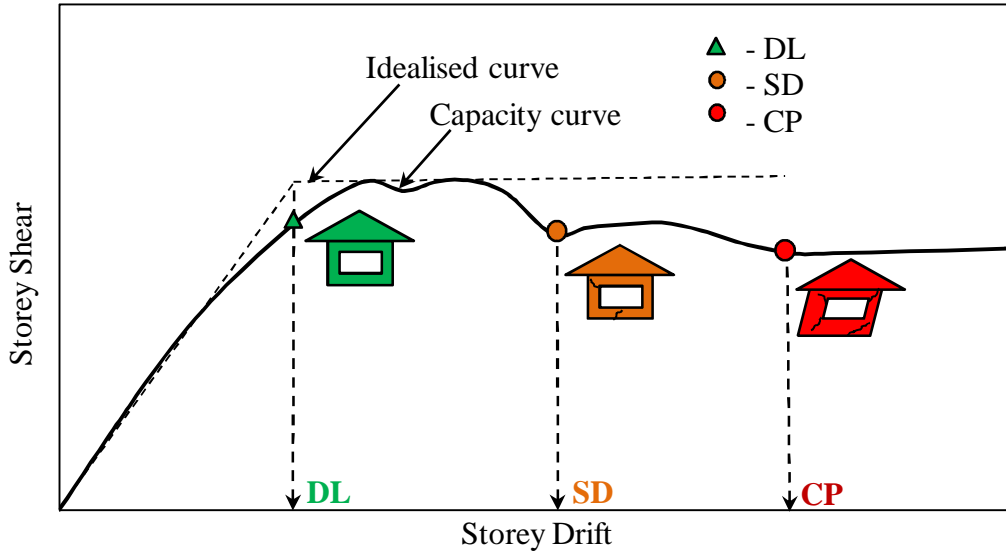


Fig. 4.22: Typical performance levels for bare frame

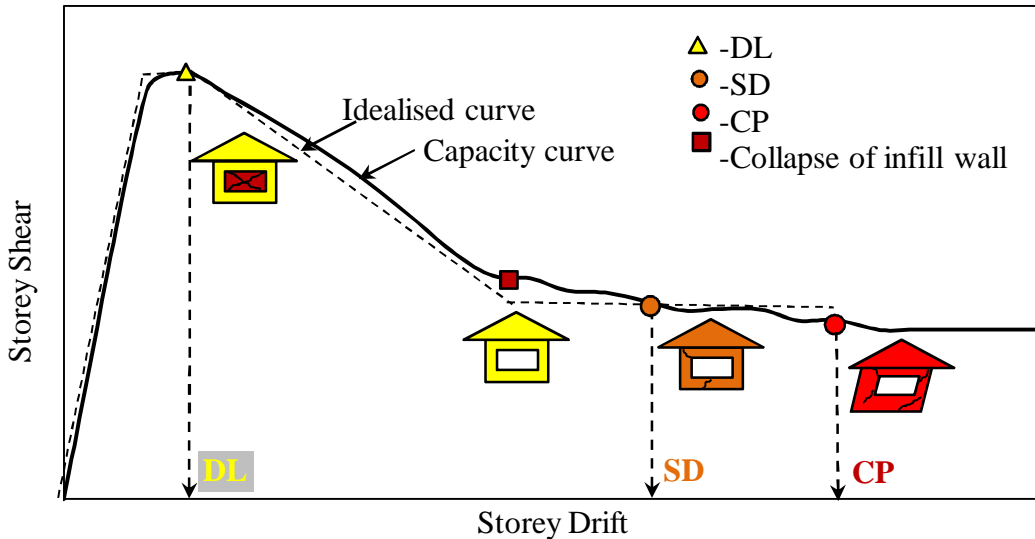


Fig. 4.23: Typical performance levels for fully infilled frame

is demonstrated in Fig 4.24 with a typical frame ($4O_1$). The boundary conditions of the frame, pushover load profile and the corresponding storey capacity curves in terms of storey shear vs. storey drift are shown. Capacity curve is idealised as bilinear curve for storeys without infill wall whereas it is idealised as quadric-linear curve for infilled storey. The three different limit state capacities DL , SD and CP are found out and marked in the capacity curve of each storey. Similarly, storeys limit state capacities for all the selected frames are calculated and shown in the Tables 4.4-4.7.

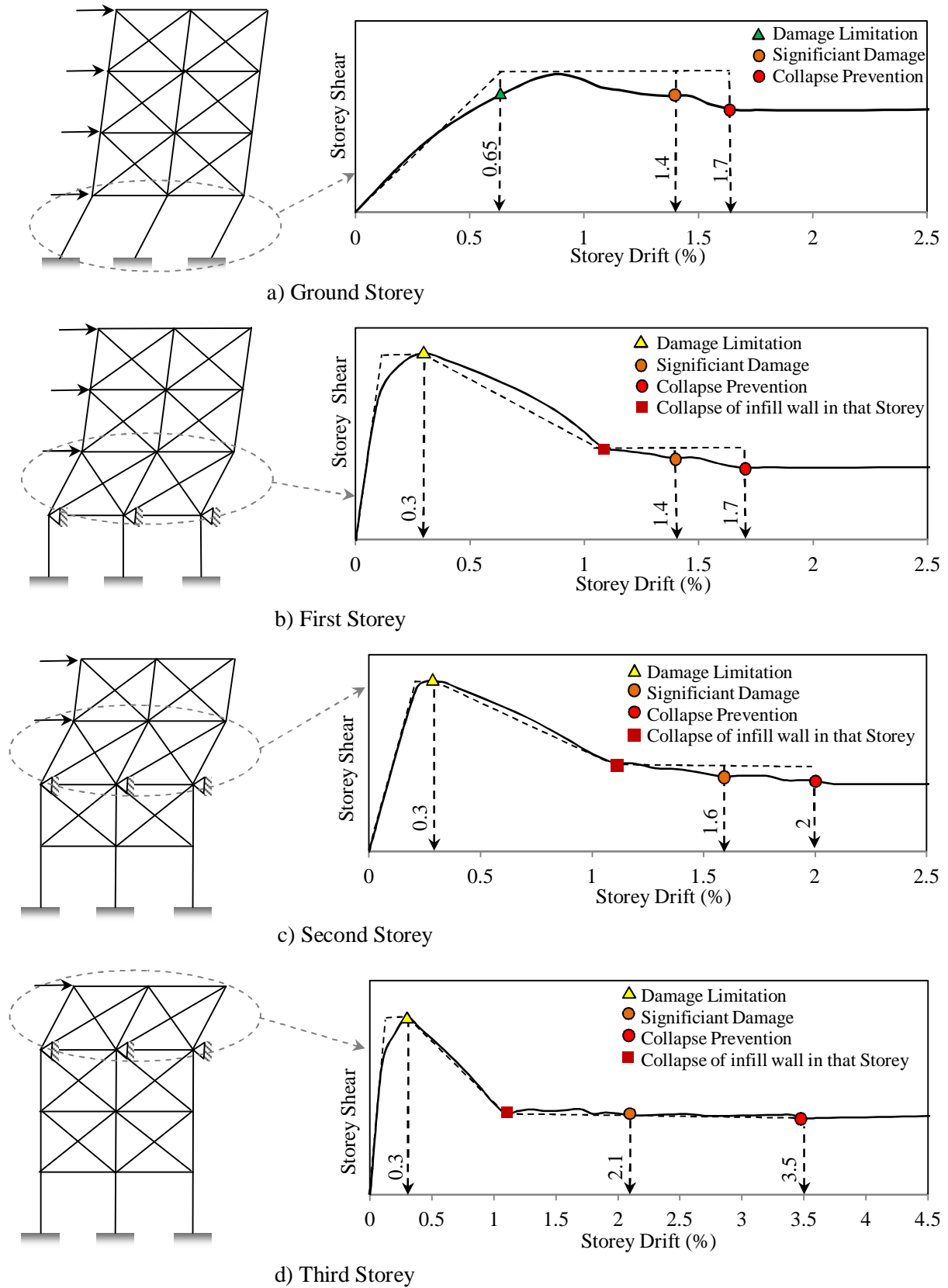


Fig. 4.24: Evaluation of storey limit state capacity for typical frame (4O₁)

Table 4.4: Limit State Capacities for 2-storey frames

Frame Identity	Storey level	ISD (%)		
		DL	SD	CP
2B	G*	1.3	2.7	3.4
	I st	0.9	2.3	2.9
2F	G	0.3	1.7	2.4
	I st	0.3	1.9	2.9
2O	G	0.8	1.8	2.3
	I st	0.3	1.9	2.9
2O _{1.5}	G	0.65	1.9	2.2
	I st	0.3	1.9	2.9
2O ₂	G	0.7	1.7	2.4
	I st	0.3	1.9	2.9
2O _{2.5}	G	0.65	1.5	2.4
	I st	0.3	1.9	2.9
2O _{1.5,1.5}	G	0.65	1.9	2.2
	I st	0.3	2.0	3.3
2O _{2,2}	G	0.7	1.7	2.4
	I st	0.3	1.9	2.4
2O _{2.5,2.5}	G	0.65	1.5	2.4
	I st	0.3	1.9	2.3
2O _{2,1.5}	G	0.7	1.7	2.4
	I st	0.3	2.0	3.3
2O _{2.5,2}	G	0.65	1.5	2.4
	I st	0.3	1.9	2.9

*G-Ground

Table 4.5: Limit State Capacities for 4-storey frames

Frame Identity	Storey level	ISD (%)		
		DL	SD	CP
4B	G	0.65	1.3	1.9
	I st	0.65	1.3	1.9
	II nd	0.65	1.8	2.4
	III rd	0.8	2.1	3.5
4F	G	0.3	1.4	1.7
	I st	0.3	1.4	1.7
	II nd	0.3	1.6	2.0
	III rd	0.3	2.1	3.5
4O ₁	G	0.65	1.4	1.7
	I st	0.3	1.4	1.7
	II nd	0.3	1.6	2.0
	III rd	0.3	2.1	3.5
4O _{1.5}	G	0.65	1.3	1.9
	I st	0.3	1.4	1.7
	II nd	0.3	1.6	2.0
	III rd	0.3	2.1	3.5
4O ₂	G	0.7	1.7	2.3
	I st	0.3	1.4	1.7
	II nd	0.3	1.6	2.0
	III rd	0.3	2.1	3.5
4O _{2.5}	G	0.7	1.7	2.3
	I st	0.3	1.4	1.7
	II nd	0.3	1.6	2.0
	III rd	0.3	2.1	3.5
4O ₃	G	0.65	1.7	2.3
	I st	0.3	1.4	1.7
	II nd	0.3	1.6	2.0
	III rd	0.3	2.1	3.5

Frame Identity	Storey level	ISD (%)		
		DL	SD	CP
4O _{1.5,1.5}	G	0.65	1.3	1.9
	I st	0.3	1.4	2.0
	II nd	0.3	1.6	2.0
	III rd	0.3	2.1	3.5
4O _{2,2}	G	0.7	1.7	2.3
	I st	0.3	1.4	2.4
	II nd	0.3	1.6	2.0
	III rd	0.3	2.1	3.5
4O _{2.5,2.5}	G	0.7	1.7	2.3
	I st	0.3	1.4	2.4
	II nd	0.3	1.6	2.0
	III rd	0.3	2.1	3.5
4O _{3,3}	G	0.65	1.7	2.3
	I st	0.3	1.4	2.4
	II nd	0.3	1.6	2.0
	III rd	0.3	2.1	3.5
4O _{2.5,2,1.5}	G	0.7	1.7	2.3
	I st	0.3	1.4	2.4
	II nd	0.3	1.6	2.0
	III rd	0.3	2.1	3.5
4O _{3,2.5,2}	G	0.65	1.7	2.3
	I st	0.3	1.4	2.4
	II nd	0.3	1.6	2.0
	III rd	0.3	2.1	3.5

Table 4.6: Limit State Capacities for 6-storey frames

Frame Identity	Storey level	ISD (%)		
		DL	SD	CP
6B	G	0.5	1.25	1.7
	I st	0.5	1.25	1.7
	II nd	0.5	1.25	1.7
	III rd	0.6	1.9	2.4
	IV th	0.65	2.0	2.8
	V th	0.65	2.3	2.8
6F	G	0.6	1.2	1.5
	I st	0.6	1.2	1.5
	II nd	0.6	1.2	1.5
	III rd	0.3	1.3	1.7
	IV th	0.3	1.7	2.3
	V th	0.3	2.0	2.8
6O ₁	G	0.5	1.0	1.5
	I st	0.6	1.2	1.5
	II nd	0.6	1.2	1.5
	III rd	0.3	1.3	1.7
	IV th	0.3	1.7	2.3
	V th	0.3	2.0	2.8
6O _{1.5}	G	0.75	1.5	2
	I st	0.6	1.2	1.5
	II nd	0.6	1.2	1.5
	III rd	0.3	1.3	1.7
	IV th	0.3	1.7	2.3
	V th	0.3	2.0	2.8
6O ₂	G	0.6	1.3	1.5
	I st	0.6	1.2	1.5
	II nd	0.6	1.2	1.5
	III rd	0.3	1.3	1.7
	IV th	0.3	1.7	2.3
	V th	0.3	2.0	2.8
6O _{2.5}	G	0.6	1.2	1.5
	I st	0.6	1.2	1.5
	II nd	0.6	1.2	1.5
	III rd	0.3	1.3	1.7
	IV th	0.3	1.7	2.3
	V th	0.3	2.0	2.8
6O _{1.5,1.5}	G	0.75	1.5	2.0
	I st	0.6	1.4	1.9
	II nd	0.6	1.2	1.5
	III rd	0.3	1.3	1.7
	IV th	0.3	1.7	2.3
	V th	0.3	2.0	2.8

Frame Identity	Storey level	ISD (%)		
		DL	SD	CP
6O _{1.5,1.5}	G	0.75	1.5	2
	I st	0.6	1.4	1.9
	II nd	0.6	1.2	1.5
	III rd	0.3	1.3	1.7
	IV th	0.3	1.7	2.3
	V th	0.3	2.0	2.8
6O _{2,2}	G	0.6	1.3	1.5
	I st	0.6	1.3	1.6
	II nd	0.6	1.2	1.5
	III rd	0.3	1.3	1.7
	IV th	0.3	1.7	2.3
	V th	0.3	2.0	2.8
6O _{2.5,2.5}	G	0.6	1.2	1.5
	I st	0.6	1.2	1.5
	II nd	0.6	1.2	1.5
	III rd	0.3	1.3	1.7
	IV th	0.3	1.7	2.3
	V th	0.3	2.0	2.8
6O _{2,2,2}	G	0.6	1.3	1.5
	I st	0.6	1.3	1.6
	II nd	0.6	1.3	1.8
	III rd	0.3	1.3	1.7
	IV th	0.3	1.7	2.3
	V th	0.3	2.0	2.8
6O _{2.5,2.5,2.5}	G	0.6	1.2	1.5
	I st	0.6	1.2	1.5
	II nd	0.6	1.2	1.7
	III rd	0.3	1.3	1.7
	IV th	0.3	1.7	2.3
	V th	0.3	2.0	2.8
6O _{2.5,2,1.5}	G	0.6	1.2	1.5
	I st	0.6	1.3	1.6
	II nd	0.6	1.6	2
	III rd	0.3	1.3	1.7
	IV th	0.3	1.7	2.3
	V th	0.3	2.0	2.8

Table 4.7: Limit State Capacities for 8-storey frames

Frame Identity	Storey level	ISD (%)		
		DL	SD	CP
8B	G	0.9	2.0	3.2
	I st	0.9	1.9	2.4
	II nd	0.9	2.0	3.2
	III rd	0.9	1.7	3.2
	IV th	0.9	2.1	3.2
	V th	0.9	1.9	2.8
	VI th	0.9	1.9	2.8
	VII th	0.9	1.9	2.8
8F	G	0.6	2.0	3.2
	I st	0.6	1.9	2.4
	II nd	0.6	2.0	3.2
	III rd	0.6	1.7	3.2
	IV th	0.6	2.1	3.2
	V th	0.6	1.9	2.8
	VI th	0.6	1.9	2.8
	VII th	0.6	1.9	2.8
8O ₁	G	0.9	2.0	3.2
	I st	0.6	1.9	2.4
	II nd	0.6	2.0	3.2
	III rd	0.6	1.7	3.2
	IV th	0.6	2.1	3.2
	V th	0.6	1.9	2.8
	VI th	0.6	1.9	2.8
	VII th	0.6	1.9	2.8
8O _{1.5}	G	0.9	2.0	3.2
	I st	0.6	1.9	2.4
	II nd	0.6	2.0	3.2
	III rd	0.6	1.7	3.2
	IV th	0.6	2.1	3.2
	V th	0.6	1.9	2.8
	VI th	0.6	1.9	2.8
	VII th	0.6	1.9	2.8
8O ₂	G	0.9	1.9	3.2
	I st	0.6	1.9	2.4
	II nd	0.6	2.0	3.2
	III rd	0.6	1.7	3.2
	IV th	0.6	2.1	3.2
	V th	0.6	1.9	2.8
	VI th	0.6	1.9	2.8
	VII th	0.6	1.9	2.8
8O _{2.5}	G	0.9	1.9	3.2
	I st	0.6	1.9	2.4
	II nd	0.6	2.0	3.2
	III rd	0.6	1.7	3.2
	IV th	0.6	2.1	3.2
	V th	0.6	1.9	2.8
	VI th	0.6	1.9	2.8
	VII th	0.6	1.9	2.8
8O _{1.5,1.5}	G	0.9	1.9	3.2
	I st	0.6	1.9	2.4
	II nd	0.6	2.0	3.2
	III rd	0.6	1.7	3.2
	IV th	0.6	2.1	3.2
	V th	0.6	1.9	2.8
	VI th	0.6	1.9	2.8
	VII th	0.6	1.9	2.8
8O _{2,2}	G	0.9	1.9	3.2
	I st	0.6	1.9	2.4
	II nd	0.6	2.0	3.2
	III rd	0.6	1.7	3.2
	IV th	0.6	2.1	3.2
	V th	0.6	1.9	2.8
	VI th	0.6	1.9	2.8
	VII th	0.6	1.9	2.8
8O _{2.5,2.5}	G	0.9	1.9	3.2
	I st	0.6	1.9	2.4
	II nd	0.6	2.0	3.2
	III rd	0.6	1.7	3.2
	IV th	0.6	2.1	3.2
	V th	0.6	1.9	2.8
	VI th	0.6	1.9	2.8
	VII th	0.6	1.9	2.8
8O _{2,2,2}	G	0.9	1.9	3.2
	I st	0.6	1.9	2.4
	II nd	0.6	2.0	3.2
	III rd	0.6	1.7	3.2
	IV th	0.6	2.1	3.2
	V th	0.6	1.9	2.8
	VI th	0.6	1.9	2.8
	VII th	0.6	1.9	2.8

Table 4.7: Limit State Capacities for 8-storey frames (Continue)

Frame Identity	Storey level	ISD (%)			Frame Identity	Storey level	ISD (%)		
		DL	SD	CP			DL	SD	CP
8O _{2.5,2.5,2.5}	G	0.9	1.9	3.2	8O _{2.5,2.5,2.5,2.5}	G	0.9	1.9	3.2
	I st	0.6	1.9	2.4		I st	0.6	1.9	2.4
	II nd	0.6	2.0	3.2		II nd	0.6	2.0	3.2
	III rd	0.6	1.7	3.2		III rd	0.6	1.7	3.2
	IV th	0.6	2.1	3.2		IV th	0.6	2.1	3.2
	V th	0.6	1.9	2.8		V th	0.6	1.9	2.8
	VI th	0.6	1.9	2.8		VI th	0.6	1.9	2.8
	VII th	0.6	1.9	2.8		VII th	0.6	1.9	2.8

4.10 SELECTION OF APPROPRIATE INTENSITY MEASURE

In order to develop PSDMs and fragility curves different parameters can be used to represent the earthquake ground motion. Selection of this parameter (defines as intensity measure) may alter the resulting fragility curves. A list of such parameters used as intensity measures (*IM*) in previous research for development of fragility curves are as follows: peak ground acceleration (*PGA*), permanent ground deformation (*PGD*), spectral acceleration at a fundamental period ($S_a [T_1]$), etc. HAZUS (FEMA, 1997) used peak ground acceleration (*PGA*) and permanent ground deformation (*PGD*) as specific intensity measures. The latest version of HAZUS has switched to the use of $S_a [T_1]$ and *PGD*. Mackie and Stojadinovic (2003) identified 23 intensity measures that could be used for PSDMs of highway bridges. Nielson *et al.* (2005) used four different intensity measures to develop fragility curves for bridges.

However, commonly used *IMs* are *PGA* and $S_a [T_1]$ for buildings. To understand the sensitiveness of *IM*, fragility curves are developed considering these two *IMs* separately as per the methodology outlined in the Section 3.2.2. The resulting PSDM models and corresponding fragility curves are shown in Figs. 4.25 and 4.26 respectively for *PGA* and $S_a [T_1]$ as *IMs*. It can be seen from these figures that the trend of the fragility curves is same and there is no much differences in the exceedance probability.

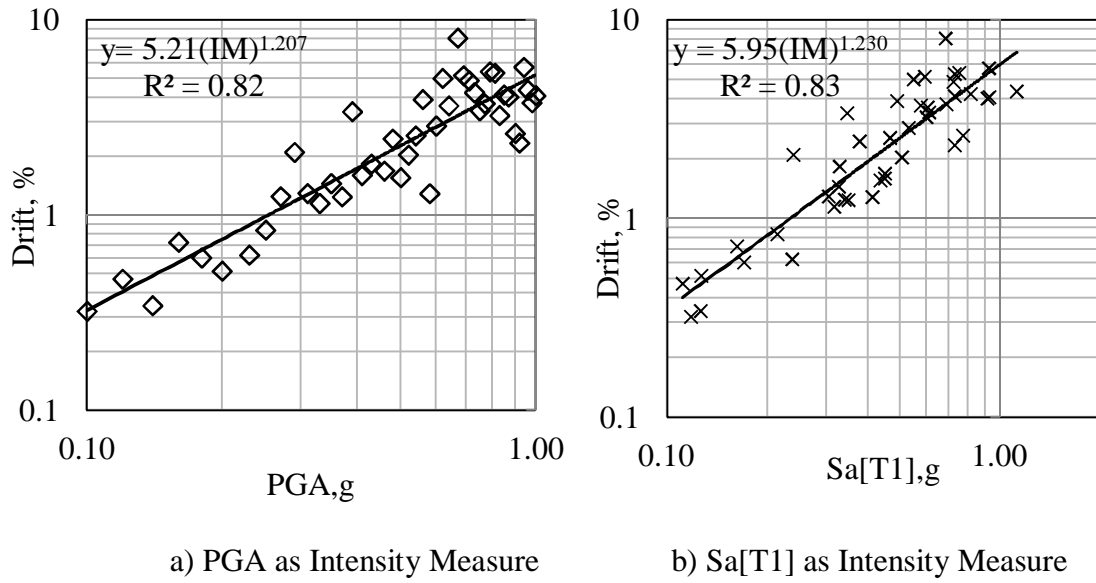


Fig. 4.25: PSDMs of selected bare frame (4B)

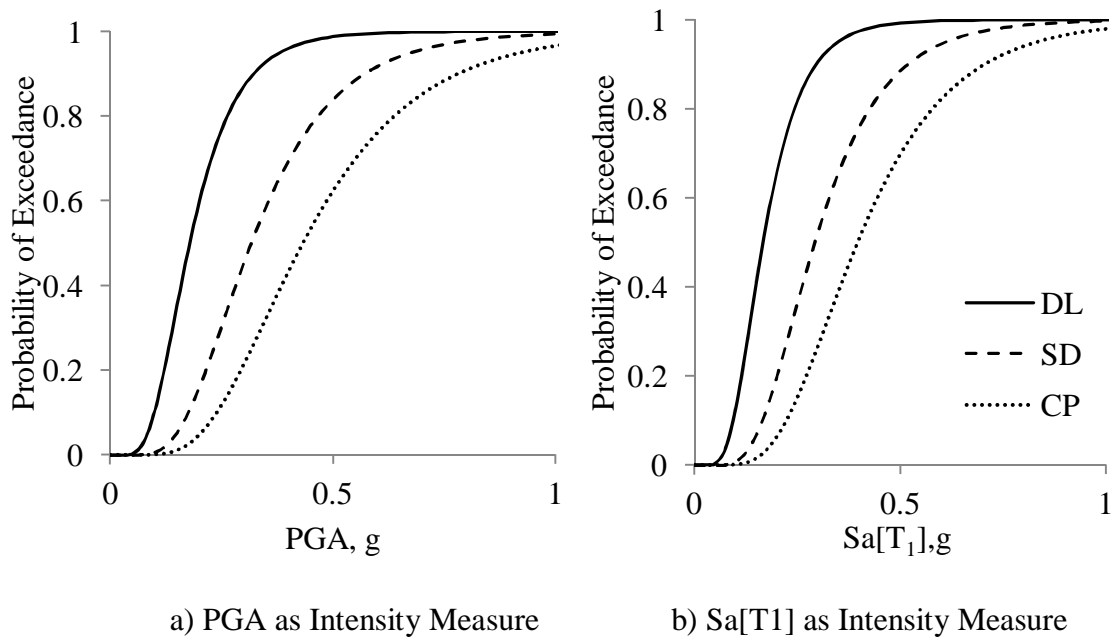


Fig. 4.26: Fragility Curves of selected bare frame (4B)

Scatter plot of selected earthquakes of different PGA and the corresponding Sa[T1] for a typical building frame is presented in Fig. 4.27. This figure shows that there is a linear relation exists between these two parameters. Therefore, the fragility curves developed using one of these two IMs can be converted to a fragility curve as a function of other IM.

Fig. 4.28 presents the fragility curves as a function of both of these two IMs developed using the fitted relation as given in Fig. 4.27.

It can be concluded from this results that the both PGA and Sa[T1] will result same fragility curves for RC framed buildings. The present study focuses on the evaluation of seismic risk which involves the fragility curves and seismic hazard curves. The standard seismic hazard curves in Indian region are available in terms of PGA, hence PGA is chosen as the IM in this study.

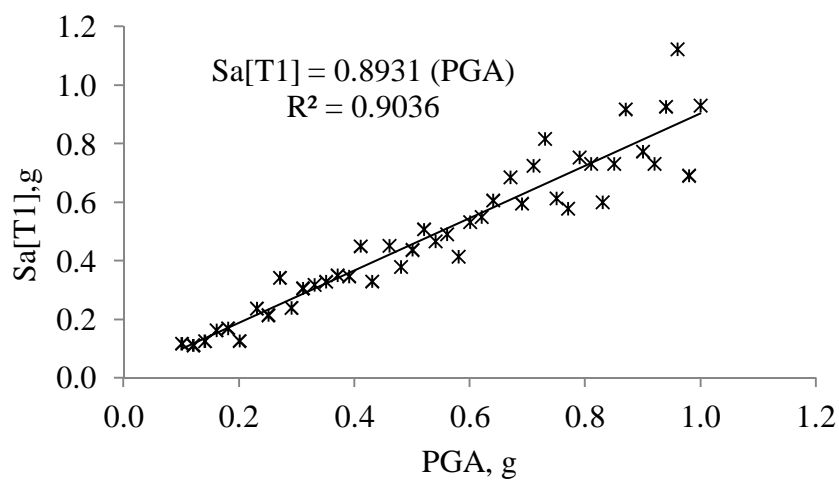


Fig. 4.27: Relation between Sa[T1] and PGA

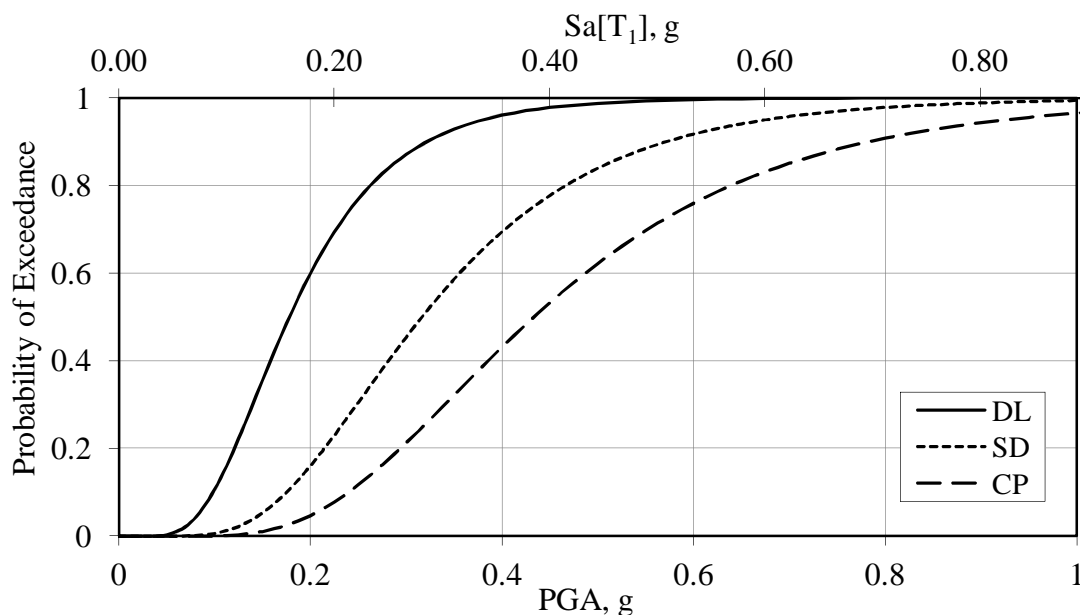


Fig. 4.28: Fragility curves of frame for different performance levels in terms of PGA and Sa[T1]

4.11 SELECTION OF GROUND MOTIONS

Uncertainty in the seismic load is considered in the study by the use of a suite of earthquake ground motions. Earthquake ground motions in a suite should be obtained from the past records of the region of interest. In this study, far-field earthquakes are chosen which represents that the building site is located at least 10km away from faults (Ravichandran and Klinger, 2012). Although India has experienced several major earthquakes in last few decades, the number of available earthquake records in Indian region is limited. Thirteen pairs of far field ground motion records of past earthquakes are only available for Indian region in CESMD website (<http://strongmotioncenter.org/>). A suite of these ground motions are considered for the present study. In order to have statistically sufficient number of ground motions a suite of synthetic ground motions with sufficiently large numbers of samples may be required for the analyses. Therefore, another suite of synthetic ground motions are generated in the present study NTHA of selected building model. The 22 pairs of far field natural ground motion records given in FEMA P695 (2012) are modified to match the design spectrum of Indian Standard IS 1893 (2002). Fragility curves of selected building frames are developed separately for the two suites of ground motions (natural and synthetic) for identifying the suite of ground motion that yields conservative results. This section discusses the details of the two suits of selected ground motions and compares the fragility curves obtained using these two suites of ground motions.

4.11.1 Natural Ground Motions from Indian Region

CESMD website has record of only thirteen earthquakes from Indian region. One pair of ground motion records from each earthquake is considered. These records with PGA ranging from 0.1g to 1.48g are selected for locations with hypo-central distance more

than 10 km. Table 4.8 presents the summary of these earthquakes. The detailed time-history data for these earthquakes are presented in Appendix-B. Response spectrums of these earthquakes are shown in Fig. 4.29 along with IS-1893 (2002) design spectrum.

Table 4.8: Selected Indian Ground motions events (<http://strongmotioncenter.org/>)

S.No	Event	Magnitude	PGA, g		Hypo-central distance (km)	Site Geology	Location
			Direction				
			I	II			
1	Chamoli Aftershock 1999-03-29	4.6	0.10	0.11	24.6	Rock	Gopeshwar, Uttarakhand
2	Chamoli 1999-03-28	6.6	0.16	0.22	123.7	Rock	Barkot, Uttarakhand
3	Chamba 1995-03-24	4.9	0.24	0.29	37.5	Rock	Rakh, Maharashtra
4	India-Burma Border 1995-05-06	6.4	0.30	0.42	261.9	Soil	Haflong, Assam
5	India-Burma Border 1987-05-18	5.9	0.46	0.39	155	Rock	Panimur, Assam
6	India-Burma Border 1990-01-09	6.1	0.55	0.6	233.5	Rock	Laisong, Assam
7	India-Bangladesh Border 1988-02-06	5.8	0.64	0.78	117.5	Rock	Khliehriat, Assam
8	Xizang-India Border 1996-03-26	4.8	0.76	0.37	49.9	Rock	Ukhimath, Uttarakhand
9	NE India 1986-09-10	4.5	0.88	0.87	50.9	Rock	Dauki, Uttar pradesh
10	India-Burma Border 1988-08-06	7.2	0.96	0.9	206.5	Rock	Hajadisa, Assam
11	Bhuj/Kachchh 2001-01-26	7.0	1.03	0.9	239	N/A	Ahmedabad Gujarat
12	Uttarkashi 1991-10-19	7.0	1.15	1.16	39.3	Rock	Ghansiali, Uttarakhand
13	India-Burma Border 1997-05-08	5.6	1.48	0.93	65.4	Soil	Silchar, Assam

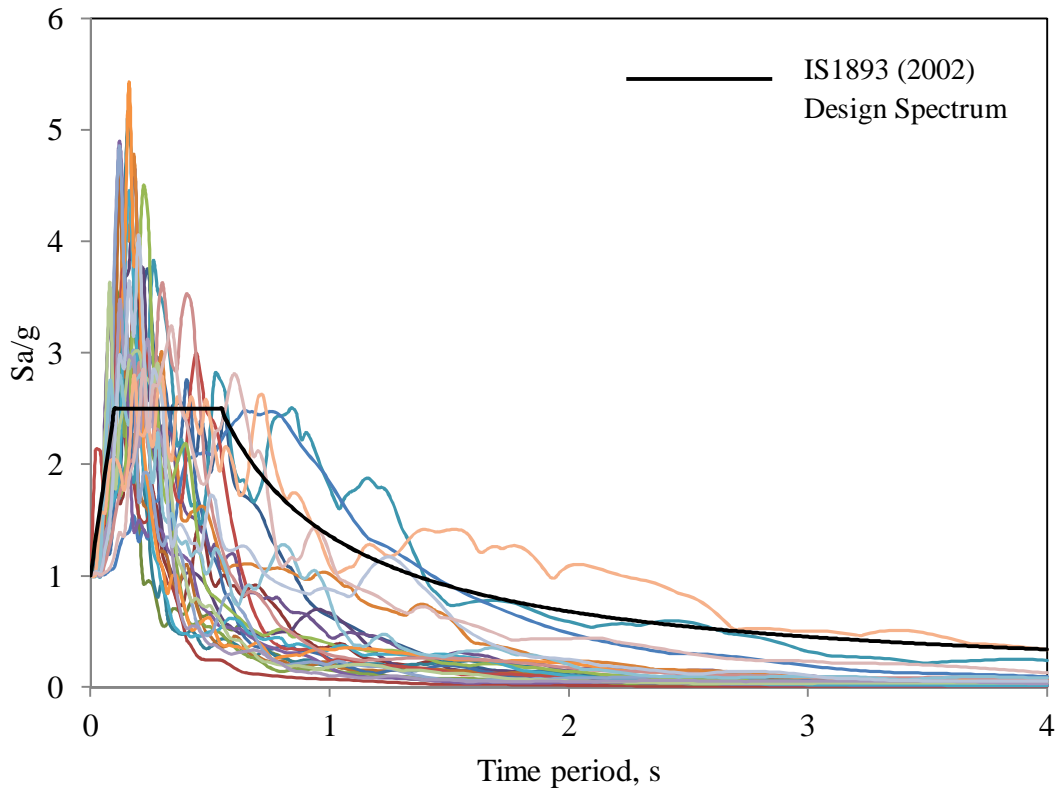


Fig.4.29: Response Spectra for natural ground motions

4.11.2 Synthetic Ground Motion Records

A suite of natural earthquake records from other regions are collected and converted to match the design spectrum of Indian Standard IS 1893 (2002). FEMA P695 (2012) has a of strong ground motion database for evaluation of building performances. The same database is also used by Haselton *et al.* (2012) and available in the website of California (http://www.csuchico.edu/structural/researchdatabases/ground_motion_sets.shtml) State University Chico. 22 pairs of available far-field ground motion records from this database are selected in this study. Table 4.9 presents the details of these 22 pairs of ground motion records. Following conditions were considered by FEMA P695 (2012) for selecting this set of earthquakes:

- i) Magnitude > 6.5 in Richter Scale
- ii) Distance from source to site > 10 km

- iii) Peak ground acceleration $> 0.2g$ and peak ground velocity > 15 cm/sec. Soil shear wave velocity in upper 30m of soil > 180 m/s
- iv) Limit of six records from a single seismic event, if more than six records pass the initial criteria, then the six records with largest PGV are selected, but in some cases a lower PGV record is used if the PGA is much larger.
- v) Lowest useable frequency < 0.25 Hz, to ensure that the low frequency content was not removed by the ground motion filtering process
- vi) Strike-slip and thrust faults

These earthquakes are converted to match with design spectrum of Indian Standard IS 1893 (2002) using a computer program WavGen, developed by Mukherjee and Gupta (2002). It decomposes a recorded accelerogram into a finite number of time histories with energy in non-overlapping frequency bands and scales these time histories up/down iteratively such that the assembled time-history is compatible with a specified design spectrum. Details about the generation of synthetic accelerogram can be found in Mukherjee and Gupta (2002). Fig. 4.30 shows the response spectrums of all 22 pairs of converted ground motions along with design spectrum of Indian standards. These accelerograms are said to be synthetic accelerograms, which are later scaled linearly varying PGA from 0.1g to 1g for NTHA. Acceleration vs. time data for all the synthetic ground motion records are presented in Appendix C.

Table 4.9: Far-field ground motions events suggested by FEMA P695 (2012).

S.No	Event	Magnitude	PGA, g		Epicentral distance (km)	Source (Fault Type)	Recording station
			Direction				
			I	II			
1	Northridge 1994	6.7	0.42	0.52	13.3	Thrust	Beverly Hills -
2	Northridge 1994	6.7	0.41	0.48	26.5	Thrust	Canyon Country-
3	Duzce, Turkey 1999	7.1	0.73	0.82	41.3	Strike-slip	Bolu
4	Hector Mine 1999	7.1	0.27	0.34	26.5	Strike-slip	Hector
5	Imperial Valley	6.5	0.24	0.35	33.7	Strike-slip	Delta
6	Imperial Valley	6.5	0.36	0.38	29.4	Strike-slip	El Centro Array #11
7	Kobe, Japan 1995	6.9	0.51	0.5	8.7	Strike-slip	Nishi-Akashi
8	Kobe, Japan 1995	6.9	0.24	0.21	46	Strike-slip	Shin-Osaka
9	Kocaeli, Turkey 1999	7.5	0.31	0.36	98.2	Strike-slip	Duzce
10	Kocaeli, Turkey 1999	7.5	0.22	0.15	53.7	Strike-slip	Arcelik
11	Landers 1992	7.3	0.24	0.15	86	Strike-slip	Yermo Fire Station
12	Landers 1992	7.3	0.28	0.42	82.1	Strike-slip	Coolwater
13	Loma Prieta 1989	6.9	0.53	0.44	9.8	Strike-slip	Capitola
14	Loma Prieta 1989	6.9	0.56	0.37	31.4	Strike-slip	Gilroy Array #3
15	Manjil, Iran 1990	7.4	0.51	0.5	40.4	Strike-slip	Abbar
16	Superstition Hills 1987	6.5	0.36	0.26	35.8	Strike-slip	El Centro Imp. Co.
17	Superstition Hills 1987	6.5	0.45	0.3	11.2	Strike-slip	Poe Road
18	Cape Mendocino	7.0	0.39	0.55	22.7	Thrust	Rio Dell Overpass
19	Chi-Chi, Taiwan 1999	7.6	0.35	0.44	32	Thrust	CHY101
20	Chi-Chi, Taiwan 1999	7.6	0.47	0.51	77.5	Thrust	TCU045
21	San Fernando 1971	6.6	0.21	0.17	39.5	Thrust	LA - Hollywood
22	Friuli, Italy 1976	6.5	0.35	0.31	20.2	Thrust	Tolmezzo

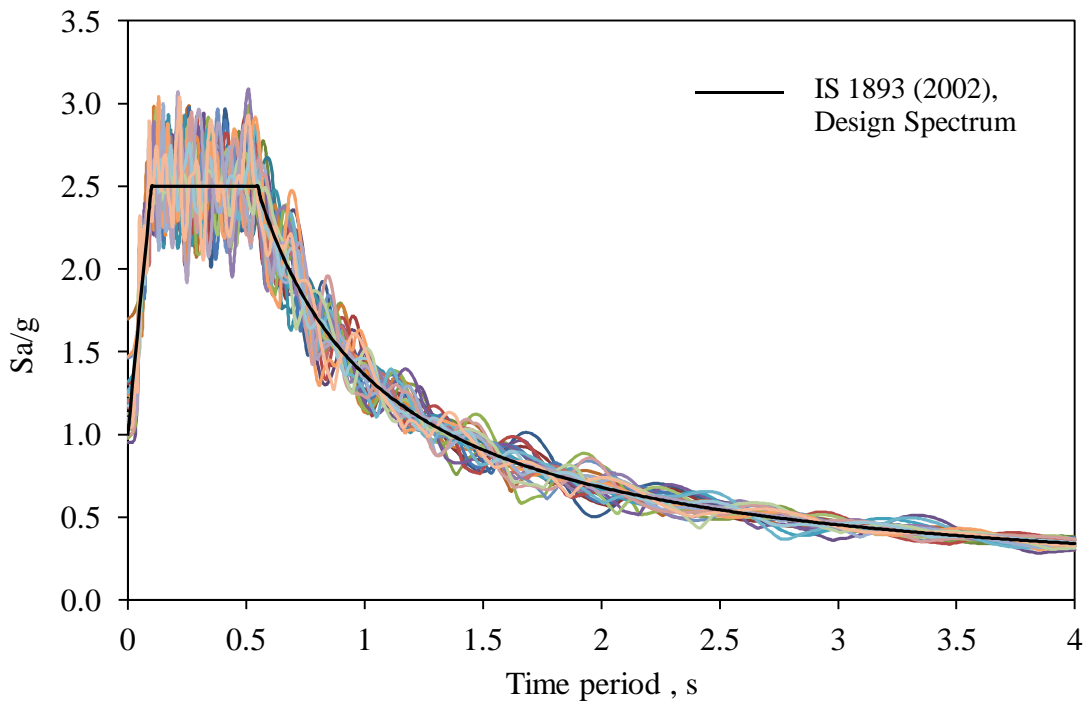


Fig.4.30: Response Spectra for 22 pairs of synthetic ground motion records

4.11.3 Effect of Earthquake Records on Fragility Curves

In order to choose a particular suite of earthquake data to be used further in the present study, fragility curves are developed according to procedure explained in Section 3.2.2 using the following two suites of ground motions separately: Case-I: natural records and Case-II: synthetic records. A typical four storeyed bare frame (4B) and corresponding fully infilled frame (4F) are chosen (refer Chapter 4 for details). This section compares the fragility curves of the buildings obtained from these two cases.

a) Case –I: A set of twenty six models are generated as per LHS scheme for each of the two frame configurations to perform NTHA using the natural earthquakes. PGA of each input ground motion and corresponding maximum inter storey drifts are recorded for all the analyses. Fig. 4.31a shows the plot between the PGA and the maximum inter-storey drifts logarithmic scale.

a) Case –II: Similarly, a set of forty four models are generated as per LHS scheme for each of the two frame configurations to perform NTHA using the synthetic earthquakes.

From each of the forty four analyses, the PGA of input ground motion and corresponding maximum inter storey drifts are recorded and plotted in Fig. 4.31b.

From the cloud analysis plot of PGA versus inter-storey drift, PSDMs models are developed using power law regression analysis (refer Eq. 3.9) and shown in Fig. 4.31. Table 4.10 shows the PSDM models along with its R square and dispersions in intensity measures. It can be observed from Fig. 4.31 that the inter-storey drift (ISD) given by PSDM models generated by synthetic accelerogram (case II) is more than that of natural accelerogram (case I) for both of the two buildings for given PGA level.

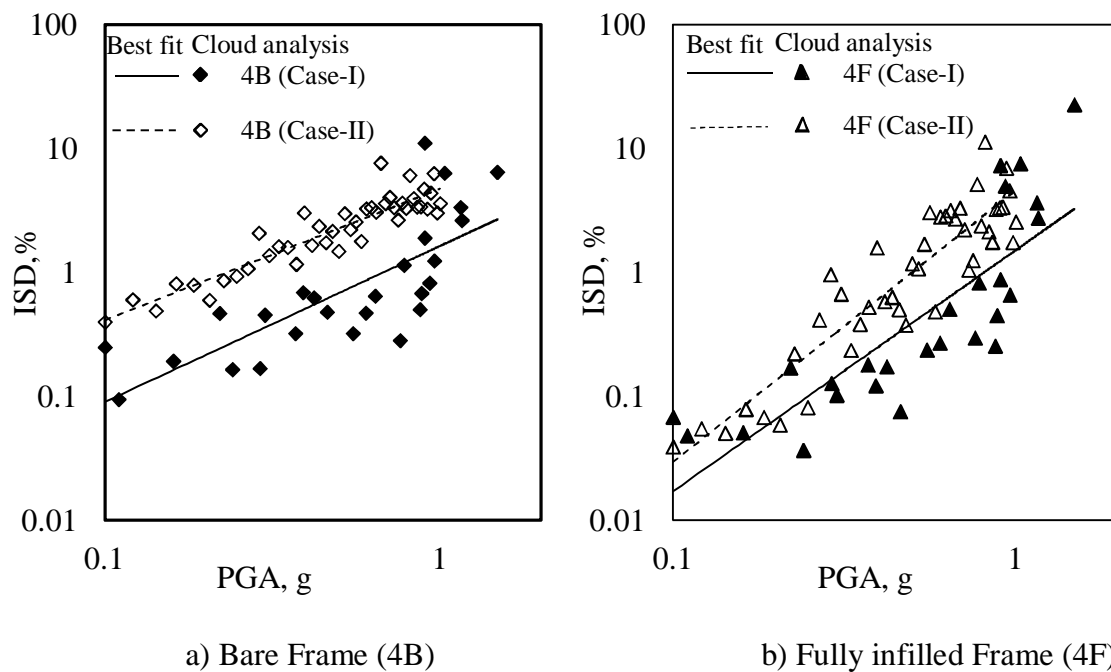


Fig.4.31: Cloud analysis results and corresponding PSDM

Table 4.10: Comparison of PSDM models developed from two suites of ground motions

Frame Identity	Case 1- Natural Ground Motion			Case 2- Synthetic Ground Motion		
	PSDM	R^2	$\beta_{D/PGA}$	PSDM	R^2	$\beta_{D/PGA}$
4B	$1.64(PGA)^{1.260}$	0.594	0.791	$4.76(PGA)^{1.063}$	0.852	0.277
4F	$1.52(PGA)^{1.949}$	0.678	1.021	$4.61(PGA)^{2.189}$	0.838	0.605

Figs. 4.32-4.33 show the fragility curves of the two building models for SD and CP performance levels developed for two different cases of ground motion records. It can be seen that the exceedance probabilities for both the frames (at SD and CP) using synthetic accelerogram set is found to be higher than that of natural accelerogram set. It can be concluded from this study that the synthetic ground motion records yield conservative results for the assessment of the buildings. Therefore, the further studies presented in this thesis are carried out based on the suite of 22 pairs of synthetic ground motions.

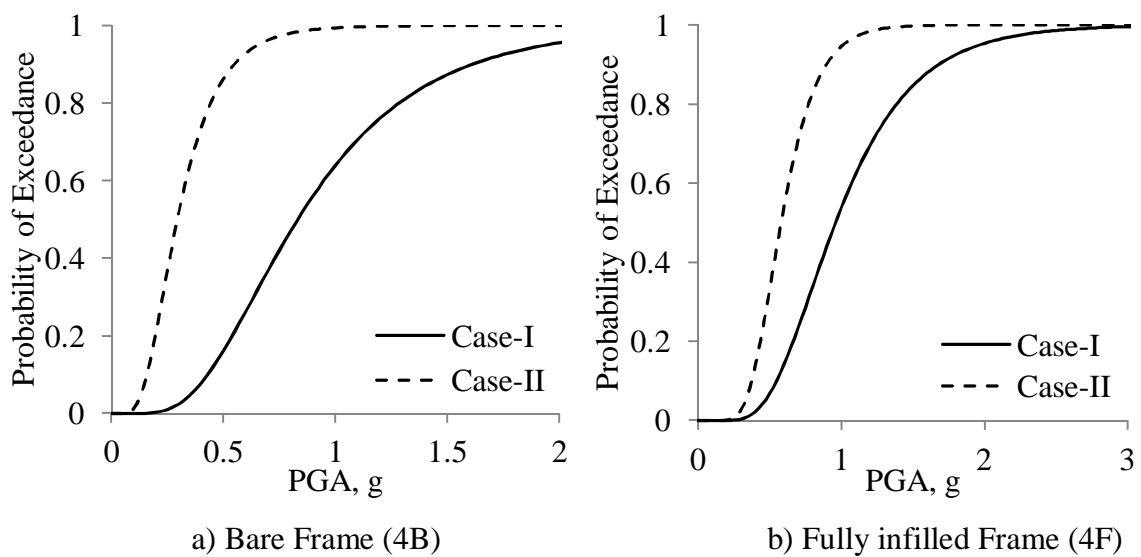


Fig. 4.32: Fragility Curves for SD performance levels

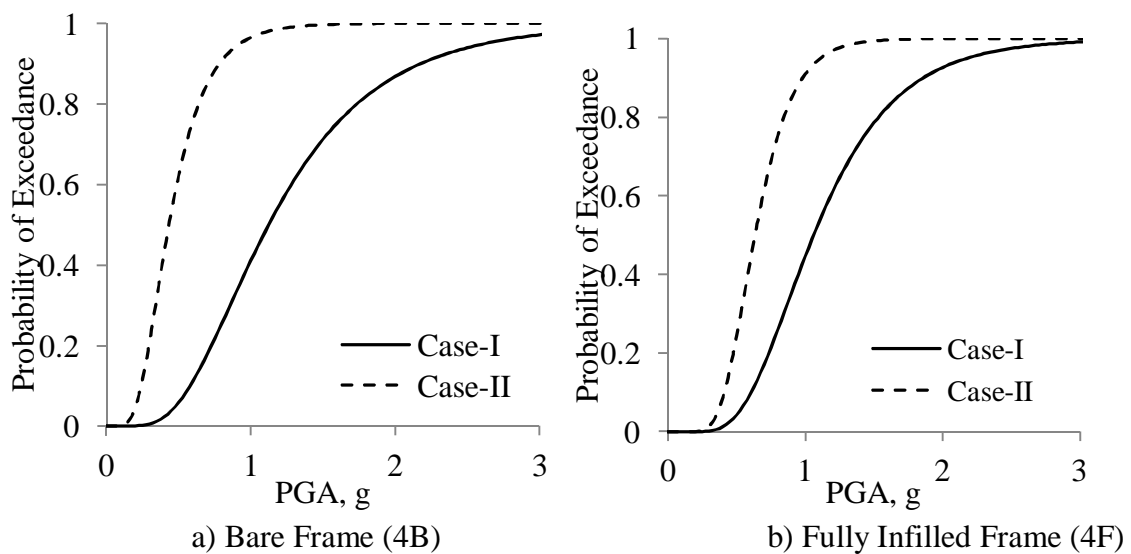


Fig. 4.33: Fragility curves for CP performance levels

4.12 SUMMARY

This chapter presents details of the basic modelling technique for nonlinear analyses of RC framed structures with and without infill walls. This includes nonlinear material models for concrete, steel rebar and infilled masonry and modelling different structural parameters. Validation study is done to verify the accuracy of the computational model used in this study. It also describes the building geometries selected for the present study and the scheme of different MFs used for designing. This chapter, summaries the sampling of random variables based on LHS scheme. Later part of this chapter presents an alternative approach to calculate the storey limit state capacities suitable for OGS buildings (and other vertically irregular buildings). Finally, selection of earthquake ground motion records required for the evaluation of building performances are discussed in this chapter.

CHAPTER 5

FRAGILITY BASED ASSESSMENT OF OGS BUILDINGS

5.1 INTRODUCTION

To gain an insight of the behaviour OGS frames, displacement responses from NTHA of four-storeyed frames are considered and compared in the first part of this chapter. Second part of the chapter presents the comparison of fragility curves developed using 2000 SAC-FEMA method with a more rigorous LHS Monte Carlo method for typical four stored frame. 2000 SAC-FEMA method is an approximate method based on a generalised correlation between demand parameter and intensity measure (PSDM) whereas LHS Monte Carlo simulation (modified Monte Carlo simulation with less computation cost) can produce more accurate results. Last part of this chapter presents the PSDM models and fragility curves for all the selected frames and analysed them to identify the effect of the different schemes of MFs on the building response.

5.2 RESPONSE OF OGS FRAMES – A DETERMINISTIC STUDY

In order to understand the behaviour of each building frame designed with different MF schemes, maximum storey displacement responses of the buildings subjected to a particular ground motion (at PGA 0.5g) are calculated using time history analyses. The results of storey displacements and inter-storey drifts for OGS frames are compared with bare and fully infilled frames and shown in Fig. 5.1-5.3. The storey displacement profile (Fig. 5.1) shows that the behaviour of OGS (4O₁) frames are different from that of fully infilled frame (4F) and bare frame (4B). Different kind of storey displacements profiles

are obtained for OGS frames designed with different schemes of MF. OGS frames designed with $MF = 1$ display the highest displacements among all the OGS frames. As the MF increases, the displacement at each storey decreases. The OGS frame, $4O_{3,2.5,2}$ shows the lowest displacements among the OGS frames, even lower than that of fully infilled frame for the selected earthquake ($PGA = 0.5g$). The decreasing order of the storey displacements among the OGS frames follow the trend, $4O_1, 4O_{1.5}, 4O_{1.5,1.5}, 4O_2, 4O_{2,2}, 4O_{2.5}, 4O_{2.5, 2,1.5}, 4O_{2.5,2.5}, 4O_3, 4O_{3,3}, 4O_{3,2.5,2}$.

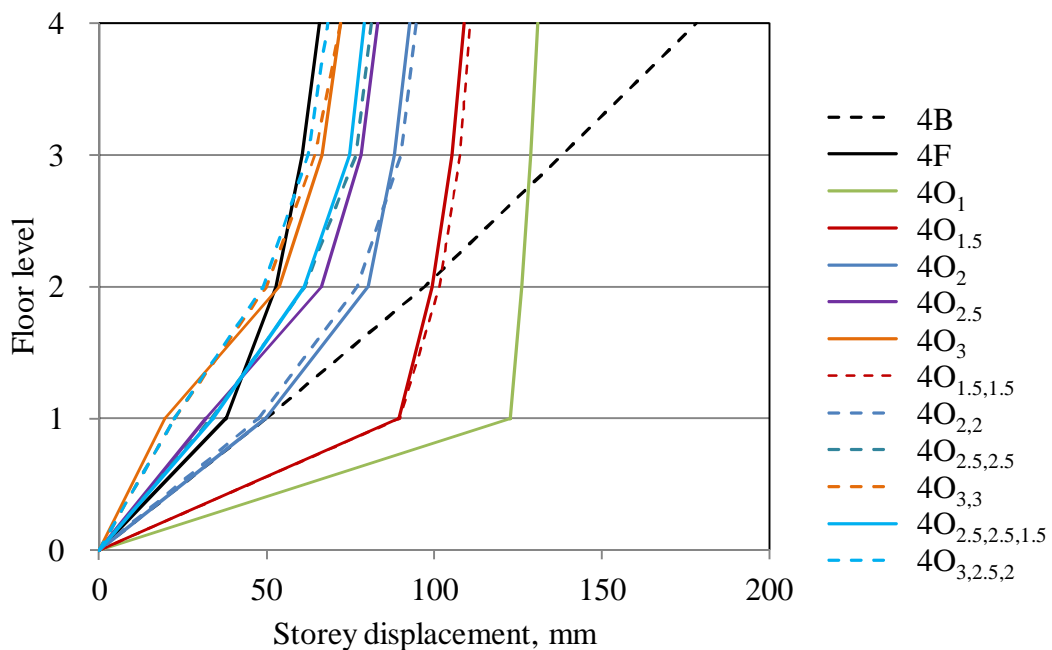


Fig. 5.1: Maximum displacement profile for four-storeyed frames subjected to particular ground motion

A Comparison of ISD (EDP in the fragility curves) among all four-storeyed frames is considered to study the effectiveness of MF in the OGS frames. Fig. 5.2 shows the ISD at each storey level for each frame. Horizontal axis represents the ISD in terms of percentage and vertical axis represents the storey levels of each frame with its designations. It can be seen that the ISD decreases from ground storey towards upper storey in a regular pattern for bare (4B) and fully infilled frame (4F). However, some of the OGS frames show an abrupt change in the distribution of ISD along the height.

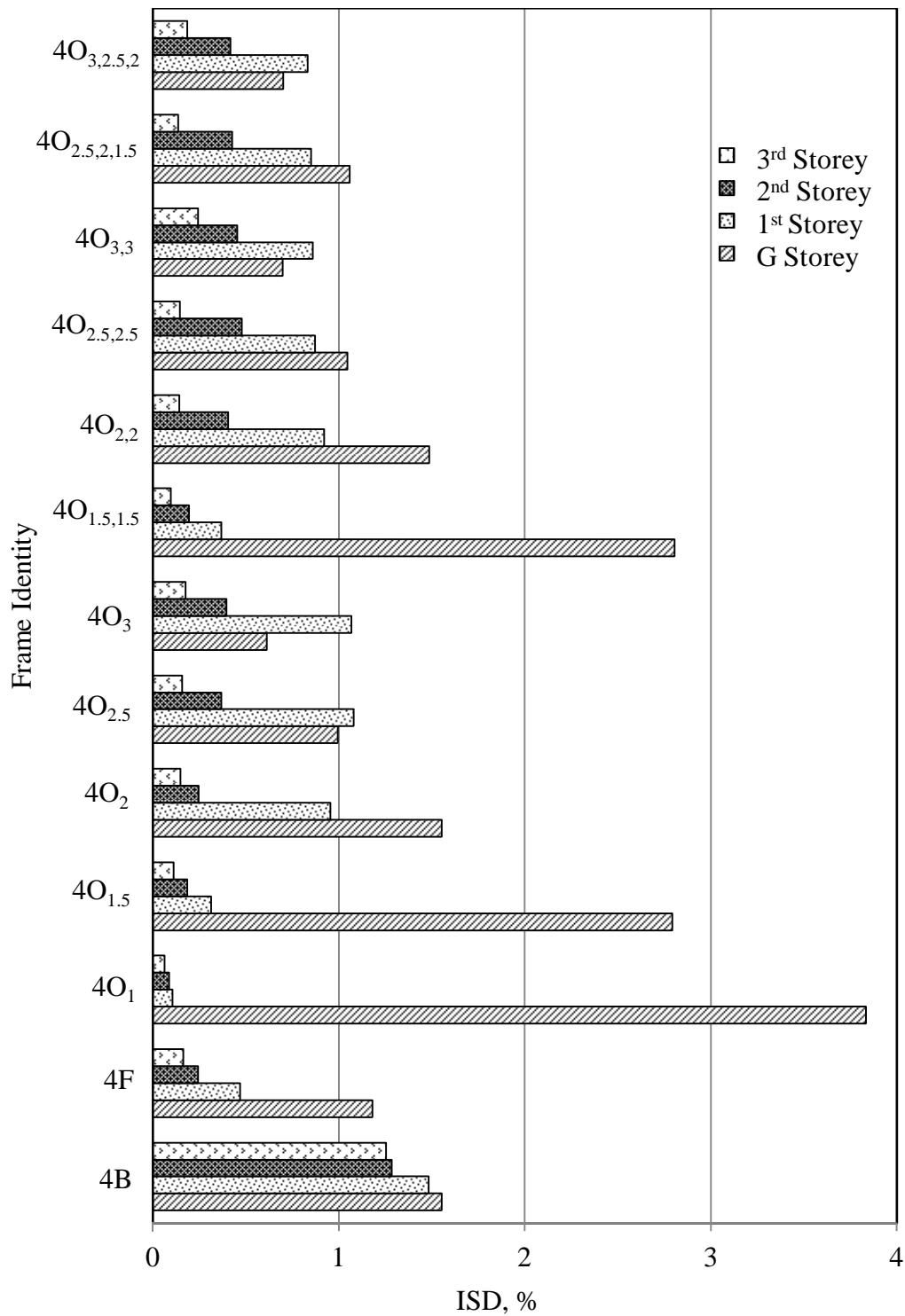


Fig. 5.2: Inter-storey-drift for four-storeyed frames.

4O₁ shows significantly large inter-storey drift at the ground storey, with low inter-storey-drifts in the upper storeys. As the MF increases to 1.5, 2.0, 2.5 and 3.0 (4O_{1,5}, 4O₂, 4O_{2,5} and 4O₃) in the ground storey, the drift in the ground storey reduces gradually. To study

the variation of ISD at ground storey with MF values, a plot between ISD and MF is drawn and shown in Fig. 5.3. As MF increases from 1.0 to 3.0 the ISD decreases by about 84% in the ground storey and increases by 913% in the first storey.

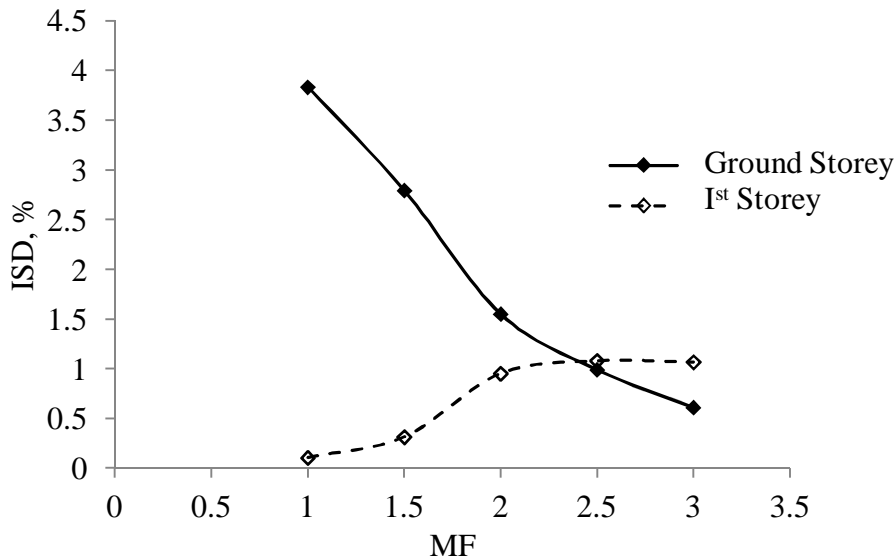


Fig. 5.3: ISD versus MF for $4O_x$ frames.

Frames $4O_{1.5,1.5}$ and $4O_{1.5}$ show identical displacement profile although $4O_{1.5,1.5}$ has slightly lesser displacement values. The same correlation can be drawn between $4O_{2,2}$ and $4O_2$ frames. However, no such correlation can be drawn between $4O_{2.5,2.5}$ and $4O_{2.5}$. Application of MF value of 2.5 in the both ground and first storey ($4O_{2.5,2.5}$) shows a regular distribution of inter-storey drift along the height as observed in the case of 4F. The same regular distribution of inter-storey drift can be observed for the frame $4O_{2.5,2,1.5}$. This study shows that the OGS buildings are most vulnerable when MF value of one is used during design. Failure of OGS building is likely to occur due to large ISD in the ground storey level for values MF lower than 2.0. Application of lower values of MF (≤ 2.0) in the both ground and first storey columns, does not change the building response significantly. Application of MF, more than 2.5 in the ground storey alone shift the failure from ground storey to adjacent first storey. A combinations of different MF values in the ground storey and upper storeys found to yield less ISD in OGS buildings. The above

discussions are based on deterministic study from a randomly selected single NTHA results.

5.3 PROBABILISTIC SEISMIC DEMAND MODELS

Probabilistic seismic demand models (PSDMs) express the Engineering Damage Parameter (EDP) as a function of Intensity Measure. A detail of PSDM as per Cornell *et al.* (2002) is discussed in Section 3.2.2. Damage of the structure can be correlated to different response quantities of the structure subjected to earthquake loading. The common response quantities that represent damage (popularly known as EDP) of a building used in the previous studies are roof displacement, inter-storey drift, base-shear, etc. In the present study, the Inter Storey Drift (ISD) is chosen as the EDP as the limit state capacities are generally expressed in terms of drift (ATC 58, 2012; Ghobarah, 2000). Also, some of the previous researchers (Nielson, 2005; Ravichandran and Klinger, 2012; Davis *et al.*, 2010b; etc) have used ISD as the EDP for the development of PSDMs.

PSDMs are generally developed from the cloud analysis of NTHA results. Step by step procedure for development of PSDM models is as follows:

- i) Select a suite of ground motions (N number of records) representing a broad range of values for the chosen intensity measure.
- ii) Create N number of statistical models of the subject structure. These models should be created by sampling on various modelling parameters which may be deemed significant (e.g. material strength, damping ratio). Thus, N statistically significant yet nominally identical samples are made.
- iii) Perform a NTHA for each ground motion for set of developed structures. Key responses (EDP) should be monitored during the analysis.

iv) For each analysis, peak responses are recorded and plotted against the value of the intensity measure for that ground motion. A regression analysis of these data is then used to develop PSDM models (refer Eq. 3.9).

5.4 VALIDATION OF THE 2000 SAC-FEMA METHOD

2000 SAC-FEMA (Cornell *et al.*, 2002) uses a closed form continuous expression for development of fragility curves. In reality, fragility functions may be discrete functions due to various kinds of uncertainties involved. In order to check the accuracy of 2000 SAC-FEMA method, the results from this method is compared with that of LHS-Monte Carlo (LHS-MC) method which was also used by many previous studies (Ghanaat *et al.*, 2012; Kim *et al.*, 2011; etc). The theoretical development and mathematical formulation of this method can be found elsewhere (McKay *et al.*, 1979). A case study on four-storeyed bare frame (4B) is considered to validate the 2000 SAC-FEMA method before developing the PSDMs for all the buildings. This section presents the results of the case study.

a) Case –I (2000 SAC-FEMA method): A set of forty-four models of selected frame are generated using LHS scheme to perform NTHA. PGA of each ground motion and corresponding maximum ISD from each analysis is recorded. PSDMs as per 2000 SAC-FEMA method and corresponding fragility curves for different performance levels are developed.

b) Case –II (LHS-Monte Carlo method):

In the present study, the same forty-four models of the selected frame are analysed for the selected ground motion. PGA of each of the selected ground motions (44 ground motions) are scaled to 0.1g to 1g (10 PGA levels) linearly and used for the NTHA. Then the forty-

four building models are analysed for randomly selected ground motion for a particular PGA. The same procedure is followed for other PGA levels. Total number analyses performed for LHS-MC is 440 (44×10). From each analysis, maximum ISD and corresponding PGA are recorded. The probability of exceedance for a particular PGA is calculated as follows:

$$\text{Probability of exceedance for a PGA level} = \frac{\text{Number of analysis cases where ISD exceeds the limit}}{\text{Total number of analysis cases at that PGA level}}$$

Fig 5.4 shows the fragility curves developed for the selected building using 2000 SAC-FEMA method and LHS-MC method for various limit states. It can be seen from Fig 5.4 that fragility curves as per 2000 SAC-FEMA method is in agreement with that of LHS-MC method. As the present study requires simulations of large number of computational models, the computationally less intensive 2000 SAC-FEMA method is used further in the present study.

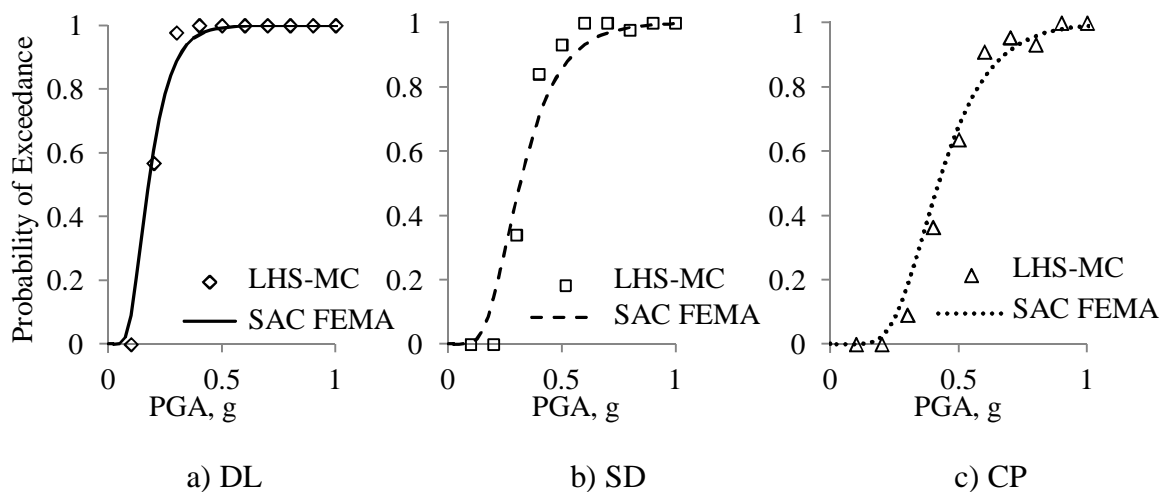


Fig. 5.4: Comparison between LHS-MC and 2000 SAC-FEMA method

5.5 PROBABILISTIC SEISMIC DEMAND MODELS FOR OGS BUILDINGS

NTHA of all the forty-four models for each of the selected building configurations are performed and ISD at each storey level are monitored. Maximum ISD at each storey is plotted against the corresponding PGA in a logarithmic plot and a regression analysis is conducted to obtain the best-fit curve that represents the PSDM for each storey level. Constants ' a ' and ' b ' of the power law model (refer Eq. 3.9) are obtained from the best fit curve. The dispersions in the intensity measure ($\beta_{EDP/IM}$) from the data set of ISD and PGA values are calculated using Eq. 3.11 for each storey of all the frames. The PSDMs for each storey of all the selected frames including the respective R^2 and $\beta_{EDP/IM}$ are presented in Tables 5.1-5.4.

The probability of exceedance of a particular damage state for a frame depends mainly on the maximum ISD among all the storeys. A PSDM describes the relation between the maximum ISD and PGA values. PSDMs are developed for each storey of all the frames considered, *i.e.*, for a frame having ' N_s ' number of storeys, ' N_s ' number of PSDM models can be developed. Governing fragility curve for a particular frame can be identified from the PSDMs of all the individual storeys for that frame. The PSDM model that produces the maximum ISD out of all PSDMs in that frame represents the governing fragility curve. For example, Fig. 5.5 shows the PSDM models and the fragility curves for each storey of the four-storey fully infilled frame (4F). Among the four fragility curves, the fragility curve of the ground storey shows the maximum probabilities of exceedance for each PGA. It can be seen from the Fig. 5.5a that the maximum ISD is given by the PSDM model of the ground storey. Hence, it can be inferred that the governing fragility curve of this frame (4F) is due to the ISD predicted by the PSDM of the ground storey as explained graphically in the Fig. 5.5. This procedure is used further to identify the governing PSDMs and fragility curves for all other frames. The governing PSDM is

identified and marked with bold text in Tables 5.1-5.4 for each frame. Figs. 5.6-5.9 show the cloud analyses results between PGA and ISD in a scatter plot along with the developed PSDMs for each frame.

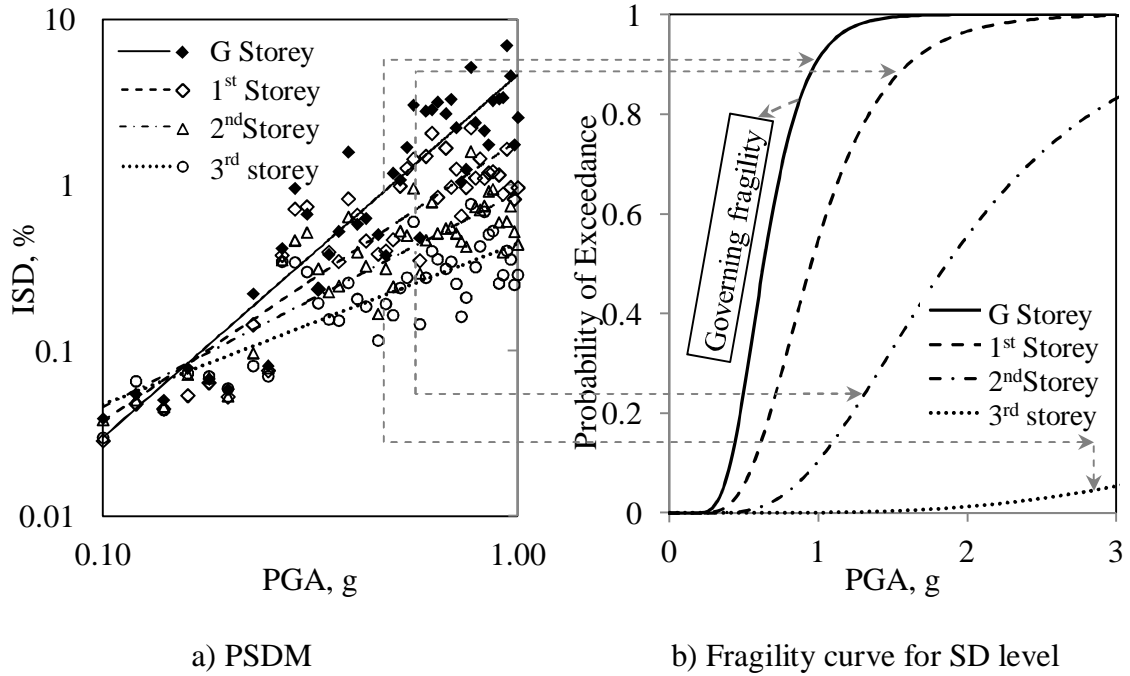


Fig. 5.5: PSDMs and fragility curves for each storey of four-storey fully infilled frame (4F).

Table 5.1: PSDMs for two-storeyed frames.

Frame Identity	Storey level	PSDM	R ²	$\beta_{D/PGA}$
2B	G	6.28(PGA)^{1.254}	0.810	0.381
	I st	2.00(PGA) ^{0.650}	0.796	0.207
2F	G	1.11(PGA)^{1.991}	0.776	0.671
	I st	0.30(PGA) ^{1.411}	0.728	0.542
2O	G	6.24(PGA)^{1.210}	0.863	0.303
	I st	0.08(PGA) ^{0.533}	0.778	0.179
2O _{1.5}	G	5.75(PGA)^{1.298}	0.863	0.324
	I st	0.10(PGA) ^{0.728}	0.746	0.267
2O ₂	G	3.85(PGA)^{1.217}	0.885	0.275
	I st	0.14(PGA) ^{0.909}	0.724	0.353
2O _{2.5}	G	3.21(PGA)^{1.299}	0.901	0.270
	I st	0.17(PGA) ^{1.029}	0.741	0.382
2O _{1.5,1.5}	G	5.72(PGA)^{1.312}	0.870	0.318
	I st	0.11(PGA) ^{0.666}	0.723	0.258
2O _{2,2}	G	3.79(PGA)^{1.246}	0.881	0.287
	I st	0.15(PGA) ^{0.810}	0.612	0.404
2O _{2.5,2.5}	G	2.96(PGA)^{1.332}	0.902	0.275
	I st	0.21(PGA) ^{0.990}	0.696	0.410
2O _{2,1.5}	G	3.82(PGA)^{1.236}	0.884	0.281
	I st	0.15(PGA) ^{0.879}	0.681	0.378
2O _{2.5,2}	G	3.07(PGA)^{1.311}	0.902	0.271
	I st	0.18(PGA) ^{0.964}	0.698	0.398

Note: G- Ground Storey, bold text -governing PSDM of the frame

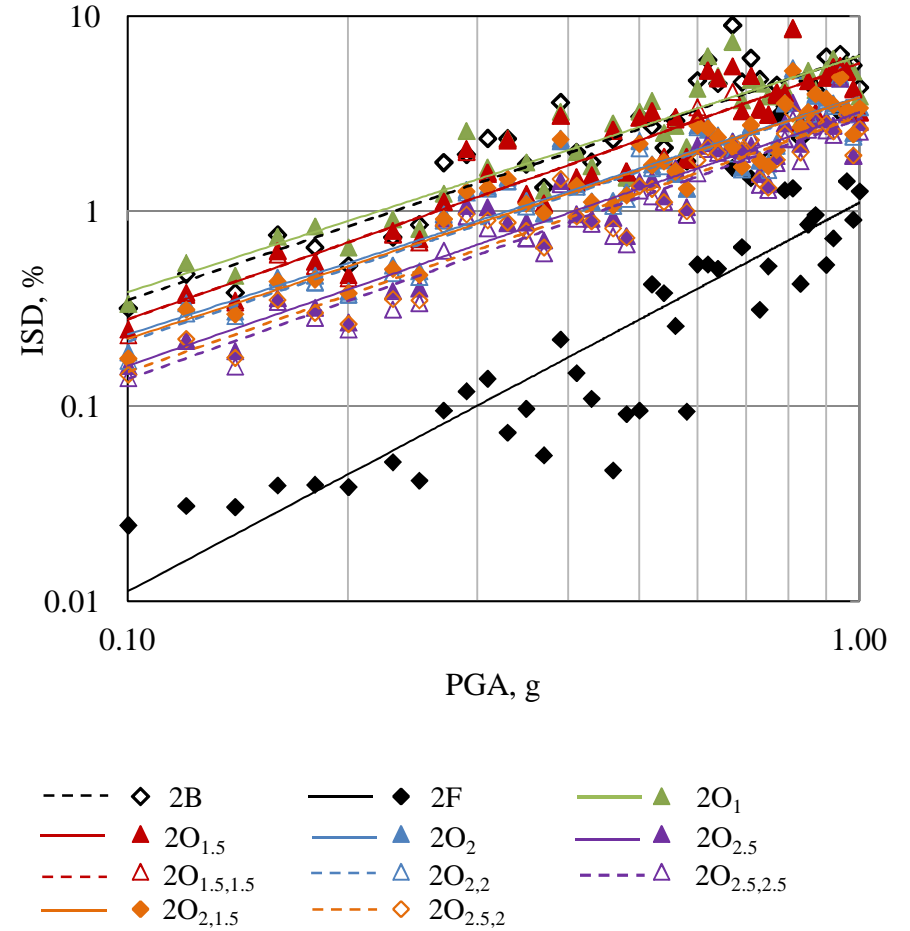


Fig. 5.6: PSDMs model for two-storeyed frame

Table 5.2: PSDMs for four-storeyed frames

Frame Identity	Storey level	PSDM	R ²	$\beta_{D/PGA}$
4B	G	5.21(PGA)^{1.207}	0.823	0.351
	I st	4.75(PGA) ^{1.059}	0.852	0.277
	II nd	2.39(PGA) ^{0.774}	0.802	0.241
	III rd	1.70(PGA) ^{0.691}	0.831	0.195
4F	G	4.61(PGA)^{2.189}	0.838	0.605
	I st	1.85(PGA) ^{1.693}	0.798	0.535
	II nd	0.89(PGA) ^{1.294}	0.746	0.473
	III rd	0.44(PGA) ^{0.971}	0.652	0.445
4O ₁	G	7.97(PGA)^{1.216}	0.816	0.362
	I st	0.19(PGA) ^{0.691}	0.761	0.243
	II nd	0.14(PGA) ^{0.709}	0.772	0.241
	III rd	0.14(PGA) ^{0.725}	0.688	0.306
4O _{1.5}	G	5.38(PGA)^{1.234}	0.849	0.326
	I st	0.80(PGA) ^{1.002}	0.642	0.469
	II nd	0.36(PGA) ^{0.885}	0.693	0.370
	III rd	0.28(PGA) ^{0.811}	0.591	0.424
4O ₂	G	2.36(PGA) ^{1.006}	0.824	0.291
	Ist	4.09(PGA)^{1.817}	0.871	0.438

Frame Identity	Storey level	PSDM	R ²	$\beta_{D/PGA}$
	II nd	1.00(PGA) ^{1.464}	0.873	0.350
	III rd	0.42(PGA) ^{1.007}	0.738	0.376
4O _{2.5}	G	1.49(PGA) ^{0.840}	0.836	0.234
	Ist	5.88(PGA)^{2.026}	0.877	0.477
	II nd	0.97(PGA) ^{1.426}	0.811	0.431
	III rd	0.48(PGA) ^{1.143}	0.710	0.458
4O ₃	G	0.94(PGA) ^{0.797}	0.795	0.254
	Ist	5.61(PGA)^{2.049}	0.874	0.489
	II nd	0.95(PGA) ^{1.409}	0.815	0.421
	III rd	0.37(PGA) ^{0.930}	0.647	0.431
4O _{1.5,1.5}	G	5.10(PGA)^{1.280}	0.863	0.320
	I st	0.72(PGA) ^{0.890}	0.748	0.324
	II nd	0.34(PGA) ^{0.915}	0.807	0.281
	III rd	0.26(PGA) ^{0.842}	0.631	0.404
4O _{2,2}	G	2.67(PGA)^{1.151}	0.869	0.281
	I st	2.37(PGA) ^{1.457}	0.884	0.330
	II nd	1.45(PGA) ^{1.706}	0.822	0.498
	III rd	0.44(PGA) ^{1.094}	0.773	0.372

Frame Identity	Storey level	PSDM	R ²	$\beta_{D/PGA}$
4O _{2.5,2.5}	G	2.14(PGA)^{1.124}	0.832	0.317
	I st	2.56(PGA) ^{1.511}	0.857	0.388
	II nd	2.36(PGA) ^{1.990}	0.866	0.492
	III rd	0.57(PGA) ^{1.288}	0.717	0.508
4O _{3,3}	G	1.25(PGA) ^{1.054}	0.796	0.335
	I st	1.83(PGA) ^{1.365}	0.852	0.357
	II nd	2.90(PGA)^{2.112}	0.853	0.550
	III rd	0.65(PGA) ^{1.345}	0.691	0.564
4O _{2.5,2,1.5}	G	2.31(PGA) ^{1.177}	0.850	0.311
	I st	2.57(PGA)^{1.532}	0.878	0.358
	II nd	1.64(PGA) ^{1.767}	0.883	0.404
	III rd	0.61(PGA) ^{1.390}	0.763	0.486
4O _{3,2.5,2}	G	1.59(PGA) ^{1.193}	0.837	0.330
	I st	2.16(PGA)^{1.487}	0.875	0.353
	II nd	1.82(PGA) ^{1.829}	0.853	0.476
	III rd	0.77(PGA) ^{1.509}	0.733	0.571

Note: G- Ground Storey, bold text -governing PSDM for the frame

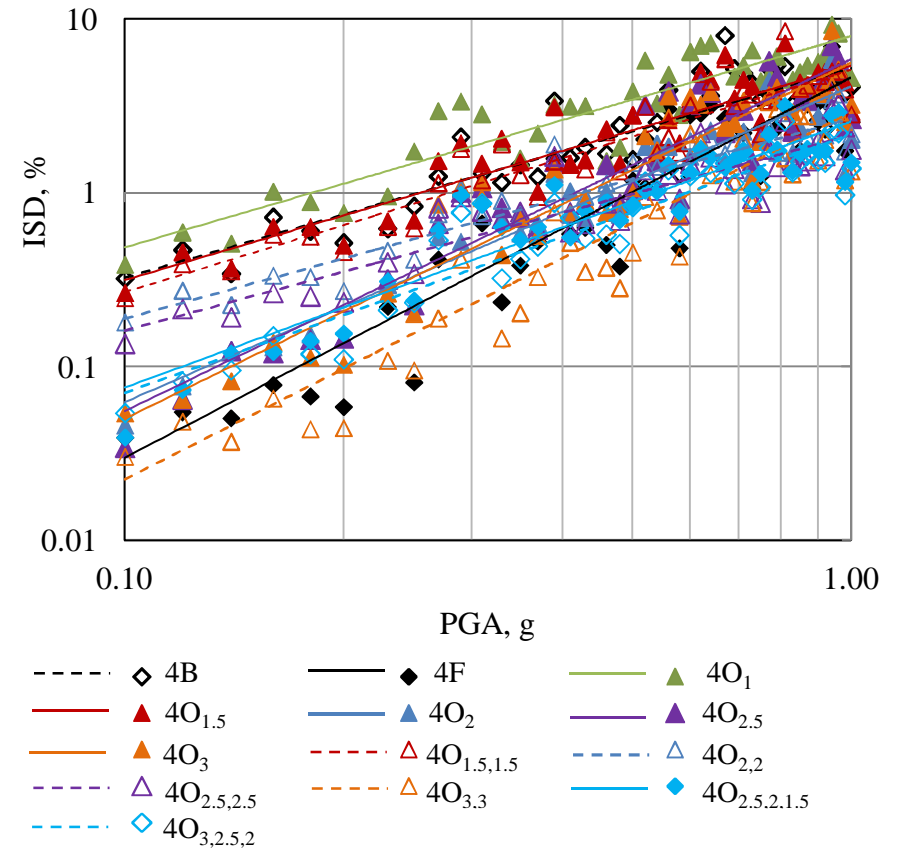


Fig. 5.7: PSDMs model for four-storeyed frame

Table 5.3: PSDMs for six-storeyed frames

Frame Identity	Storey level	PSDM	R ²	$\beta_{D/PGA}$
6B	G	5.00(PGA) ^{1.333}	0.840	0.365
	I st	4.64(PGA)^{1.121}	0.817	0.333
	II nd	2.98(PGA) ^{0.891}	0.739	0.332
	III rd	2.17(PGA) ^{0.713}	0.789	0.231
	IV th	1.79(PGA) ^{0.675}	0.811	0.205
	V th	1.31(PGA) ^{0.720}	0.798	0.227
6F	G	3.70(PGA)^{1.670}	0.806	0.514
	I st	2.56(PGA) ^{1.448}	0.842	0.394
	II nd	1.44(PGA) ^{1.162}	0.797	0.368
	III rd	0.98(PGA) ^{1.019}	0.747	0.372
	IV th	0.67(PGA) ^{0.911}	0.702	0.372
	V th	0.44(PGA) ^{0.774}	0.693	0.324
6O ₁	G	6.20(PGA)^{1.210}	0.833	0.340
	I st	0.41(PGA) ^{0.539}	0.647	0.361
	II nd	0.28(PGA) ^{0.700}	0.694	0.292
	III rd	0.27(PGA) ^{0.724}	0.753	0.260
	IV th	0.25(PGA) ^{0.706}	0.786	0.231

Frame Identity	Storey level	PSDM	R ²	$\beta_{D/PGA}$
6O ₁	V th	0.25(PGA) ^{0.760}	0.582	0.404
6O _{1.5}	G	2.74(PGA) ^{1.001}	0.764	0.349
	Ist	4.35(PGA)^{1.527}	0.806	0.470
	II nd	1.09(PGA) ^{1.083}	0.809	0.331
	III rd	0.66(PGA) ^{1.006}	0.847	0.269
	IV th	0.46(PGA) ^{0.890}	0.806	0.274
	V th	0.32(PGA) ^{0.769}	0.797	0.243
6O ₂	G	1.16(PGA) ^{0.708}	0.742	0.262
	Ist	5.44(PGA)^{1.653}	0.777	0.556
	II nd	1.49(PGA) ^{1.147}	0.800	0.359
	III rd	0.83(PGA) ^{1.058}	0.837	0.292
	IV th	0.55(PGA) ^{0.940}	0.857	0.241
	V th	0.39(PGA) ^{0.845}	0.854	0.219
6O _{2.5}	G	0.77(PGA) ^{0.663}	0.808	0.203
	Ist	5.52(PGA)^{1.731}	0.820	0.508
	II nd	1.61(PGA) ^{1.192}	0.831	0.338
	III rd	0.94(PGA) ^{1.115}	0.852	0.291
	IV th	0.60(PGA) ^{0.983}	0.846	0.263
	V th	0.41(PGA) ^{0.880}	0.829	0.251

Frame Identity	Storey level	PSDM	R ²	$\beta_{D/PGA}$
6O _{1.5,1.5}	G	3.02(PGA)^{1.094}	0.805	0.338
	I st	2.92(PGA) ^{1.289}	0.850	0.340
	II nd	2.15(PGA) ^{1.527}	0.828	0.437
	III rd	0.79(PGA) ^{1.151}	0.873	0.275
	IV th	0.49(PGA) ^{0.992}	0.773	0.337
	V th	0.29(PGA) ^{0.736}	0.789	0.239
6O _{2,2}	G	1.78(PGA) ^{1.002}	0.776	0.338
	I st	2.48(PGA) ^{1.182}	0.819	0.348
	IInd	3.65(PGA)^{1.664}	0.832	0.470
	III rd	1.09(PGA) ^{1.213}	0.787	0.396
	IV th	0.57(PGA) ^{0.973}	0.732	0.369
	V th	0.33(PGA) ^{0.768}	0.750	0.278
6O _{2.5,2.5}	G	1.11(PGA) ^{0.917}	0.783	0.303
	I st	1.90(PGA) ^{1.126}	0.831	0.319
	IInd	4.78(PGA)^{1.845}	0.817	0.549
	III rd	1.50(PGA) ^{1.401}	0.856	0.360
	IV th	0.81(PGA) ^{1.212}	0.842	0.330
	V th	0.43(PGA) ^{0.964}	0.811	0.292
6O _{2,2,2}	G	2.01(PGA) ^{1.079}	0.790	0.349

Frame Identity	Storey level	PSDM	R ²	$\beta_{D/PGA}$
6O _{2,2,2}	Ist	2.48(PGA)^{1.200}	0.833	0.337
	II nd	2.46(PGA) ^{1.444}	0.870	0.351
	III rd	1.91(PGA) ^{1.604}	0.829	0.458
	IV th	0.69(PGA) ^{1.150}	0.788	0.374
	V th	0.35(PGA) ^{0.886}	0.811	0.269
6O _{2.5,2.5,2.5}	G	1.34(PGA) ^{1.044}	0.775	0.353
	I st	2.14(PGA) ^{1.231}	0.841	0.336
	II nd	2.42(PGA) ^{1.457}	0.856	0.376
	IIIrd	2.67(PGA)^{1.736}	0.843	0.470
	IV th	1.00(PGA) ^{1.374}	0.816	0.409
	V th	0.39(PGA) ^{0.954}	0.749	0.347
6O _{2.5,2,1.5}	G	1.27(PGA) ^{0.992}	0.760	0.350
	I st	2.24(PGA) ^{1.224}	0.826	0.353
	IInd	2.65(PGA)^{1.479}	0.852	0.387
	III rd	2.48(PGA) ^{1.711}	0.808	0.523
	IV th	0.92(PGA) ^{1.286}	0.805	0.397
	V th	0.43(PGA) ^{0.975}	0.707	0.394

Note : G- Ground Storey, bold text -governing PSDM for the frame

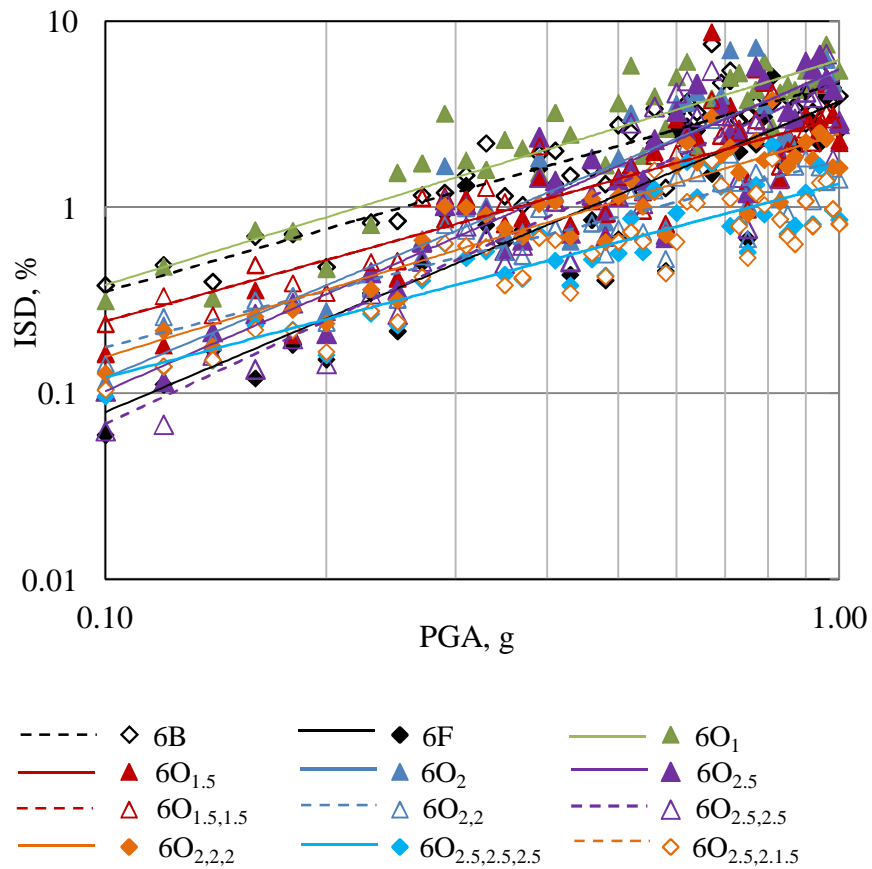


Fig. 5.8: PSDMs model for six-storey frame

Table 5.4: PSDMs for eight-storeyed frames.

Frame Identity	Storey level	PSDM	R ²	$\beta_{D/PGA}$
8B	G	$1.32(PGA)^{0.704}$	0.576	0.379
	I st	$2.74(PGA)^{0.793}$	0.621	0.389
	II nd	$5.00(PGA)^{0.980}$	0.609	0.493
	III rd	$3.16(PGA)^{0.800}$	0.506	0.496
	IV th	$1.62(PGA)^{0.544}$	0.403	0.415
	V th	$1.35(PGA)^{0.555}$	0.542	0.320
	VI th	$1.18(PGA)^{0.604}$	0.594	0.313
VII th	$0.85(PGA)^{0.620}$	0.640	0.292	
8F	G	$1.26(PGA)^{0.984}$	0.816	0.293
	I st	$2.43(PGA)^{1.258}$	0.803	0.391
	II nd	$5.65(PGA)^{1.839}$	0.789	0.597
	III rd	$1.62(PGA)^{1.210}$	0.825	0.350
	IV th	$1.03(PGA)^{1.065}$	0.794	0.340
	V th	$0.75(PGA)^{0.970}$	0.735	0.365
	VI th	$0.57(PGA)^{0.954}$	0.742	0.353
VII th	$0.34(PGA)^{0.619}$	0.602	0.316	
8O ₁	G	$4.44(PGA)^{1.091}$	0.768	0.376
	I st	$3.11(PGA)^{1.370}$	0.750	0.497
	II nd	$0.96(PGA)^{1.102}$	0.787	0.360
	III rd	$0.64(PGA)^{1.046}$	0.770	0.358
IV th	$0.48(PGA)^{0.966}$	0.831	0.273	

Frame Identity	Storey level	PSDM	R ²	$\beta_{D/PGA}$
	V th	0.38(PGA) ^{0.927}	0.825	0.267
	VI th	0.29(PGA) ^{0.866}	0.773	0.294
	VII th	0.23(PGA) ^{0.627}	0.740	0.233
8O _{1.5}	G	2.06(PGA) ^{0.906}	0.727	0.348
	I st	2.96(PGA)^{1.158}	0.768	0.399
	II nd	2.96(PGA) ^{1.463}	0.625	0.711
	III rd	1.12(PGA) ^{1.117}	0.786	0.366
	IV th	0.77(PGA) ^{1.089}	0.796	0.346
	V th	0.56(PGA) ^{1.033}	0.791	0.333
	VI th	0.44(PGA) ^{0.966}	0.767	0.334
VII th	0.30(PGA) ^{0.718}	0.739	0.267	
8O ₂	G	2.95(PGA) ^{1.104}	0.770	0.379
	I st	3.38(PGA)^{1.302}	0.791	0.420
	II nd	1.67(PGA) ^{1.244}	0.731	0.473
	III rd	0.94(PGA) ^{1.100}	0.753	0.395
	IV th	0.68(PGA) ^{1.091}	0.832	0.308
	V th	0.50(PGA) ^{1.006}	0.792	0.324
	VI th	0.38(PGA) ^{0.940}	0.746	0.344
VII th	0.28(PGA) ^{0.710}	0.749	0.258	
8O _{2.5}	G	0.98(PGA) ^{0.689}	0.625	0.335
	I st	2.33(PGA) ^{1.027}	0.736	0.386
	II nd	5.10(PGA)^{1.678}	0.744	0.618

Frame Identity	Storey level	PSDM	R ²	$\beta_{D/PGA}$
8O _{2.5}	III rd	1.46(PGA) ^{1.164}	0.822	0.340
	IV th	1.02(PGA) ^{1.207}	0.845	0.325
	V th	0.76(PGA) ^{1.154}	0.833	0.325
	VI th	0.57(PGA) ^{1.076}	0.803	0.335
	VII th	0.34(PGA) ^{0.732}	0.730	0.279
8O _{1.5,1.5}	G	1.80(PGA) ^{0.851}	0.672	0.373
	I st	2.19(PGA) ^{1.020}	0.772	0.348
	II nd	4.11(PGA)^{1.626}	0.726	0.626
	III rd	1.27(PGA) ^{1.177}	0.830	0.334
	IV th	0.83(PGA) ^{1.146}	0.843	0.310
	V th	0.63(PGA) ^{1.109}	0.845	0.298
	VI th	0.46(PGA) ^{1.000}	0.783	0.330
VII th	0.29(PGA) ^{0.723}	0.723	0.281	
8O _{2,2}	G	2.47(PGA) ^{1.028}	0.780	0.342
	I st	2.43(PGA) ^{1.124}	0.842	0.305
	II nd	3.08(PGA)^{1.531}	0.732	0.581
	III rd	0.96(PGA) ^{1.058}	0.791	0.341
	IV th	0.66(PGA) ^{1.022}	0.799	0.321
	V th	0.48(PGA) ^{0.963}	0.817	0.286
	VI th	0.38(PGA) ^{0.907}	0.758	0.321
VII th	0.26(PGA) ^{0.627}	0.686	0.266	
8O _{2.5,2.5}	G	0.96(PGA) ^{0.700}	0.654	0.319

Frame Identity	Storey level	PSDM	R ²	$\beta_{D/PGA}$
	I st	1.38(PGA) ^{0.796}	0.745	0.293
	IInd	5.72(PGA)^{1.700}	0.746	0.623
	III rd	1.51(PGA) ^{1.194}	0.802	0.372
	IV th	0.96(PGA) ^{1.153}	0.813	0.347
	V th	0.66(PGA) ^{1.076}	0.782	0.356
	VI th	0.49(PGA) ^{1.004}	0.798	0.317
	VII th	0.31(PGA) ^{0.707}	0.727	0.272
8O _{2,2,2}	G	2.76(PGA)^{1.093}	0.778	0.366
	I st	2.47(PGA) ^{1.152}	0.817	0.342
	II nd	1.91(PGA) ^{1.312}	0.806	0.404
	III rd	1.67(PGA) ^{1.430}	0.783	0.472
	IV th	0.81(PGA) ^{1.206}	0.839	0.332
	V th	0.59(PGA) ^{1.147}	0.826	0.331
	VI th	0.44(PGA) ^{1.098}	0.819	0.324
VII th	0.27(PGA) ^{0.741}	0.803	0.230	
8O _{2.5,2.5,2.5}	G	1.00(PGA) ^{0.719}	0.597	0.371
	I st	1.44(PGA) ^{0.870}	0.748	0.317
	II nd	1.59(PGA) ^{1.077}	0.807	0.331
	IIIrd	3.45(PGA)^{1.684}	0.780	0.561
IV th	1.19(PGA) ^{1.268}	0.837	0.351	

Frame Identity	Storey level	PSDM	R ²	$\beta_{D/PGA}$
8O _{2.5,2.5,2.5}	V th	0.74(PGA) ^{1.158}	0.807	0.356
	VI th	0.58(PGA) ^{1.151}	0.724	0.446
	VII th	0.29(PGA) ^{0.706}	0.705	0.286
8O _{2.5,2.5,2.5,2.5}	G	1.70(PGA) ^{1.065}	0.721	0.416
	I st	2.11(PGA) ^{1.111}	0.794	0.355
	II nd	2.04(PGA) ^{1.250}	0.831	0.353
	III rd	1.83(PGA) ^{1.310}	0.832	0.369
	IVth	2.00(PGA)^{1.580}	0.822	0.462
	V th	0.89(PGA) ^{1.273}	0.833	0.357
	VI th	0.59(PGA) ^{1.199}	0.852	0.314
VII th	0.32(PGA) ^{0.780}	0.703	0.318	

Note : G- Ground Storey, bold text -governing PSDM for the frame

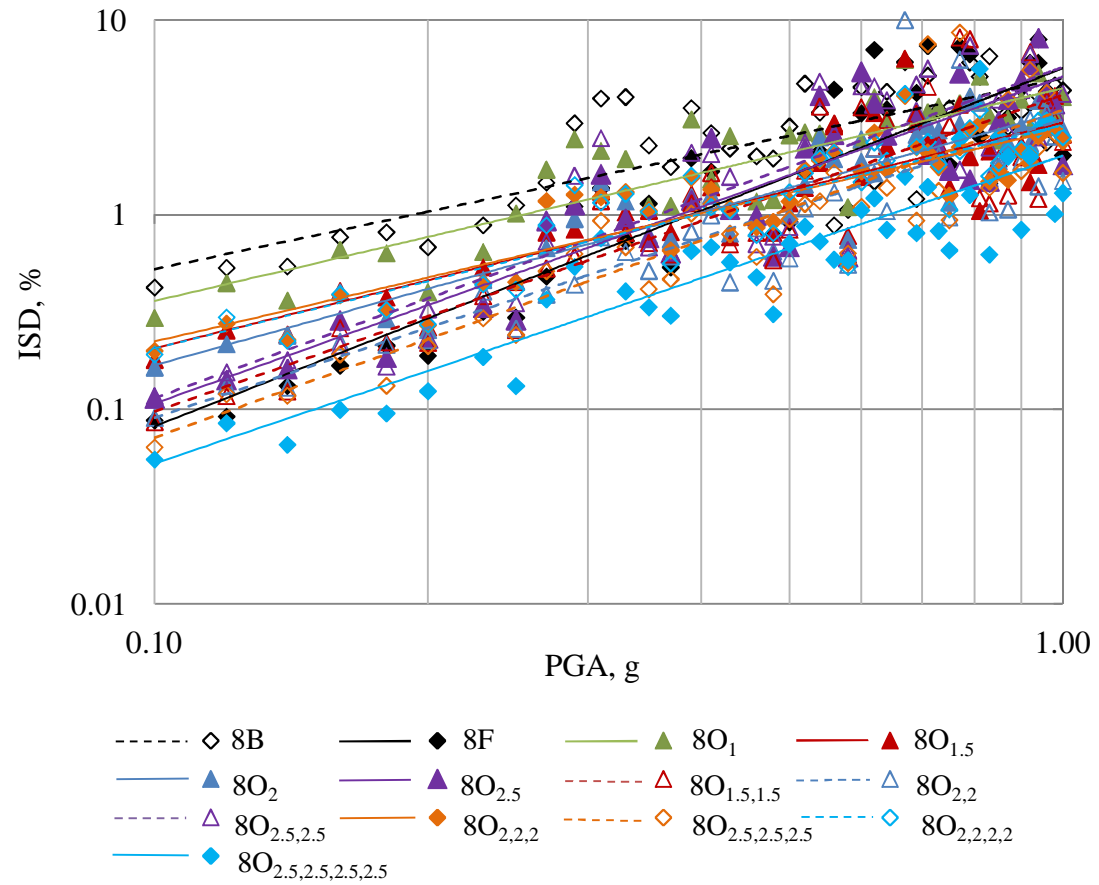


Fig. 5.9: PSDMs model for eight-storeyed frame

5.6 FRAGILITY CURVES

Once PSDM models and dispersions ($\beta_{D/PGA}$, β_c , and β_m) for all the frame models are computed, fragility curves for various performance levels are developed using the Eq. 3.10 for different performance levels namely Damage Limitation (DL), Significant Damage (DM) and Collapse prevention (CP). Fragility curves for all the storeys in each frame are evaluated. The curve which has the maximum probability of exceedance for the particular frame among all the storeys is considered as the governing fragility curve of the building.

5.6.1 Two-storey Buildings

Fragility curves for two-storey buildings designed with different schemes of MF (refer Chapter 3) for various performance levels (DL, SD and CP) are shown in Fig. 5.10. It is found that OGS building frame with MF value of 1.0 ($2O_1$) has maximum probability of exceedance among all the selected two-storey frames. This indicates that Frame $2O_1$ is most vulnerable among others. Fully infilled frame (2F) displays lowest probability of exceedance for all the selected performance levels. As MF value increases in ground storey columns ($2O_{1.5}$, $2O_2$ and $2O_{2.5}$) the probability of exceedance reduces for all performance levels. Similarly, for a scheme of same MF applied in both ground and first storeys ($2O_{1.5,1.5}$, $2O_{2,2}$ and $2O_{2.5,2.5}$), the probability of exceedance decreases as the MF value increases. However, there is no much difference in probability of exceedance for any damage state between the frames $2O_{2.5}$ & $2O_{2.5, 2.5}$. To understand the effect of different schemes of MF in the building performance, percentage decrease in probability of exceedance (with respect to $2O_1$) for CP performance level at a PGA of 0.75g for each OGS frames are computed and shown in the Fig. 5.11. The horizontal axis represents the frame identity and the vertical axis represents the probability of exceedance of ISD at

0.75g for CP level. It can be observed from the figure that the probability of exceedance of frame $2O_{1.5}$ is reduced by about 3% compared to $2O_1$. Similarly, the reductions in the probabilities of exceedance for other frames with different schemes of MFs are shown in the same figure. The maximum reduction in the exceedance probability at CP level is found to be 59% for the frame $2O_{2.5,2.5}$. Similar observation is found for frame $2O_{2.5}$ where the reduction in exceedance probability at CP level is 51%.

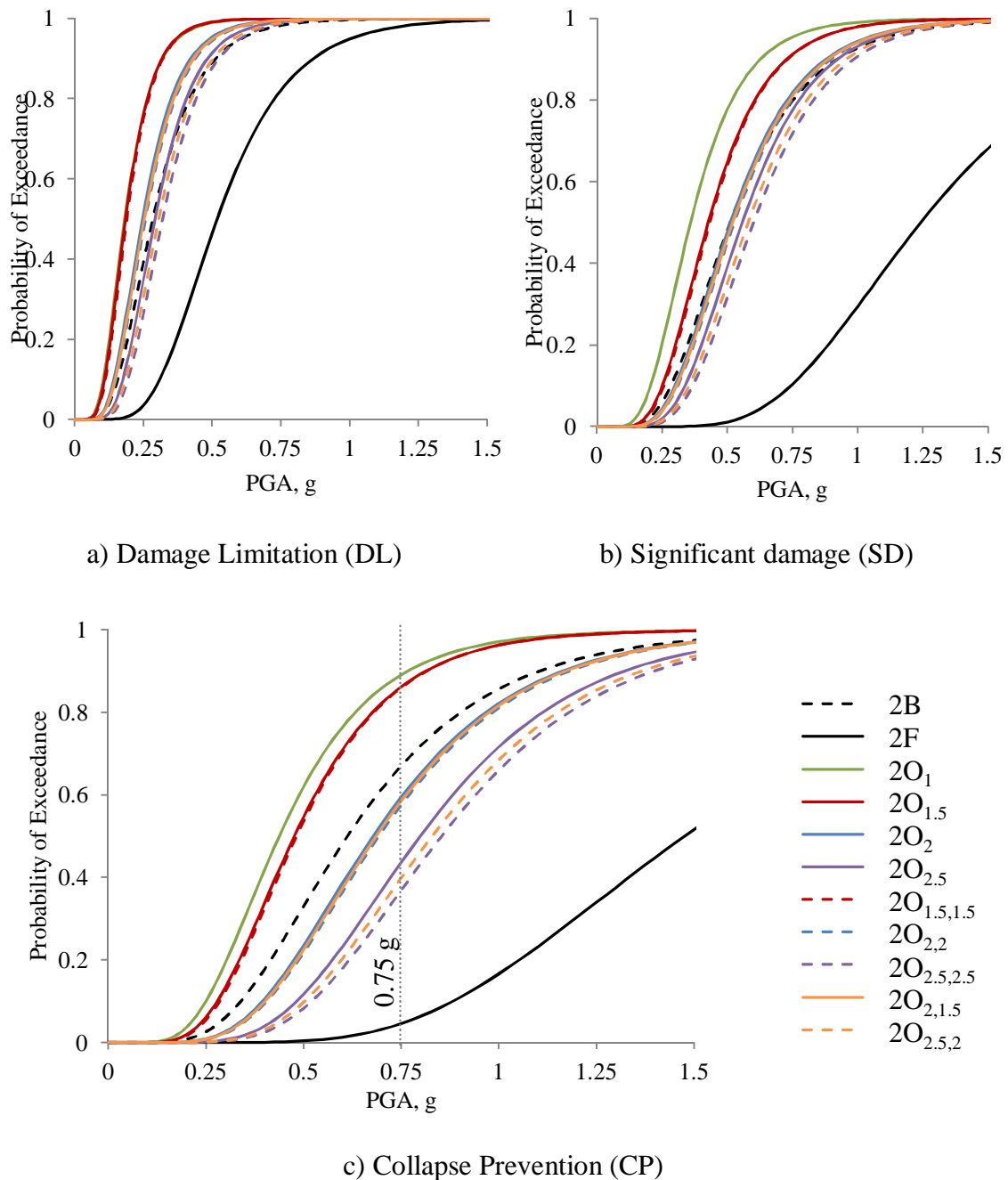


Fig. 5.10: Fragility curves for two-storey frames

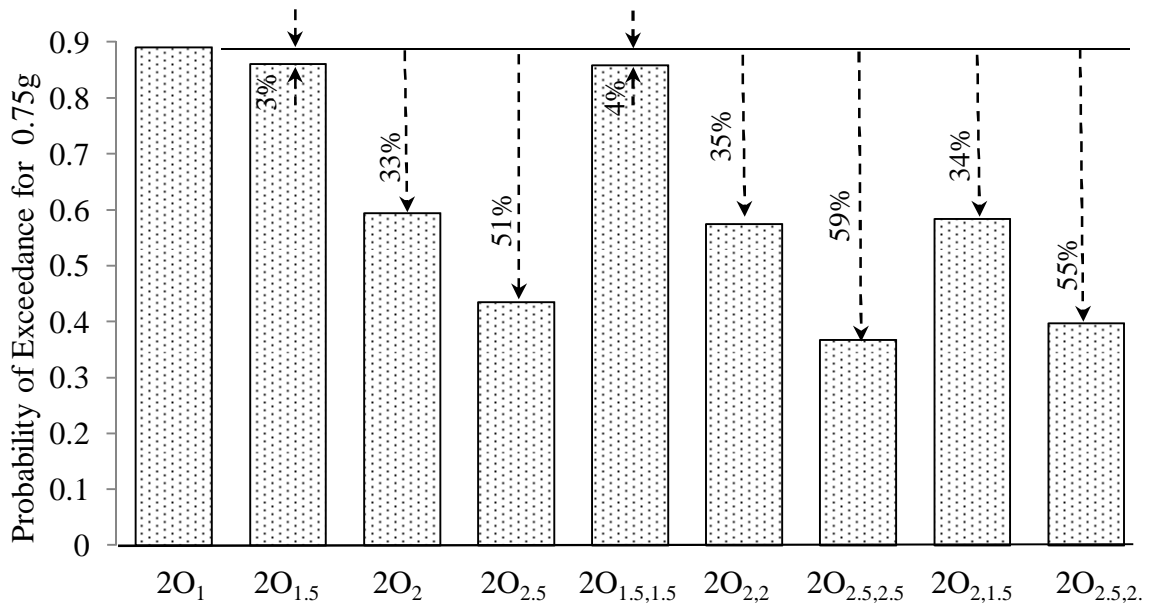


Fig. 5.11: Comparison of different schemes of MF at CP for 2-storey frames

5.6.2 Four-storey Buildings

Fragility curves for selected four-storey frames for various performance levels are shown in Fig. 5.12. It is found that OGS without any MF (4O₁) has maximum probability of exceedance as expected in all the performance levels. The 4F frame shows less probability of exceedance compared to 4B and 4O₁.

Fig. 5.13 shows a comparative performance (relative to Frame 4O₁) of four-storeyed OGS frames designed with different MF schemes for CP performance level at a PGA of 0.75g. It can be observed from the figure that the probability of exceedance of frame 4O_{1.5} is reduced by about 9% compared to 4O₁. As MF value increases from 1.5 to 2.0, (for frames 4O_{1.5} and 4O₂) the probability of exceedance is also reduced by 9% and 27% respectively. However, for the frames with MF of 2.5 and 3.0 (4O_{2.5} and 4O₃), the reduction of exceedance probability is only 16% and 11% which is less than that of 4O₂. This is due to the fact that ISD in the first storey is more than that of ground storey for the frames 4O_{2.5} and 4O₃. This phenomenon is schematically explained in the Fig 5.14. Fig 5.14 shows that the ISD is found to be maximum at the ground storey for the frames 4O_{1.5}

and $4O_2$ whereas it is at first storey for the frames $4O_{2.5}$ and $4O_3$. The maximum reduction in the exceedance probability at CP level is found to be 78%, 73%, 74% and 83% for the frames $4O_{2,2}$, $4O_{2.5,2.5}$, $4O_{2.5,2,1.5}$ and $4O_{3,2.5,2}$ respectively.

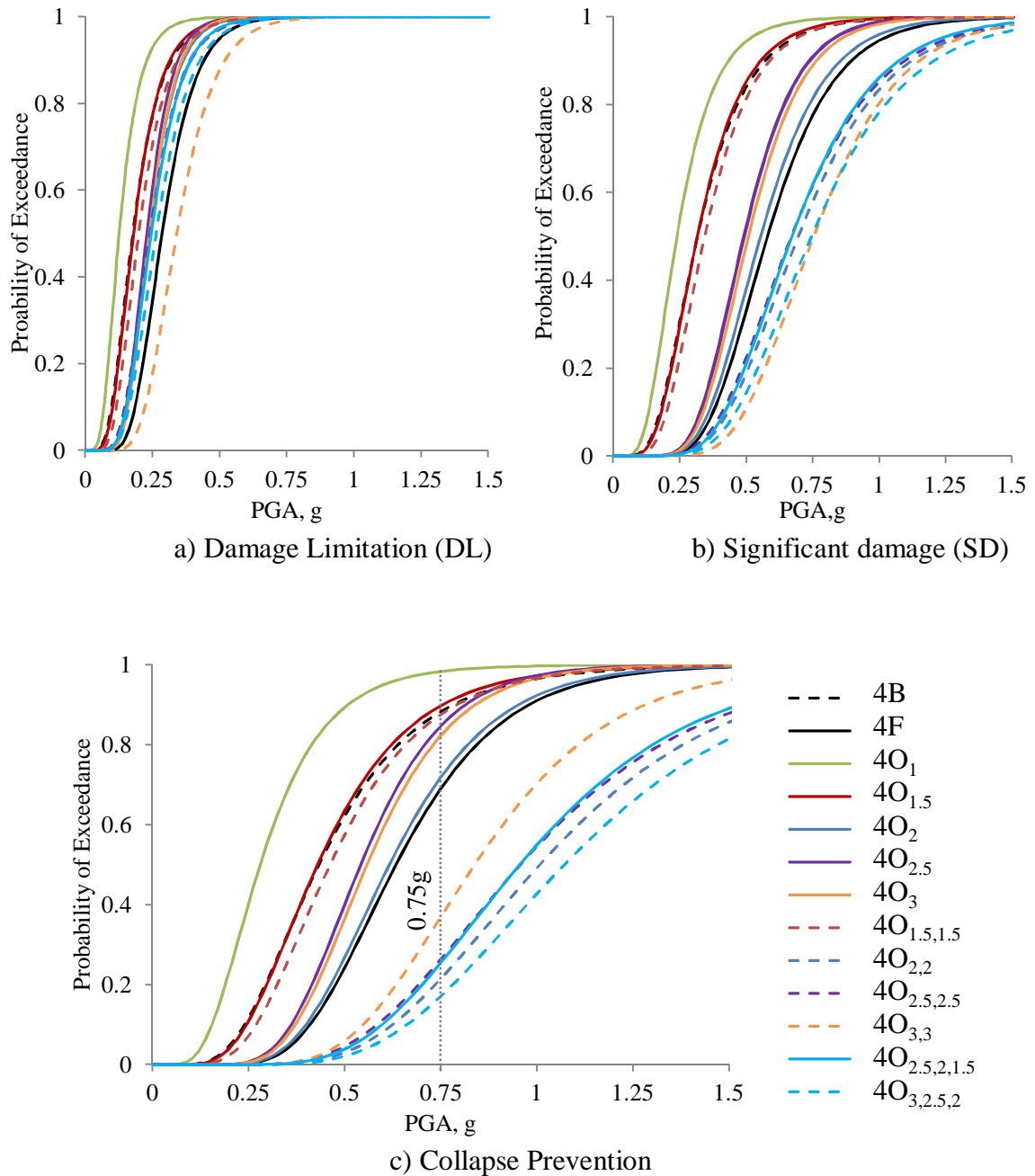


Fig. 5.12: Fragility curves for four-storey frames

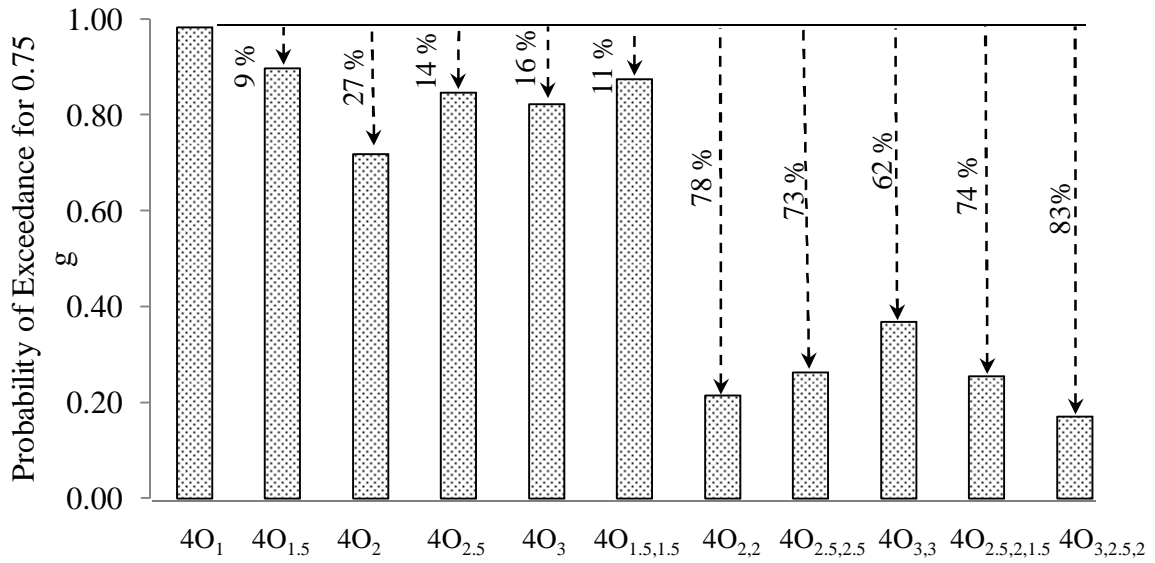


Fig. 5.13: Comparison of different schemes of MF at CP for 4-storey frames

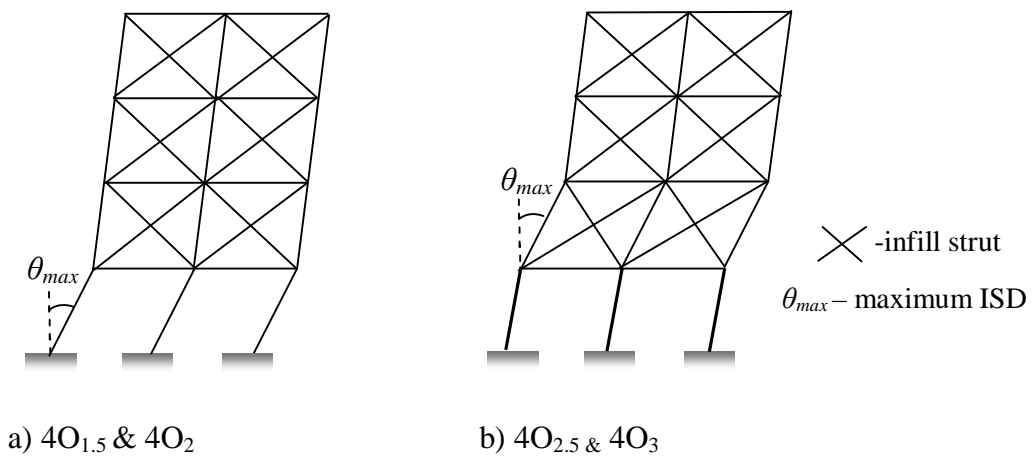


Fig. 5.14: Typical displacement profile for four-storeyed OGS frame

5.6.3 Six-storey Buildings

Similarly, the fragility curves are developed for six-storey building frames and shown in Fig. 5.15. It is found that OGS with MF value of 1.0 (6O₁) shows highest probability of exceedance as expected. Frame 6F shows less probability of exceedance compared to 6B and 6O₁. Fig. 5.16 shows a comparative performance (relative to 6O₁) of six-storeyed OGS frames for CP performance level at a PGA of 0.75g.

It can be observed from the figure that the probability of exceedance for frame 6O_{1.5} is reduced by about 14% compared to 6O₁. The probability of exceedance of the frame 6O₂ and 6O_{2.5} is reduced by 10% and 9% respectively which shows the poor performance of these frames compared 6O_{1.5}. This is due to the larger ISD in the first storey, compared to the ground storey, for the frame 6O₂ and 6O_{2.5}. This behaviour is shown schematically in the Fig. 5.17.

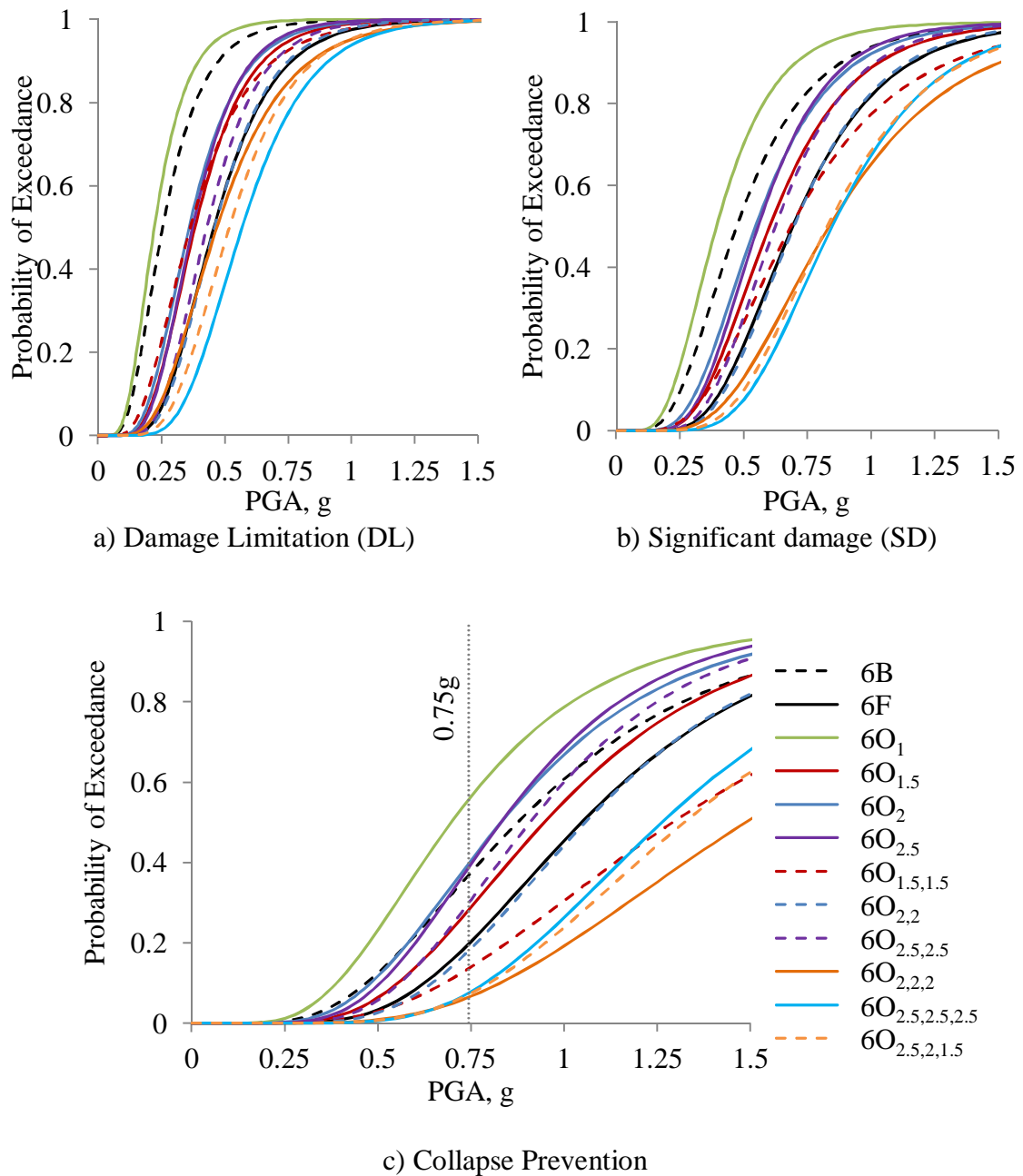


Fig. 5.15: Fragility curves for six-storey frames

The $6O_{1.5,1.5}$ shows better performance compared to $6O_1$ with a reduction in probability of exceedance by 41%. But the performance of frames $6O_{2,2}$ and $6O_{2.5,2.5}$ is not as good as $6O_{1.5,1.5}$ due to the large inter-storey drift at the second storey level as shown in the Fig. 5.17c. Fig. 5.16 shows that the application of MF in three storeys ($6O_{2,2,2}$, $6O_{2.5,2.5,2.5}$ and $6O_{2.5,2.1.5}$) perform better with substantial reduction in probabilities of exceedance of these frames compared that of $6O_1$.

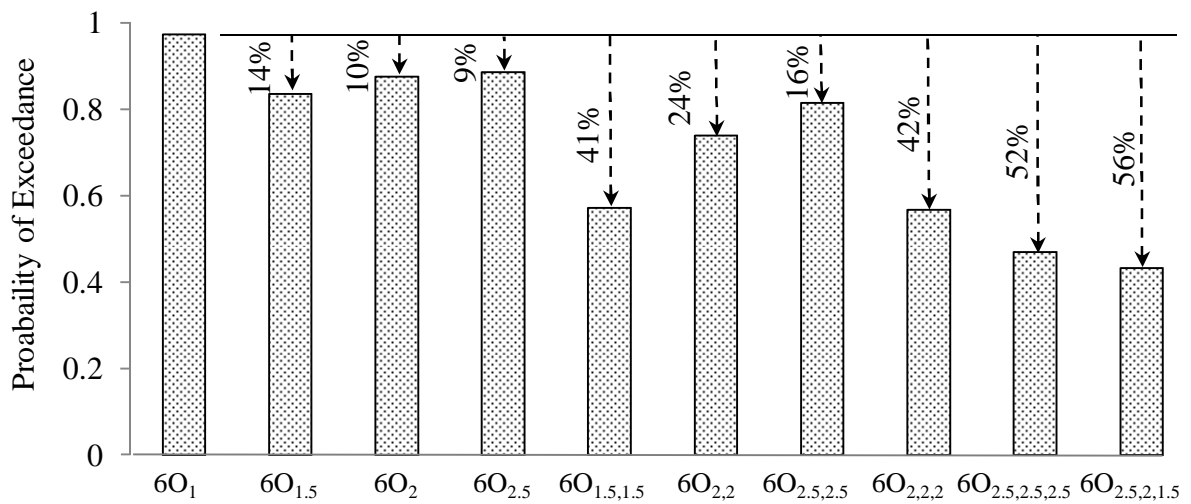


Fig. 5.16: Comparison of different schemes of MF at CP for 6-storey frames

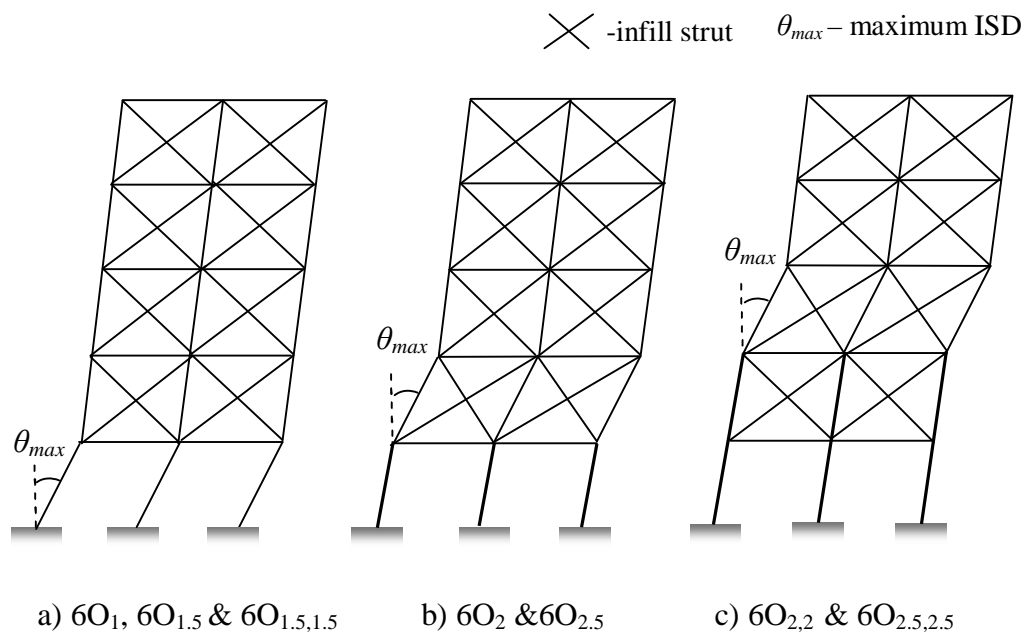


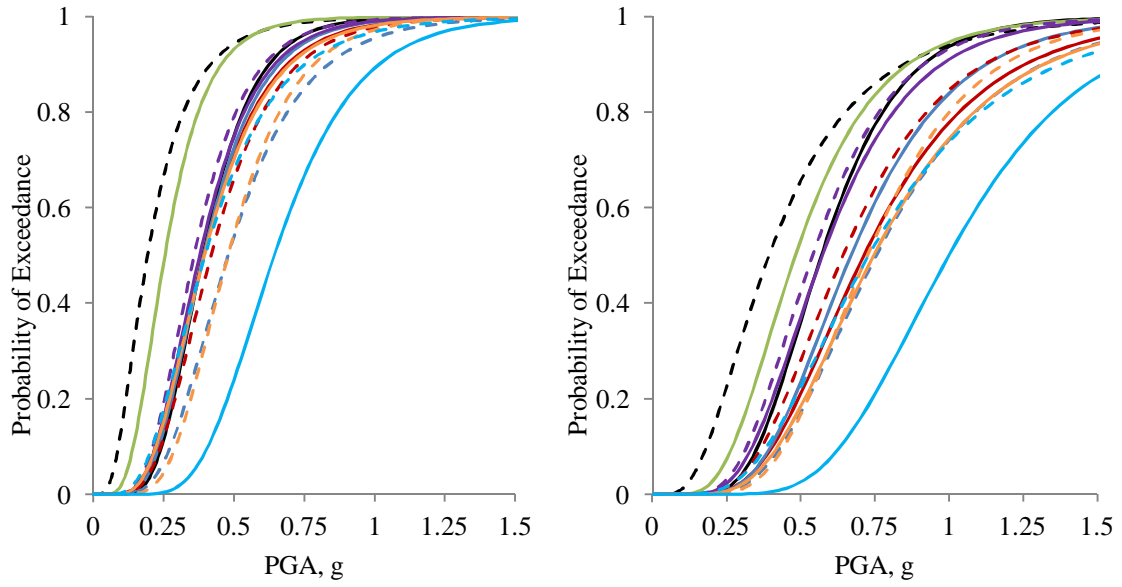
Fig. 5.17: Typical displacement profile for six-storeyed OGS frame

5.6.4 Eight-storey Buildings

Fragility curves are developed for selected eight-storey building frames designed with different scheme of MF and shown in Fig. 5.18. OGS with M.F value of 1.0 (8O₁) display poor performance by showing highest probability of exceedance as expected. Frame 8F shows less probability of exceedance compared to 8B and 8O₁. Fig. 5.19 shows a comparative performance (relative to 8O₁) of eight-storeyed OGS frames for CP performance level at a PGA of 0.75g.

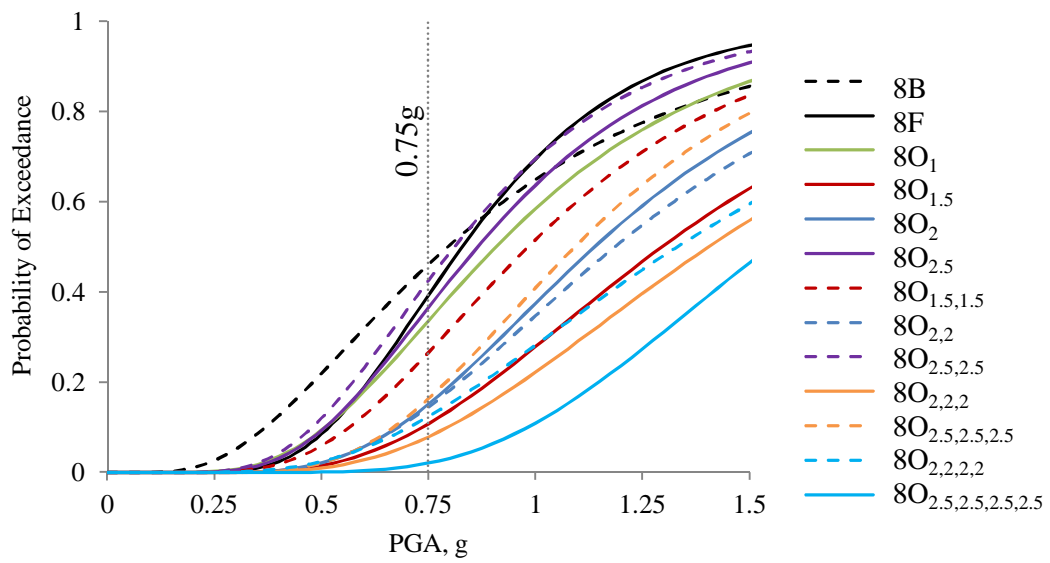
It can be observed from the figure that the probability of exceedance for frame 8O_{1.5} is reduced by about 18% compared to 8O₁. The probability of exceedance of frame 8O₂ is reduced by 6% compared that of 8O₁. 8O_{1.5} found to be performing better than 8O₂ and 8O_{2.5}. The behaviour of these (8O₂ and 8O_{2.5}.) frames is governed by the ISD at first storey level as shown in Fig. 5.21b.

The frame 8O_{2,2} shows a better performance compared to 8O_{1.5,1.5} and 8O_{2.5,2.5} as shown in the Fig. 5.19. The frame 8O_{2,2,2} shows comparatively good performance than 8O_{2.5,2.5,2.5}. The OGS frame 8O_{2.5,2.5,2.5,2.5} perform better than all other frames with the maximum reduction in the probability of exceedance of 86%. Fig. 5.20c and 5.20d show the displacement profile of these frames schematically.



a) Damage Limitation (DL)

b) Significant damage (SD)



c) Collapse Prevention

Fig. 5.18: Fragility curves for eight-storeyed frames

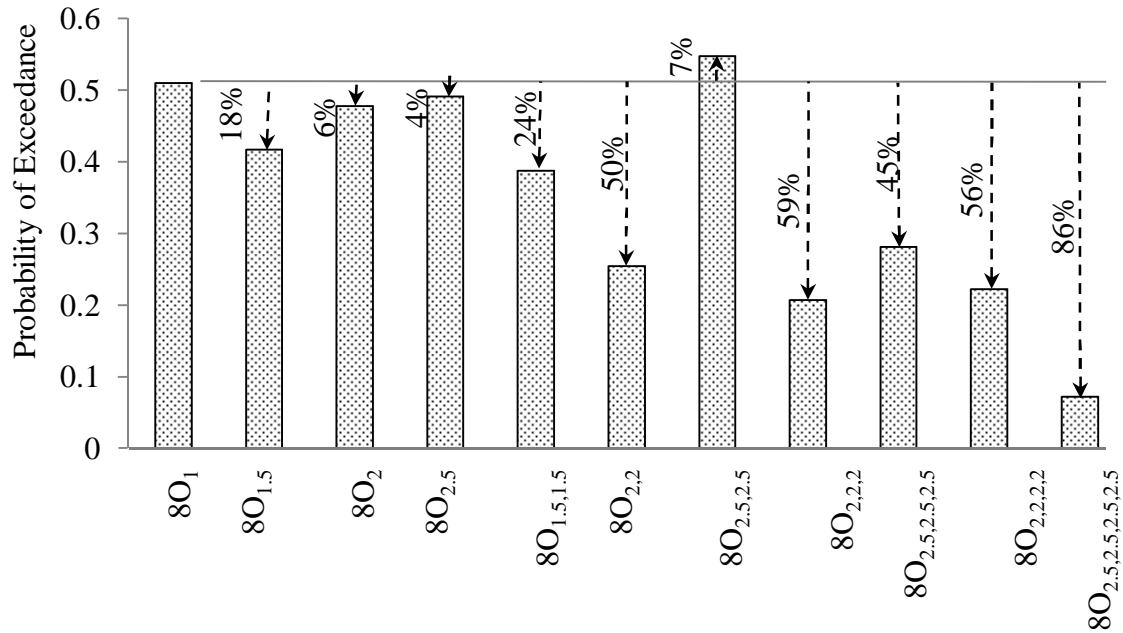


Fig. 5.19: Comparison of different schemes of MF at CP for 8-storey frames

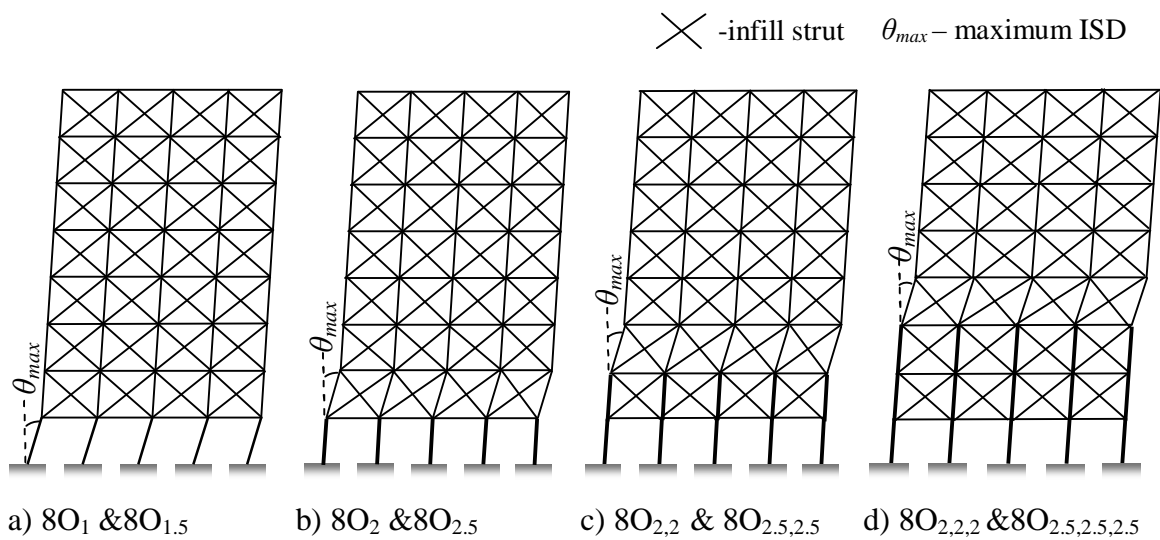


Fig. 5.20: Typical displacement profile for eight-storeyed OGS frame

5.7 SUMMARY AND CONCLUSIONS

Storey displacement responses from NTHA of four-storeyed frames are compared to understand the effect of various MF schemes in OGS frames. It is found that the storey displacement profile of OGS frames designed with MF value of 1.0 is different from that of fully infilled frame and bare frame. With regard OGS frames with MF applied only in ground storey, as the MF value increases from 1.0 to 3.0 the ISD decreases by 84% in the

ground storey and increases by 913% in the first storey. This implies that application of MF only in the ground storey make the adjacent first storey to be vulnerable.

Comparison of fragility curves developed using 2000 SAC-FEMA method with a more rigorous LHS Monte Carlo method for typical four storey frame is carried out. It is found that the fragility curves developed using 2000 SAC-FEMA method is in agreement with computationally more intensive LHS-MC method.

PSDMs and corresponding fragility curves are developed using 2000 SAC-FEMA method for all the selected frames. Comparisons of the fragility curves are presented to study the effectiveness of different schemes of MF for the design of OGS buildings.

It is found that, for two-storey frames, application of MF in ground storey alone shows good performances. However, in case of four-storey frames, it makes first storey as vulnerable. When MF is used in ground and first storey for four-storey frames, the exceedance probability of ISD is reduced considerably. Similarly, six-storey frames shows less probability of exceedance of ISD when MF is applied in ground, first and second storey. For eight-storey frames, shows good performance (less exceedance probability) when MF is applied in ground, first, second and third storey.

CHAPTER 6

RELIABILITY BASED ASSESSMENT OF OGS BUILDINGS

6.1 INTRODUCTION

The fragility curves derived so far presents the probability that the frames considered will fail if subjected to earthquakes of a given intensity (in terms of PGA). However, to assess the risk of any structures, these fragility curves should be combined with the probability of occurrence of earthquakes of a given intensity at the location of interest (seismic hazard). The risk of building frames is expressed in this study through the statistical parameter 'reliability index'. Reliability indices are calculated and analysed for all the selected frames against seismic hazards of selected locations in India. The first part of this chapter describes the selection of seismic hazard curves from available literature. Risk of a structure can be calculated for different levels of earthquake and for building performance limit states. Therefore, it is necessary to establish the desired performance limit states of buildings when subjected to different earthquake levels. These performance objectives are discussed in the next part of this chapter. Reliability indices are calculated for all the OGS frames against the selected hazard curves and presented in this chapter. This chapter presents detailed discussions on the effect of different schemes of MF used for the design of OGS buildings on the reliability indices. In order to have an acceptable degree of reliability, target reliability values for different performance objective are established based on available literature and present studies on benchmark buildings (fully infilled frames). The most effective schemes of MF for the design of OGS building are proposed based on the above discussions.

6.2 SELECTION OF SEISMIC HAZARD CURVE

Hazard curve represents the probability of occurrence of an earthquake of a given maximum intensity. Appropriate hazard curve should be considered for assessment of seismic risk in order to adequately represent an area of seismicity for which the frame has been designed. The seismic hazard function (G_A) at a site is the annual frequency of motion intensity at or above a given level (x), which is expressed through a complementary cumulative distribution function. Chapter 3 summarizes the procedure for the development of seismic hazard curves for a particular site based on the earthquake sources, magnitude (m) and source to site distance (r).

The building frames considered in this study are designed for the highest seismic zones of India (Zone-V as per IS 1893, 2002). Also, the building characteristics including the material properties, configurations, their variations, etc. are considered in the context of Indian construction practice. Therefore, two different seismically active locations from Zone-V of Indian seismic map (Guwahati and Bhuj) are considered in this study. Seismic hazard curves of Guwahati and Bhuj are available in literature (Nath and Thingbaijam, 2012) as shown in Fig. 6.1. The mean annual rate of exceedance for three levels of earthquake such as 50%, 10% and 2% in 50years (with return periods of 72, 475 and 2475 years respectively) is marked in the figure. The PGA values corresponding to these three levels of earthquakes for the selected locations are shown in Table 6.1.

Table: 6.1: Different earthquake levels at selected regions

Location	Probability of exceedance for 50% in 50 years PGA (g)	Probability of exceedance for 10% in 50 years PGA (g)	Probability of exceedance for 2 % in 50 years PGA (g)
Guwahati	0.28	0.67	1.35
Bhuj	0.15	0.43	0.95

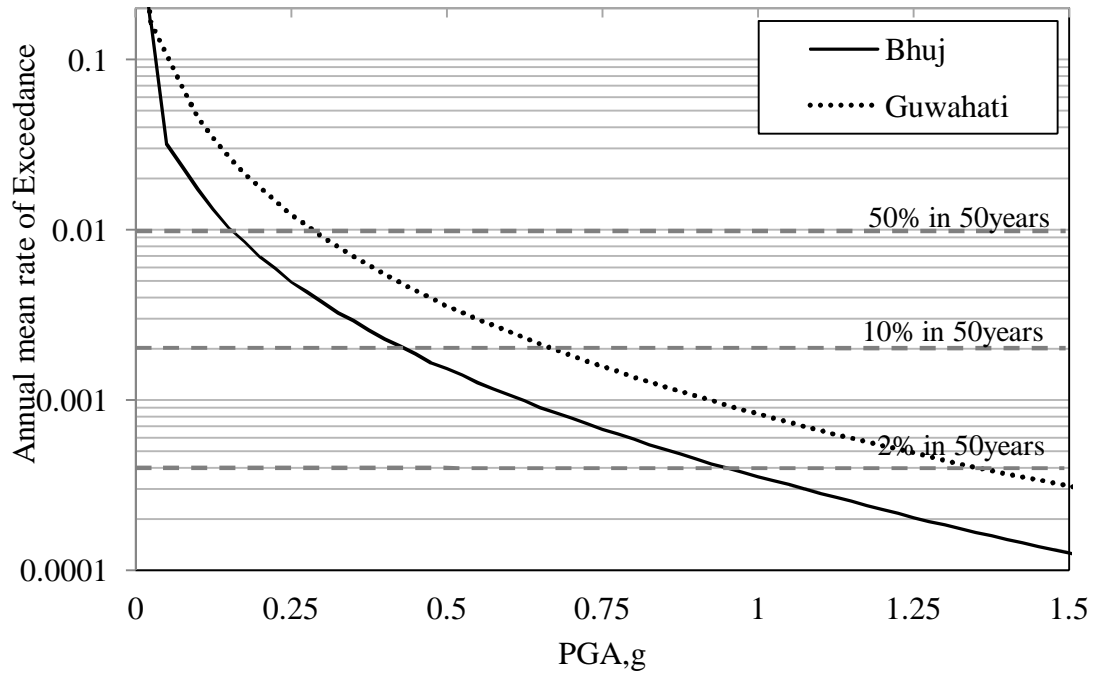


Fig. 6.1: Seismic hazard curves of selected regions

6.3 PERFORMANCE OBJECTIVES

Performance objective of an analysis constitutes the target building performance level under the selected level of seismic hazard. Details of the different performance levels considered in the present study are discussed in Sections 3.3 and 4.8. SEAOC (1995) proposed performance objectives in the form of a matrix mapping earthquake hazards with the performance levels as shown in Fig. 6.2. As per SEAOC (1995) multiple levels of performance objectives can be defined. A basic safety objective (BSO) is defined by SEAOC (1995) as multiple requirements of ‘fully operational’ under ‘frequent’ earthquakes, ‘operational’ under ‘occasional’ earthquakes, ‘Life Safety’ under ‘rare’ earthquake and ‘near collapse’ under ‘very rare’ earthquake. The aim of BSO is to have a low risk of life threatening injury during a rare earthquake and to check the collapse of the system during a very rare earthquake.

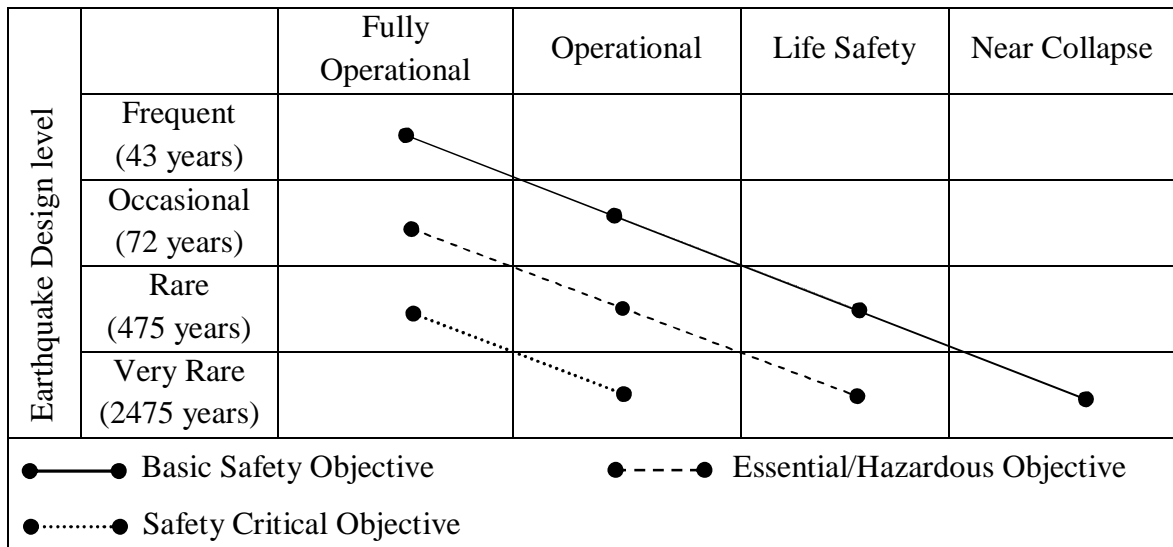


Fig. 6.2: Seismic performance and design objective matrix as per SEAOC (1995)

These same BSO proposed by SEAOC (1995) is selected in the present study with selected three performance levels (discussed in Section 3.3) as follows:

Performance Objective I (PO-I): Damage Limitation (DL) for an occasional earthquake hazard level having probability of occurrence of 50% in 50 years (return period of 72 years).

Performance Objective II (PO-II): Significant Damage (SD) for a rare earthquake hazard level having probability of occurrence of 10% in 50 years (return period of 475 years).

Performance Objective III (PO-III): Collapse Prevention (CP) for a very rare earthquake hazard level having probability of occurrence of 2% in 50 years (return period of 2475 years).

6.4 RELIABILITY CURVES

Reliability indices are calculated for all the selected buildings for different performance objectives using Eq. 3.2 through a numerical integration. Fig. 6.3 presents a schematic representation for the computation of reliability index of each frame. The fragility curve,

$F_R(x)$ and seismic hazard curve $G_A(x)$ are combined to evaluate the limit state probability, $P[LS_i]$ and the corresponding reliability index, β_{pf} . The details of this procedure are discussed in Section 3.2.

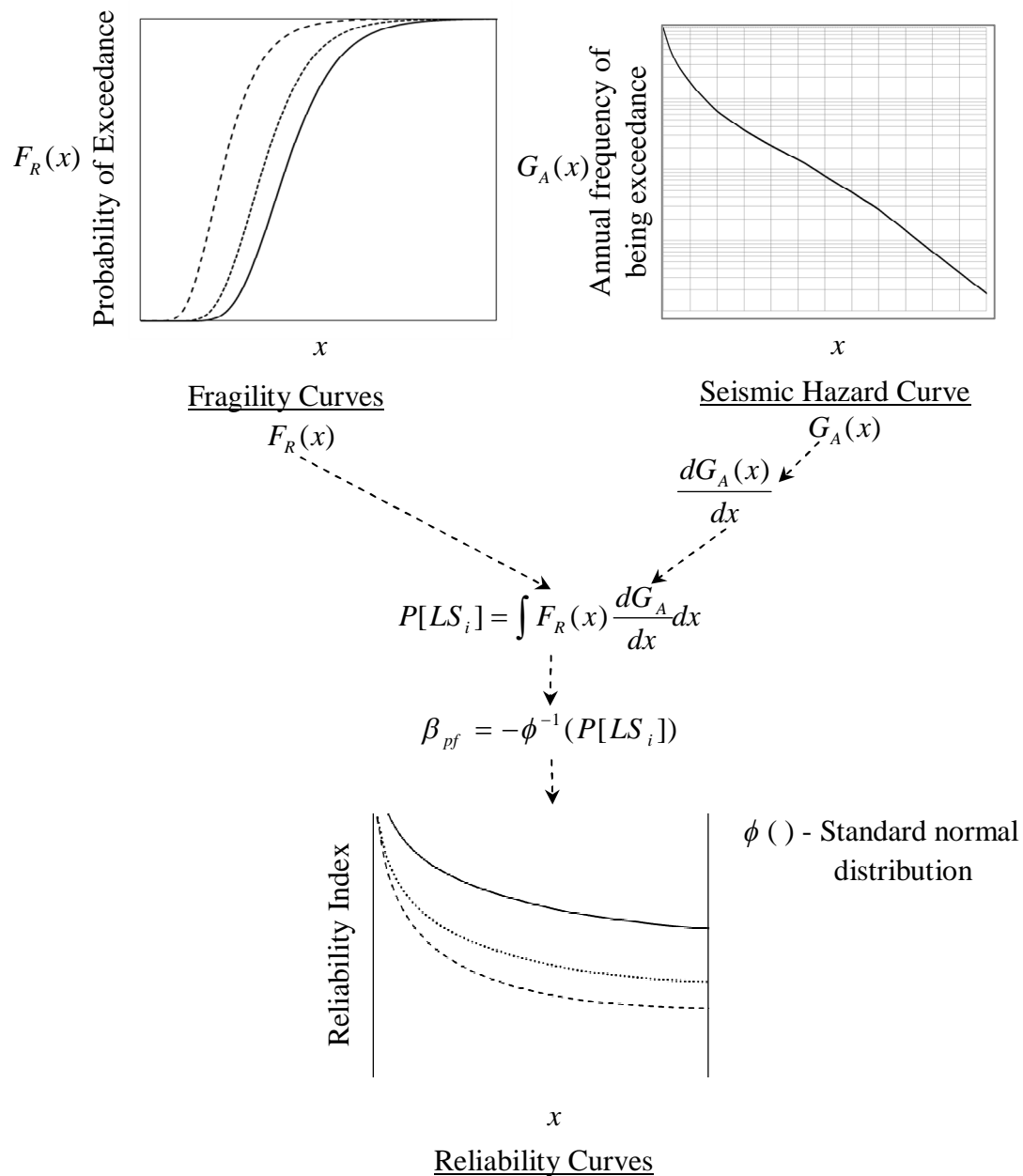


Fig 6.3: Schematic representation for development of reliability index (β_{pf})

Reliability curve is the plot of reliability index as a function of PGA. Figs. 6.4-6.7 show the reliability curves for two, four, six and eight storey OGS frames designed with various MF schemes for Guwahati region.

6.4.1 Two Storey Frames

Fig. 6.4 presents the reliability curves (reliability index versus PGA) for different performance levels, DL, SD and CP for two storey frames at Guwahati region. It is observed that, as the PGA increases the reliability index decreases. It can be seen that Frame $2O_1$ yields the lowest values of reliability index for all PGAs, *i.e.*, this building frame is most vulnerable. The frames $2F$, $2O_{2.5}$, $2O_{2.5,2.5}$ and $2O_{2.5,2}$ show relatively higher values of reliability index compared to $2O_1$. To find out the reliability index values corresponding to the selected performance objectives, PO-I, PO-II and PO-III, the corresponding PGAs are marked in the figure.

6.4.2 Four Storey Frames

Fig. 6.5 shows the reliability curves for different performance levels, DL, SD and CP for four storey frames at Guwahati region. It can be seen that Frame $4O_1$ yields the lowest values of reliability index for all PGAs. The frames $4O_{2,2}$, $4O_{2.5,2.5}$, $4O_{3,3}$, $4O_{2.5,2,1.5}$ and $4O_{3,2.5,2}$ show relatively higher values of reliability index compared to $4O_1$. To find out the reliability index values corresponding to the selected performance objectives, PO-I, PO-II and PO-III, the corresponding PGAs are marked in the figure.

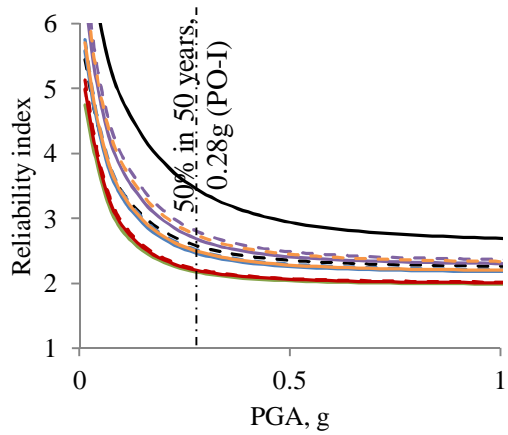
6.4.3 Six Storey Frames

Fig. 6.6 shows the reliability curves for different performance levels, DL, SD and CP for six storey frames at Guwahati region. It can be seen that Frame $6O_1$ yields the lowest values of reliability index for all PGAs. The frames $6O_{2,2,2}$, $6O_{2.5,2.5,2.5}$ and $6O_{2.5,2,1.5}$ show relatively higher values of reliability index compared to $6O_1$. To find out the reliability index values corresponding to the selected performance objectives, PO-I, PO-II and PO-III, the corresponding PGAs are marked in the figure.

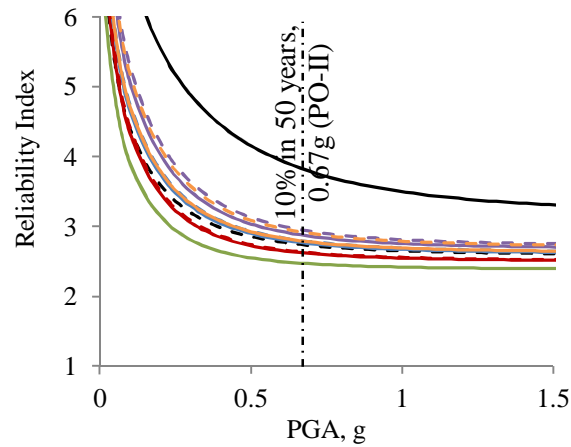
6.4.4 Eight Storey Frames

Fig. 6.7 shows the reliability curves for different performance levels, DL, SD and CP for eight storey frames at Guwahati region. It can be seen that Frame $8O_1$ yields the lowest values of reliability index for all PGAs. The frames $8O_{2.5,2.5,2.5,2.5}$ show relatively higher values of reliability index compared to $8O_1$. To find out the reliability index values corresponding to the selected performance objectives, PO-I, PO-II and PO-III, the corresponding PGAs are marked in the figure.

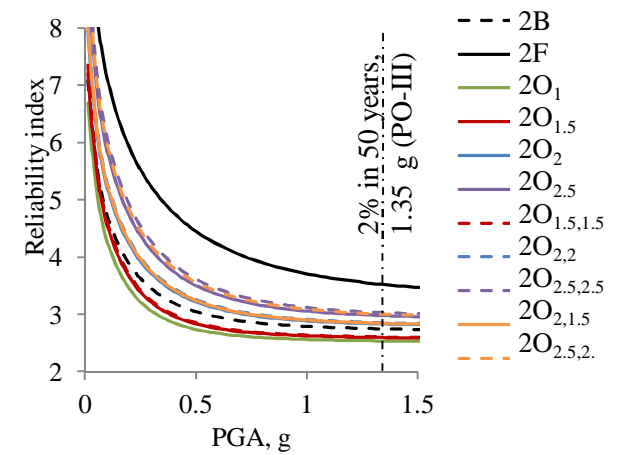
Reliability curves for all performance levels are also developed and similar observations are found for Bhuj region. Reliability index corresponding to the PGAs of selected performance objectives are recorded for both the selected regions and used for further analyses.



a) Reliability curves for DL Performance

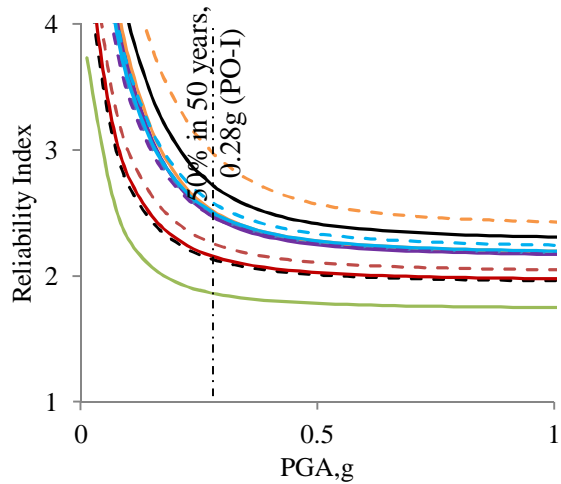


b) Reliability curves for SD Performance

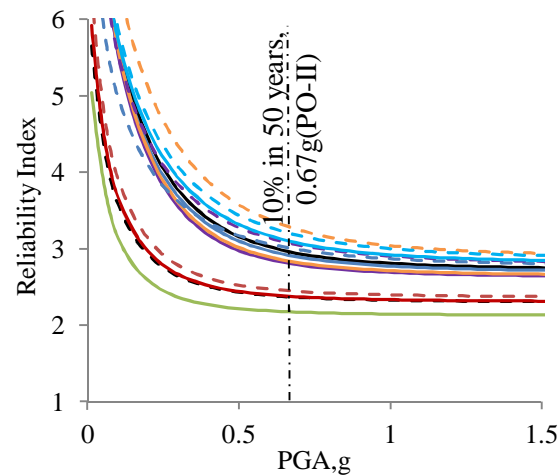


c) Reliability curves for CP Performance

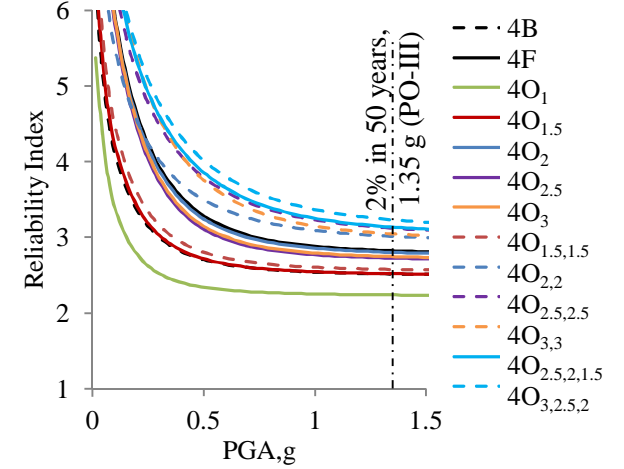
Fig. 6.4: Reliability Curves for 2 storey frame



a) Reliability curves for DL Performance

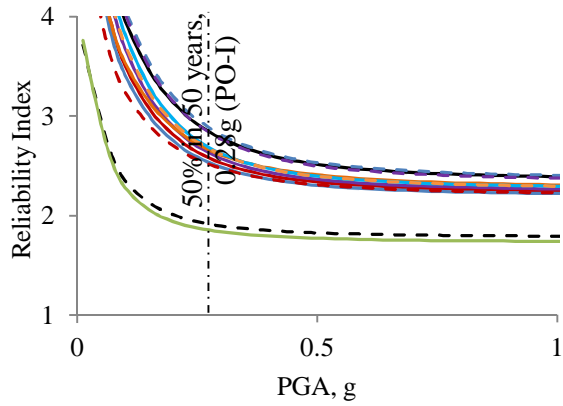


b) Reliability curves for SD Performance

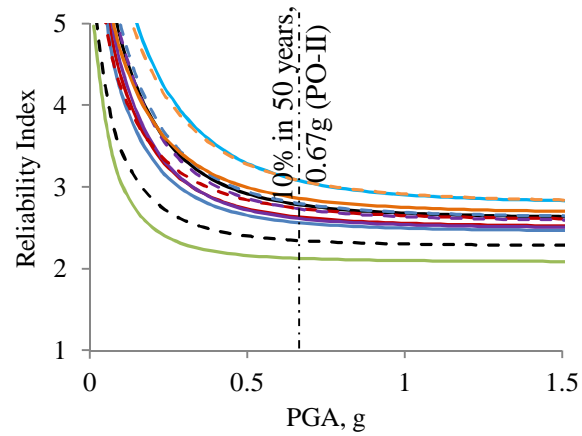


c) Reliability curves for CP Performance

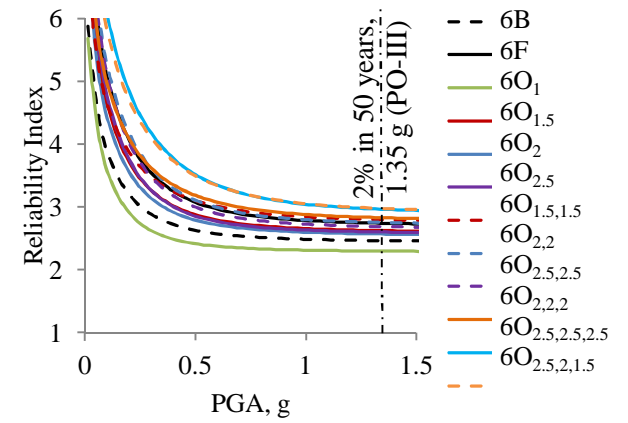
Fig. 6.5: Reliability Curves for 4 storey frame



a) Reliability curves for DL Performance

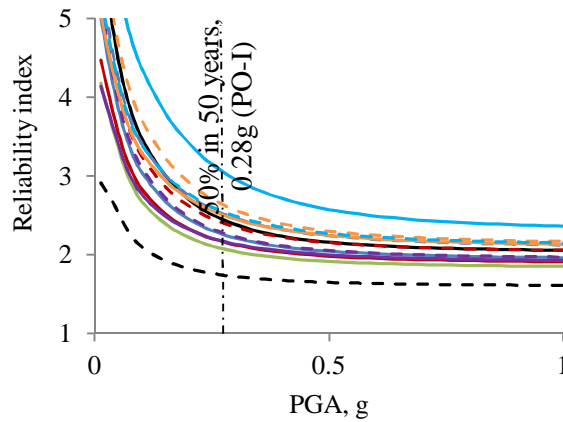


b) Reliability curves for SD Performance

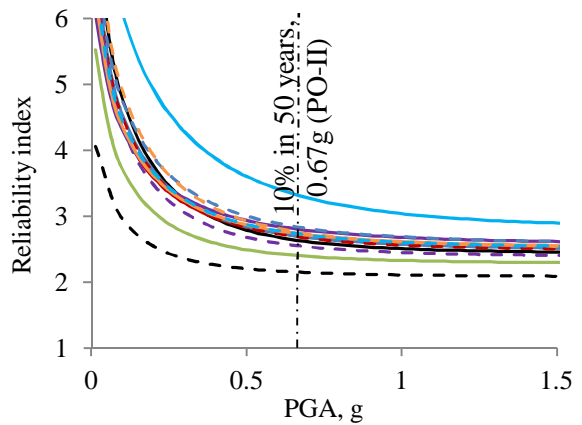


c) Reliability curves for CP Performance

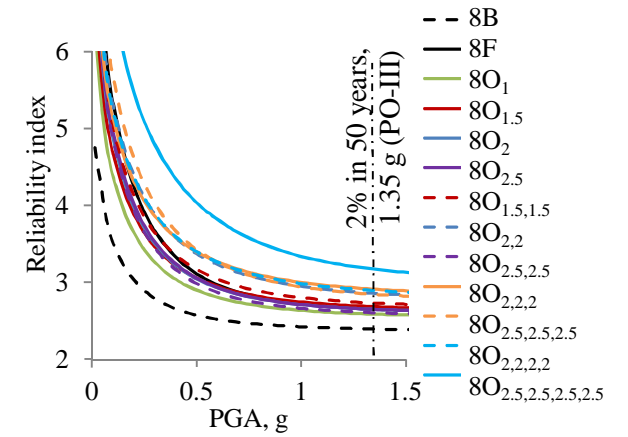
Fig. 6.6: Reliability Curves for 6 storey frame



a) Reliability curves for DL Performance



b) Reliability curves for SD Performance



c) Reliability curves for CP Performance

Fig. 6.7: Reliability Curves for 8 storey frame

6.5 RELIABILITY INDEX FOR DIFFERENT PERFORMANCE OBJECTIVES

Reliability indices for selected performance objectives are calculated from the reliability curves presented in the previous section. Reliability index can be a direct measure of the safety of the buildings. Higher the value of reliability index lesser the probability of failure and vice-versa. This section presents the reliability index achieved by the selected frames for different performance objectives.

6.5.1 Two Storey Frames

Reliability index at three selected performance objectives for both of the two selected regions are presented in Fig. 6.8 in the form of bar charts. This figure shows the comparison of reliability indices for all the two storeys frames designed with various schemes of MF. It can be seen that the reliability indices at PO-I level are in the range of 2.1 to 3.5 for Guwahati region and 2.8 to 4.4 for Bhuj region. It is found that OGS building frame without any MF ($2O_1$) has the lowest reliability index whereas fully infilled frame (2F) has the highest reliability index in all the performance objectives. This indicates the good performance of the 2F frame.

As MF value increases ($2O_{1.5}$, $2O_2$ & $2O_{2.5}$) in ground storey columns, the reliability index increases for all performance objectives. Similarly, as the MF value increases the reliability index increases when equal magnitude of MFs are applied in both ground and first storeys ($2O_{1.5,1.5}$, $2O_{2,2}$ & $2O_{2.5,2.5}$). The OGS frames with different magnitude of MFs in ground and first storey ($2O_{2,0,1.5}$ and $2O_{2.5,2,0}$) also show good performance as indicated in their respective reliability index values.

6.5.2 Four Storey Frames

Reliability indices for four storey building frames at different performance objectives for different regions are presented Fig. 6.9. This figure shows the comparison of reliability indices achieved by the four storeys frames designed with various schemes of MF. It can be seen that the reliability indices at PO-I level are in the range of 1.7 to 2.7 for Guwahati region and 2.4 to 3.6 for Bhuj region. It is found that OGS building frame without any MF ($4O_1$) has the lowest reliability index. Unlike the case of two storey buildings, the fully infilled frame in this case (4F) does not have the maximum reliability index.

Fig. 6.9 presents the following interesting observation: the reliability indices are not increasing with the increase of MF values after a certain limit when the MF is applied only in the ground storey. As the MF values increase from 1.5 to 2.0 in the ground storey (for frames $4O_{1.5}$ and $4O_2$), reliability index increases for all performance objectives. However, the reliability index reduces for the further increase of MFs in the ground storey ($4O_{2.5}$ and $4O_3$). This is due to the shift of failure mechanism from ground storey to the adjacent first storey when MF in the ground storey exceeds a value 2.0. This can be clearly seen from Fig. 5.14. This can be concluded from this observation that the application of MF only in ground storey may not increase the reliability index of that frame but it may lead to vulnerable adjacent first storey. The Frames $4O_{2,2}$, $4O_{2.5,2.5}$, $4O_{2.5,2,1.5}$ and $4O_{3,2.5,2}$ show higher reliability indices as compared with $4O_1$ in all performance objectives.

6.5.3 Six Storey Frames

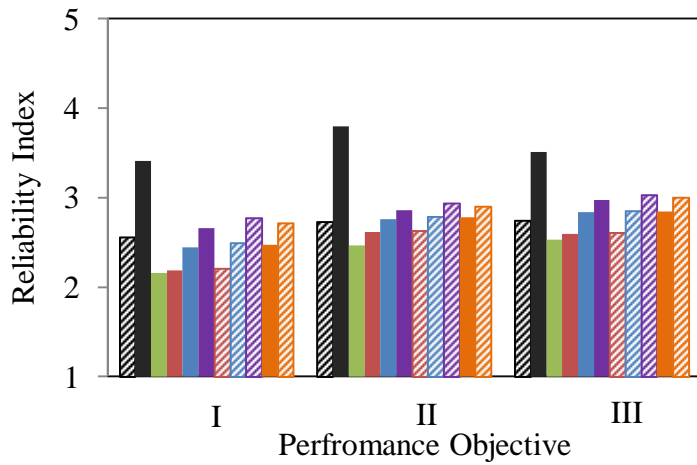
Fig. 6.10 shows the comparison of reliability indices for all the six storeys frames designed with various schemes of MF for three performance objectives. It is found that OGS without any MF ($6O_1$) is having the lowest reliability index. In line with the results

of four storey frames the reliability indices are analysed for six storey building frames with MFs applied in two lower storeys (ground and first). It is found that these schemes make the second storey vulnerable after a certain limit. However, when the MFs are applied in first three storeys of six storey frames ($6O_{2,2,2}$, $6O_{2.5,2.5,2.5}$ and $6O_{2.5,2,1.5}$), it shows relatively higher reliability index in all performance objectives.

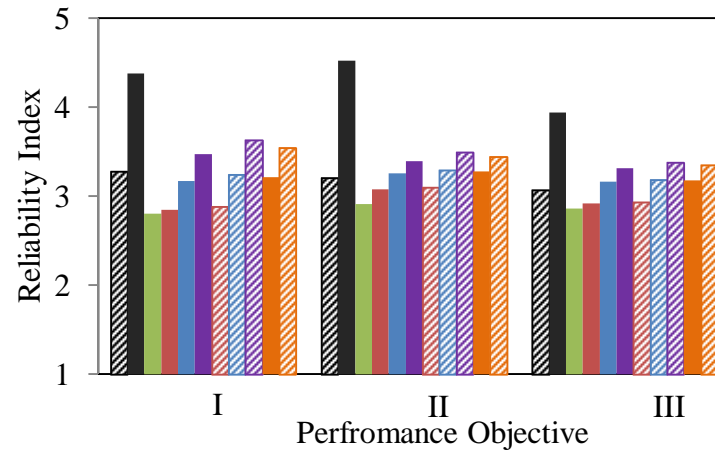
6.5.4 Eight Storey Frames

Fig. 6.11 figure shows the comparison of reliability indices for all the eight storeys frames designed with various schemes of MF for selected three performance objectives. OGS building frame without any MF ($8O_1$) found to have the lowest reliability index in this case also. Frame $8O_{2.5,2.5,2.5,2.5}$ found to result in maximum reliability index among all the eight storey frames considered.

The above observations are generally true for both of the two selected regions (Guwahati and Bhuj) as shown in the Figs. 6.8-6.11. However, the reliability index of all the frames for Guwahati region is found to be the little lower as compared to the Bhuj region for each performance objectives. This is due to the higher probability of occurrence of earthquake at Guwahati region as shown in Fig. 6.1.



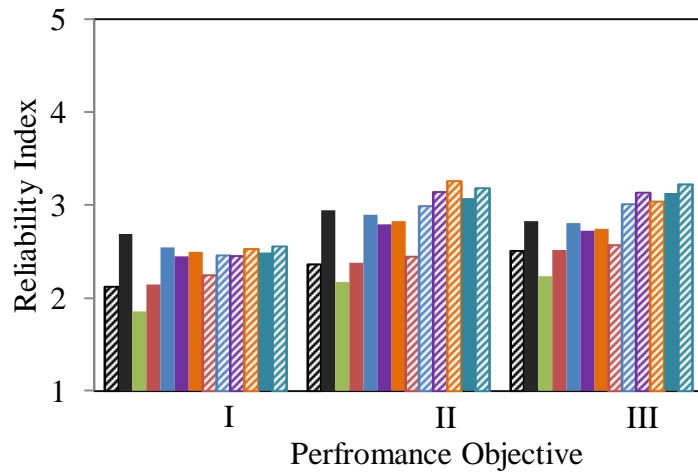
a) Guwahati Region



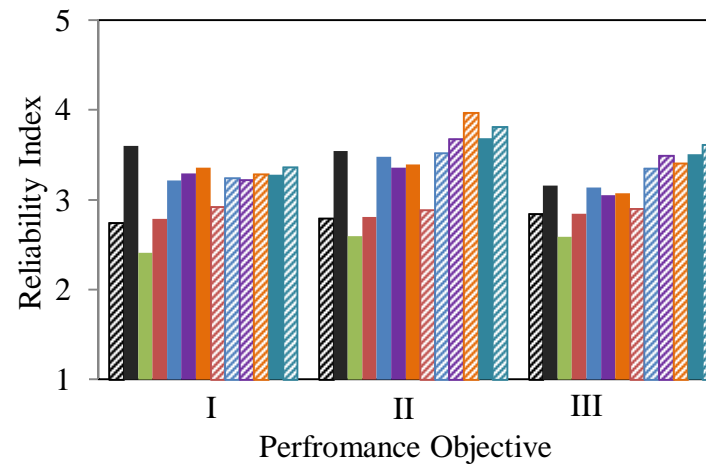
b) Bhuj Region

- 2B
- 2F
- 2O₁
- 2O_{1.5}
- 2O₂
- 2O_{2.5}
- 2O_{1.5,1.5}
- 2O_{2,2}
- 2O_{2.5,2.5}
- 2O_{2,1.5}
- 2O_{2.5,2}

Fig. 6.8: Reliability index for different performance objectives for 2- storey frames



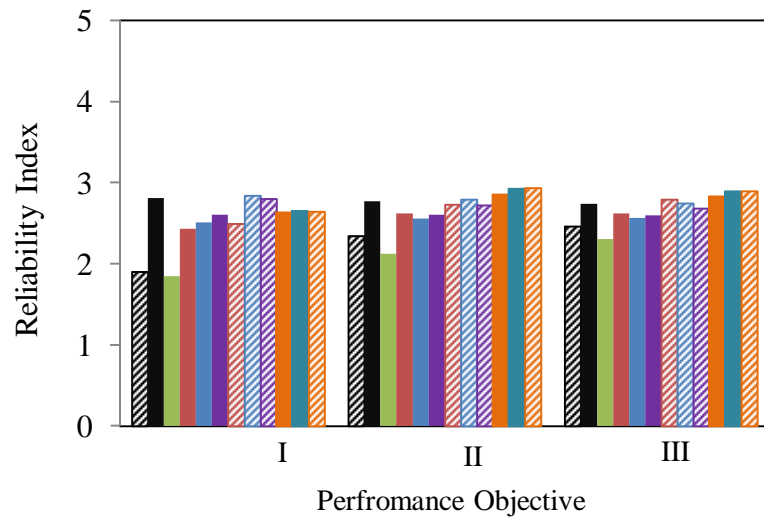
a) Guwahati Region



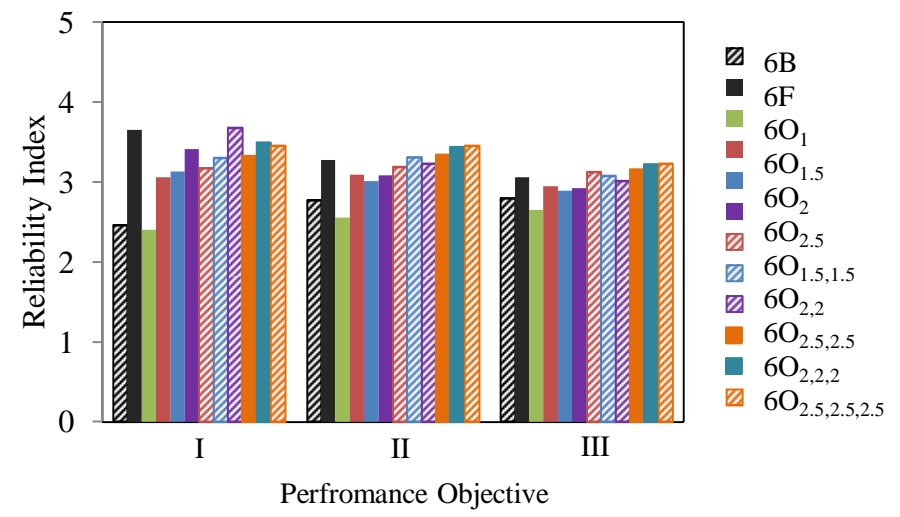
b) Bhuj Region

- 4B
- 4F
- 4O₁
- 4O_{1.5}
- 4O₂
- 4O_{2.5}
- 4O₃
- 4O_{1.5,1.5}
- 4O_{2,2}
- 4O_{2.5,2.5}
- 4O_{3,3}
- 4O_{2.5,2,1.5}
- 4O_{3,2.5,2}

Fig. 6.9: Reliability index for different performance objectives for 4- storey frames



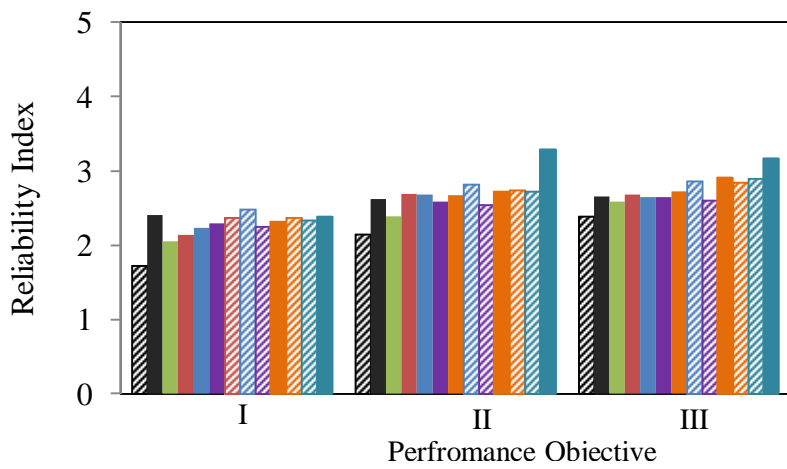
a) Guwahati Region



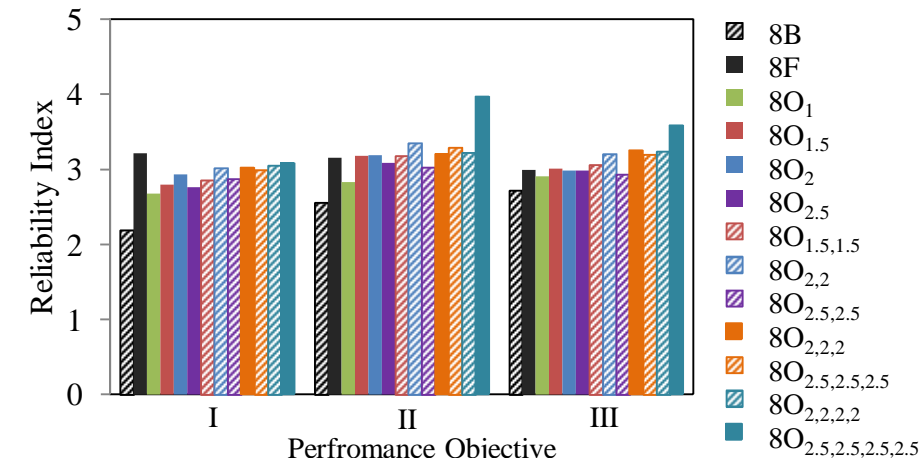
b) Bhuj Region

- ▨ 6B
- 6F
- 6O₁
- 6O_{1.5}
- 6O₂
- 6O_{2.5}
- ▨ 6O_{1.5,1.5}
- ▨ 6O_{2,2}
- ▨ 6O_{2.5,2.5}
- 6O_{2,2,2}
- ▨ 6O_{2.5,2.5,2.5}

Fig. 6.10: Reliability index for different performance objectives for 6- storey frames



a) Guwahati Region



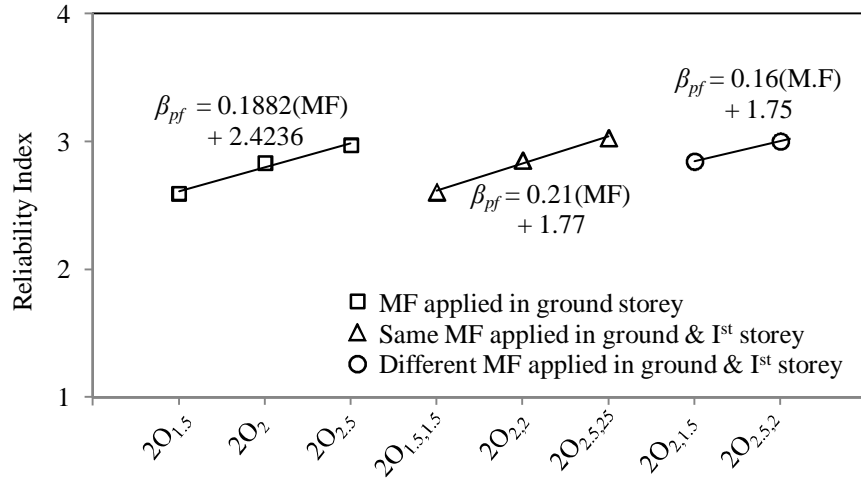
b) Bhuj Region

- ▨ 8B
- 8F
- 8O₁
- 8O_{1.5}
- 8O₂
- 8O_{2.5}
- ▨ 8O_{1.5,1.5}
- ▨ 8O_{2,2}
- ▨ 8O_{2.5,2.5}
- 8O_{2,2,2}
- ▨ 8O_{2.5,2.5,2.5}
- ▨ 8O_{2,2,2,2}
- 8O_{2.5,2.5,2.5,2.5}

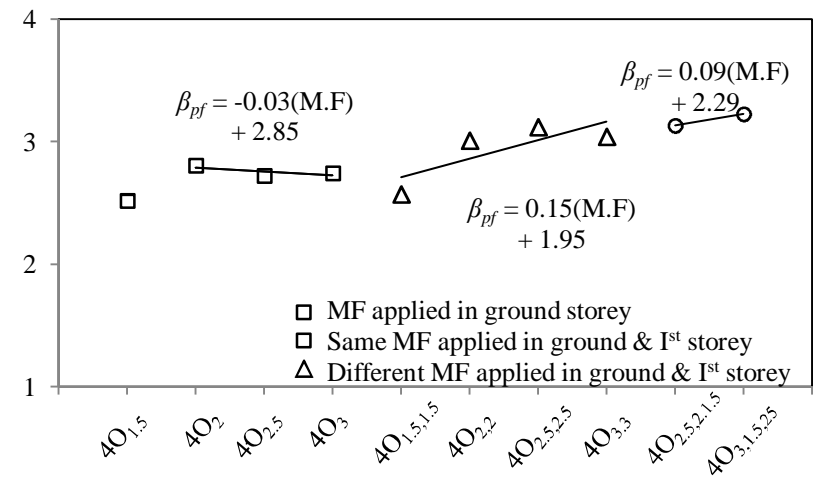
Fig. 6.11: Reliability index for different performance objectives for 8- storey frames

6.6 EFFECT OF MF SCHEMES ON THE BEHAVIOUR OF OGS FRAME

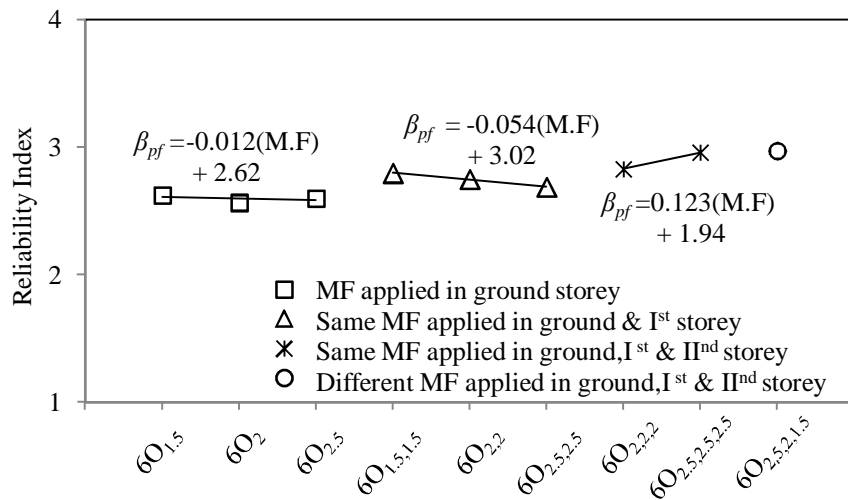
In order to understand the effect of different schemes of MFs on the performance of OGS buildings, variation of 'reliability index' a function of values of MF (separately for each scheme) are drawn for all the OGS frames at PO-III level as shown in Figs. 6.12-6.13. A careful attention to these figures reveals that the increase in the value of MF does not necessarily improve the performance of the OGS buildings which is against the common perceptions about the use of MF in the OGS buildings. This fact can be measured quantitatively through trendline as shown in the Figs. 6.12-6.13. Although a relation cannot be established based few discrete points, this study is carried out with an interest to understand the relative behaviour of the OGS buildings designed with various schemes of MF. Reliability index (β_{pf}) is found to be proportional to the MF values for all the schemes (indicated by the positive slope of the trendline) in two storey frames as shown in the Figs. 6.12a and 6.13a. This behaviour is not the same for four storey frames when MF applied only in the ground storey as indicated by the negative slope of the trendline in the Figs. 6.12b and 6.13b. In case of six storey frames, when the MF applied only in the ground storey (first trendline in Figs. 6.12c and 6.13c) and MF applied in ground and first storey (second trendline in Figs. 6.12c and 6.13c), the reliability index is found to be negatively proportional to the MF values. In case of eight storey frames, when the MF applied only in the ground storey (first trendline in Figs. 6.12d and 6.13d), MF applied in ground and first storey (second trendline in Figs. 6.12d and 6.13d) and MF applied in ground, first and second storey (third trendline in Figs. 6.12d and 6.13d), the reliability index is again found to be negatively proportional to the MF values. This indicates that only increasing the MF values in ground storey alone as recommended by most of the international design codes and the published literature is not the appropriate solution for the OGS buildings.



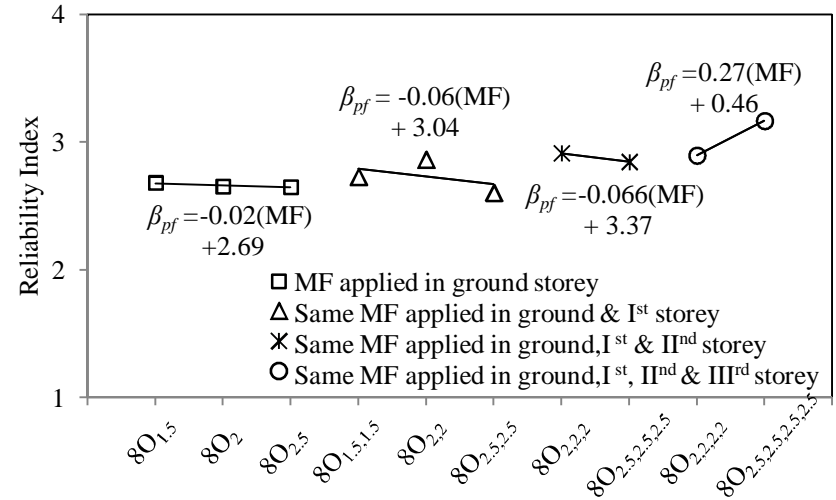
a) Two storey frame



b) Four storey frame

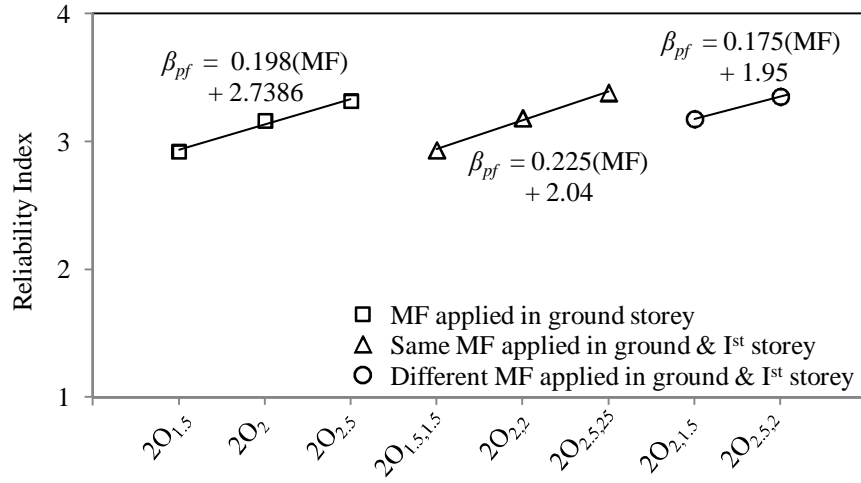


a) Six storey frame

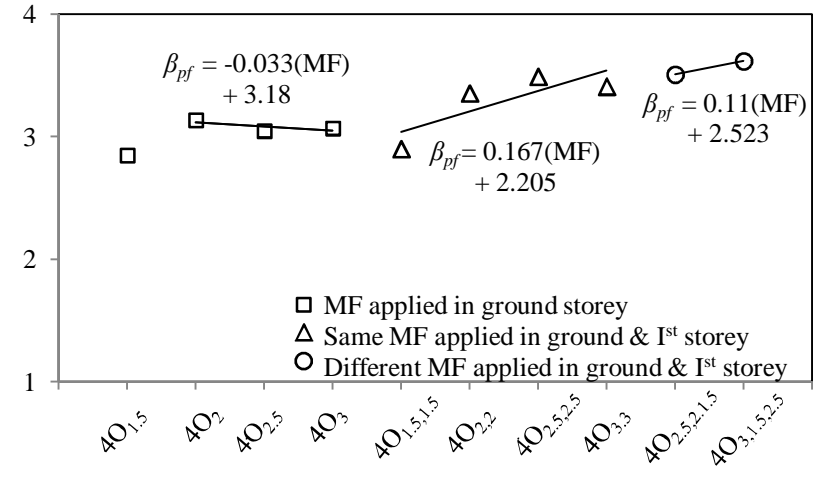


b) Eight storey frame

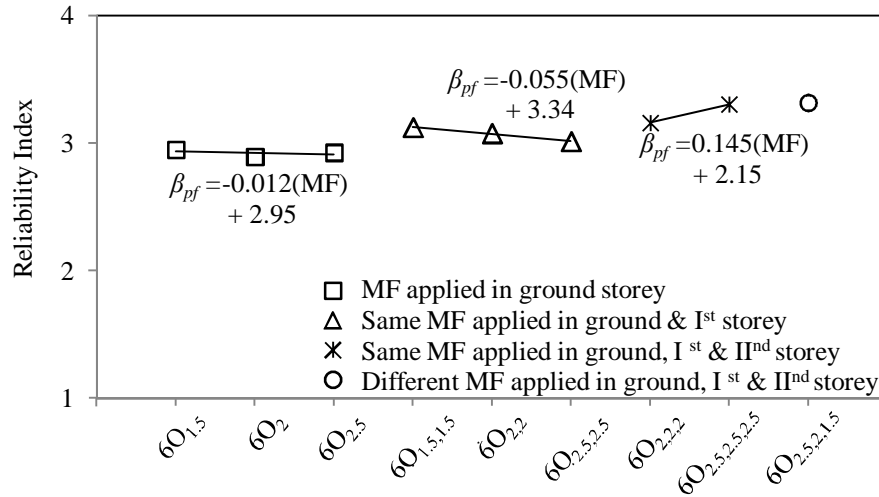
Fig. 6.12: Variation of Reliability index with various scheme of MF (Guwahati region)



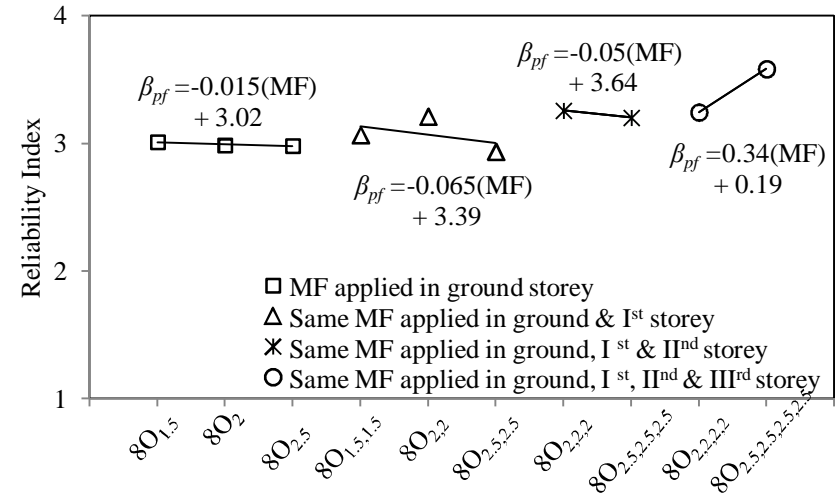
a) Two storey frame



b) Four storey frame



a) Six storey frame



b) Eight storey frame

Fig. 6.13: Variation of Reliability index with various scheme of MF (Bhuj region)

6.7 TARGET RELIABILITY

Target reliability for any structure can be defined as the reliability index of benchmark structures of the same class that has a history of successful service (in terms of safety and cost). In order to evaluate the effective scheme of MF among various OGS frames on the basis of optimum performance, target reliability shall be established. Several standards (NKB 55, 1987; JCSS, 2001; EN 1990, 2002; ISO 13822, 2010; etc.) recommend target reliabilities for general loadings. Wen (1995) reported the probability of failure of buildings designed in accordance with prevailing US codes as in the order of 10^{-4} per year (which corresponds to a reliability index of 3.71) based on the empirical evidence. Chryssanthopoulos *et al.* (2000) compared the achieved reliability of RC buildings subjected to earthquake loading with the target reliability index recommended by Eurocode-8 (2003) and Wen *et al.* (1996) in absence of any other recommendation for seismic target reliabilities. Seismic target reliability values proposed by Aoki *et al.* (2000) for different performance levels based on buildings designed for Japanese code. Table 6.2 presents the values of target reliability proposed by Aoki *et al.* (2000).

An extensive literature review found no uniform guidelines on target reliability for RC buildings subjected to earthquake forces. Almost all the recommendation are based on the specific regions. This may be because of the fact that the target reliability ideally should be developed considering the requirements of different stakeholders, the socio-economic and technical factors. Also, there is no research effort found in the literature on the target reliability of RC buildings for Indian region.

Fully infilled frames designed as per prevailing Indian Standard codes are assumed to perform with an acceptable degree of reliability. Therefore, the reliability indices of fully infilled frame can be considered as target reliability for evaluating OGS buildings of same

class. Table 6.3 presents the values of reliability index achieved by fully infilled frame for different performance objectives at selected regions.

Table 6.2: Target reliability index used by Aoki *et al.* (2000)

Performance of Building	Reliability Index
Damage on secondary elements	1.0
Failure of structural elements	2.0
Collapse of building	3.0

Table 6.3: Target reliability index based on achieved reliability index of fully infilled frame

Building Category	Guwahati Region			Bhuj Region		
	PO-I	PO-II	PO-III	PO-I	PO-II	PO-III
2-storeyed	3.4	3.8	3.5	4.4	4.5	3.9
4-storeyed	2.7	2.9	2.8	3.6	3.5	3.2
6-storeyed	2.8	2.8	2.7	3.6	3.3	3.1
8-storeyed	2.4	2.6	2.7	3.2	3.2	2.9

In the present study two target reliabilities are used for evaluation of OGS building designed with different scheme of MFs: (i) the target reliability values proposed by Aoki *et al.* (2000) as shown in Table 6.2 and (ii) reliability indices achieved by the fully infilled frames as shown in Table 6.3

6.7.1 Evaluation Based on Target Reliabilities of Aoki *et al.* (2000)

Figs. 6.8-6.11 show that the achieved reliability indices for all the frames meet the target reliability values of 1.0 and 2.0 (Aoki *et al.*, 2000) respectively for PO-I and PO-II. This implies that the designed frames (including O₁) satisfy the performance requirements for frequent earthquakes with probabilities of occurrences of 50% and 10% in 50years. However, only a few frames achieve the target reliability of 3.0 for PO-III. To identify the

selected frames that satisfy the target reliability (by Akoi *et al.*, 2000), a parameter, κ_{ak} is defined as follows.

$$\kappa_{ak} = \frac{\text{Achieved reliability index for PO-III}}{\text{Target reliability proposed by Akoi } et al. (2000)} - 1 \quad (6.1)$$

The parameter κ_{ak} is computed and plotted for all the frames as shown in Fig. 6.14. It can be seen from the figure that the following frames achieve the target reliability of PO-III: $2O_{2.5}$, $2O_{2.5,2.5}$, $2O_{2.5,2}$, $4O_{2,2}$, $4O_{2.5,2.5}$, $4O_{3,3}$, $4O_{2.5,2,1.5}$, $4O_{3,2.5,2}$, $6O_{2,2,2}$, $6O_{2.5,2.5,2.5}$ and $8O_{2.5,2.5,2.5,2.5}$.

6.7.2 Evaluation Based on Achieved Reliability of Fully Infilled Frame

The reliability index of the Frame 2F is close to 4.0 for both the regions at PO-III as shown in Table 6.3 and none of the two storey OGS frame has achieved this reliability index. This indicates that applying MF of the order of 1.5 – 3.0 cannot be sufficient to make the OGS frame behave similarly to that of fully infilled frame. To identify the selected frames that satisfy the target reliability (as achieved by corresponding fully infilled frame), a parameter, κ_{ff} is defined as follows.

$$\kappa_{ff} = \frac{\text{Achieved reliability index for PO-III}}{\text{Achieved reliability of fully infilled frame}} - 1 \quad (6.2)$$

The parameter κ_{ff} is computed and plotted for all the frames as shown in Fig. 6.15. From the plot, it is seen that following frames, among all the two storey OGS frames, are found to achieve the maximum reliability index: $2O_{2.5}$ (closely), $2O_{2.5,2.5}$ and $2O_{2.5,2,0}$. With regard to four storey frame, the frames $4O_{2.5,2.5}$, $4O_{3,3}$, $4O_{2.5,2,1.5}$ and $4O_{3,2.5,2}$ achieve the reliability index of 4F. Similarly, $6O_{2,2,2}$, $6O_{2.5,2.5,2.5}$, $6O_{2.5,2,1.5}$, $8O_{2.5,2.5,2.5}$, $8O_{2.5,2.5,2.5,2.5}$ achieve the reliability index of corresponding fully infilled frames.

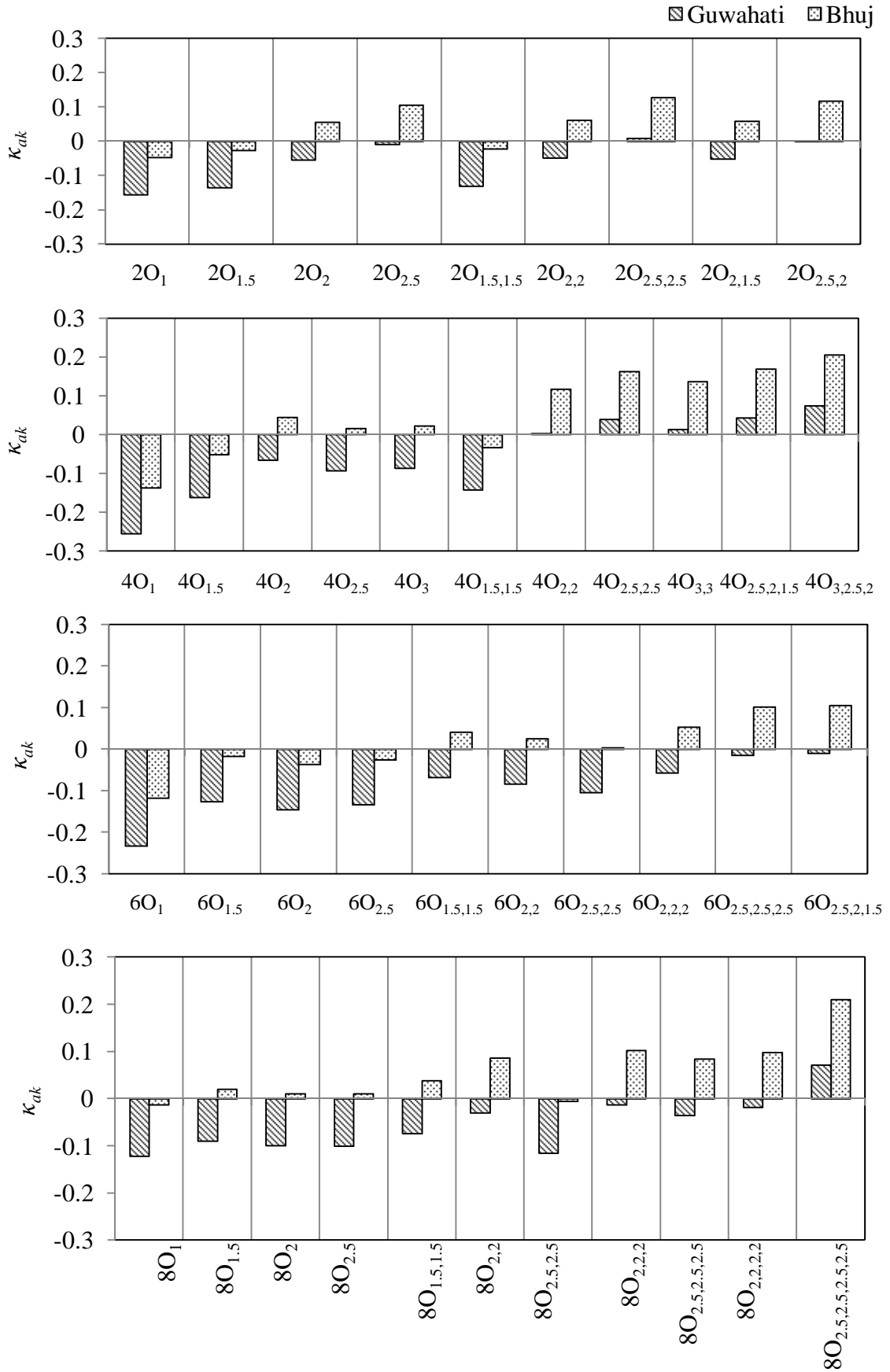


Fig. 6.14: κ_{ak} values for all the Benchmark frames

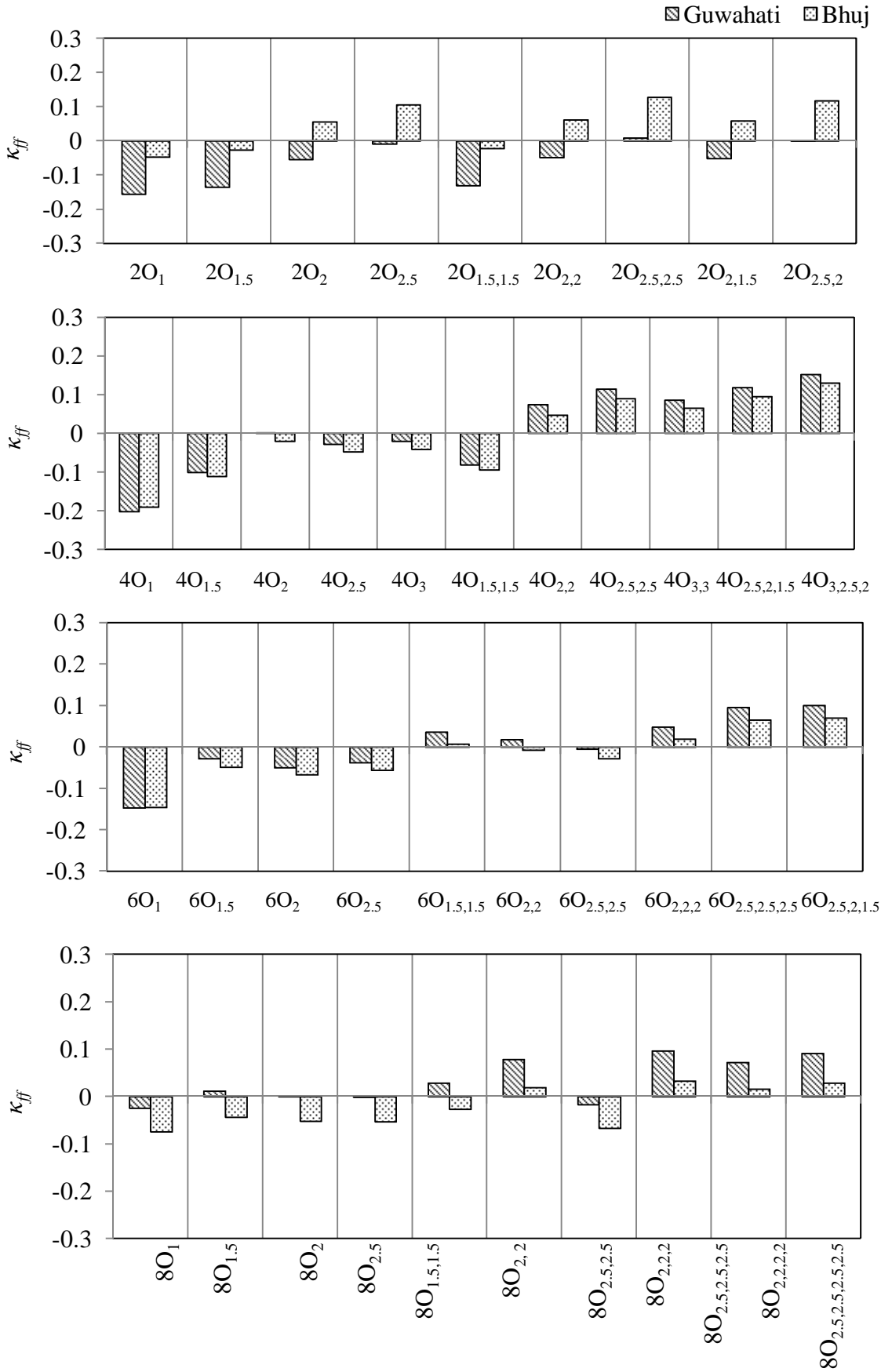


Fig. 6.15: κ_{ff} values for all the Benchmark frames

6.8 SUITABLE MF SCHEMES FOR THE DESIGN OF OGS BUILDINGS

The list of the frames that satisfies the both of the above target reliability criteria are considered for developing a scheme of MF suitable for design of OGS buildings. This list rules out the scheme of MF applied to the ground storey alone. Using different values of MFs in different storeys of a building can result in different sizes and/or reinforcement details of the column sections at every storey and this scheme of using different MFs at different storey may be inconvenient for construction. Therefore, the scheme of using same MF in required number of storeys in a building is chosen for the design of OGS buildings. Following schemes of MF is considered based on the results of building reliability discussed above and convenience in construction:

$$\left. \begin{array}{l} \text{Scheme 1: MF} = 2.5 \\ \text{Scheme 2: MF} = 3.0 \end{array} \right\} \text{MF to be applied to 'n' number of storeys} \\ \text{starting from OGS}$$

where,

$$n = \frac{N}{2} \quad \text{when } N \text{ is an even number} \\ = \frac{N+1}{2} \quad \text{when } N \text{ is an odd number}$$

and N = Total number of storey.

Two schemes of MF are considered with two different values of MF. Table 6.4 presents the reliability index achieved by the two considered schemes at PO-III level and compared them with other available schemes recommended by international codes and published literature for the design of OGS buildings. This includes Eurocode 8 (2003), Indian code (IS 1893, 2002) and the studies carried out by Scarlet (1997), Fardis *et al.* (1999), Davis *et al.* (2010a). The table shows that OGS buildings designed with all of the international codes considered achieve an acceptable degree of reliability (assumed to have $\beta_{pf} > 3$) only for two storey buildings. In case of four storey buildings, all the

international codes except Israel Code (SI, 1995) fail to achieve the acceptable degree of reliability. For six and eight storey buildings, none of the international code achieves the acceptable reliability. The reliability index achieved by the frames designed with both of the schemes considered here found to be always greater than that of other international code and published literature. This proves the efficacy of the considered scheme for design of OGS buildings.

Table 6.5 presents probability of failure for the OGS buildings designed with the two schemes at PO-I and PO-III performance objectives. This table can be treated as a guideline for choosing the appropriate scheme. The difference between the reliability indices and the corresponding probability of failure among the schemes considered are only marginal. Considering the cost involved among the two schemes, it may be judicial to select the Scheme 1 for the design.

Table 6.4: Comparison of proposed schemes with the schemes available in literature

Literature/Code	Achieved Reliability Index (Guwahati Region)			
	Total number of storeys			
	Two	Four	Six	Eight
Bulgarian code (1987)	> 3.0	2.7	<2.6	<2.8
Eurocode 8 (2003)	> 3.0	<2.7	<2.6	<2.8
Israel code (SI, 1995)	3.2	3.0	<2.7	2.8
Indian code (IS 1893, 2002)	3.0	2.7	2.6	2.8
Scarlet (1997)	<3	<2.7	< 2.6	< 2.8
Davis <i>et al.</i> (2010a)	<2.6	< 2.5	< 2.6	< 2.8
Proposed Scheme -1	3.0	3.1	2.9	3.2
Proposed Scheme- 2	3.0	3.1	3.0	3.1

This proposal is based on building frames up to eight storey height and should be used for this category of buildings. However, stakeholders can choose any one of these two schemes can be chosen based on the requirements.

Table 6.5: Expected probability of failure (at Guwahati) for proposed schemes

Proposed Schemes	Performance Objectives	Frames			
		2-storey	4-storey	6-storey	8-storey
Scheme -1	PO-I	2.78×10^{-03}	7.05×10^{-04}	4.08×10^{-03}	8.57×10^{-03}
	PO-III	1.48×10^{-03}	8.49×10^{-04}	1.89×10^{-03}	7.74×10^{-04}
Scheme- 2	PO-I	2.11×10^{-03}	5.72×10^{-03}	1.04×10^{-02}	9.25×10^{-03}
	PO-III	1.14×10^{-03}	8.70×10^{-04}	1.50×10^{-03}	8.74×10^{-04}

6.9 SUMMARY

The reliability based evaluation requires both fragility curves and seismic hazard curves. Chapter 5 discusses details about the fragility curves developed for the selected buildings at different limit state capacities. This chapter starts with discussing the seismic hazard curves of selected regions found in literature. Multiple performance objectives are then established combining the levels of earthquakes and limit state capacities based on available literature. Reliability curves are developed for all the frames for various performance objectives at selected regions and critical discussions are reported. The reliability indices achieved by different frames need to be compared with a target reliability to understand the expected behaviour of the frames. A brief discussion on the target reliability for RC buildings for seismic loading is presented in this chapter. Improved schemes of MF for the design of OGS buildings are proposed based on the comparison between the achieved and target reliability indices.

CHAPTER 7

CONCLUSIONS

7.1 SUMMARY

The main objective of the present study has been identified as to propose suitable scheme of MF for seismic design of OGS buildings considering possible uncertainties. The sub-objectives are divided into the following parts:

- i) To establish limit state capacities of each storey of framed building for various performance levels.
- ii) To develop probabilistic seismic demand model (PSDM) and fragility curves for benchmark OGS framed buildings designed with various schemes of MF.
- iii) To develop reliability index for OGS framed buildings designed with various schemes of MF.
- iv) To propose appropriate schemes of MF for design of OGS buildings based on the reliability indices achieved by the benchmark frames.

To achieve the above objectives, an extensive literature review is carried out on following three areas: (i) existing design methodologies for OGS buildings as per various international codes and literatures, (ii) fragility curves and reliability analysis on RC framed buildings and (iii) macro-models available in literature for modelling infill walls.

A detailed report of literature review is presented in Chapter 2.

The procedure for seismic risk assessment suggested by Ellingwood (2001) is considered in the present study. This procedure involves the development of PSDMs, fragility curves and PSHAs. The uncertainties in the material properties are considered using LHS

scheme. Limit state capacities for RC frames are defined in this study based on the approach used by FEMA HAZUS-MH (2003) and Dolsek and Fajfar (2008).

OpenSees (2013) is used in this study for modelling and analysis of all the building frames. The computational models of buildings frame considered in the present study has two parts: nonlinear material model and structural models. 'concrete02', 'steel02' and 'pinchingdamage' uniaxial material models available in OpenSees library are used for modelling of concrete, steel rebar and infill wall respectively. Frame elements (beams and columns) are modelled using forced-based 'Nonlinear beam-column elements' and the equivalent struts representing infill walls are modelled with 'truss' elements. A number of studies are carried out to validate the modelling procedure adopted in the present study. Different configurations of benchmark frames are selected and designed with different schemes of MFs. To consider the uncertainties in the computational models, material and structural properties are developed through LHS scheme. Pushover analyses of the designed frames are carried out to obtain the structural capacities at different limit states. Two suites of ground motion records are selected and the effects of these two suites on the building performance are studied. Finally, the suite of synthetic ground motion is used for further analysis as it gives conservative results.

SAC-FEMA method (Cornell *et al.*, 2002) is used in this study for developing fragility curves. This method is compared with the more exact LHS MC method and validated. PSDM and corresponding fragility curves are developed using SAC-FEMA method for all the frames at each limit states.

Seismic hazard curves of selected regions are used for the estimation of reliability index. Reliability indices are calculated through numerical integration of fragility curve and seismic hazard curves. Different performance objectives are selected from literature for

calculation of reliability indices. A review on the target reliability index is carried out and the achieved reliability indices of all the frames are compared with selected target reliability. A new scheme of MF for the design of OGS buildings is proposed based on the above results.

7.2 CONCLUSIONS

It is observed that the existing design codes and the literature have not adequately addressed the problem of earthquake-resistant design of OGS buildings. Major international design codes (ASCE/SEI-7, 2010; NZS 1170.5, 2004 and ICC IBC, 2012) prohibit the construction of such buildings. However, the developing countries like India cannot avoid such type of building due to the scarcity of land in the urban areas. Other international codes (IS 1893, Eurocode 8, SI, Bulgarian code, etc.) allows this building category with a magnification of design forces (MF) in the ground storey columns. There is a wide disparity among these codes on the value of the MF. From the fragility curves and achieved reliability indices of the benchmark frames developed in this study the following generalised conclusions can be drawn:

- i) OGS frames designed without any MF always found to have maximum probability of exceedance indicating vulnerability of these frames.
- ii) In case of two storey frames, the application of MF only in ground storey columns improves the building performance. However, for building with more than two storeys, application of MF only in the ground storey makes the adjacent storey vulnerable. This shows that the scheme of MF applying in ground storey alone recommended by most of the international codes is not an effective solution.

- iii) In general, an MF of magnitude less than 2.0 does not meet the acceptable degree of reliability.
- iv) It is found that the application of MF in the increasing order does not necessarily improve the performance of the buildings beyond certain limits.
- v) It is found that in case of two storey buildings MF applied only in ground storey meets the target reliability, similarly MF in ground and first storey for four storey buildings, MF in ground, first and second for six storey buildings and MF in ground, first, second and third storey for eight storey buildings meets the target reliability.
- vi) It is found that the scheme of uniform value and the scheme of different values of MF in the different storeys results in similar performance.
- vii) Based on the discussions presented in Section 6.8, following schemes of MF are proposed for design of OGS buildings:

$$\text{Scheme 1: MF} = 2.5 \left\{ \begin{array}{l} \text{MF to be applied to 'n' number of storeys} \\ \text{starting from OGS} \end{array} \right.$$

where,

$$n = \frac{N}{2} \quad \text{when } N \text{ is an even number}$$

$$= \frac{N+1}{2} \quad \text{when } N \text{ is an odd number}$$

and $N = \text{Total number of storey.}$

7.3 CONTRIBUTIONS OF THE RESEARCH

Followings are the main contribution from the present study:

- i) Existing design manuals and published literature define the limit state capacities in terms of roof displacements of regular multi-storeyed buildings.

The present study develops an improved approach for evaluating the limit state capacities of each storey suitable for OGS/vertically irregular buildings.

- ii) Probabilistic seismic demand model (PSDM) and corresponding fragility curves are developed for OGS framed buildings designed with various schemes of MF to assess the performance. This is the first attempt to develop such models for Indian construction practice.
- iii) The reliability indices against the hazard curves associated with highest seismic zone of India are calculated for OGS framed buildings designed with various schemes of MF. The result shows that OGS buildings designed with MF suggested by international codes and published literature failed to achieve the target reliability.
- iv) The present study proposes a new scheme of MF to design the columns of the OGS as well as storeys above on the basis of Target reliability index. The proposed scheme of MF for the design of OGS buildings found to meet Target reliability.

7.4 SCOPE OF FUTURE WORK

The present study is limited to reinforced concrete multi-storey framed buildings that are regular in plan. Irregular distribution of infill walls in the upper storeys of OGS building can lead to plan irregularity. This study can be extended to such buildings considering the torsional effects arising out of the plan irregularity. Also, similar studies can be carried out on steel framed buildings.

The present study can be extended to OGS buildings with basement, shear walls and plinth beams.

Soil-structure interaction effects are ignored in the present study. It will be interesting to study the response of the OGS buildings considering the soil-structure interaction.

The floor slabs are considered in the present study as rigid diaphragms. This study can be extended for buildings with flexible diaphragms.

Full scale shake table tests can be conducted for further clarity on the responses of OGS buildings subjected to lateral loading.

APPENDIX-A

FINITE ELEMENT FORMULATION

A.1 INTRODUCTION

The governing differential equation of motion for multi-degree of freedom system to be solved for dynamic analysis is generally express as follows:

$$[M]\{\ddot{x}\} + [C]\{\dot{x}\} + [K]\{x\} = \{P(t)\} \quad (\text{A.1})$$

\ddot{x} is the acceleration vector relative to the ground, \dot{x} is the relative velocity vector, x is the relative displacement vector and the external load vector is $\{P(t)\} = -[M]\{1\}\ddot{a}_g$ in the case of earthquake loading, where \ddot{a}_g is the ground acceleration. $[M]$ $[C]$ and $[K]$ are the mass, damping, and stiffness matrix, respectively. These matrices are described in the following sections.

A.2 ELEMENT STIFFNESS FORMULATION, K_e (LEE AND MOSALAM, 2004)

Consider the element displacement vector u , element force vector p , section deformations $v_s(x)$ and section force $q(x)$ as specified in Section 4.4.3. Section displacements are determined from the element nodal displacements through the shape functions. The generalized relationship between section displacement vector $v_s(x)$ and the element nodal displacement vector ' u ' can be expressed as

$$v_s(x) = \begin{Bmatrix} u(x) \\ v(x) \end{Bmatrix} \quad (\text{A.2})$$

$$= N_d(x) \cdot [u_1 \quad u_2 \quad u_3 \quad u_4 \quad u_5 \quad u_6] \quad (\text{A.3})$$

where, $N_d(x)$ is the matrix of displacement interpolation functions which can be expressed as

$$N_d(x) = \begin{bmatrix} \psi_1(x) & 0 & 0 & \psi_2(x) & 0 & 0 \\ 0 & \phi_1(x) & \phi_2(x) & 0 & \phi_3(x) & \phi_4(x) \end{bmatrix} \quad (\text{A.4})$$

where, ψ_1 , ψ_2 , ϕ_1 , ϕ_2 , ϕ_3 and ϕ_4 are the interpolation functions for axial and transverse displacements respectively and are given by

$$\begin{aligned} \psi_1(x) &= -\frac{x}{L} + 1 & \psi_2(x) &= -\frac{x}{L} \\ \phi_1(x) &= 2\frac{x^3}{L^3} - 3\frac{x^2}{L^2} + 1 & \phi_2(x) &= \frac{x^3}{L^2} - 2\frac{x^2}{L} + x \\ \phi_3(x) &= -2\frac{x^3}{L^3} + 3\frac{x^2}{L^2} & \phi_4(x) &= \frac{x^3}{L^2} - \frac{x^2}{L} \end{aligned} \quad (\text{A.5})$$

where, L is the length of the member. Let, $\varepsilon(x)$ is the axial strain considering the second order effect, such that

$$\varepsilon(x) = \varepsilon_0(x) + \frac{1}{2}v(x)'^2 \quad (\text{A.6})$$

$$= u(x)' + \frac{1}{2}v(x)'^2 \quad (\text{A.7})$$

where, $u(x)$ and $v(x)$ are the axial and transverse displacements at x respectively and ' denotes a partial derivative with respect to the coordinate x . In the subsequent derivations, the argument x will be dropped for convenience. The principle of virtual work implies

$$\delta u^T P = \int_L [\delta\varepsilon \quad \delta\varphi] \begin{bmatrix} N \\ M \end{bmatrix} dx \quad (\text{A.8})$$

Since $\delta\varepsilon = \delta u' + v' \delta v'$, Eq. A.8 can be rewritten as

$$\delta u^T p = \int_L [\delta u' + v' \delta v' \quad \delta\varphi] \begin{bmatrix} N \\ M \end{bmatrix} dx \quad (\text{A.9})$$

$$= \int_L [\delta u' \quad \delta\varphi] \begin{bmatrix} N \\ M \end{bmatrix} dx + \int_L v' \delta v' N dx \quad (\text{A.10})$$

Now consider two interpolation functions

$$B(x) = \begin{bmatrix} -\frac{1}{L} & 0 & 0 & \frac{1}{L} & 0 & 0 \\ 0 & -6\frac{x}{L^2} + 12\frac{x^2}{L^3} & \left(-4\frac{x}{L^2} + 6\frac{x^2}{L^3}\right)L & 0 & 6\frac{x}{L^2} - 12\frac{x^2}{L^3} & \left(-2\frac{x}{L^2} + 6\frac{x^2}{L^3}\right)L \end{bmatrix} \quad (\text{A.11})$$

and

$$C(x) = \begin{bmatrix} 0 & 0 & 0 & 0 & 0 & 0 \\ 0 & -6\frac{x}{L^2} + 12\frac{x^2}{L^3} & \left(\frac{1}{L} - 4\frac{x}{L^2} + 3\frac{x^2}{L^3}\right)L & 0 & 6\frac{x}{L^2} - 6\frac{x^2}{L^3} & \left(-2\frac{x}{L^2} + 3\frac{x^2}{L^3}\right)L \end{bmatrix} \quad (\text{A.12})$$

such that $\begin{bmatrix} u' \\ \varphi \end{bmatrix} = Bu$ and $\begin{bmatrix} 0 \\ v' \end{bmatrix} = Cu$. Substituting variational forms of these equations into

(A.10) gives

$$\delta u^T P = \int_L (B \delta u)^T \begin{bmatrix} N \\ M \end{bmatrix} dx + \int_L (C \delta u)^T Cu N dx \quad (\text{A.13})$$

Then we get the weak form of equilibrium as

$$p = \int_L B^T q dx + \int_L C^T Cu N dx \quad (\text{A.14})$$

where, $q = q(x) = \begin{bmatrix} N \\ M \end{bmatrix}^T$, To obtain the element stiffness matrix k_e , take the derivative of p with respect to u as

$$k_e = \frac{\partial p}{\partial u} = \int_L B^T \frac{\partial q}{\partial u} dx + \int_L C^T Cu \frac{\partial N}{\partial u} dx + \int_L C^T CN dx \quad (\text{A.15})$$

From the section equilibrium,

$$\begin{aligned} q &= k_s \begin{bmatrix} \varepsilon \\ \varphi \end{bmatrix} = k_s \begin{bmatrix} u' + \frac{1}{2} v'^2 \\ \varphi \end{bmatrix} \\ &= k_s \left\{ B + \frac{1}{2} \begin{bmatrix} 1 \\ 0 \end{bmatrix} (Cu)^T C \right\} u \end{aligned} \quad (\text{A.16})$$

where $k_s = k_s(x)$ is the section stiffness matrix. Therefore,

$$\frac{\partial q}{\partial u} = k_s \left\{ B + \begin{bmatrix} 1 \\ 0 \end{bmatrix} (Cu)^T C \right\}$$

$$=k_s (B + G) \quad (\text{A.17})$$

where $G = \begin{bmatrix} 1 \\ 0 \end{bmatrix} (Cu)^T C$. Moreover,

$$\frac{\partial N}{\partial u} = [1 \quad 0] k_s (B + G) \quad (\text{A.18})$$

Consequently,

$$\begin{aligned} k_e &= \int_L B^T k_s (B + G) dx + \int_L C^T Cu [1 \quad 0] k_s (B + G) dx + \int_L C^T CN dx \\ &= \int_L B^T k_s (B + G) dx + \int_L G^T k_s (B + G) dx + \int_L C^T CN dx \\ &= \int_L (B + G)^T k_s (B + G) dx + \int_L C^T CN dx \\ &= \int_L T^T k_s T dx + \int_L C^T CN dx \end{aligned} \quad (\text{A.19})$$

where $T = B + G$.

A.3 MASS MATRIX

Lumped mass system is used (Selna, 1977)

$$\text{Element mass matrix, } M = \begin{bmatrix} m_1 & 0 & 0 & 0 & 0 & 0 \\ 0 & m_2 & 0 & 0 & 0 & 0 \\ 0 & 0 & m_3 & 0 & 0 & 0 \\ 0 & 0 & 0 & m_4 & 0 & 0 \\ 0 & 0 & 0 & 0 & m_5 & 0 \\ 0 & 0 & 0 & 0 & 0 & m_6 \end{bmatrix} \quad (\text{A.20})$$

where, m_i represent the mass at i^{th} degree of freedom.

A.4 DAMPING MATRIX

Rayleigh damping is used for dynamic analysis (Rayleigh, 1954). It is assumed to be proportional to the mass and stiffness matrices as follows:

$$[C] = \eta [M] + \delta [K] \quad (\text{A.21})$$

where, η is the mass-proportional damping coefficient and δ is the stiffness-proportional damping coefficient. These coefficients can be derived by assuming suitable damping ratios for any two modes of vibrations. Relationships between the modal equations and orthogonality conditions allow this equation to be rewritten as

$$\xi_n = \frac{\eta}{2\omega_n} + \delta \frac{\omega_n}{2} \quad (\text{A.22})$$

where, ξ_n is the damping ratio and ω_n is the natural frequency for n^{th} mode. After selecting the damping ratios for two modes of vibration, the constants η and δ can be obtained as follows (Clough and Penzien, 1975):

$$\begin{bmatrix} \lambda_m \\ \lambda_n \end{bmatrix} = \frac{1}{2} \begin{bmatrix} 1/\omega_m & \omega_m \\ 1/\omega_n & \omega_n \end{bmatrix} \cdot \begin{Bmatrix} \eta \\ \delta \end{Bmatrix} \quad (\text{A.23})$$

A.5 EVALUATION OF STRUCTURAL RESPONSE

The structural response is to be evaluated by solving the governing differential equation presented in Eq. A.1. Analytical solution of this equation of motion is not possible as the earthquake ground acceleration varies arbitrarily with time and the system considered is nonlinear (Chopra, 2012). Therefore, numerical integration techniques proposed by Newmark (1959) is utilised for solving the above differential equation. The details of this method can be available in literature (Chopra, 2012). To illustrate the use of Newmark's integration methods, consider the dynamic equilibrium equations as shown in equation A.1. The direct use of Taylor's series provides following two additional equations:

$$u_t = u_{t-\Delta t} + \Delta t \cdot \dot{u}_{t-\Delta t} + \frac{\Delta t^2}{2} \ddot{u}_{t-\Delta t} + \frac{\Delta t^3}{6} \dddot{u}_{t-\Delta t} + \dots \quad (\text{A.24})$$

$$\dot{u}_t = \dot{u}_{t-\Delta t} + \Delta t \cdot \ddot{u}_{t-\Delta t} + \frac{\Delta t^2}{2} \dddot{u}_{t-\Delta t} \dots \quad (\text{A.25})$$

Newmark truncated those equations and expressed them in the following form:

$$u_t = u_{t-\Delta t} + \Delta t \cdot \dot{u}_{t-\Delta t} + \frac{\Delta t^2}{2} \ddot{u}_{t-\Delta t} + \beta \Delta t^3 \dddot{u} \quad (\text{A.26})$$

$$\dot{u}_t = \dot{u}_{t-\Delta t} + \Delta t \cdot \ddot{u}_{t-\Delta t} + \gamma \Delta t^2 \ddot{u} \quad (\text{A.27})$$

Here β and γ are known as Newmark's constants. If the acceleration is assumed to be linear within the time step, the following equation can be written:

$$\ddot{u} = \frac{(\ddot{u}_t - \ddot{u}_{t-\Delta t})}{\Delta t} \quad (\text{A.28})$$

The substitution of Eq. A.28 into Eq. A.26 and A.27 produces Newmark's equations in standard form:

$$u_t = u_{t-\Delta t} + \Delta t \cdot \dot{u}_{t-\Delta t} + \left(\frac{1}{2} - \beta\right) \Delta t^2 \ddot{u}_{t-\Delta t} + \beta \Delta t^2 \ddot{u}_t \quad (\text{A.29})$$

$$\dot{u}_t = \dot{u}_{t-\Delta t} + (1 - \gamma) \Delta t \cdot \ddot{u}_{t-\Delta t} + \gamma \Delta t \cdot \ddot{u}_t \quad (\text{A.30})$$

Newmark solved Eq. A.29, A.30 and A.1 by iteration for each time step for each displacement DOF of the structural system.

APPENDIX-B

REINFORCEMENT DETAILS OF SELECTED BUILDINGS DESIGNED AS PER INDIAN STANDARDS

Table B-1: Column sections and reinforcement details for 2-storey frames

Frame Configurations	Storey number	Width (mm)	Depth (mm)	Reinforcement Details (uniformly distributed)	Lateral ties
2B	G-I st	300	300	8 - ϕ 20	8mm ϕ rectangular ties, @ 150mm c/c throughout
2F	G-I st	300	300	8 - ϕ 20	
2O	G-I st	300	300	8 - ϕ 20	
2O _{1.5}	G	350	350	8 - ϕ 18	
	I st	300	300	8 - ϕ 20	
2O ₂	G	350	350	8 - ϕ 25	
	I st	300	300	8 - ϕ 20	
2O _{2.5}	G	425	425	8 - ϕ 22	
	I st	300	300	8 - ϕ 20	
2O _{1.5,1.5}	G-I st	350	350	8 - ϕ 18	
2O _{2,2}	G-I st	350	350	8 - ϕ 25	
2O _{2.5,2.5}	G-I st	425	425	8 - ϕ 22	
2O _{2,1.5}	G	350	350	8 - ϕ 25	
	I st	350	350	8 - ϕ 18	
2O _{2.5,2}	G	425	425	8 - ϕ 22	
	I st	350	350	8 - ϕ 25	

Table B-2: Beam sections and reinforcement details for 2-storey frames

Frame	Floor	Width (mm)	Depth (mm)	Reinforcements details		Stirrups
				Top	Bottom	
2B	I st	300	350	4 - ϕ 25	4 - ϕ 20	2 legged 8mm ϕ , @ 150mm c/c throughout and 2 legged 8mm ϕ , @ 100mm c/c for a distance of 500mm from supports,
	II nd	300	350	4 - ϕ 22	2 - ϕ 22	
2F	I st	300	350	4 - ϕ 25	4 - ϕ 20	
	II nd	300	350	4 - ϕ 22	2 - ϕ 22	
2O	I st	300	350	4 - ϕ 25	4 - ϕ 20	
	II nd	300	350	4 - ϕ 22	2 - ϕ 22	
2O _{1.5}	I st	300	350	4 - ϕ 25	4 - ϕ 20	
	II nd	300	350	4 - ϕ 22	2 - ϕ 22	
2O ₂	I st	300	350	4 - ϕ 25	4 - ϕ 20	
	II nd	300	350	4 - ϕ 22	2 - ϕ 22	
2O _{2.5}	I st	300	350	4 - ϕ 25	4 - ϕ 20	
	II nd	300	350	4 - ϕ 22	2 - ϕ 22	
2O _{1.5,1.5}	I st	300	350	4 - ϕ 25	4 - ϕ 20	
	II nd	300	350	4 - ϕ 22	2 - ϕ 22	
2O _{2,2}	I st	300	350	4 - ϕ 25	4 - ϕ 20	
	II nd	300	350	4 - ϕ 22	2 - ϕ 22	
2O _{2.5,2.5}	I st	300	350	4 - ϕ 25	4 - ϕ 20	
	II nd	300	350	4 - ϕ 22	2 - ϕ 22	
2O _{2,1.5}	I st	300	350	4 - ϕ 25	4 - ϕ 20	
	II nd	300	350	4 - ϕ 22	2 - ϕ 22	
2O _{2.5,2}	I st	300	350	4 - ϕ 25	4 - ϕ 20	
	II nd	300	350	4 - ϕ 22	2 - ϕ 22	

Table B-3: Column sections and reinforcement details for 4-storey frames

Frame	Storey	Width (mm)	Depth (mm)	Reinforcement Details (uniformly distributed)	Lateral ties	
4B	G	350	350	8 - 20 ϕ	8mm ϕ rectangular ties, @ 175mm c/c throughout	
	I st - III rd	350	350	8 - 18 ϕ		
4F	G	350	350	8 - 20 ϕ		
	I st - III rd	350	350	8 - 18 ϕ		
4O _{1.0}	G	350	350	8 - 20 ϕ		
	I st - III rd	350	350	8 - 18 ϕ		
4O _{1.5}	G	425	425	8 - 22 ϕ		
	I st - III rd	350	350	8 - 18 ϕ		
4O _{2.0}	G	425	425	8 - 25 ϕ		
	I st - III rd	350	350	8 - 18 ϕ		
4O _{2.5}	G	475	475	12 - 25 ϕ		16mm ϕ rectangular ties, @ 85mm c/c for a distance of 535mm from supports,
	I st - III rd	350	350	8 - 18 ϕ		
4O _{3.0}	G	600	600	16 - 25 ϕ		
	I st - III rd	350	350	8 - 18 ϕ		
4O _{1.5,1.5}	G, I st	425	425	8 - 22 ϕ		
	II nd - III rd	350	350	8 - 18 ϕ		
4O _{2.0,2.0}	G, I st	425	425	8 - 25 ϕ		
	II nd - III rd	350	350	8 - 18 ϕ		
4O _{2.5,2.5}	G, I st	475	475	12 - 25 ϕ		
	II nd - III rd	350	350	8 - 18 ϕ		
4O _{3.0,3.0}	G, I st	600	600	16 - 25 ϕ		
	II nd - III rd	350	350	8 - 18 ϕ		

Table B-4: Beam sections and reinforcement details for 4-storey frames

Frame	Floor	Width (mm)	Depth (mm)	Reinforcements details		Stirrups
				Top	Bottom	
4B	I st -II nd	300	375	5 - 20 ϕ	4 - 20 ϕ	2 legged 8mm ϕ , @ 140mm c/c throughout and 2 legged 8mm ϕ , @ 100mm c/c for a distance of 500mm from supports,
	III rd	300	375	4 - 20 ϕ	3 - 20 ϕ	
	IV th	300	325	4 - 20 ϕ	3 - 20 ϕ	
4F	I st -II nd	300	375	5 - 20 ϕ	4 - 20 ϕ	
	III rd	300	375	4 - 20 ϕ	3 - 20 ϕ	
	IV th	300	325	4 - 20 ϕ	3 - 20 ϕ	
4O _{1.0}	I st -II nd	300	375	5 - 20 ϕ	4 - 20 ϕ	
	III rd	300	375	4 - 20 ϕ	3 - 20 ϕ	
	IV th	300	325	4 - 20 ϕ	3 - 20 ϕ	
4O _{1.5}	I st -II nd	300	375	5 - 20 ϕ	4 - 20 ϕ	
	III rd	300	375	4 - 20 ϕ	3 - 20 ϕ	
	IV th	300	325	4 - 20 ϕ	3 - 20 ϕ	
4O _{2.0}	I st -II nd	300	375	5 - 20 ϕ	4 - 20 ϕ	
	III rd	300	375	4 - 20 ϕ	3 - 20 ϕ	
	IV th	300	325	4 - 20 ϕ	3 - 20 ϕ	
4O _{2.5}	I st -II nd	300	375	5 - 20 ϕ	4 - 20 ϕ	
	III rd	300	375	4 - 20 ϕ	3 - 20 ϕ	
	IV th	300	325	4 - 20 ϕ	3 - 20 ϕ	
4O _{3.0}	I st -II nd	300	375	5 - 20 ϕ	4 - 20 ϕ	
	III rd	300	375	4 - 20 ϕ	3 - 20 ϕ	
	IV th	300	325	4 - 20 ϕ	3 - 20 ϕ	
4O _{1.5,1.5}	I st -II nd	300	375	5 - 20 ϕ	4 - 20 ϕ	
	III rd	300	375	4 - 20 ϕ	3 - 20 ϕ	
	IV th	300	325	4 - 20 ϕ	3 - 20 ϕ	
4O _{2.2}	I st -II nd	300	375	5 - 20 ϕ	4 - 20 ϕ	
	III rd	300	375	4 - 20 ϕ	3 - 20 ϕ	
	IV th	300	325	4 - 20 ϕ	3 - 20 ϕ	
4O _{2.5,2.5}	I st -II nd	300	375	5 - 20 ϕ	4 - 20 ϕ	
	III rd	300	375	4 - 20 ϕ	3 - 20 ϕ	
	IV th	300	325	4 - 20 ϕ	3 - 20 ϕ	
4O _{3.0,3.0}	I st -II nd	300	375	5 - 20 ϕ	4 - 20 ϕ	
	III rd	300	375	4 - 20 ϕ	3 - 20 ϕ	
	IV th	300	325	4 - 20 ϕ	3 - 20 ϕ	

Table B-5: Column sections and reinforcement details for 6-storey frames

Frame	Storey	Width (mm)	Depth (mm)	Reinforcement Details (uniformly distributed)	Lateral ties	
6B	G	450	450	8 - 20 ϕ	8mm ϕ rectangular ties, @ 175mm c/c throughout	
	I st - V th	450	450	8 - 18 ϕ		
6F	G	450	450	8 - 20 ϕ		
	I st - V th	450	450	8 - 18 ϕ		
6O _{1.0}	G	450	450	8 - 20 ϕ		
	I st - V th	450	450	8 - 18 ϕ		
6O _{1.5}	G	450	450	16 - 25 ϕ		
	I st - V th	450	450	8 - 18 ϕ		
6O _{2.0}	G	550	550	16 - 25 ϕ		16mm ϕ rectangular ties, @ 85mm c/c for a distance of 535mm from supports,
	I st - V th	450	450	8 - 18 ϕ		
6O _{2.5}	G	650	650	12 - 32 ϕ		
	I st - V th	450	450	8 - 18 ϕ		
6O _{1.5,1.5}	G - I st	450	450	16 - 25 ϕ		
	II nd - V th	450	450	8 - 18 ϕ		
6O _{2.0,2.0}	G - I st	550	550	16 - 25 ϕ		
	II nd - V th	450	450	8 - 18 ϕ		
6O _{2.5,2.5}	G - I st	650	650	12 - 32 ϕ		
	II nd - V th	450	450	8 - 18 ϕ		
6O _{2.0,2.0,2.0}	G - II nd	550	550	16 - 25 ϕ		
	III rd - V th	450	450	8 - 18 ϕ		
6O _{2.5,2.5,2.5}	G - II nd	650	650	12 - 32 ϕ		
	III rd - V th	450	450	8 - 18 ϕ		
6O _{2.5,2.0,1.5}	G	650	650	12 - 32 ϕ		
	I st	550	550	16 - 25 ϕ		
	II nd	450	450	16 - 25 ϕ		
	III rd - V th	450	450	8 - 18 ϕ		

Table B-6: Beam sections and reinforcement details for 6-storey frames

Frame	Floor	Width (mm)	Depth (mm)	Reinforcements details		Stirrups
				Top	Bottom	
6B	G- III rd	300	375	5 - 25 ϕ	4 - 20 ϕ	2 legged 8mm ϕ , @ 140mm c/c throughout and 2 legged 8mm ϕ , @ 100mm c/c for a distance of 500mm from supports,
	IV th	300	375	4 - 25 ϕ	2 - 20 ϕ	
	V th	300	375	4 - 20 ϕ	2 - 20 ϕ	
6F	G- III rd	300	375	5 - 25 ϕ	4 - 20 ϕ	
	IV th	300	375	4 - 25 ϕ	2 - 20 ϕ	
	V th	300	375	4 - 20 ϕ	2 - 20 ϕ	
6O _{1.0}	G- III rd	300	375	5 - 25 ϕ	4 - 20 ϕ	
	IV th	300	375	4 - 25 ϕ	2 - 20 ϕ	
	V th	300	375	4 - 20 ϕ	2 - 20 ϕ	
6O _{1.5}	G- III rd	300	375	5 - 25 ϕ	4 - 20 ϕ	
	IV th	300	375	4 - 25 ϕ	2 - 20 ϕ	
	V th	300	375	4 - 20 ϕ	2 - 20 ϕ	
6O _{2.0}	G- III rd	300	375	5 - 25 ϕ	4 - 20 ϕ	
	IV th	300	375	4 - 25 ϕ	2 - 20 ϕ	
	V th	300	375	4 - 20 ϕ	2 - 20 ϕ	
6O _{2.5}	G- III rd	300	375	5 - 25 ϕ	4 - 20 ϕ	
	IV th	300	375	4 - 25 ϕ	2 - 20 ϕ	
	V th	300	375	4 - 20 ϕ	2 - 20 ϕ	
6O _{1.5,1.5}	G- III rd	300	375	5 - 25 ϕ	4 - 20 ϕ	
	IV th	300	375	4 - 25 ϕ	2 - 20 ϕ	
	V th	300	375	4 - 20 ϕ	2 - 20 ϕ	
6O _{2.0,2.0}	G- III rd	300	375	5 - 25 ϕ	4 - 20 ϕ	
	IV th	300	375	4 - 25 ϕ	2 - 20 ϕ	
	V th	300	375	4 - 20 ϕ	2 - 20 ϕ	
6O _{2.5,2.5}	G- III rd	300	375	5 - 25 ϕ	4 - 20 ϕ	
	IV th	300	375	4 - 25 ϕ	2 - 20 ϕ	
	V th	300	375	4 - 20 ϕ	2 - 20 ϕ	
6O _{2.0,2.0,2.0}	G- III rd	300	375	5 - 25 ϕ	4 - 20 ϕ	
	IV th	300	375	4 - 25 ϕ	2 - 20 ϕ	
	V th	300	375	4 - 20 ϕ	2 - 20 ϕ	
6O _{2.5,2.5,2.5}	G- III rd	300	375	5 - 25 ϕ	4 - 20 ϕ	
	IV th	300	375	4 - 25 ϕ	2 - 20 ϕ	
	V th	300	375	4 - 20 ϕ	2 - 20 ϕ	
6O _{2.5,2.0,1.5}	G- III rd	300	375	5 - 25 ϕ	4 - 20 ϕ	
	IV th	300	375	4 - 25 ϕ	2 - 20 ϕ	
	V th	300	375	4 - 20 ϕ	2 - 20 ϕ	

Table B-7: Columns sections and reinforcement details for 8-storey frames

Frame	Storey	Width (mm)	Depth (mm)	Reinforcement Details (uniformly distributed)	Lateral ties
8B	G	450	450	8 - 32 ϕ	8mm ϕ rectangular ties, @ 175mm c/c throughout
	I st - II nd	450	450	8 - 25 ϕ	
	III rd - VII th	450	450	4 - 25 ϕ	
8F	G	450	450	8 - 32 ϕ	
	I st - II nd	450	450	8 - 25 ϕ	
	III rd - VII th	450	450	4 - 25 ϕ	
8O _{1.0}	G	450	450	8 - 32 ϕ	
	I st - II nd	450	450	8 - 25 ϕ	
	III rd - VII th	450	450	4 - 25 ϕ	
8O _{1.5}	G	550	550	12 - 32 ϕ	
	I st - II nd	450	450	8 - 25 ϕ	
	III rd - VII th	450	450	4 - 25 ϕ	
8O _{2.0}	G	600	600	12 - 25 ϕ	
	I st - II nd	450	450	8 - 25 ϕ	
	III rd - VII th	450	450	4 - 25 ϕ	
8O _{2.5}	G	700	700	16 - 25 ϕ	
	I st - II nd	450	450	8 - 25 ϕ	
	III rd - VII th	450	450	4 - 25 ϕ	
8O _{1.5,1.5}	G- I st	550	550	12 - 32 ϕ	16mm ϕ rectangular ties, @ 85mm c/c for a distance of 535mm from supports,
	II nd	450	450	8 - 25 ϕ	
	III rd - VII th	450	450	4 - 25 ϕ	
8O _{2.0,2.0}	G- I st	600	600	12 - 25 ϕ	
	II nd	450	450	8 - 25 ϕ	
	III rd - VII th	450	450	4 - 25 ϕ	
8O _{2.5,2.5}	G- I st	700	700	16 - 25 ϕ	
	II nd	450	450	8 - 25 ϕ	
	III rd - VII th	450	450	4 - 25 ϕ	
8O _{2.0,2.0,2.0}	G- II nd	600	600	12 - 25 ϕ	
	III rd - VII th	450	450	4 - 25 ϕ	
8O _{2.5,2.5,2.5}	G- II nd	700	700	16 - 25 ϕ	
	III rd - VII th	450	450	4 - 25 ϕ	
8O _{2.5,2.5,2.5,2.5}	G- III rd	700	700	16 - 25 ϕ	
	IV th - VII th	450	450	4 - 25 ϕ	

Table B-8: Beam sections and reinforcement details for 8-storey frames

Frame	Floor	Width (mm)	Depth (mm)	Reinforcements details		Stirrups	
				Top	Bottom		
8B	G- V th	400	300	5 - 25 ϕ	4 - 20 ϕ	2 legged 8mm ϕ , @ 140mm c/c throughout and	
	VI th	400	300	4 - 25 ϕ	3 - 20 ϕ		
	VII th	300	300	3 - 22 ϕ	2 - 20 ϕ		
8F	G- V th	400	300	5 - 25 ϕ	4 - 20 ϕ		
	VI th	400	300	4 - 25 ϕ	3 - 20 ϕ		
	VII th	300	300	3 - 22 ϕ	2 - 20 ϕ		
8O _{1.0}	G- V th	400	300	5 - 25 ϕ	4 - 20 ϕ		
	VI th	400	300	4 - 25 ϕ	3 - 20 ϕ		
	VII th	300	300	3 - 22 ϕ	2 - 20 ϕ		
8O _{1.5}	G- V th	400	300	5 - 25 ϕ	4 - 20 ϕ		
	VI th	400	300	4 - 25 ϕ	3 - 20 ϕ		
	VII th	300	300	3 - 22 ϕ	2 - 20 ϕ		
8O _{2.0}	G- V th	400	300	5 - 25 ϕ	4 - 20 ϕ		
	VI th	400	300	4 - 25 ϕ	3 - 20 ϕ		
	VII th	300	300	3 - 22 ϕ	2 - 20 ϕ		
8O _{2.5}	G- V th	400	300	5 - 25 ϕ	4 - 20 ϕ		
	VI th	400	300	4 - 25 ϕ	3 - 20 ϕ		
	VII th	300	300	3 - 22 ϕ	2 - 20 ϕ		
8O _{1.5,1.5}	G- V th	400	300	5 - 25 ϕ	4 - 20 ϕ		2 legged 8mm ϕ , @ 100mm c/c for a distance of 500mm from supports,
	VI th	400	300	4 - 25 ϕ	3 - 20 ϕ		
	VII th	300	300	3 - 22 ϕ	2 - 20 ϕ		
8O _{2.0,2.0}	G- V th	400	300	5 - 25 ϕ	4 - 20 ϕ		
	VI th	400	300	4 - 25 ϕ	3 - 20 ϕ		
	VII th	300	300	3 - 22 ϕ	2 - 20 ϕ		
8O _{2.5,2.5}	G- V th	400	300	5 - 25 ϕ	4 - 20 ϕ		
	VI th	400	300	4 - 25 ϕ	3 - 20 ϕ		
	VII th	300	300	3 - 22 ϕ	2 - 20 ϕ		
8O _{2.0,2.0,2.0}	G- V th	400	300	5 - 25 ϕ	4 - 20 ϕ		
	VI th	400	300	4 - 25 ϕ	3 - 20 ϕ		
	VII th	300	300	3 - 22 ϕ	2 - 20 ϕ		
8O _{2.5,2.5,2.5}	G- V th	400	300	5 - 25 ϕ	4 - 20 ϕ		
	VI th	400	300	4 - 25 ϕ	3 - 20 ϕ		
	VII th	300	300	3 - 22 ϕ	2 - 20 ϕ		
8O _{2.5,2.5,2.5,2.5}	G- V th	400	300	5 - 25 ϕ	4 - 20 ϕ		
	VI th	400	300	4 - 25 ϕ	3 - 20 ϕ		
	VII th	300	300	3 - 22 ϕ	2 - 20 ϕ		

APPENDIX-C

GROUND MOTIONS

C.1 NATURAL GROUND MOTION

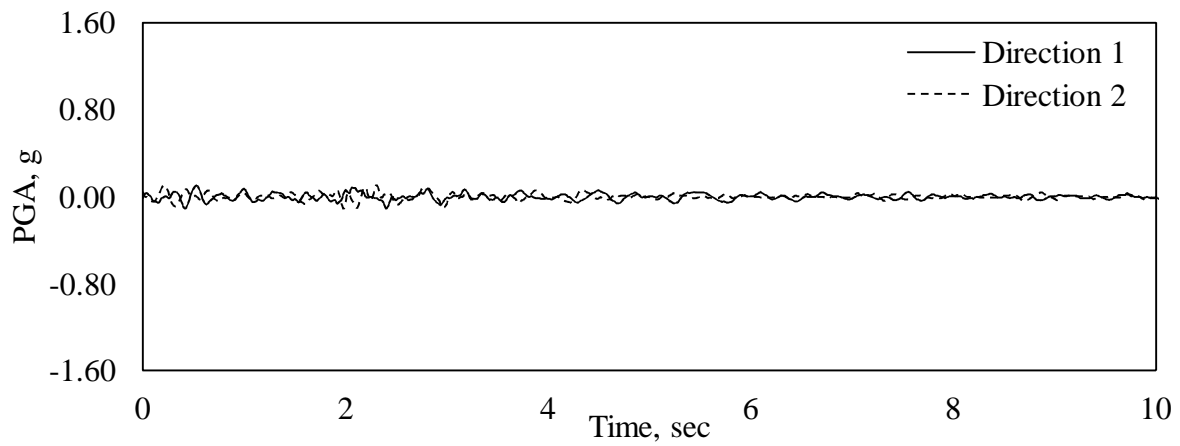


Fig. C.1: Chamoli Aftershock 1999-03-29, Gopeshwar, Uttarakhand

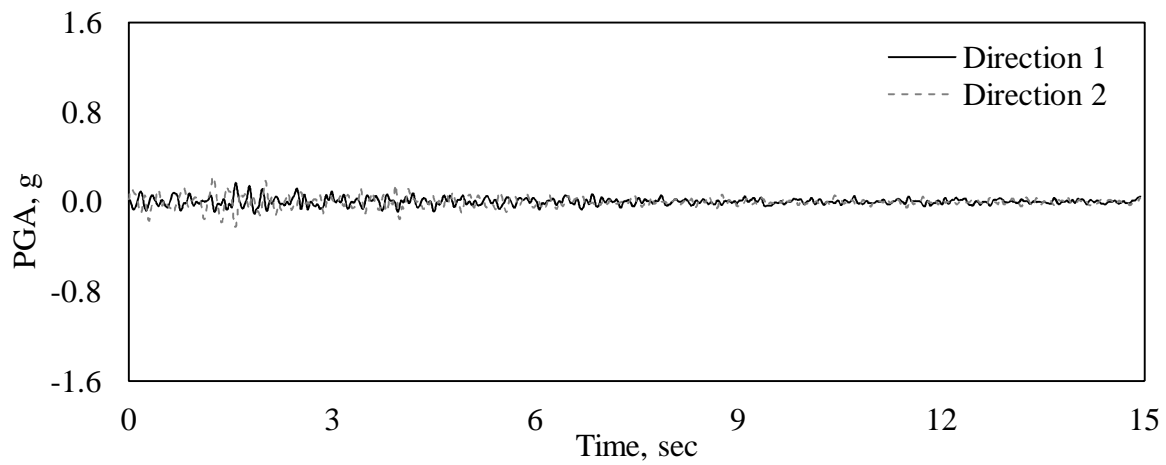


Fig. C.2: Chamoli 1999-03-28, Barkot, Uttarakhand

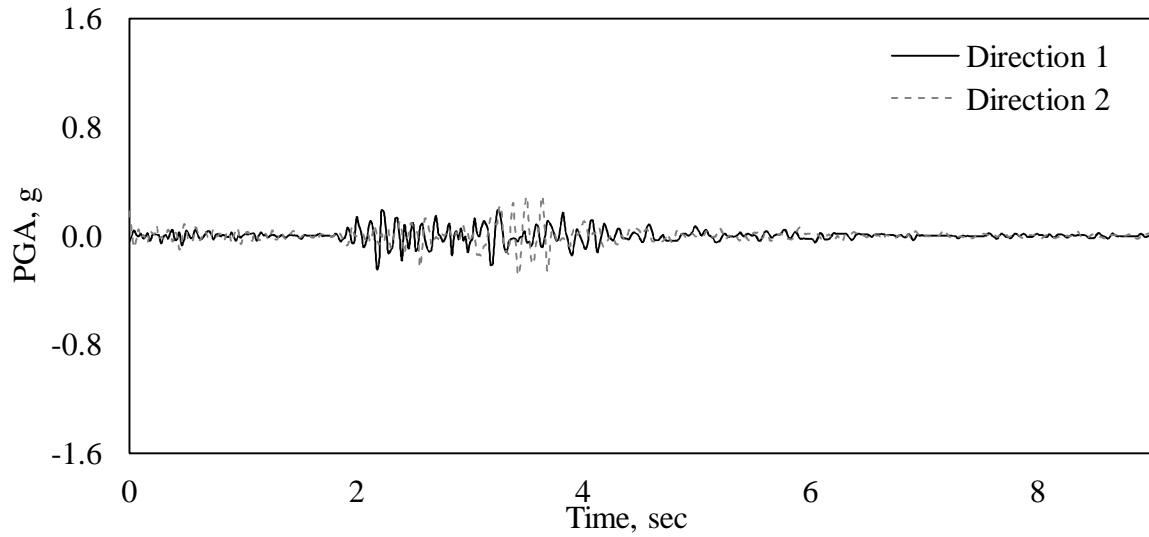


Fig. C.3: Chamba 1995-03-24, Rakh, Maharashtra

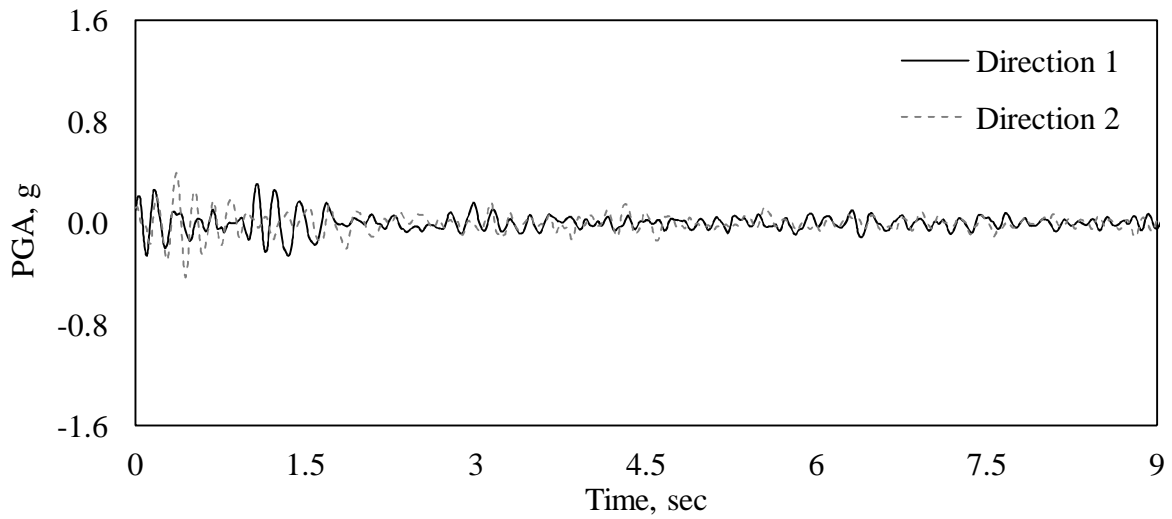


Fig. C.4: India-Burma Border 1995-05-06, Haflong, Assam

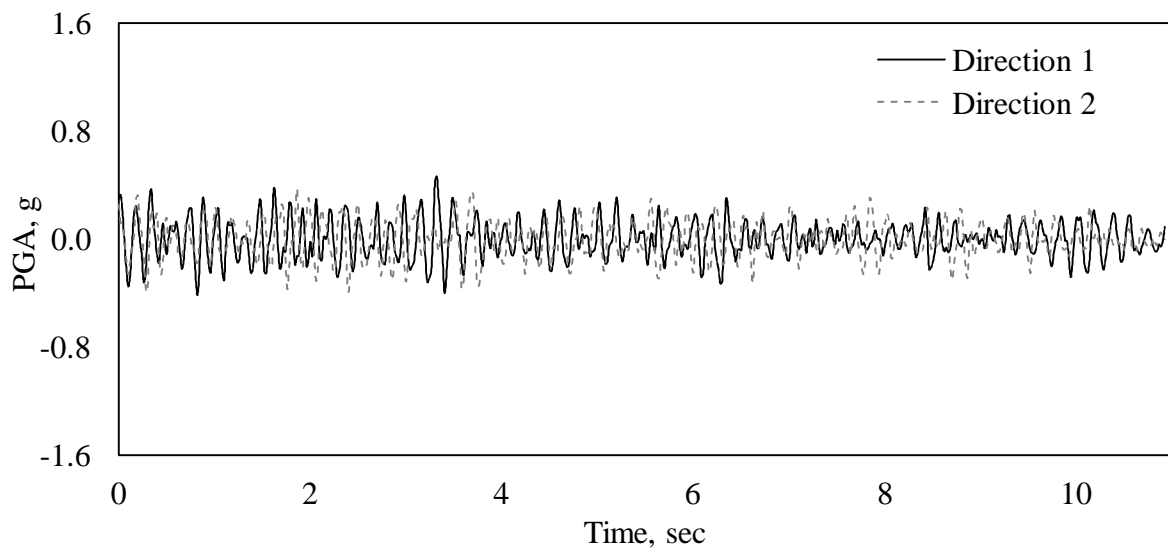


Fig. C.5: India-Burma Border, 1987-05-18, Panimur, Assam

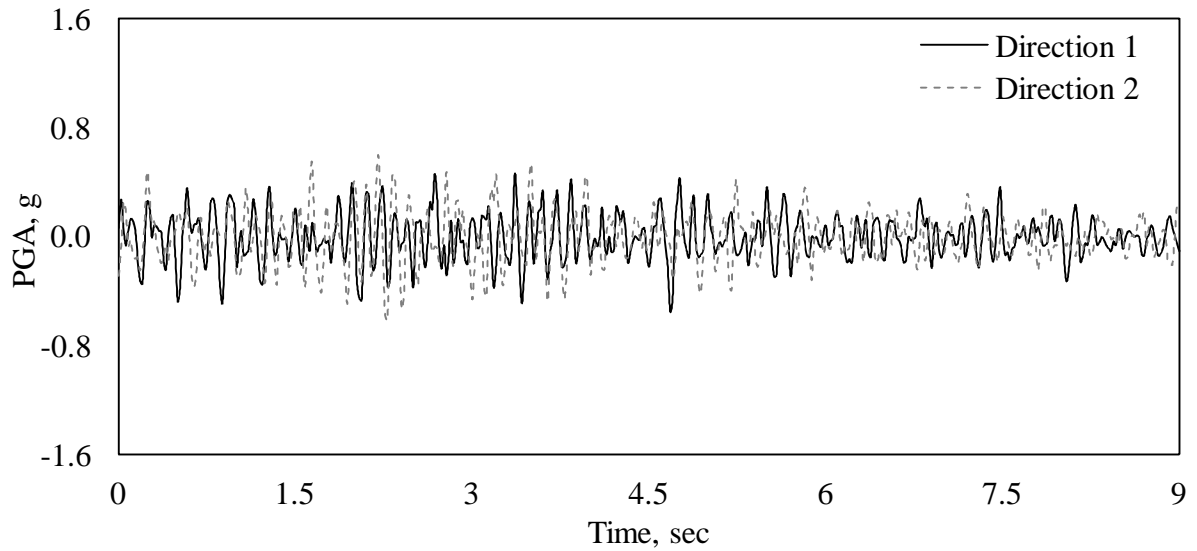


Fig. C.6: India-Burma Border, 1990-01-09, Laisong, Assam

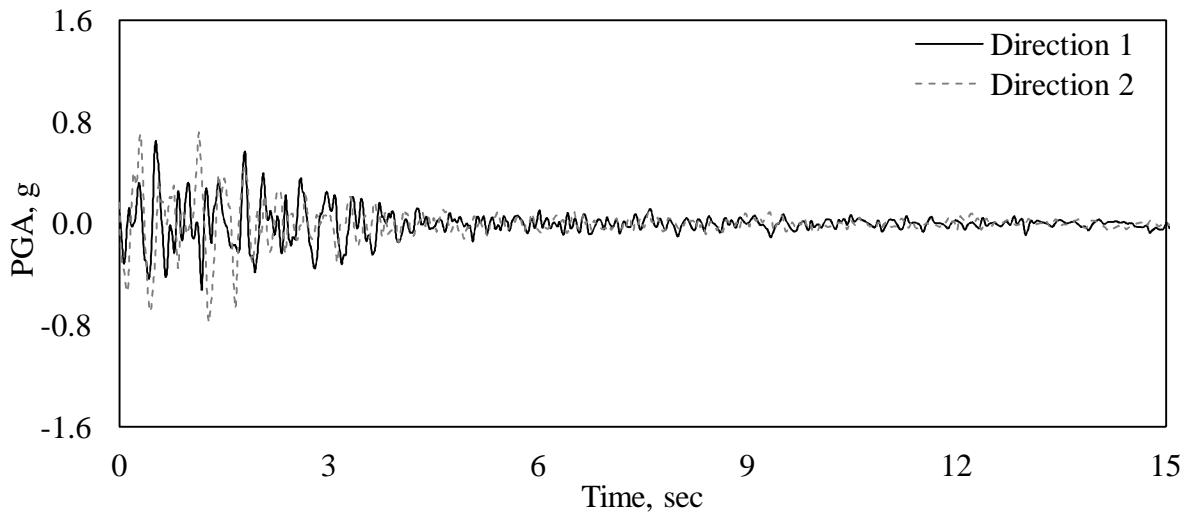


Fig. C.7: India-Bangladesh Border, 1988-02-06, Khliehriat, Assam

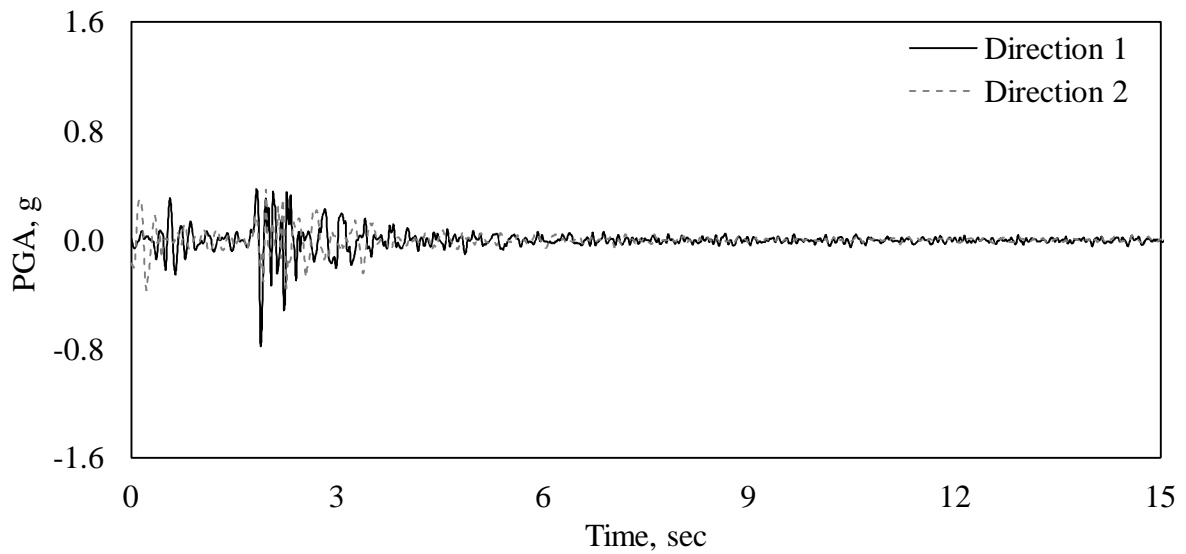


Fig. C.8: Xizang-India Border, 1996-03-26, Ukhimath, Uttarakhand

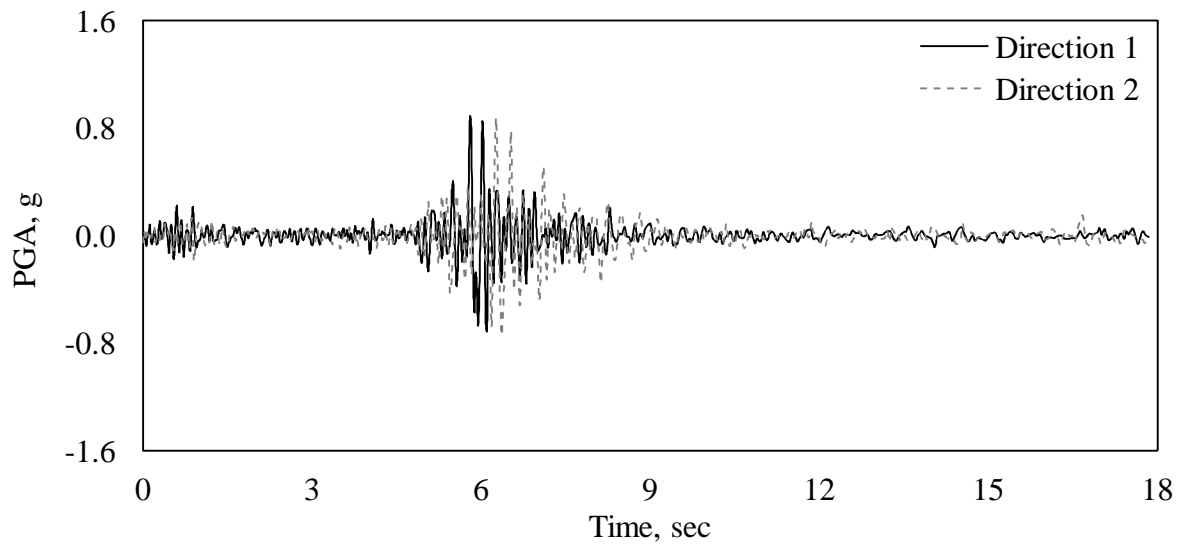


Fig. C.9: NE India, 1986-09-10, Dauki, Uttar Pradesh

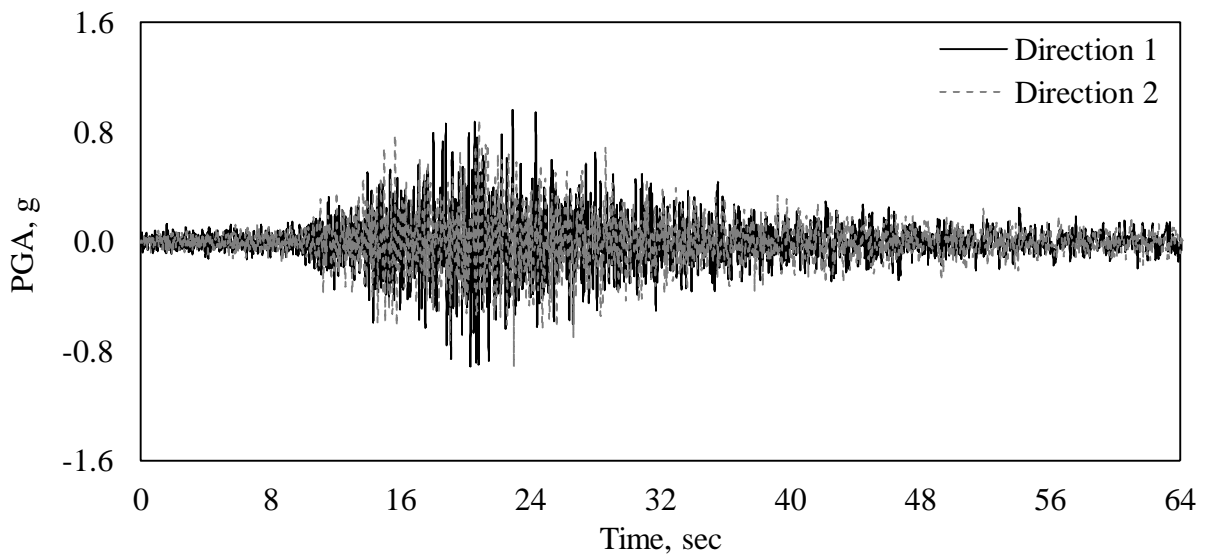


Fig. C.10: India-Burma Border, 1988-08-06, Hajadisa, Assam

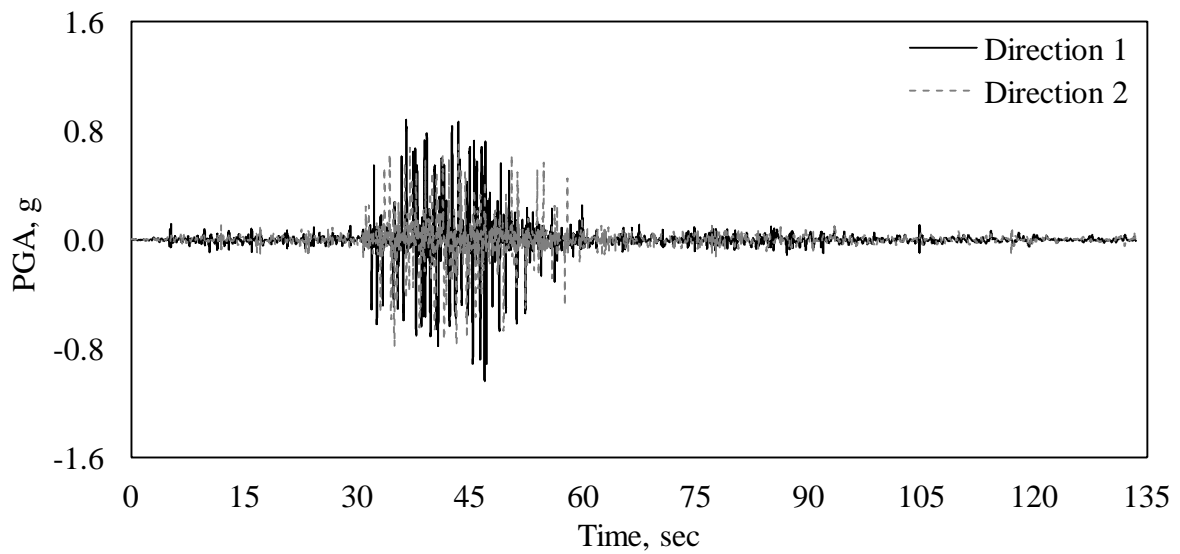


Fig. C.11: Bhuj/Kachchh, 2001-01-26, Ahmedabad Gujarat

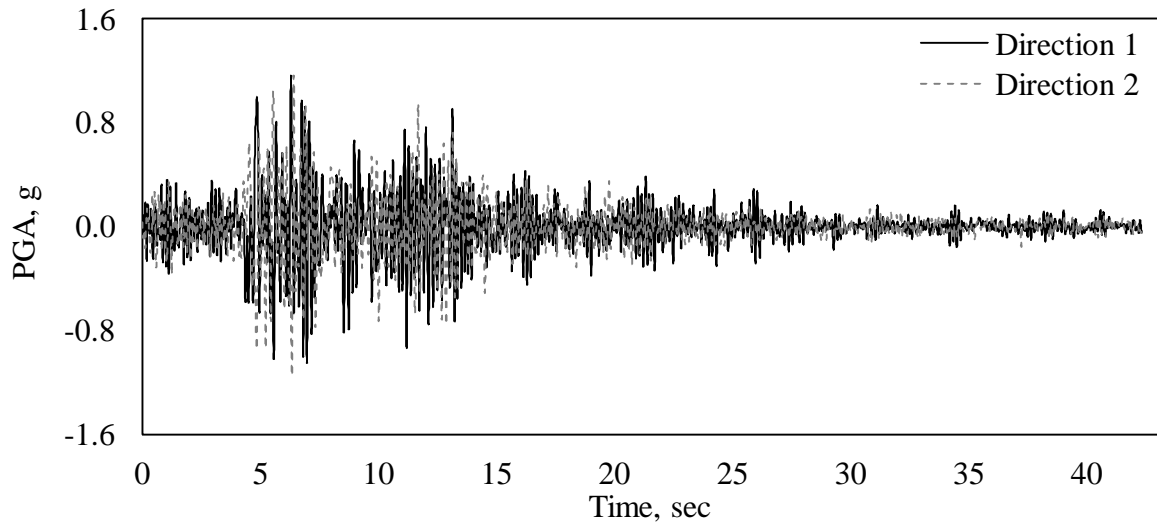


Fig. C.12: Uttarkashi , 1991-10-19, Ghansiali, Uttarakhand

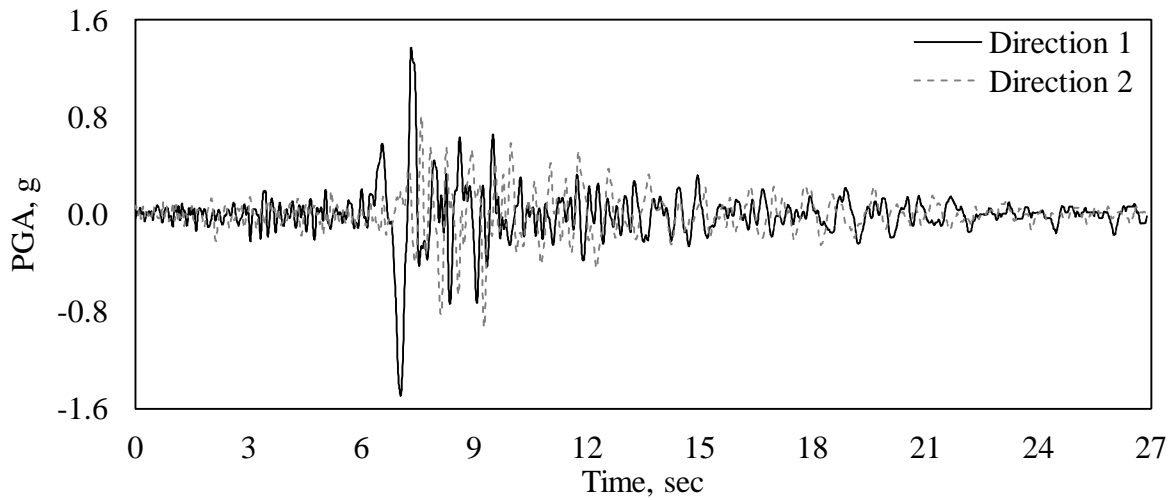


Fig. C.13: India-Burma Border, 1997-05-08, Silchar, Assam

C.2 SYNTHETIC GROUND MOTION (CONSISTENT TO INDIAN SPECTRUM)

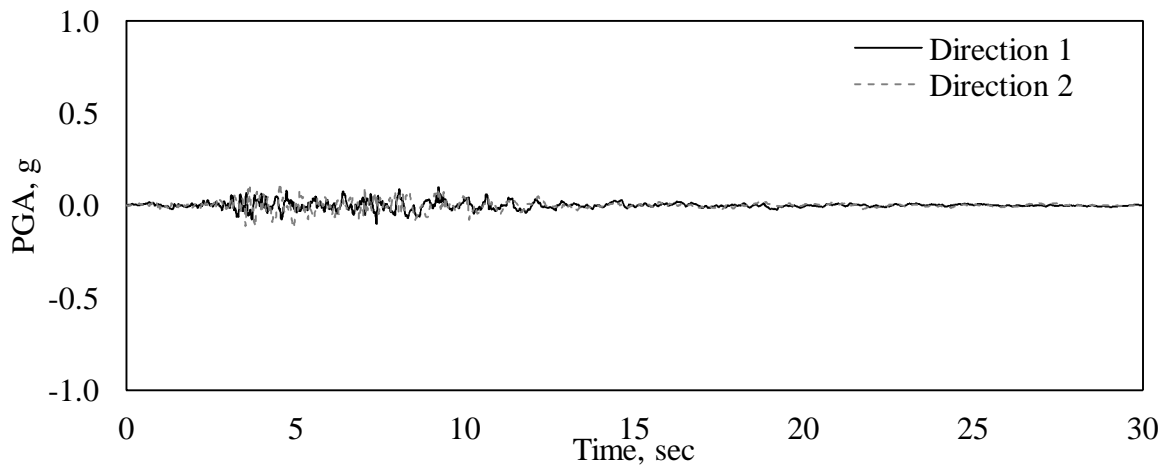


Fig. C.14: Northridge 1994, Beverly Hills

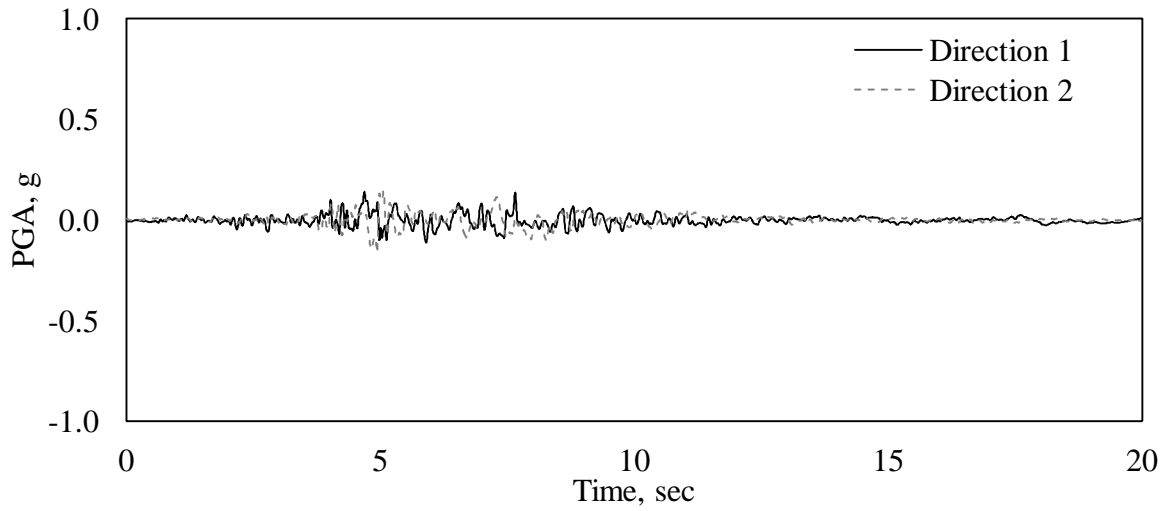


Fig. C.15: Northridge 1994, Canyon Country

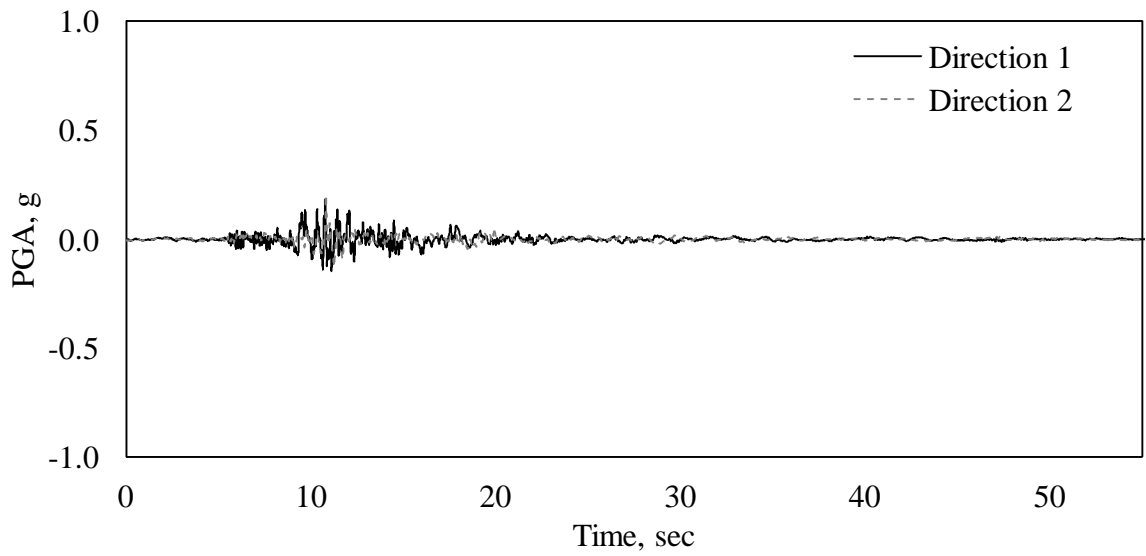


Fig. C.16: Duzce, Turkey, 1999, Bolu

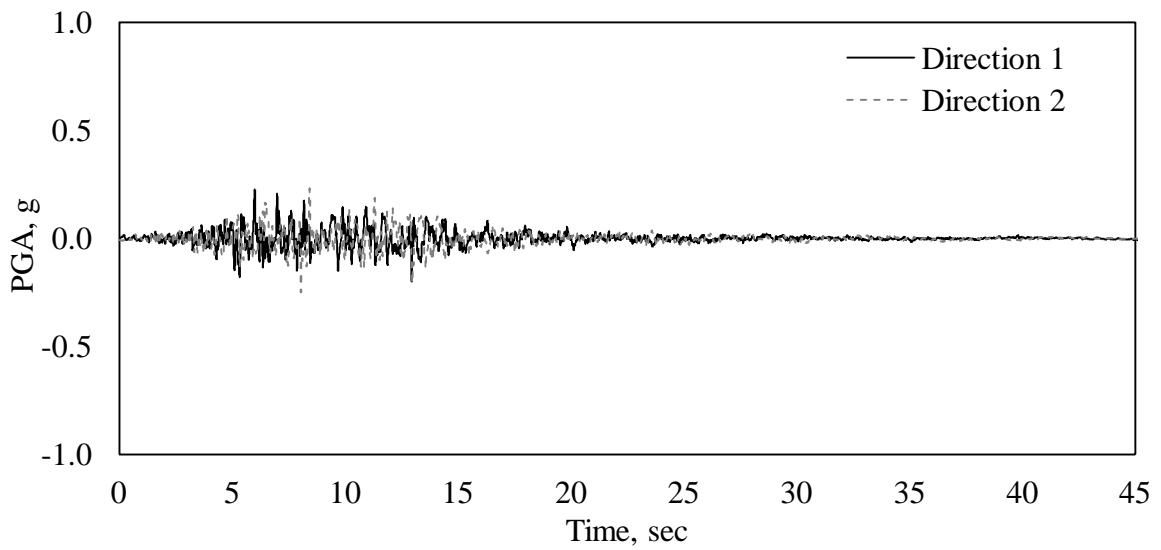


Fig. C.17: Hector Mine 1999, Hector

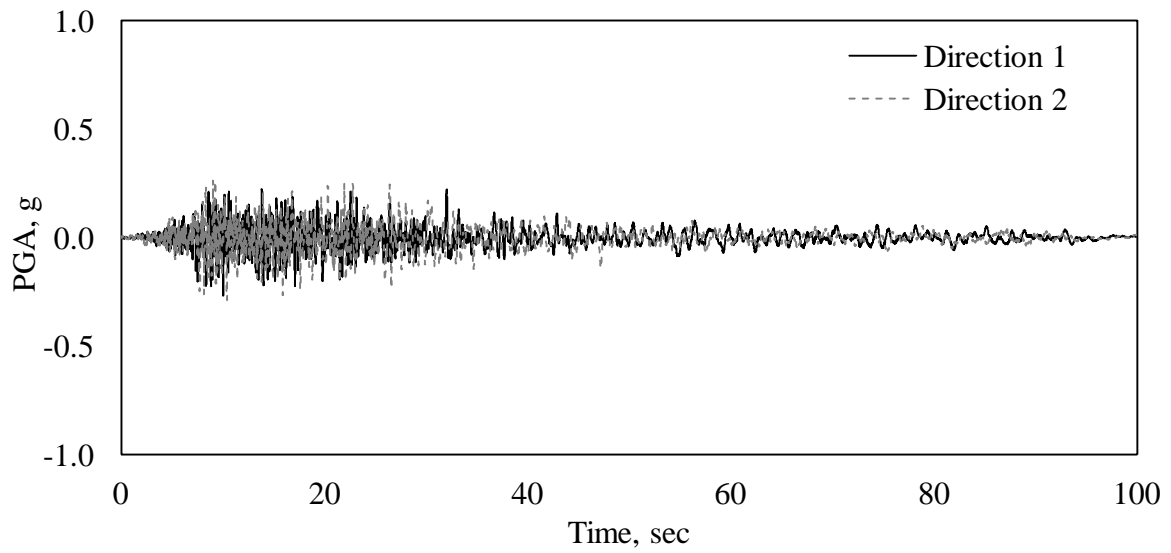


Fig. C.18: Imperial Valley, Delta

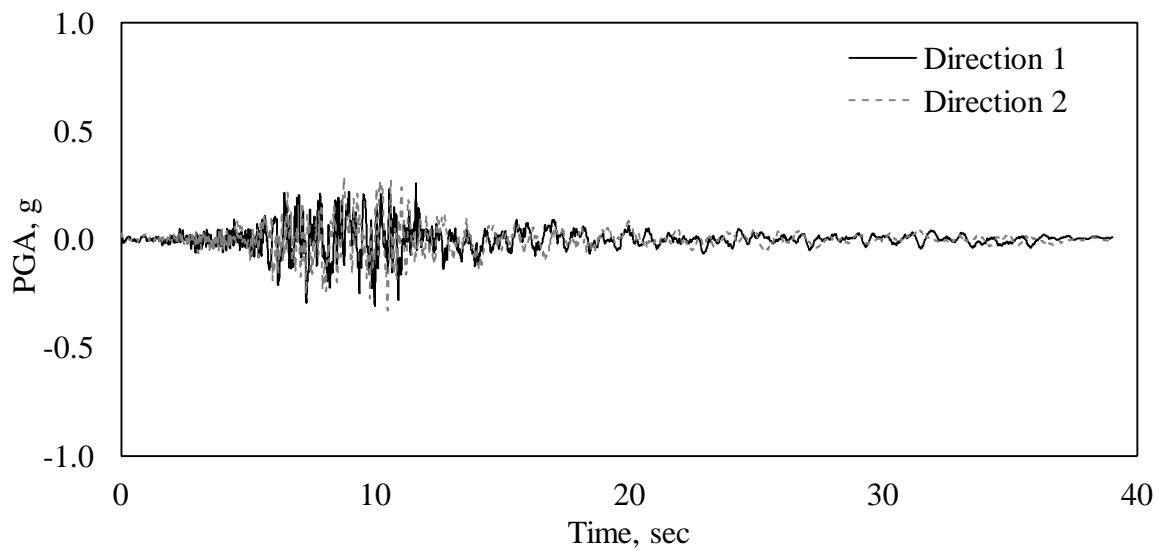


Fig. C.19: Imperial Valley, El Centro

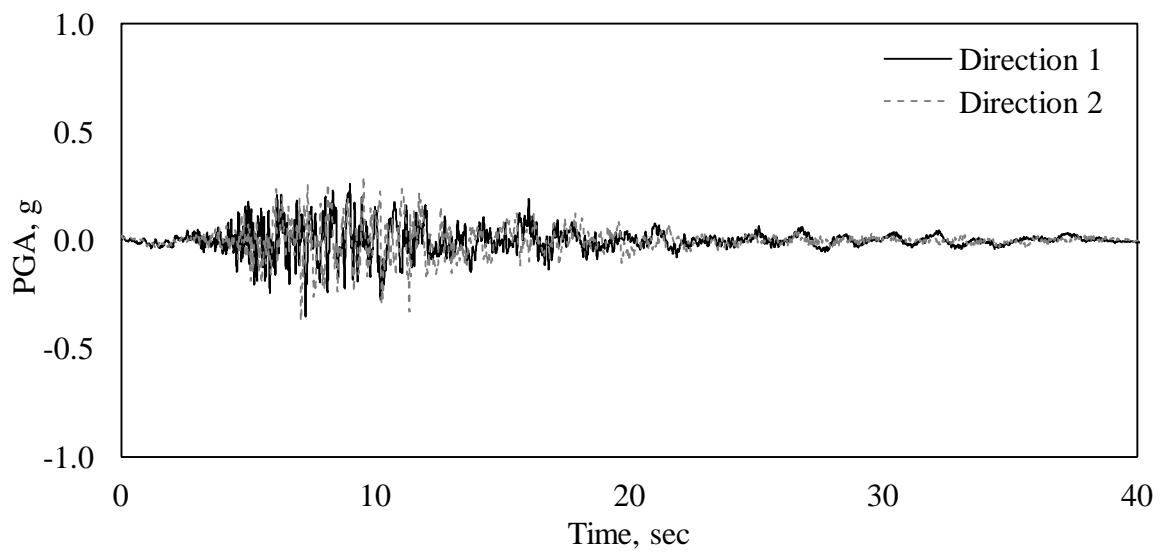


Fig. C.20: Kobe, Japan 1995, Nishi-Akashi

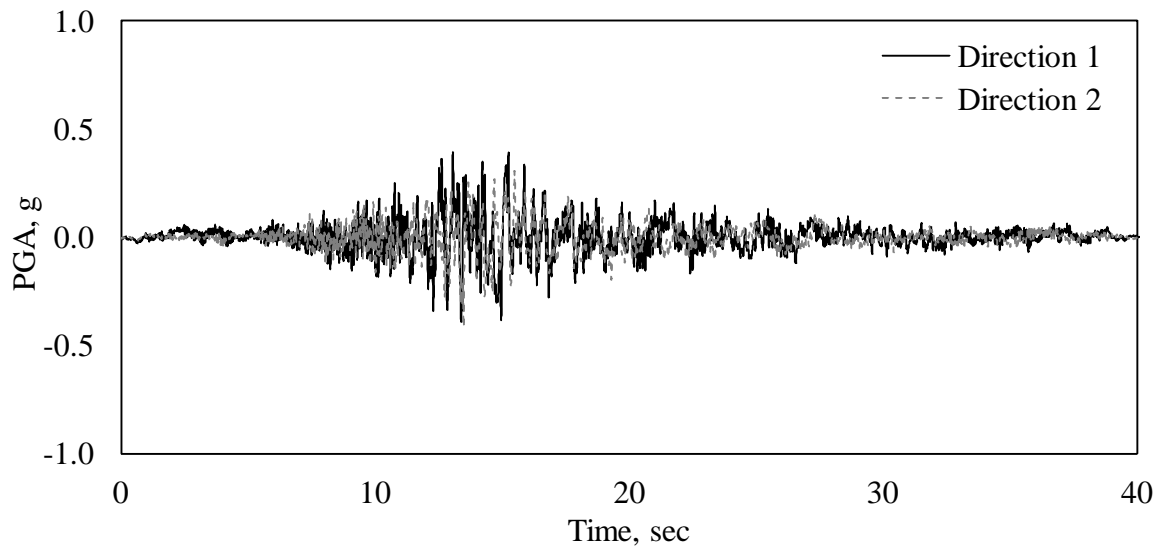


Fig. C.21: Kobe, Japan 1995, Shin-Osaka

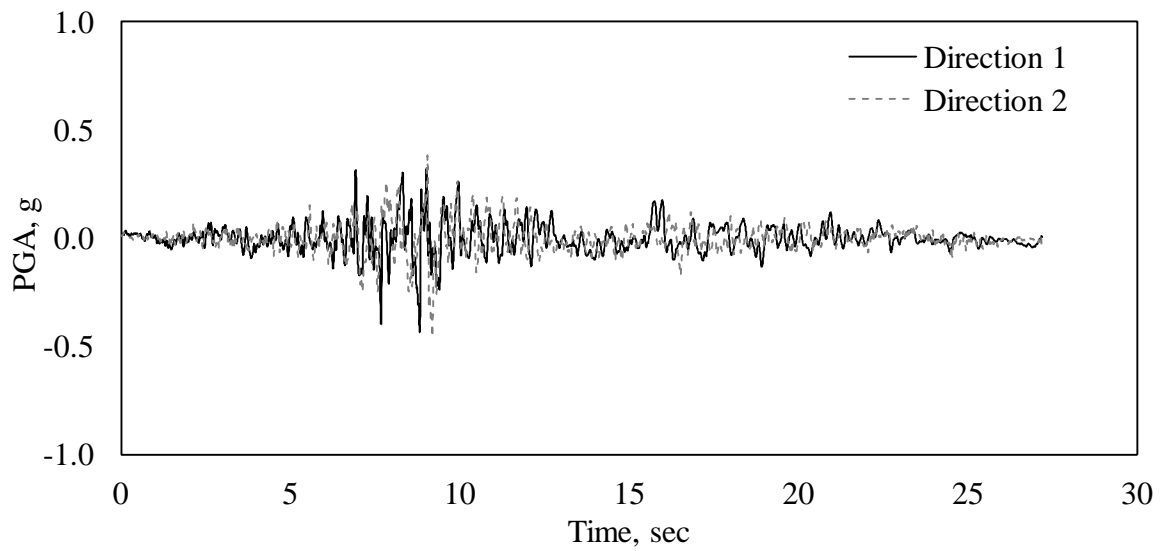


Fig. C.22: Kocaeli, Turkey 1999, Duzce

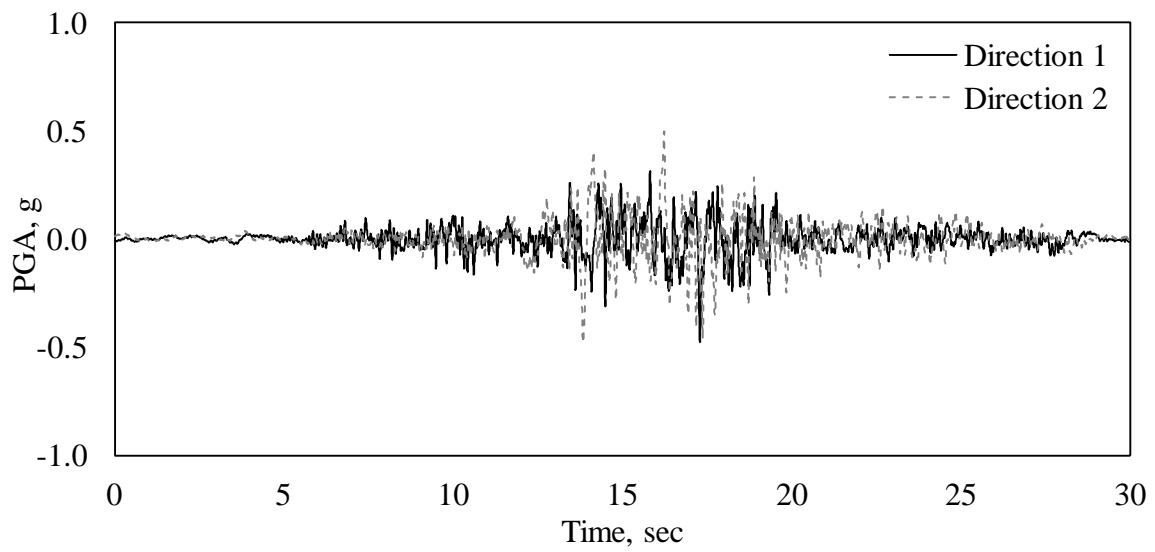


Fig. C.23: Kocaeli, Turkey 1999, Arcelik

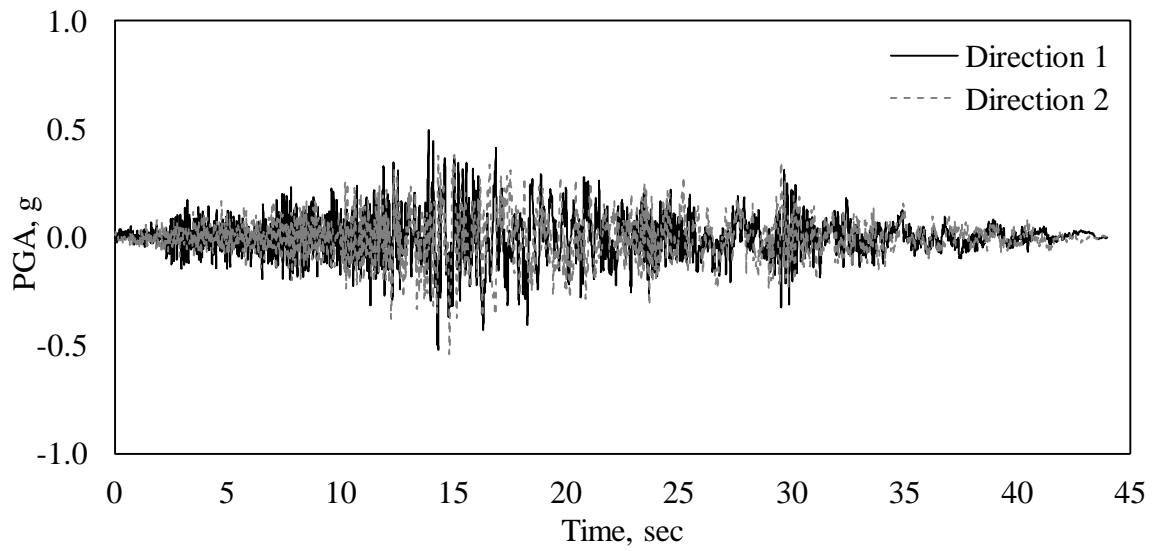


Fig. C.24: Landers 1992, Yermo Fire Station

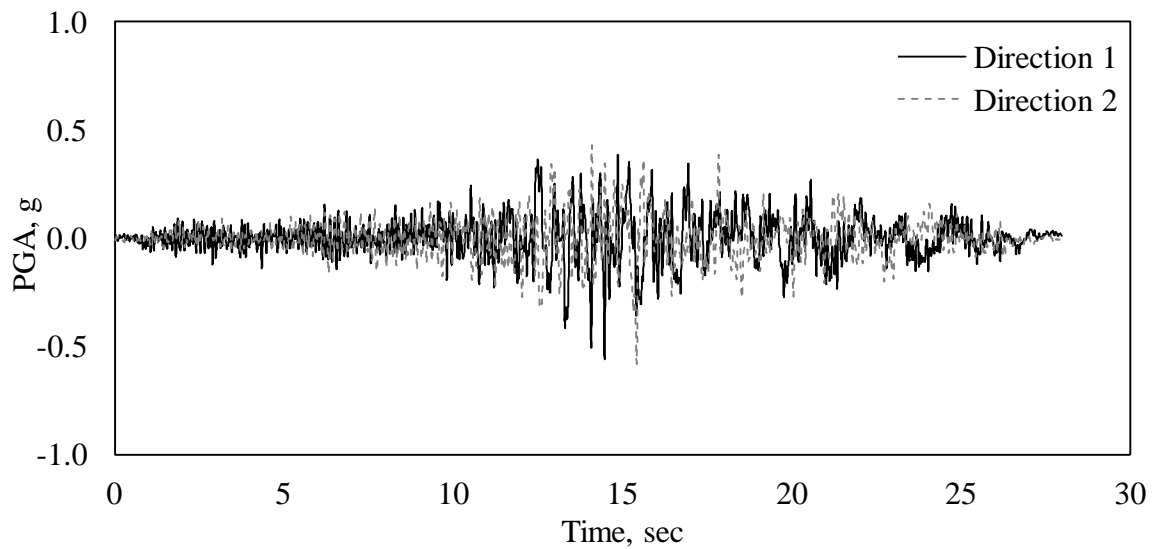


Fig. C.25: Landers 1992, Coolwater

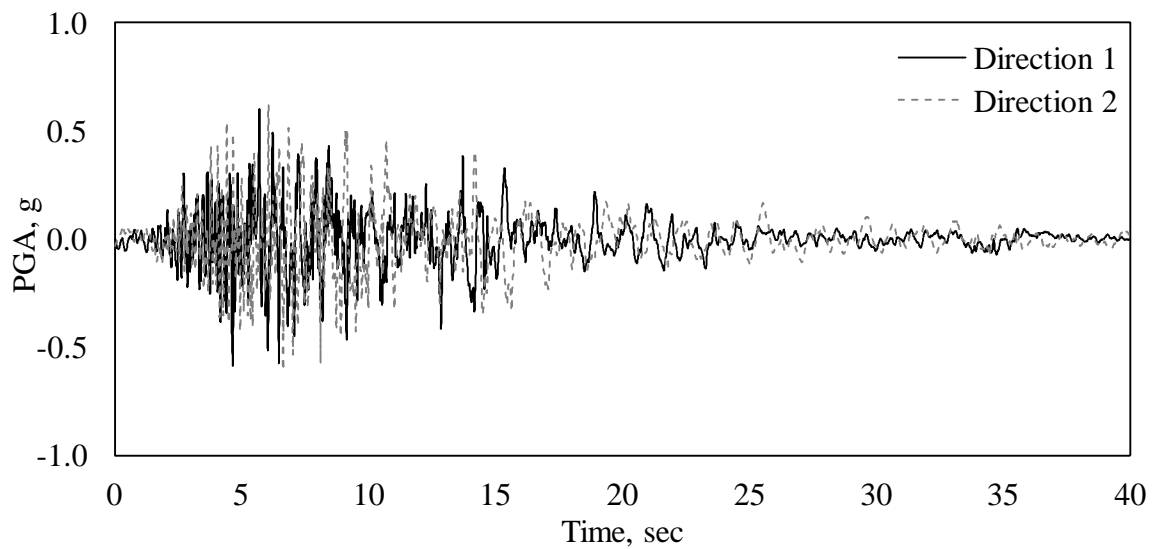


Fig. C.26: Loma Prieta 1989, Capitola

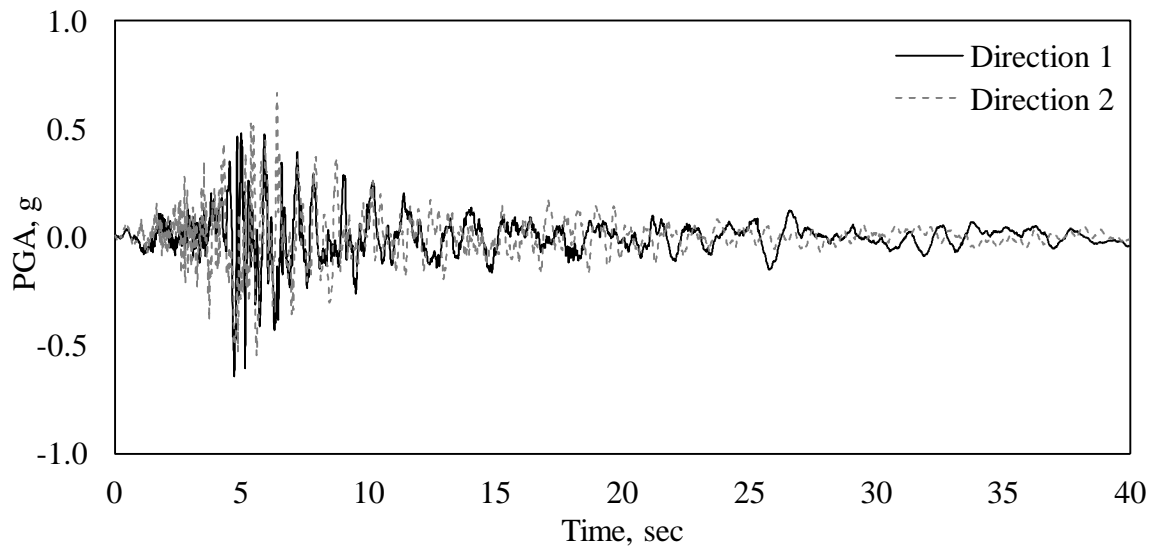


Fig. C.27: Loma Prieta 1989, Gilroy

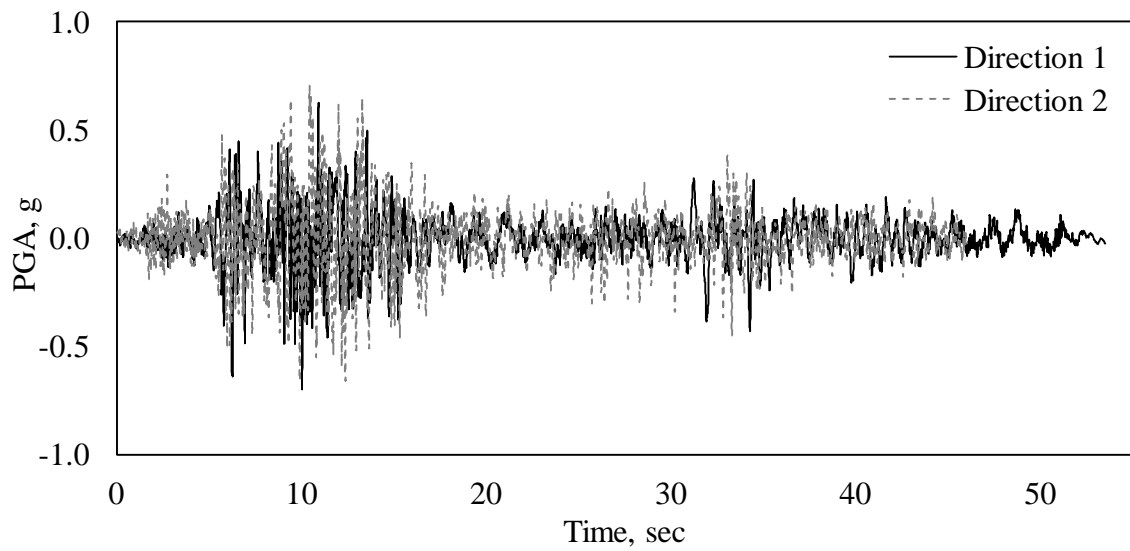


Fig. C.28: Manjil, Iran 1990, Abbar

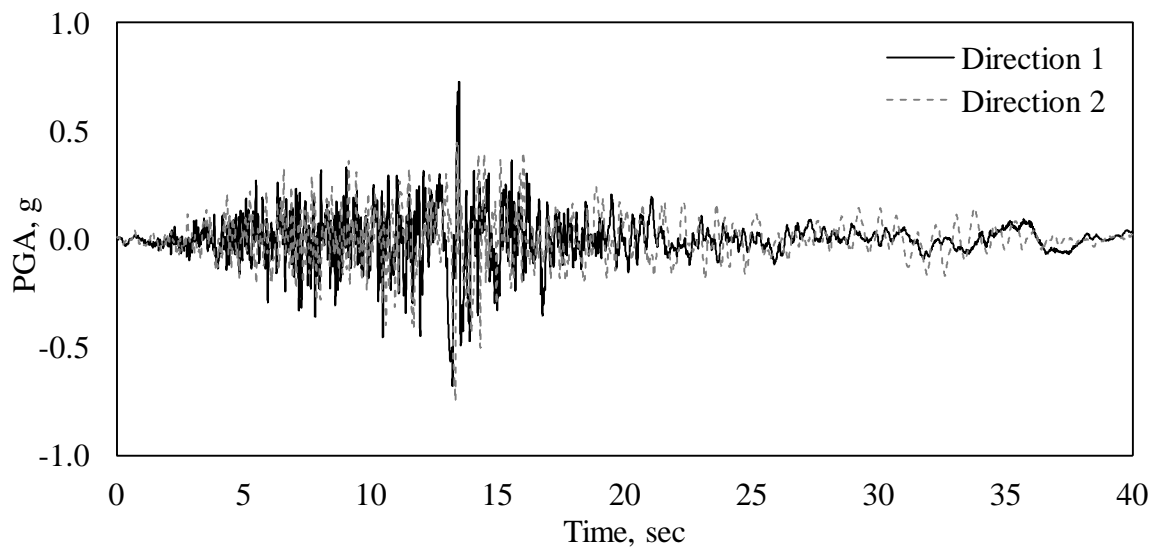


Fig. C.29: Superstition Hills 1987, El Centro

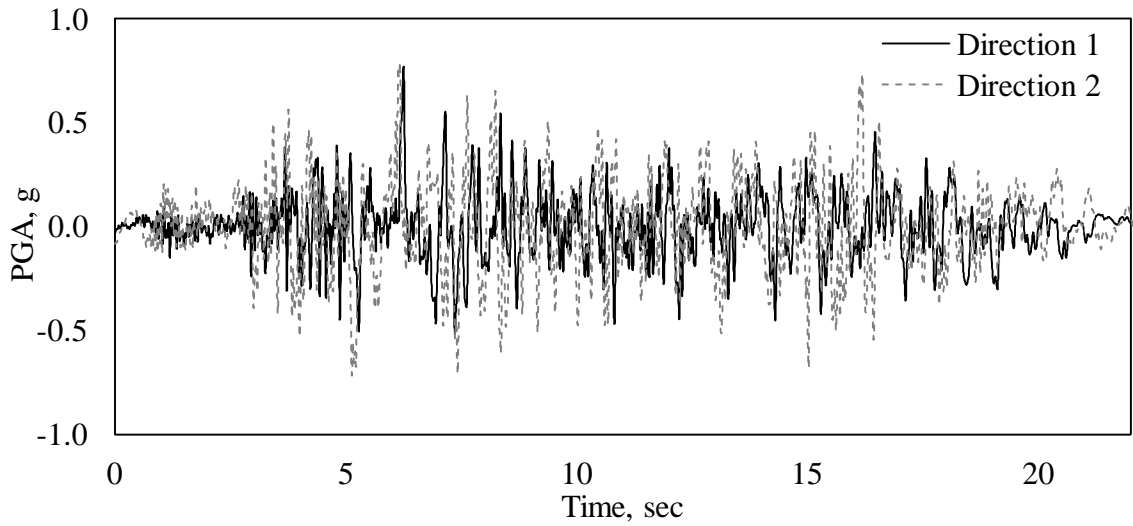


Fig. C.30: Superstition Hills 1987, Poe Road

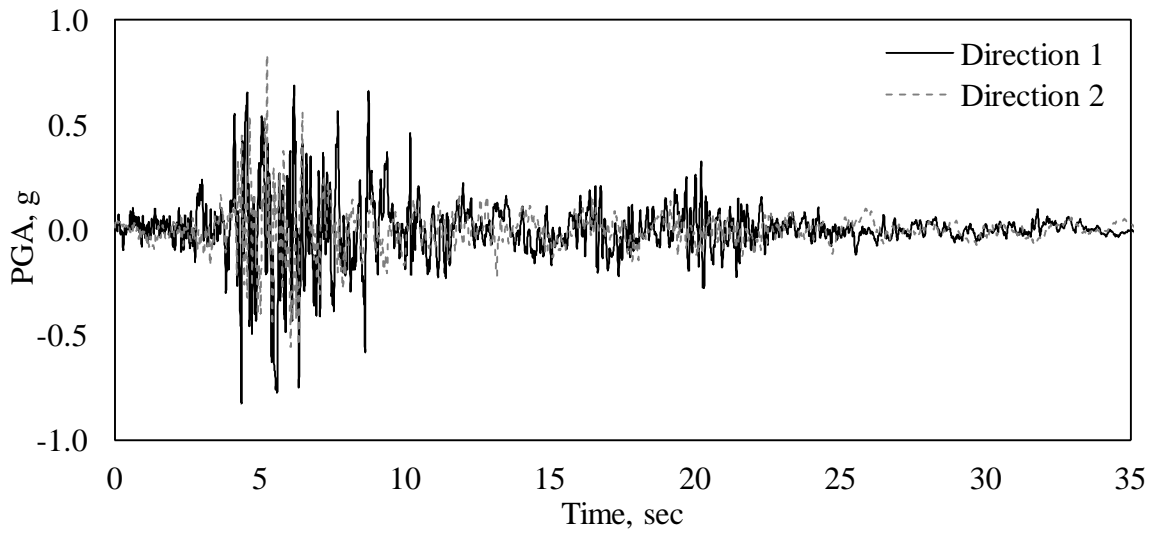


Fig. C.31: Cape Mendocino, Rio Dell Overpass

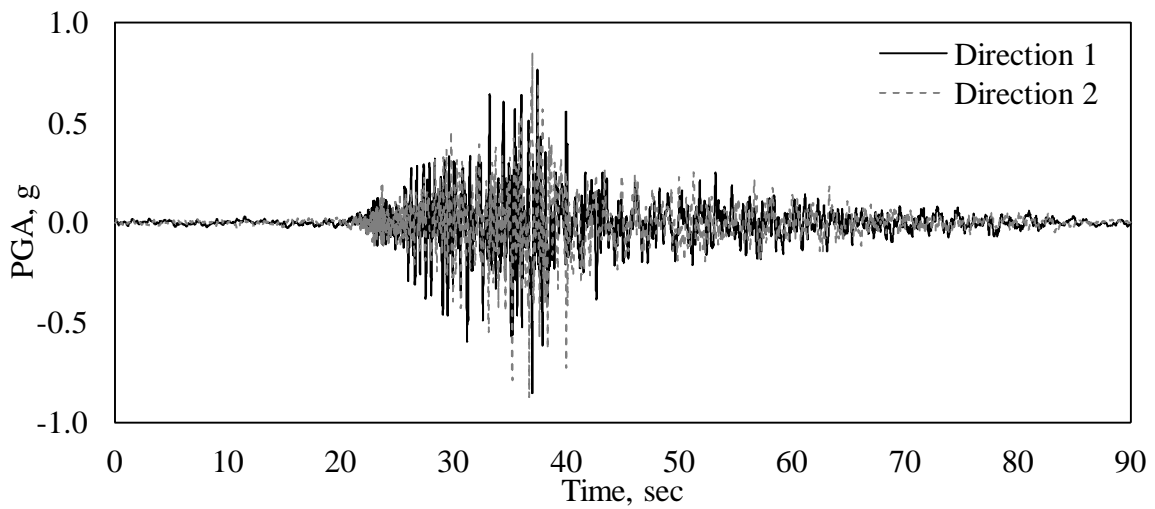


Fig. C.32: Chi-Chi, Taiwan 1999, CHY101

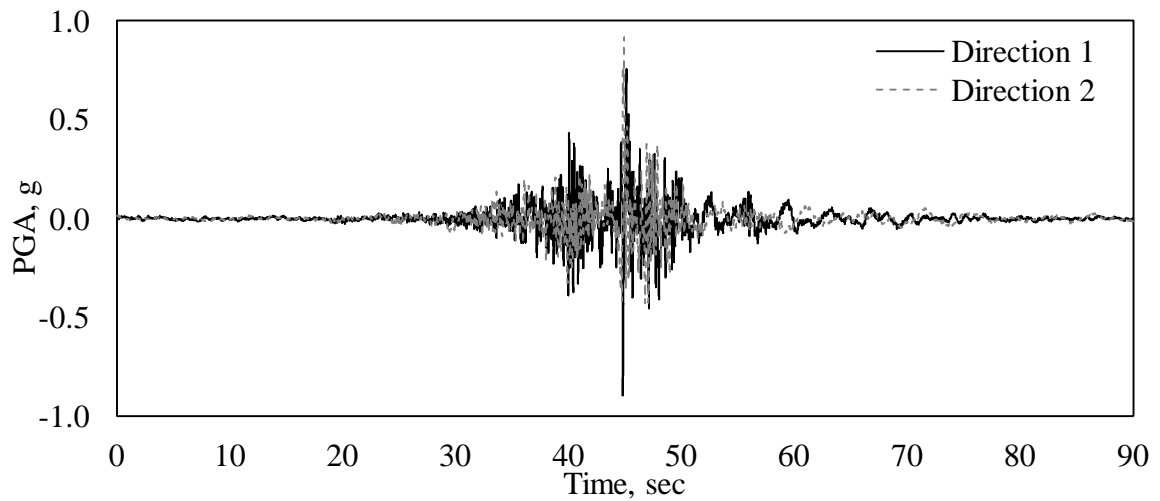


Fig. C.33: Chi-Chi, Taiwan 1999, TCU045

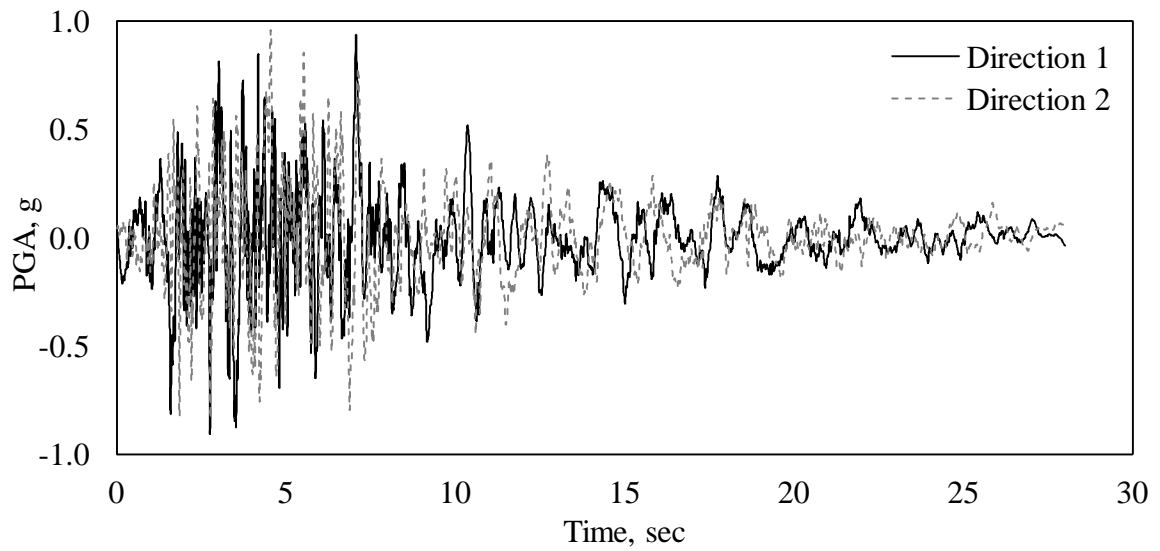


Fig. C.34: San Fernando 1971, LA - Hollywood

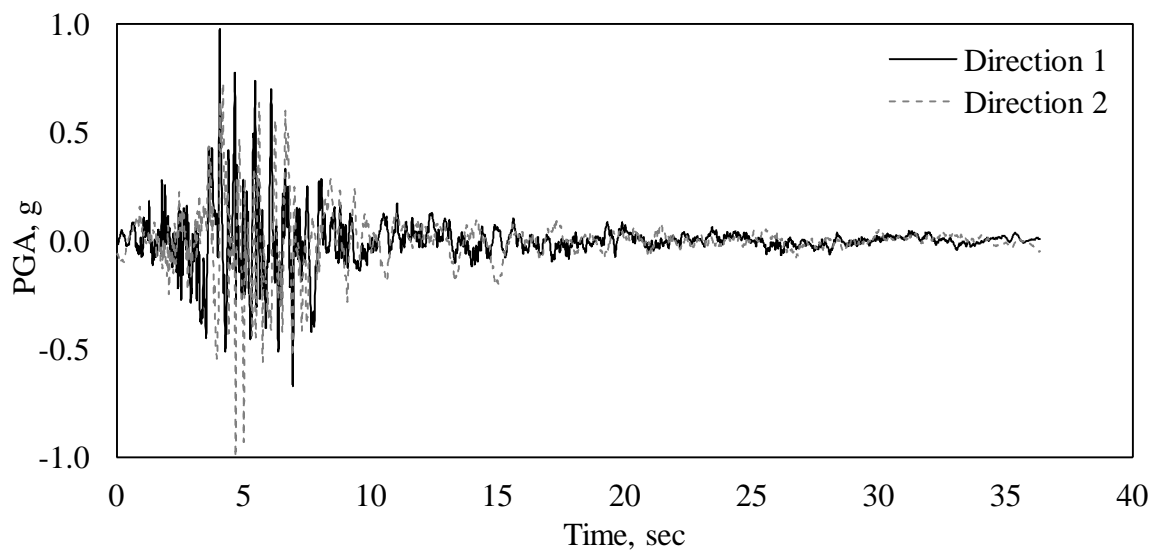


Fig. C.35: Friuli, Italy 1976, Tolmezzo

REFERENCES

- A Agarwal, P. and Thakkar, S. K.** (2001). A comparative study of brick masonry house model under quasi-static and dynamic loading, *Journal of Earthquake Technology*, paper No. 414, 38(2-4):103-122.
- Al-Chaar, G.** (2002). Evaluating strength and stiffness of unreinforced masonry infill structures, US Army Corp of Engineers, Engineer Research and Development Center.
- Anderson, J.G.** (1997). Benefits of Scenario Ground Motion Maps, *Engineering Geology*, 48(1):43–57.
- Aoki, Y., Kanda, J., Emoto, T., Kohno, M., Ohashi, Y., Fujitani, H. and Saito, T.** (2000). Target seismic performance levels in structural design for buildings, *Proceedings 12th World Conference on Earthquake Engineering*, Auckland, New Zealand.
- Arlekar, J. N., Jain, S. K. and Murty, C. V. R.** (1997). Seismic response of RC frame buildings with soft first storeys, *Proceedings of the CBRI golden jubilee conference on natural hazards in urban habitat*, New Delhi.
- ASCE/SEI 41-06** (2007). *Seismic Rehabilitation of Existing Buildings*, American Society of Civil Engineers, USA.
- ASCE/SEI 7** (2010). *Minimum Design Loads for Buildings and Other Structures*, American Society of Civil engineers, Reston, VA.
- Asteris, P.G., Antoniou, S.T., Sophianopoulos, D.S. and Chrysostomou, C. Z.** (2011). Mathematical macro modeling of infilled frames: State of the art, *Journal of Structural Engineering*, 137(12):1508–1517.
- ATC 13**, (1985). *Earthquake damage evaluation data for California*, Applied Technology Council, Redwood City, CA.
- ATC 58**, 100% Draft (2012). *Guidelines for Seismic Performance Assessment of Buildings*, Applied Technology Council, Redwood City, CA.

- Attarchian, N., Kalantari, A. and Moghaddam, A. S.** (2013). Cyclic behaviour modelling of rectangular RC bridge piers using OpenSees, 4th ECCOMAS Thematic Conference on Computational Methods in Structural Dynamics and Earthquake Engineering, Kos Island, Greece.
- Ayyub, B.M. and K.-L. Lai.** (1989). Structural Reliability Assessment using Latin Hypercube Sampling, 5th International Conference on Structural Safety and Reliability, ICOSSAR, 1177-1184.
- B Baker, J. W.** (2008). An Introduction to Probabilistic Seismic Hazard Analysis (PSHA). Hnandbook, versions 1.3, October.
- Basoz, N. and Kiremidjian, A. S.** (1999). Development of Empirical Fragility Curves for Bridges, 5th US Conference on Lifeline Earthquake Engineering, Seattle, WA, USA.
- Bianchi, F., Sousa, R. and Pinho R.** (2011). Blind prediction of a full-scale RC bridge column tested under dynamic conditions, Proceedings of 3rd International Conference on Computational Methods in Structural Dynamics and Earthquake Engineering (COMPDYN 2011), Paper no. 294, Corfu, Greece.
- Biondi, S., Colangelo, F. and Nuti, C.** (2000). La Risposta Sismica dei Telai con Tamponature Muraie, (in Italian), Gruppo Nazionale per la Difesa dai Terremoti, Rome.
- Bracci, J. M., Reinhorn, A. M. and Mander, J. B.** (1995). Seismic resistance of reinforced concrete frame structures designed for gravity loads: Performance of structural system, ACI Structural Journal 92(5):597–609.
- Bulgarian Seismic Code** (1987). Code for design of buildings and structures in seismic regions, Bulgarian Academy of Science Committee of Territorial and Town System at the Council of Ministers, Sofia, Bulgaria.
- C Celarec, D., Ricci, P. and Dolsek, M.** (2012). The sensitivity of seismic response parameters to the uncertain modeling variables of masonry-infilled reinforced concrete frames, Engineering Structures, 35:165–177.
- Celik, O. C. and Ellingwood, B. R.** (2010). Seismic fragilities for non-ductile reinforced concrete frames - Role of aleatoric and epistemic uncertainties, Structural Safety, 32(1):1-12.

Chen, P. and Collins, K. R. (2001). Some observations on performance-based and reliability-based seismic design of asymmetric building structures, *Engineering Structures*, 23(8):1005–1010.

Chopra, A. K. (2012). *Dynamics of Structures*, 4th Edition. Prentice Hall.

Chryssanthopoulos, M. K., Dymiotis, C. and Kappos, A. J. (2000). Probabilistic Evaluation of Behaviour Factors in EC8-Designed R/C Frames, *Engineering Structures*, 22(8):1028–1041.

Clough, R. W. and Penzien, J. (1975). *Dynamics of Structures*, McGraw-Hill International Editions.

Colangelo, F. (1999). Qualificazione, Risposta Sismica Pseudodinamica e Modelli Fenomenologici di Portali di C.A.Tamponati con Laterizio, (in Italian). DISAT, Italy.

Colangelo, F. (2004). Pseudo-dynamic seismic response of infilled RC frames designed for gravity load, 13th World Conference on Earthquake Engineering, Vancouver, Canada, Paper no. 3021.

Collins, K. R., Wen, Y.K. and Foutch D.A. (1996). Dual-level seismic design: a reliability-based methodology *Earthquake Engineering and Structural Dynamics*., 25(12):1433–1467

Combescure, D. and Pegon, P. (2000). Application of the local to global approach to the study of infilled frame structures under seismic loading, *Proceedings 12th World Conference on Earthquake Engineering*, Auckland, New Zealand.

Center for Engineering Strong Motion Data (CESMD), Retrieved from <http://www.strongmotioncenter.org/> (Last Accessed: Sep. 20, 2014)

Cornell, C. A. (1969). A Probability-Based Structural Code, *ACI-Journal*, 66,974-985.

Cornell, C. A., Jalayer, F., Hamburger, R. O. and Foutch, D. A. (2002). The probabilistic basis for the 2000 SAC/FEMA steel moment frame guidelines, *Journal of Structural Engineering*, 128(4):526-533.

Crisafulli, F. J. (1997). Seismic behaviour of reinforced concrete structures with Masonry infills, Ph.D.Thesis, University of Canterbury, Christchurch, New Zealand.

- Crisafulli, F. J., Carr, A. J. and Park, R.** (2000). Analytical modelling of infilled frame structures-a general overview, *Bull New Zealand Soc, Earthquake Engineering*, 33(1):30-47.
- D Das, S. and Nau, J. M.** (2003). Seismic Design Aspects of Vertically Irregular Reinforced Concrete Buildings, *Earthquake Spectra*, 19(3):455-477.
- Davenport, A. G. and Carroll, H.** (1986). Damping in tall buildings: its variability and treatment in design, ASCE Spring Convention, Seattle, USA, *Building Motion in wind*, 42-57.
- Davis P. R., Padhy K. T, Menon D. and Prasad. A. M.** (2010b). Seismic fragility of open ground storey buildings in India, 9th US National and 10th Canadian Conference on Earthquake Engineering, Toronto, Paper no. 926.
- Davis, P. R., Krishnan, P., Menon, D. and A Meher Prasad, A. M.** (2004). Effect of infill stiffness on seismic performance of multi-storey RC framed buildings in India, Proc. of the 13th World Conf. on Earthquake Engineering, Vancouver, Canada, Paper No. 1198.
- Davis, P. R., Menon D. and Prasad, A. M. (2010a).** Earthquake-resistant design of open ground storey RC framed buildings, *Journal of Structural Engineering*, 37(2): 117-124.
- Dhanasekhar, M. and Page, A. W. (1986).** The influence of brick masonry infill properties on the behavior of infilled frames, *Proceedings of the Institution of Civil Engineers*, 81(2):593–605.
- Dolsek, M. and Fajfar, P.** (2001). Soft Storey effects in uniformly infilled reinforced concrete frames, *Journal of Earthquake Engineering*, 5(1):1-12.
- Dolsek, M. and Fajfar, P.** (2002). Mathematical modeling of an infilled RC frame structure based on the results of pseudo-dynamic tests, *Earthquake Engineering & Structural Dynamics*, 31(6):1215–1230.
- Dolsek, M. and Fajfar, P.** (2008). The effect of masonry infills on the seismic response of a four-storey reinforced concrete frame – a deterministic assessment, *Engineering Structures*, 30(7):1991–2001.
- Dymiotis, C., Kappos, J. A. and Chryssanthopoulos, K. M.** (2001). Seismic reliability of masonry-infilled RC frames, *Journal of Structural Engineering*, 127:296-

305.

- E** **Ellingwood, B. R.** (1994). Probability-based codified design for earthquakes, *Engineering Structures*, 16(7): 498–506.
- Ellingwood, B. R.** (2001). Earthquake risk assessment of building structures, *Reliability Engineering and System Safety*, 74(3):251-262.
- Earthquake Database**, California State University, Chico. Retrieved from <http://www.csuchico.edu/> (Last Accessed: Sep. 30, 2014)
- Earthquake Engineering Library**, Richmond, Retrieved from <http://nisee2.berkeley.edu/> (Last Accessed: Jan. 20, 2015)
- EN 1990** (2002). Eurocode - Basis of structural design, Brussels, CEN.
- Erberik, M. A. and Elnashai, A. S.** (2004). Fragility analysis of flat-slab structures, *Engineering Structures*, 26(7):937–948.
- Esteva, L.** (1992). Non-linear response of weak-ground-storey buildings to narrow-band accerelation time histories, Report 544, Institute of Engineering, UNAM (in Spanish).
- Eurocode 8** (2003). Design of structures for earth-quake resistance—Part 1: General Rules, Seismic Actions and Rules for Buildings, European Committee of Standardization, prEN1998-1, Brussels, Belgium.
- F** **Fajfar, P.** (2000). A Nonlinear Analysis Method for Performance-Based Seismic Design, *Earthquake Spectra*, 16(3):573-592.
- Fardis, M. N. and Panagiotakos, T. B.** (1997). Seismic design and response of bare and masonry-infilled reinforced concrete buildings, Part II: Infilled structures, *Journal of Earthquake Engineering*, 1(3):475–503.
- Fardis, M. N., Negro, P., Bousias, S. N. and Colombo, A.** (1999). Seismic design of open-storey infilled RC buildings, *Journal of Earthquake Engineering*, 3(2):173-197.
- Favvata M. J., Naoum M. C. and Karayannis C. G.** (2013). Limit States of RC structures with first floor Irregularities. *Journal Structural Engineering and Mechanics*, 47 (6), 791-818.
- FCEACR** (1986). Seismic Code of Costa Rica, Federal College of Engineers and Architects of Costa Rica, San Jose, Costa Rica.

- FEMA HAZUS-MH MR-1** (2003). Technical Manual, Federal Emergency Management Agency, Washington, D.C., USA.
- FEMA P695** (2012). Quantification of building seismic performance factors, Applied Technology Council, Redwood City: California for the Federal Emergency Management Agency, Washington, D.C.
- Filippou, F. C., Ambrisi, A. D. and Issa, A.** (1992), Nonlinear Static and Dynamic Analysis of RC Sub assemblages, UCB/EERC-92/08, Earthquake Engineering Research Center, University of California, Berkeley.
- Filippou, F. C., Popov, E. P. and Bertero, V. V.** (1983). Effects of bond deterioration on hysteretic behavior of reinforced concrete joints, Report EERC 83-19, Earthquake Engineering Research Center, University of California, Berkeley.
- Flanagan, R., and Bennett, R.** (1999). In- Plane Behavior of Structural Clay Tile Infilled Frames. J. of Struct. Eng , 125 (6), 590-599
- Framed Infill Network**, An Initiative of GeoHazards International, Retrieved from <http://framedinfill.org/> (Last Accessed: Nov. 30, 2014)
- G Ghanaat, Y., Patev, R. C. and Chudgar, A. K.** (2012). Seismic fragility analysis of concrete gravity dams, Proceedings of the 15th World Conference on Earthquake Engineering, Lisboa, Portugal.
- NEES**, George E. Brown, Jr. Network for Earthquake Engineering Simulation, Retrieved from <https://nees.org/> (Last Accessed: Dec. 30, 2014)
- Ghobarah, A.** (2000). Performance-based design in earthquake engineering: state of development, Engineering Structures, 23(8):878-884.
- Guneyisi, E. M. and Altay, G.** (2008). Seismic fragility assessment of effectiveness of viscous dampers in R/C buildings under scenario earthquakes, Structural Safety, 30(5):461–480.
- H Haldar, P., Singh, Y. and Paul, D. K.** (2012). Effect of URM infills on seismic vulnerability of Indian code designed RC frame buildings, Earthquake Engineering and Engineering Vibration, 11(2):233-241.

- Hasofer, A. M** and **Lind, N. C.** (1974). Exact and invariant second moment code format. *Journal of the Engineering Mechanics Division, Proceedings of the ASCE* 100(1):111–121.
- Haselton, C. B., Whittaker A. S., Hortacsu, A., Baker, J. W., Bray, J. and Grant, D. N.** (2012). Selecting and scaling earthquake ground motions for performing response-history analyses, *Proceedings of the 15th World Conference on Earthquake Engineering*, Lisboa, Portugal.
- Hashmi, A. K. and Madan, A.** (2008). Damage forecast for masonry infilled reinforced concrete framed buildings subjected to earthquakes in India, *Current Science*, 94(1):61-73.
- Heo, Y. and Kunnath, S. K.** (2008). Sensitivity to material modelling choices in seismic demand estimation for reinforced concrete frames, *Proceedings of the 14th World Conference on Earthquake Engineering*, Beijing, China.
- Holmes, M.,** (1961). Steel frame with brickwork and concrete infilling, *Proceedings of the Institution of Civil Engineers*, 19(4):473–478.
- Hwang, H. H. M. and Jaw, J. W.** (1990). Probabilistic damage analysis of structures, *Journal of Structural Engineering*, 116(7):1992-2007.
- I Ibarra, L. F., Medina, A., and Krawinkler, H.** (2005). Hysteretic models that incorporate strength and stiffness deterioration. *Earthquake Engineering and Structural Dynamics*, 34(12):1489-1511.
- ICC IBC** (2012). *International Building Code*, International Code Consortium, USA.
- Iman, R. L., and Conover, W. J.** (1980). Small sample sensitivity analysis techniques for computer models, with an application to risk assessment. *Communications in Statistics: Theory and Methods*, A9(17):1749-1874.
- IS 13920** (1993). *Ductile detailing of reinforced concrete structures subjected to seismic forces - code of practice*, Bureau of Indian Standards, New Delhi.
- IS 1893 Part I** (2002). *Indian standard criteria for earthquake resistant design of structures, Part – 1: General provisions and buildings, Fifth Revision*, Bureau of Indian Standards, New Delhi.
- IS 456** (2000). *Plain and reinforced concrete - code of practice, Fourth Revision*,

Bureau of Indian Standards, New Delhi.

ISO 13822 (2010). Bases for design of structures - Assessment of existing structures, Geneva, Switzerland, ISO TC98/SC2.

J Janardhana, M. (2010). Cyclic behaviour of glass fiber reinforced gypsum wall panels, Ph.D. Thesis, Department of Civil Engineering, IIT Madras, Chennai, India.

JCSS, (2001). JCSS Probabilistic Model Code, Zurich, Joint Committee on Structural Safety.

K Kanitkar, R. and Kanitkar, V. (2004). Seismic performance of conventional multi-storey building with open ground floors for vehicular parking, *The Indian Concrete Journal*, 78(2):99-104.

Kaushik, H. B., Rai, D. C. and Jain, S. K. (2009). Effectiveness of some strengthening options for masonry-infilled RC frames with open first storey, *Journal of Structural Engineering*, 135(8):925-937.

Kaushik, H. B., Rai, D. C., and Jain, S. K. (2006). Code approaches to seismic design of masonry infilled reinforced concrete frames: A state-of-the-art review, *Earthquake Spectra*, 22(4):961-983.

Kermani, A. H. and Fadaee, M. J. (2013). Assessment of seismic reliability of RC framed buildings using a vector-valued intensity measure, *Asian journal of Civil engineering (BHRC)*, 14(1):17-32.

Khatibinia, M., Fadaee, M. J., Salajegheh, J. and Salajegheh, E. (2013). Seismic reliability assessment of RC structures including soil–structure interaction using wavelet weighted least squares support vector machine, *Reliability Engineering & System Safety*, 110:22–33.

Kim, J. H., Choi, I. and Park, J. (2011). Uncertainty analysis of system fragility for seismic safety evaluation of NPP, *Nuclear Engineering and Design*, 241(7):2570–2579.

Kim, S. H. and Shinozuka, M. (2004). Development of fragility curves of bridges retrofitted by column jacketing, *Probabilistic Engineering Mechanics*, 19(1-2):105–112.

Kircil, M. S. and Polat, Z. (2006). Fragility analysis of mid-rise R/C frame buildings, *Engineering Structures*, 28(9):1335-1345.

Klingner R.E. and Bertero V. V. (1976), *Infilled Frames in Earthquake Resistant*

Construction, Report no.EERC 76-32, Earthquake Engineering Research Center, University of California, Berkeley.

Klingner, R. E. and Bertero, V. V. (1978), Earthquake Resistance of Infilled Frames, ASCE, Journal of the Structural Division, 104(ST6):973-989.

Koutromanos, I., Stavridis, A., Shing, P.B. and Willam, K. (2011). Numerical modeling of masonry-infilled RC frames subjected to seismic loads, Computers and Structures, 89(11-12):1026–1037.

Krinitzsky, E.L. (2002). How to obtain Earthquake Ground Motions for Engineering Design, Engineering Geology, 65(1):1–16.

Krishnan, J. (2006). Reliability analysis and design of transmission line towers, Ph.D. Thesis, Indian Institute of Technology, Madras.

Kumar, C. R. (2013). Implications of major international codal design provisions for pen ground storey buildings, M.Tech Thesis, National Institute of Technology, Rourkela.

Kunnath, S. K. (2007). Application of the PEER PBEE methodology to the I-880 viaduct, Pacific Earthquake Engineering Research Center, University of California, Berkeley.

Kwon, O. S. and Elnashai, A. (2006). The effect of material and ground motion uncertainty on the seismic vulnerability of RC structure, Engineering Structures, 28(2):289–303.

L Lagaros, N. D. (2008). Probabilistic fragility analysis: A tool for assessing design rules of RC buildings, Earthquake engineering and engineering vibration, 7(1):45–56.

Landi, L., Diotallevi, P., P. and Tardini, A. (2012). Calibration of an equivalent strut model for the nonlinear seismic analysis of infilled RC frames, 15th World Conference on Earthquake Engineering, Lisboa, Portugal.

Lee, T. H. and Mosalam, K. M. (2004). Probabilistic fiber element modeling of reinforced concrete structures, Computers and Structures, 82(27):2285-2299.

Liauw, T. C. and Kwan, K. H. (1984). Nonlinear behaviour of non-integral infilled frames, Computers and Structures, 18(3):551-560.

Liauw, T. C., and Kwan, K. H. (1983). Plastic Theory of Nonintegral Infilled Frames,

Proceedings of the Institution of Civil Engineers (London), Part 2, 75:379-396.

Liu, P. L., and Der Kiureghian, A. (1991). Finite element reliability of geometrically nonlinear uncertain structures. Journal of the Engineering Mechanics Division, Proceedings of the ASCE 117(8):1806–1825.

Lupoi, G. (2005). Fragility analysis of the seismic response of freestanding equipment, Ph.D Thesis, European School of Advanced studies in Reduction of Seismic Risk- Rose school.

M Mackie, K. and Stojadinovic, B. (2003). Seismic Demands for Performance-Based Design of Bridges. Report No. PEER 312.

Madan A., Reinhorn A. M., Mandar J. B. and Valles R. E.(1997). Modeling of Masonry Infill Panels for Structural Analysis, Journal of Structural Engineering, 123(10):1295-1302.

Mainstone, R. J. (1962). Discussion on Steel Frames with Brickwork and Concrete Infilling, Proceedings of the Institution of Civil Engineers, 23:94-99.

Mainstone, R. J. (1971). On the stiffness and strength of infilled frames, Proceedings of the Institution of Civil Engineers, 4:57-90.

Mainstone, R. J. and Weeks, G. A. (1970). The influence of a bounding frame on the racking stiffness and strengths of brick walls. SIBMAC Proceeding, Presented at the Second International Brick Masonry Conference, Building Research Station, England.

Mander J. B., Priestley, M. J. N. and Park R. (1988). Theoretical stress-strain model for confined concrete, Journal of Structural Engineering, 114(8):1804-1826.

Mazzoni and McKenna, Algorithm for Push over and Non-linear time history analysis, Retrieved from <http://opensees.berkeley.edu/> (Last Accessed: Dec. 15, 2014)

Mazzoni, S., McKenna, F., Scott, M. H. and Fenves, G. L. (2009). OpenSees Command Language Manual, Open System for Earthquake Engineering Simulations.

McKay, M., Beckman, R. and Conover, W. (1979). A comparison of three methods for selecting values of input variables in the analysis of output from a computer code, Technometrics, 21:239–245.

McKenna, F., McGann, C., Arduino, P. and Harmon, J. A. (2014). OpenSees Laboratory, <https://nees.org/resources/openseeslab>.

- Mehrabi A. B. and Shing P. B.** (2002). Behaviour and analysis of masonry-infilled frames, *Progress in Structural Engineering and Materials*, 4(3):320-331.
- Mehrabi, A. B. and Shing, P. B.** (1997). Finite Element Modeling of Masonry-Infilled RC frames, *Journal of Structural Engineering*, ASCE, 123(5):604-613.
- Melchers, R. E.** (1987) *Structural Reliability Analysis and Prediction*, 1st Edition, Ellis Horwood Limited, Market Cross House, Cooper Street, Chichester, West Sussex, PO19 1EB, England.
- Melchers, R. E.** (1999). *Structural Reliability Analysis and Prediction* (2nd ed.). Chichester, West Sussex, England: John Wiley and Sons Ltd.
- Menegotto M. and Pinto P. E.** (1973). Method of analysis for cyclically loaded R.C. plane frames including changes in geometry and non-elastic behaviour of elements under combined normal force and bending, *Symposium on the Resistance and Ultimate Deformability of Structures Acted on by Well Defined Repeated Loads*, International Association for Bridge and Structural Engineering, Zurich, Switzerland, 15-22.
- Mosalam, K. M., Ayala, G., White, R. N. and Roth, C.** (1997). Seismic fragility of LRC frames with and without masonry infill walls, *Journal of Earthquake Engineering*, 1(4):693-720.
- Mukherjee, S. and Gupta, V. K.** (2002). Wavelet-based generation of spectrum compatible time histories, *Soil dynamics and Earthquake engineering*, 22(9):799-804.
- Murthy, C.V. R.** (2002). What are the Seismic Effects on Structures?, *Earthquake tip 05*, IITK –BMTPC.
- N Nath, S. K. and Thingbaijam, K. K. S.** (2012). Probabilistic Seismic hazard assessment of India, *Seismological Research Letters*, 83(1):135-149.
- NICEE**, National Information Centre of Earthquake Engineering, Retrieved from <http://www.nicee.org/> (Last Accessed: May. 20, 2014)
- NBC-201** (1995). *Nepal National Building Code for Mandatory Rules of Thumb for Reinforced Concrete Buildings with Masonry Infill*, Ministry of Housing and Physical Planning, Department of Buildings, Kathmandu, Nepal.
- Negro, P. and Colombo, A.** (1997). Irregularities induced by non-structural masonry panels in framed buildings, *Engineering Structures*, 19(7):576-585.

- Newmark, N. M.** (1959). A Method of Computation for Structural Dynamics, ASCE Journal of the Engineering Mechanics Division. 85(EM3):67-94.
- Nie, J. and Ellingwood B. R.** (2005), Finite Element-based structural reliability assessment using efficient directional simulation, Journal of Engineering Mechanics, ASCE, 131(3):259-267.
- Nielson, B. G.** (2005). Analytical fragility curves for highway bridges in moderate seismic zones, Ph.D Thesis, Georgia Institute of Technology.
- Nielson, B. G. and DesRoches, R.** (2007). Analytical seismic fragility curves for typical bridges in the Central and South eastern US, Earthquake Spectra, 23(3):615–633.
- NKB 55** (1987). Retningslinier for Last-og sikkerhedsbestemmelser for Bærende konstruktioner (Recommendations for loading and safety regulations for structural design, in Swedish), ISBN 87-509-6991-1, ISSN 0359-9981, Visoprint as, Köpenhamn.
- NZS 1170.5** (2004). Structural design actions, Part 5: Earthquake actions -New Zealand-Commentary, Standards Association of New Zealand, Wellington, New Zealand.
- O** **OpenSees** (2013). Open system for earthquake engineering simulation, A Program for Static and Dynamic Nonlinear Analysis of Structures. [online]. <<http://opensees.berkeley.edu/>>.
- Ozel, A.E. and Guneyisi, E.M.** (2011). Effects of eccentric steel bracing systems on seismic fragility curves of midrise R/C buildings: a case study, Structural Safety, 33(1):82-95.
- P** **Patel, S.** (2012). Earthquake resistant design of low-rise Open Ground Storey framed building, M.Tech Thesis, National Institute of Technology, Rourkela.
- Panagiotakos T. B. and Fardis M. N.** (1996). Seismic response of infilled RC frame structures, In: Proceedings of the 11th world conference on earthquake engineering.
- Pinto A. V.,** editor (1996). Pseudodynamic and Shaking Table Tests R.C. Bridges, ECOEST PREC, Rep.No. 8.
- Pinho, R. and Elnashai, A.S.** (2000). Dynamic collapse testing of a full-scale four storey RC frame, ISET Journal of Earthquake Technology, 37(4):143-164.

- Polyakov, S.V.** (1960). On the interaction between masonry filler walls and enclosing frame when loaded in the plane of the wall, in: construction in seismic regions, Translation in Earthquake Engineering, Earthquake Engineering Research Institute, Moscow, 36–42.
- Porter, K. A., Kiremidjian, A. S. and LeGrue, J. S.** (2001). Assembly-based vulnerability of buildings and its use in performance evaluation, *Earthquake Spectra* (EERI), 17(2): 291–312.
- R** **Rajeev, P. and Tesfamariam, S.** (2012). Seismic fragilities for reinforced concrete buildings with consideration of irregularities, *Structural Safety*, 39:1-3.
- Ramamoorthy, S. K., Gardoni, P. and Bracci, J. M.** (2006). Probabilistic demand models and fragility curves for reinforced concrete frames, *Journal of Structural Engineering*, 132(10):1563–1572.
- Ranganathan, R.** (1999). *Structural reliability analysis and design*, Jaico Publishing House, Mumbai.
- Ravichandran, S. S. and Klinger, E. R.** (2012). Seismic design factors for steel moment frames with masonry infills: Part I, *Earthquake Spectra*, 28(3):1189-1204.
- Rayleigh, L.** (1954). *Theory of Sound*, Dover Publications, New York.
- Reiter, L.** (1990). *Earthquake Hazard Analysis- Issues and Insights*, Columbia University Press, New York, x:254.
- Rossetto, T. and Elnashai, A.** (2005). A new analytical procedure for the derivation of displacement-based vulnerability curves for populations of RC structures, *Engineering Structures*, 27(3):397–409.
- S** **Sattar, S.** (2013). Influence of masonry infill walls and other building characteristics on seismic collapse of concrete frame buildings, Ph.D thesis, University of Colorado, Boulder, Colorado, USA.
- Sahoo, D. R. and Rai, D. C.** (2013). Design and Evaluation of seismic strengthening techniques for Reinforced Concrete frames with soft ground storey, *Engineering Structures*, 56(11):1933–1944.
- Saneinejad, A. and Hobbs, B.** (1995). Inelastic design of infilled frames, *Journal of Structural Engineering*, 121(ST4):634–650.

- Scarlet, A.** (1997). Design of soft stories-A simplified energy approach, *Earthquake Spectra*, 13(2):305-315.
- SEAOC Vision 2000.** (1995). Performance based seismic engineering, Structural Engineers Association of California, Sacramento, CA.
- Seismosoft** (2013). SeismoStruct v6.0 - Verification Report, Available from URL: www.seismosoft.com.
- Selna, L.G.** (1977). Modeling of Reinforced Concrete Buildings, Proceedings of a Workshop on Earthquake-Resistant Reinforced Concrete Building Construction, University of California, Berkeley, 2:887-937.
- Selvakoodalingam, B., Perumal Pillai, E. B. and Govindan, P.** (1999). Strengthening of RC Infilled frame with opening, *Concrete International*, 21(11):37-42.
- Shinozuka M, Feng MQ, Lee J. and Naganuma, T.** (2000). Statistical analysis of fragility curves, *Journal of Engineering Mechanics*, 126(12):1224–1231.
- SI-413.** (1995). Design Provisions for Earthquake Resistance of Structures, The Standards Institution of Israel, Tel-Aviv, Israel.
- Singhal A and Kiremidjian A. S.** (1996). Method for probabilistic evaluation of seismic structural damage, *Journal of Structural Engineering*, 122(12):1459–1467.
- Singhal, A. and Kiremidjian, A. S.** (1998). Bayesian updating of fragilities with application to RC frames, *Journal of Structural Engineering*, 124(8):922–929.
- Smith, B. S and Carter, C.** (1969). A method of analysis for infilled frames, *Proceedings of the Institution of Civil Engineers*, 44:31–48.
- Smith, B. S.** (1962). Lateral stiffness of infilled frames, *Journal of Structural Division*, 88:183–199.
- Song, J. and Ellingwood, B. R.** (1999). Seismic reliability of special moment steel frames with welded connections:II, *Journal of Structural Engineering*, 125(4):372.
- Stavridis, A. and Shing, P.** (2010). Finite-element modelling of nonlinear behaviour of masonry-infilled RC frames, *Journal of Structural Engineering*, 136(3):285–296.
- T Tavares, D. H., Padgett J. E., and Paultre, P.** (2012). Fragility Curves of Typical As-built Highway Bridges in Eastern Canada, *Engineering structures*, 40:107-118.

- Thomas, F. G.** (1953). The strength of brickwork, *Structural Engineer*, 31(2):44-46.
- Tian, J. and Symans, M. D.** (2012). High-Performance Seismic Retrofit of Soft-Storey Wood-framed Buildings using Energy Dissipation Systems, *Proceedings of ASCE Structures Congress, Chicago, IL*.
- V Val, Dimitri, Bljoger, F. and Yankelevsky, D.** (1997). Reliability Evaluation in Nonlinear analysis of Reinforced Concrete structures, *Structural Safety*, 19(2):203-217.
- W Wen, Y. K.** (1995). Building Reliability and Code Calibration, *Earthquake Spectra*, 11(2):269-296.
- Wen, Y. K., Collins, K. R., Han, S. W. and Elwood K. J.** (1996). Dual-level designs for buildings under seismic loads, *Structural Safety*, 18(2-3):195–224.
- Wen, Y. K.** (2001). Reliability and performance-based design, *Structural Safety*, 23:407-428.
- Wood, R. H.** (1958). The Stability of Tall Buildings, *Proceedings of the Institution of Civil Engineers*, 11:69-102.
- Y Yoshimura, M.** (1997). Nonlinear analysis of a reinforced concrete building with a soft first storey collapsed by the 1995 Hyogoken Nanbu earthquake, *Cement and Concrete Composites*, 19(3):213-221.
- Z Zarnic, R. and Gostic, S.** (1997). Masonry infilled frames as an effective structural sub-assembly, *Seismic Design Methodologies for the Next Generation of Codes: Proceedings of the International Workshop, Bled, Slovenia*.

LIST OF PUBLICATIONS

REFEREED JOURNALS

- 1) **Haran Pragalath D.C., Robin Davis P. and Pradip Sarkar** (2015). Multiplication Factors for Open Ground Storey buildings - A Reliability Based Evaluation, Earthquake Engineering and Engineering Vibration. Springer. (Accepted)
- 2) **Haran Pragalath D. C., Robin Davis P. and Pradip Sarkar** (2015). Comparison of fragility analysis for a RC frame by two major approaches, Asian Journal of Civil Engineering, 16(1):47-66.
- 3) **Haran Pragalath D.C., Robin Davis P. and Pradip Sarkar** (August, 2014). Reliability Based multiplication factors for Design of open ground storey RC building, Engineering Structures. (Under review)
- 4) **Haran Pragalath D.C., Robin Davis P. and Pradip Sarkar** (November, 2014). Performance of infilled RC frame structure having different wall thickness under Seismic Excitation, Iranian Journal of Science and Technology Transactions of Civil Engineering. (Under review).
- 5) **Haran Pragalath D.C., Robin Davis P., Pradip Sarkar and Monalisa Priyadharshini** (2014). Seismic reliability assessment of RC Frame in a High Seismic Zone – India, International Journal of Emerging Technology and Advanced Engineering, 4(4):28-32.

PRESENTATIONS IN CONFERENCES

- 1) **Haran Pragalath D.C., Robin Davis P. and Pradip Sarkar** (2014). Efficacy of Multiplication Factors Suggested by International codes for Open Ground Storey Buildings – A Reliability Based Evaluation, 8th National Frontiers of Engineering, INAE and IIT Gandhinagar, Gandhinagar, India.
- 2) **Robin Davis P., Haran Pragalath D.C. and Pradip Sarkar** (2014). Open Ground Storey Buildings designed as per various International Codes – A Seismic Performance Comparison Study – A Reliability Based Evaluation, Recent Innovations in Civil Engineering and Technology, Ilahiya College of Engineering and Technology, Kerala, India.

- 3) **Haran Pragalath D. C., Pradip Sarkar and Robin Davis P.** (2013). Comparison of Fragility Analysis for a RC Frame by two major approaches, National Conferences on New Horizons in Civil Engineering, Manipal Institute of Technology, Manipal, Karnataka, India, Paper # 76.
- 4) **Ranjith Kumar C. H., Robin Davis P., Pradip Sarkar and Haran Pragalath D. C.** (2013). Seismic performance of typical Open Ground Storey framed buildings. National Conferences on New Horizons in Civil Engineering, Manipal Institute of Technology, Manipal, Karnataka, India. Paper # 91.
- 5) **Ganesh R., Haran Pragalath D. C., Robin Davis P., Pradip Sarkar and S.P.Singh** (2013). Seismic fragility analysis of axially loaded single pile, International conference on Structural Engineering and Mechanics, National Institute of Technology Rourkela, Odisha, India, Paper # 132.
- 6) **Haran Pragalath D. C., Robin Davis P. and Pradip Sarkar** (2014). Seismic Performance of an Open Ground Storey framed buildings designed as per Indian code, International Conference on Recent Trends in Engineering and Technology, Kerala, India.
- 7) **Haran Pragalath D.C., Robin Davis P., Pradip Sarkar and Monalisa Priyadarshini** (2014). Seismic reliability assessment of RC frames in a high seismic zone – India, International Conference on Advances in Civil Engineering and Chemistry of Innovative Materials, Chennai, India.
- 8) **Monalisa Priyadarshini, Robin Davis P., Haran Pragalath D. C. and Pradip Sarkar** (2013). Seismic reliability assessment of typical soft-storey RC building in manipur region, International Conference on Innovations in civil engineering, SCMS School of Engineering & Technology, Kerala, India, Paper # 71.
- 9) **Monalisa Priyadarshini, Robin Davis P. and Haran Pragalath D. C.** (2013). Performance assessment of vertical irregular buildings using fragility curves, Proceedings of Symposium on Sustainable Infrastructure Development (SID), IIT Bhubaneswar, Bhubaneswar, Odisha, India, Pg # 245-251.
- 10) **Monalisa Priyadarshini, Robin Davis P., Pradip Sarkar and Haran Pragalath D.C.** (2013). Seismic reliability assessment of R/C stepped frames, International conference on Structural Engineering and Mechanics, National Institute of Technology Rourkela, Odisha, India, Paper # 124.

BIO-DATA

NAME : D.C. Haran Pragalath
DATE OF BIRTH : May 28, 1988
PERMANENT ADDRESS : No: 10, 45th street, D-sector,
Sivasakthi Nagar,
Annanur, Chennai,
Tamil Nadu, India - 600 109.
Ph: +91-9840661998
haran5441@gmail.com.

EDUCATIONAL QUALIFICATION

Diploma in Engineering (Diploma)

Specialisation : Civil Engineering (secured 90.38%)
Institution : S.A. Polytechnic College,
DOTE, Govt. of Tamil Nadu, Chennai, TN.

Bachelor of Engineering (B. E.)

Specialisation : Civil Engineering (secured 80.22%)
Institution : Jaya Engineering College,
Anna University, Chennai, TN.

Master of Technology (M. Tech.)

Specialisation : Structural Engineering (secured 9.37 CGPA)
Institution : National Institute of Technology Rourkela,
Rourkela, Odisha.

Doctor of Philosophy (Ph. D) - pursuing

Specialisation : Civil Engineering (secured 9.49 CGPA)
Institution : National Institute of Technology Rourkela,
Rourkela, Odisha.